CHAPTER III - SUMMARY OF TROPICAL CYCLONES

1. WESTERN NORTH PACIFIC TROPICAL CYCLONES

During 1982, the western North Pacific experienced the fourth consecutive year of below average tropical cyclone activity. Twenty-eight tropical cyclones occurred in 1982, three and one-half less than the annual average. Only two significant tropical cyclones failed to develop beyond the tropical depression (TD) stage and seven tropical storms (TS) failed to reach typhoon intensity. Of the 19 tropical cyclones that developed to typhoon (TY) intensity (the highest frequency since 1972), only two reached the 130 kt (67 m/sec) intensity necessary to be classified as super typhoons (STY). In the western North Pacific, tropical cyclones reaching tropical storm intensity or greater are assigned names in alphabetical order from a list of alternating male/female names (refer to Appendix 3). Table 3-1 provides a summary of key statistics for western North Pacific tropical cyclones. Each tropical cyclone's maximum surface winds (in knots) and minimum observed sea level pressure (in millibars) were obtained from best estimates based on all available data. The distance traveled (in nautical miles) was calculated from the JTWC official best tracks (see Annex A).

Table 3-2 through 3-5 provide further information on the monthly distribution of tropical cyclones and statistics on Tropical Cyclone Formation Alerts and Warnings.

TABLE 3-1. WESTERN NORTH PACIFIC

1982 SIGNIFICANT TROPICAL CYCLONES

TROPICAL CYCLONE	PERIOD OF WARNING	CALENDAR DAYS OF WARNING	NUMBER OF WARNINGS ISSUED	MAXIMUM SURFACE WIND (KT)	OBSERVED MSLP (MB)	BEST TRACK DISTANCE TRAVELED (NM)
01 TS MAMIE	16 MAR - 24 MAR	9	35	60	990	2733
02 TY NELSON	19 MAR - 1 APR	14	53	105	934	3063
03 TY ODESSA	29 MAR - 4 APR	7	25	75	964	1528
04 TY PAT	17 MAY - 23 MAY	7	24	105	947	1994
05 TY RUBY	21 JUN - 27 JUN	7	25	75	970	2173
06 TS TESS	29 JUN - 2 JUL	4	14	35	999	585
07 TS SKIP	30 JUN - 1 JUL	2	8	50	991	1197
08 TS VAL	3 JUL - 4 JUL	2	7	55	987	867
09 TS WINONA	12 JUL - 17 JUL	6	22	55	985	1486
10 TY ANDY	22 JUL - 30 JUL	9	32	120	920	2072
11 STY BESS	22 JUL - 2 AUG	12	43	140	901	2811
12 TY CECIL	5 AUG - 14 AUG	10	39	125	914	1665
13 TY DOT	9 AUG - 15 AUG	7	27	80	960	2435
14 TY ELLIS	18 AUG - 27 AUG	10	36	125	913	2640
15 TY FAYE	21 AUG - 3 SEP	14	50	90	960	2454
16 TY GORDON	27 AUG - 5 SEP	10	38	100	944	2014
17 TS HOPE	4 SEP - 6 SEP	3	10	60	979	630
18 TY IRVING	5 SEP - 16 SEP	12	44	90	952	1778
19 TY JUDY	5 SEP - 12 SEP	8	29	90	953	2133
20 TY KEN	16 SEP - 25 SEP	10	37	110	936	1647
21 TS LOLA	16 SEP - 19 SEP	4	12	50	993	1424
22 TD 22	21 SEP - 22 SEP	2	5	30	1001	282
23 STY MAC	1 OCT - 9 OCT	9	32	140	895	2287
24 TY NANCY	11 OCT - 18 OCT	8	29	115	926	2400
25 TD 25	15 OCT - 16 OCT	2	5	20	1002	228
26 TY OWEN	15 OCT - 27 OCT***	12	40	105	939	3604
27 TY PAMELA	24 NOV - 9 DEC	16	60	100	940	4291
28 TY ROGER	8 DEC - 10 DEC	3	12	65	985	906
1982 TOTALS:		150*	793**			

* OVERLAPPING DAYS INCLUDED ONLY ONCE IN SUM
** IN ADDITION, 17 AMENDED WARNINGS WERE ISSUED DURING 1982
*** NO WARNINGS WERE ISSUED FOR TY OWEN ON 23 OCTOBER

TABLE 3-2.

1982 SIGNIFICANT TROPICAL CYCLONES

WESTERN NORTH PACIFIC	JAN	FEB	MAR	APR	MAY	JUN	JUL	AUG	SEP	OCT	NOV	DEC	TOTAL	(1959-1981) AVERAGE	(1959-1981) CASES
TROPICAL DEPRESSIONS	0	0	0	0	0	0	0	0	1	1	0	0	2	4.0	91
TROPICAL STORMS	0	0	1	0	0	2	2	0	2	0	0	0	7	9.8	225
TYPHOONS	0	0	2	0	1	1	2	5	3	3	1	1	19	17.8	409
ALL TROPICAL CYCLONES	0	0	3	0	1	3	4	5	6	4	1	1	28	31.5	725

1959-1981	JAN	FEB	MAR	APR	MAY	JUN	JUL	AUG	SEP	OCT	NOV	DEC	TOTAL
AVERAGE	.6	.3	.7	1.0	1.4	2.0	5.0	6.3	5.9	4.4	2.7	1.4	31.5
CASES	13	8	15	22	32	45	115	144	136	101	62	32	725

PREVIOUS 23-YEAR HISTORY

FORMATION ALERTS: 26 of 36 Formation Alert Events developed into significant tropical cyclones. Tropical Cyclone Formation Alerts were issued for all but two of the significant tropical cyclones that developed during 1982.

WARNINGS:

Number of warning days:	150
Number of warning days with two tropical cyclones in region:	56
Number of warning days with three or more tropical cyclones in region:	6

TABLE 3-3.

FREQUENCY OF TYPHOONS BY MONTH AND YEAR

YEAR	JAN	FEB	MAR	APR	MAY	JUN	JUL	AUG	SEP	OCT	NOV	DEC	TOTAL
(1945-1958) AVERAGE	.4	.1	.3	.4	.7	1.1	2.0	2.9	3.2	2.4	2.0	.9	16.3
1959	0	0	0	1	0	0	1	5	3	3	2	2	17
1960	0	0	0	1	0	2	2	8	0	4	1	1	19
1961	0	0	1	0	2	1	3	3	5	3	1	1	20
1962	0	0	0	1	2	0	5	7	2	4	3	0	24
1963	0	0	0	1	1	2	3	3	3	4	0	2	19
1964	0	0	0	0	2	2	6	3	5	3	4	1	26
1965	1	0	0	1	2	2	4	3	5	2	1	0	21
1966	0	0	0	1	2	1	3	6	4	2	0	1	20
1967	0	0	1	1	0	1	3	4	4	3	3	0	20
1968	0	0	0	1	1	1	1	4	3	5	4	0	20
1969	1	0	0	1	0	0	2	3	2	3	1	0	13
1970	0	1	0	0	0	1	0	4	2	3	1	0	12
1971	0	0	0	3	1	2	6	3	5	3	1	0	24
1972	1	0	0	0	1	1	4	4	3	4	2	2	22
1973	0	0	0	0	0	0	4	2	2	4	0	0	12
1974	0	0	0	0	1	2	1	2	3	4	2	0	14
1975	1	0	0	0	0	0	1	3	4	3	2	0	15
1976	1	0	0	1	2	2	2	1	4	1	1	0	15
1977	0	0	0	0	0	0	3	0	2	3	2	1	11
1978	0	0	0	1	0	0	3	2	4	3	2	0	15
1979	1	0	1	1	0	0	2	2	3	2	1	1	14
1980	0	0	0	0	2	0	3	2	5	2	1	0	15
1981	0	0	1	0	0	2	2	2	4	1	2	2	16
1982	0	0	2	0	1	1	2	5	3	3	1	1	19
(1959-1982) AVERAGE	.3	.04	.3	.6	.9	1.0	2.8	3.4	3.3	3.0	1.6	.7	17.8
CASES	6	1	6	15	20	23	66	81	80	72	38	15	423

TABLE 3-4.

FREQUENCY OF TROPICAL STORMS AND TYPHOONS BY MONTH AND YEAR

YEAR	JAN	FEB	MAR	APR	MAY	JUN	JUL	AUG	SEP	OCT	NOV	DEC	TOTAL
(1945-1958) AVERAGE	.4	.1	.4	.5	.8	1.3	3.0	3.9	4.1	3.3	2.7	1.1	21.6
1959	0	1	1	1	0	0	3	6	6	4	2	2	26
1960	0	0	0	1	1	3	3	10	3	4	1	1	27
1961	1	1	1	1	3	2	5	4	6	5	1	1	31
1962	0	1	0	1	2	0	6	7	3	5	3	2	30
1963	0	0	0	1	1	3	4	3	5	5	0	3	25
1964	0	0	0	0	2	2	7	9	7	6	6	1	40
1965	2	2	1	1	2	3	5	6	7	2	2	1	34
1966	0	0	0	1	2	1	5	8	7	3	2	1	30
1967	1	0	2	1	1	1	6	8	7	4	3	1	35
1968	0	0	0	1	1	1	3	8	3	6	4	0	27
1969	1	0	1	1	0	0	3	4	3	3	2	1	19
1970	0	1	0	0	0	2	2	6	4	5	4	0	24
1971	1	0	1	3	4	2	8	4	6	4	2	0	35
1972	1	0	0	0	1	3	6	5	4	5	2	3	30
1973	0	0	0	0	0	0	7	5	2	4	3	0	21
1974	1	0	1	1	1	4	4	5	5	4	4	2	32
1975	1	0	0	0	0	0	2	4	5	5	3	0	20
1976	1	1	0	2	2	2	4	4	5	1	1	2	25
1977	0	0	1	0	0	1	4	1	5	4	2	1	19
1978	1	0	0	1	0	3	4	7	5	4	3	0	28
1979	1	0	1	1	1	0	4	2	7	3	2	2	24
1980	0	0	0	1	4	1	4	2	6	4	1	1	24
1981	0	0	1	2	0	2	5	7	4	2	3	2	28
1982	0	0	3	0	1	3	4	5	5	3	1	1	26
(1959-1982) AVERAGE	.5	.3	.6	.9	1.2	1.6	4.5	5.4	5.0	4.0	2.4	1.2	27.5
CASES	12	7	14	21	29	39	108	130	120	95	57	28	660

TABLE 3-5.

FORMATION ALERT SUMMARY

WESTERN NORTH PACIFIC

YEAR	NUMBER OF ALERT SYSTEMS	ALERT SYSTEMS WHICH BECAME NUMBERED TROPICAL CYCLONES	TOTAL NUMBERED TROPICAL CYCLONES	DEVELOPMENT RATE
1972	41	29	32	71%
1973	26	22	23	85%
1974	35	30	36	86%
1975	34	25	25	74%
1976	34	25	25	74%
1977	26	20	21	77%
1978	32	27	32	84%
1979	27	23	28	85%
1980	37	28	28	76%
1981	29	28	29	97%
1982	36	26	28	72%
(1972-1982) AVERAGE	32.5	25.7	27.9	79%

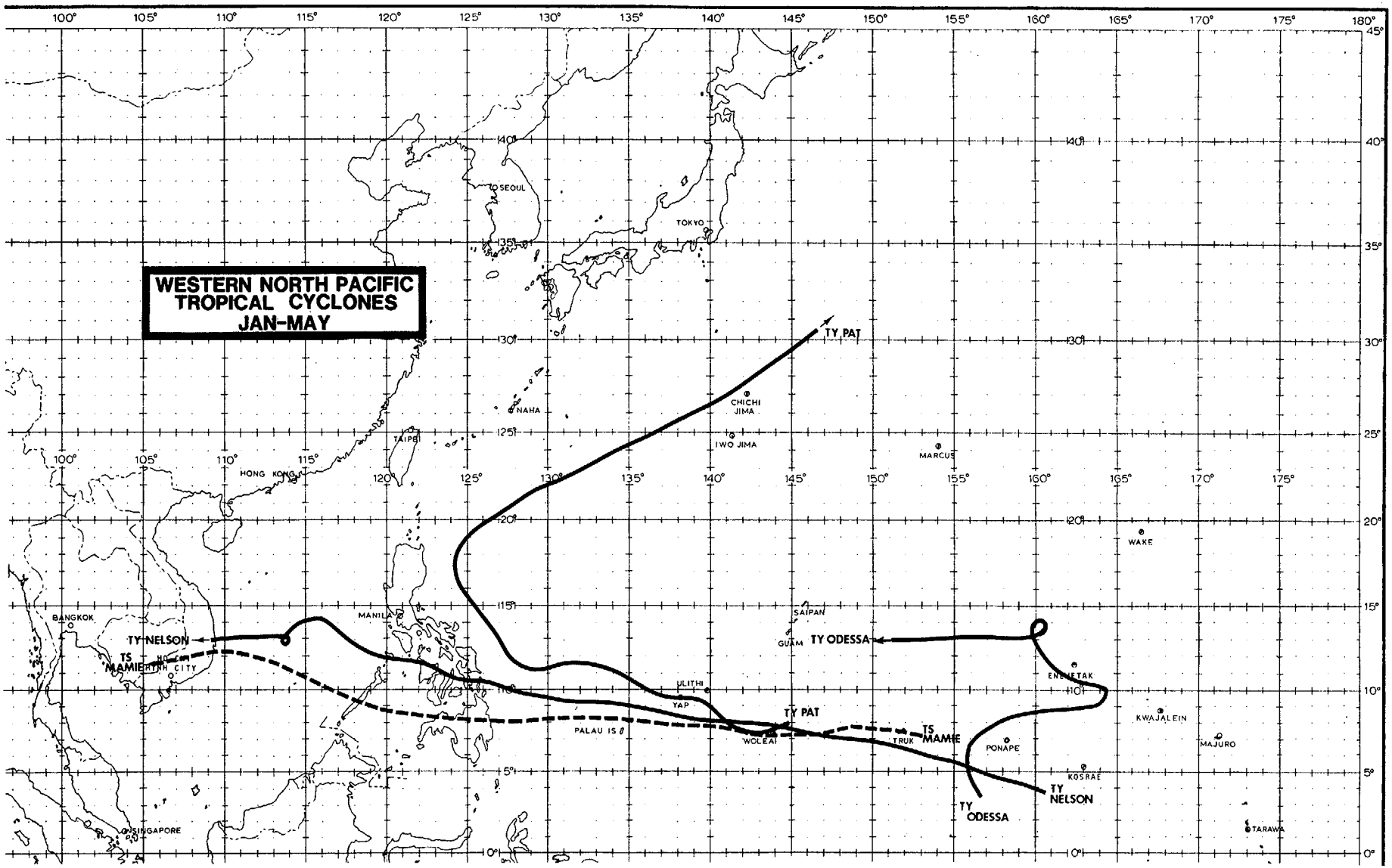
WESTERN NORTH PACIFIC
TROPICAL CYCLONES
JAN-MAY
TY PAT
TY NELSON
TS MAMIE
TY ODESSA
TY PAT
TS MAMIE
TY NELSON
TY ODESSA
SEOUL
TOKYO
NAHA
TAIPEI
HONG KONG
BANGKOK
MANILA
HO CHI MINH CITY
SINGAPORE
CHICHI JIMA
IWO JIMA
MARCUS
WAKE
SAIPAN
GUAM
ULITHI
YAP
PALAU IS
WOLEAI
TRUK
PONAPE
KOSRAE
ENEWETAK
KWAJALEIN
MAJURO
TARAWA

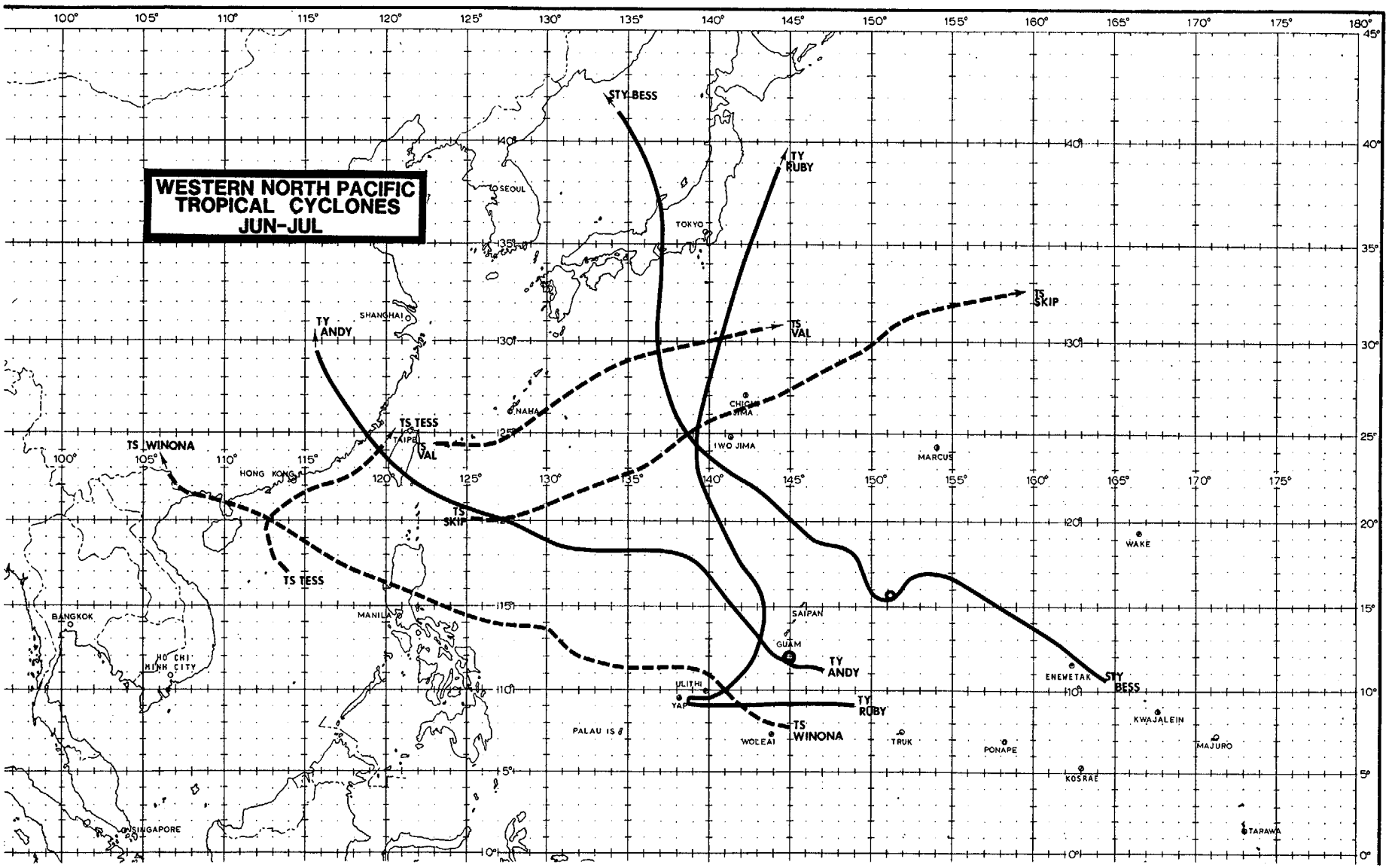
WESTERN NORTH PACIFIC
TROPICAL CYCLONES
JUN-JUL
STY BESS
TY RUBY
TS SKIP
TS VAL
TY ANDY
TS TESS
TS WINONA
SEOUL
TOKYO
SHANGHAI
NAHA
TAIPEI
HONG KONG
CHICHI JIMA
IWO JIMA
MARCUS
WAKE
SAIPAN
GUAM
MANILA
BANGKOK
HO CHI MINH CITY
SINGAPORE
PALAU IS
YAP
ULITHI
WOLEAI
TRUK
PONAPE
KOSRAE
ENEWETAK
KWAJALEIN
MAJURO
TARAWA

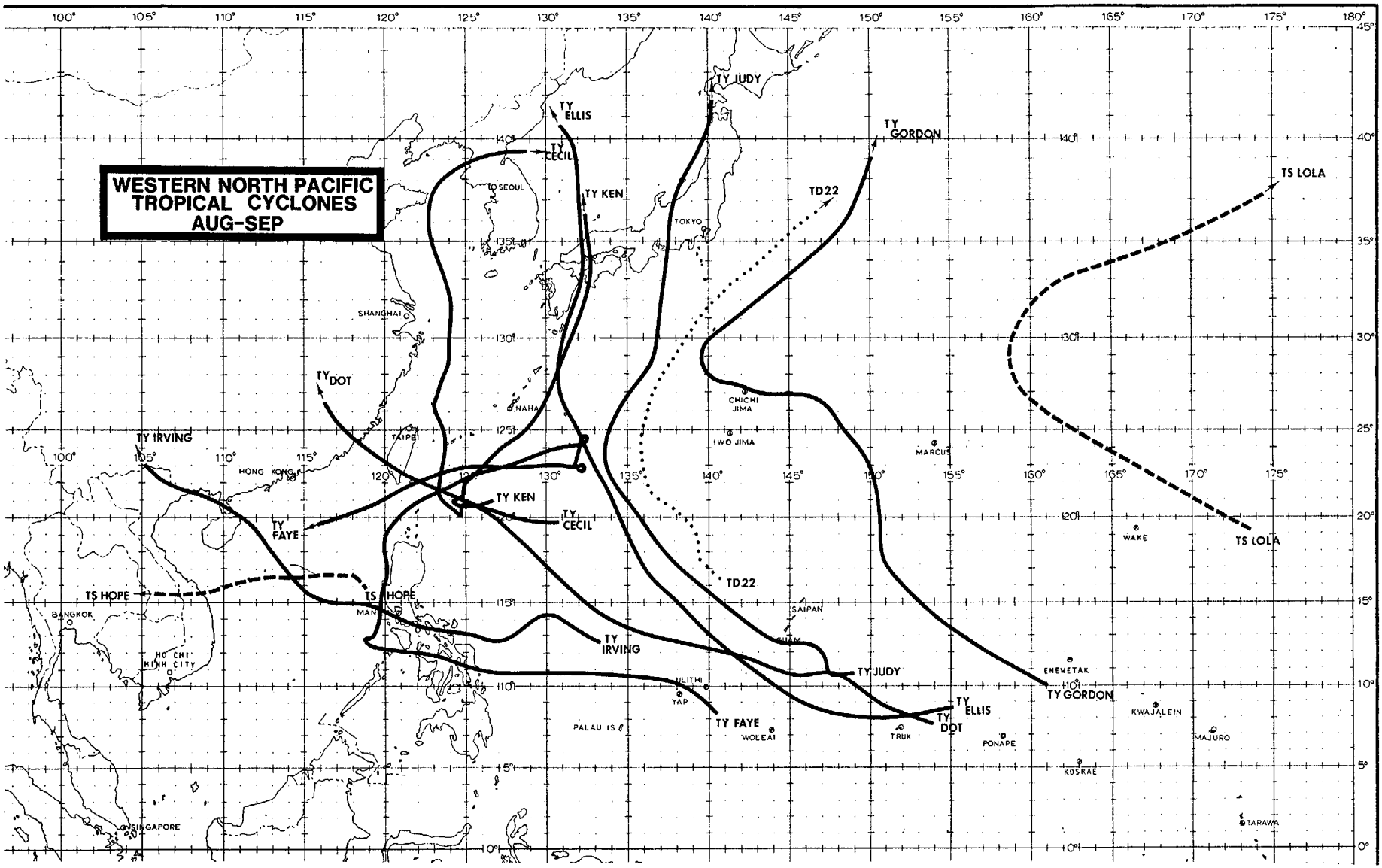
WESTERN NORTH PACIFIC
TROPICAL CYCLONES
AUG-SEP
TY JUDY
TY ELLIS
TY GORDON
TY CECIL
TY KEN
TS LOLA
TD22
TY DOT
TY IRVING
TY FAYE
TS HOPE
SEOUL
TOKYO
SHANGHAI
NAHA
TAIPEI
HONG KONG
CHICHI JIMA
IWO JIMA
MARCUS
WAKE
SAIPAN
GUAM
ENEWETAK
KWAJALEIN
MAJURO
TARAWA
KOSRAE
PONAPE
TRUK
WOLEAI
YAP
ULITHI
PALAU IS
BANGKOK
HO CHI MINH CITY
SINGAPORE

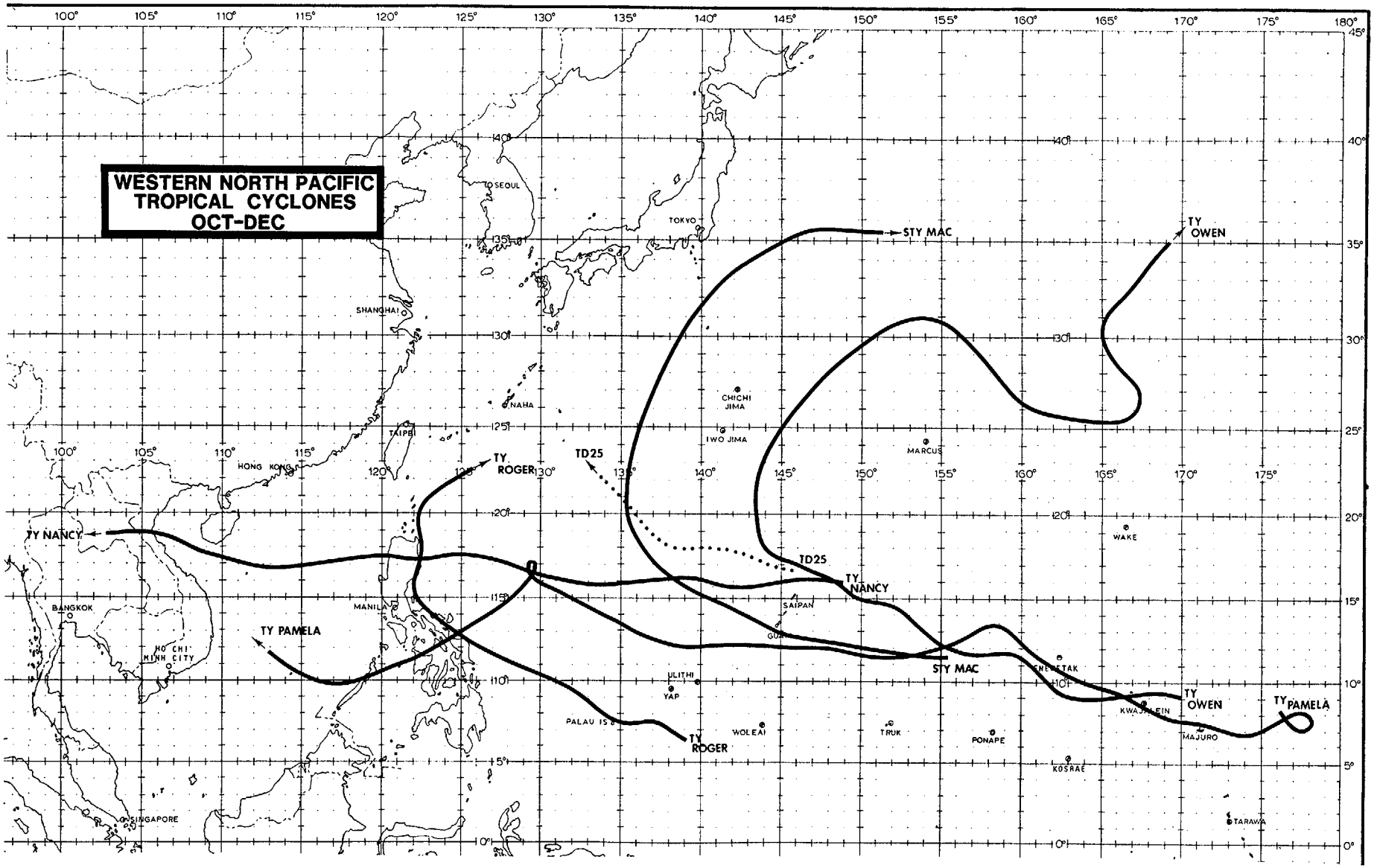
WESTERN NORTH PACIFIC
TROPICAL CYCLONES
OCT-DEC
STY MAC
TY OWEN
TY ROGER
TD25
TY NANCY
TY PAMELA
SEOUL
TOKYO
SHANGHAI
NAHA
TAIPEI
HONG KONG
CHICHI JIMA
IWO JIMA
MARCUS
WAKE
SAIPAN
GUAM
MANILA
BANGKOK
HO CHI MINH CITY
SINGAPORE
ULITHI
YAP
PALAU IS.
WOLEAI
TRUK
PONAPE
KOSRAE
KWAJALEIN
MAJURO
TARAWA

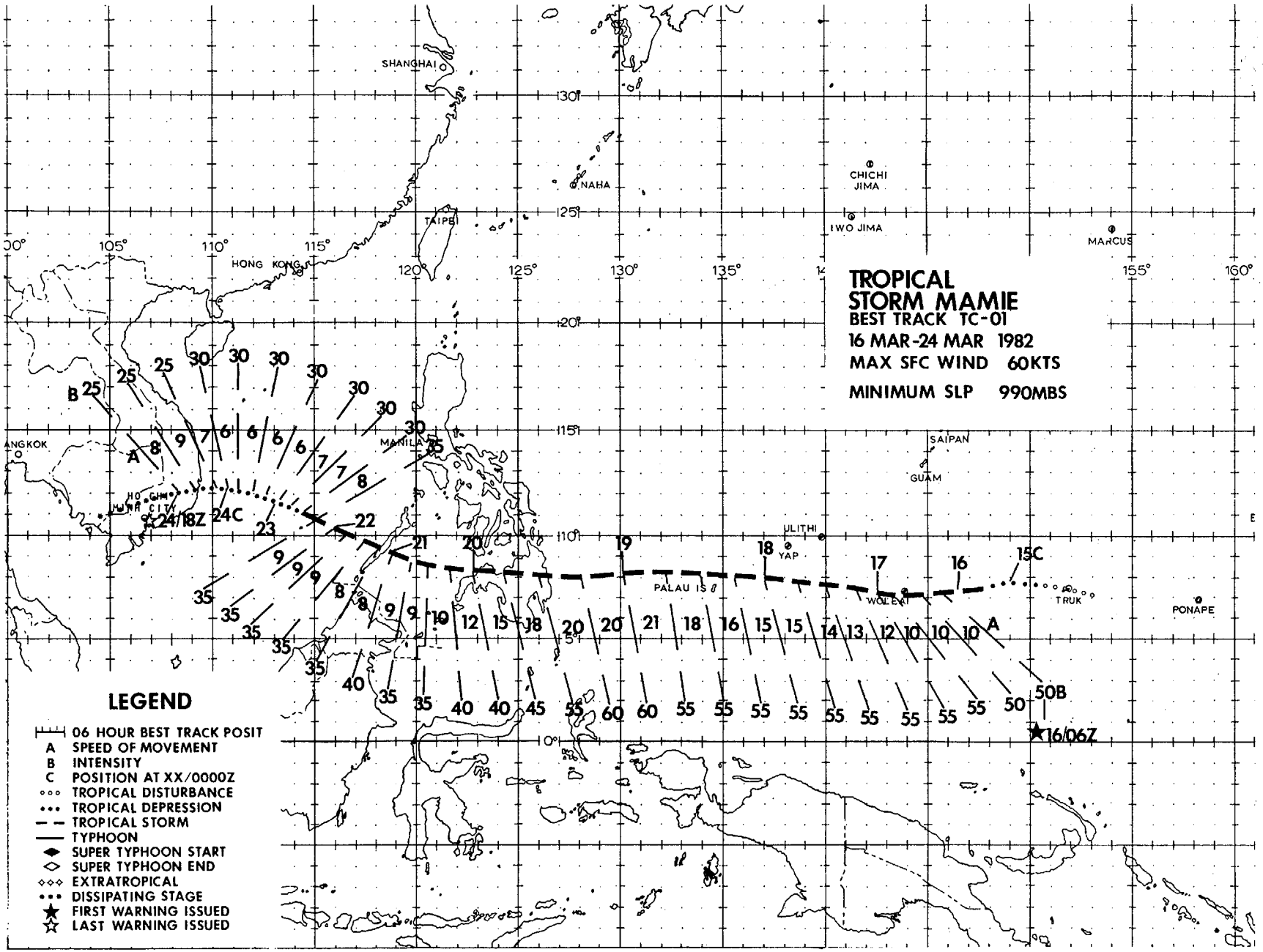
TROPICAL
STORM MAMIE
BEST TRACK TC-01
16 MAR-24 MAR 1982
MAX SFC WIND 60KTS
MINIMUM SLP 990MBS
LEGEND
06 HOUR BEST TRACK POSIT
A SPEED OF MOVEMENT
B INTENSITY
C POSITION AT XX/0000Z
TROPICAL DISTURBANCE
TROPICAL DEPRESSION
TROPICAL STORM
TYPHOON
SUPER TYPHOON START
SUPER TYPHOON END
EXTRATROPICAL
DISSIPATING STAGE
FIRST WARNING ISSUED
LAST WARNING ISSUED
SHANGHAI
NAHA
TAIPEI
HONG KONG
MANILA
BANGKOK
HO CHI MINH CITY
CHICHI JIMA
IWO JIMA
MARCUS
SAIPAN
GUAM
ULITHI
YAP
PALAU IS
WOLEAI
TRUK
PONAPE
24/18Z
16/06Z

Tropical Storm Mamie, the first tropical cyclone of the season, developed from an area of active convection which was first sighted on 7 March, near 150E and just south of the equator (Figure 3-01-1). During the next five days, this convective area was observed migrating northward as the near-equatorial trough set up south of 05N. By 12 March, the convective organization was sufficient to warrant discussion in the Significant Tropical Weather Advisory (ABEH PGTW). On 14 March, the first satellite fix located the developing disturbance approximately 104 nm (193 km) east-southeast of Truk Atoll (WMO 91344). As the disturbance tracked westward and was followed on satellite imagery, the available synoptic data indicated a relatively weak wind field with surface pressures near normal (1010 mb). However, because satellite imagery showed continued convective organization, a reconnaissance aircraft was sent on an investigative mission which proved to be very enlightening. Upon receipt of observed winds of 50 kt (26 m/sec) and evidence of a closed circulation from the reconnaissance data, the first warning on Tropical Storm Mamie was issued immediately (160600Z). Mamie's intensities up to that point can only be extrapolated backwards; however, further intensification was very slow with the maximum intensity of 60 kt (31 m/sec) reached shortly before making landfall on Mindanao on 19 March.

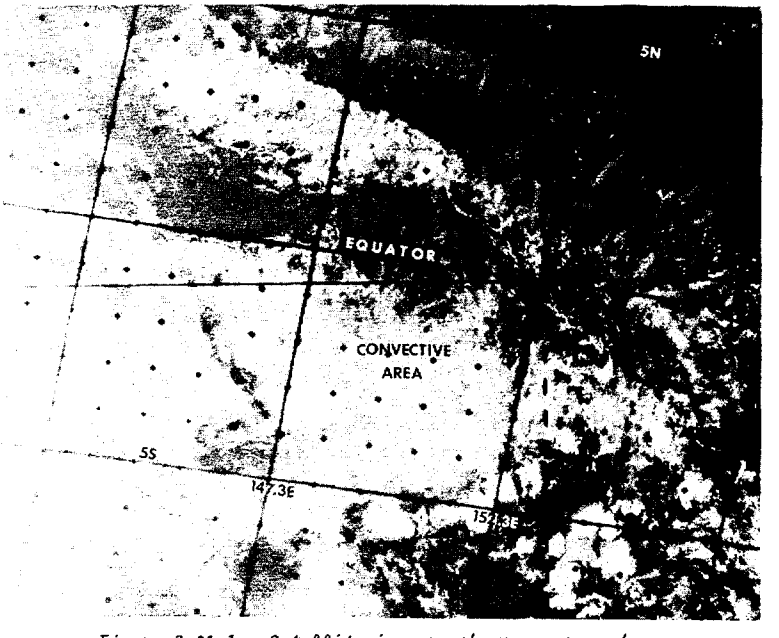

Figure 3-01-1. Satellite imagery shows an area of convection south of the equator which migrated northward and eventually became associated with the development of Tropical Storm Mamie, 070430Z March (NOAA 7 visual imagery).

From the first satellite fix to landfall on Mindanao, Mamie tracked westward along the southern periphery of a strong subtropical ridge (Figure 3-01-2). During this period, had it not been for satellite surveillance, Mamie may well have gone undetected until initial casualty reports were received from Mindanao (approximately 40 persons dead and extensive property and crop damage). Aside from winds received from the reconnaissance aircraft missions, no other surface observations were received which indicated a well-organized circulation. Even upon landfall, Mamie was not detectable from the observations of local reporting stations. Fortunately, given Mamie's track and compact circulation (less than 90 nm (167 km)), both satellite and aircraft reconnaissance platforms were available and Mamie was tracked and monitored despite the paucity of reporting stations and ships in the Philippine Sea.

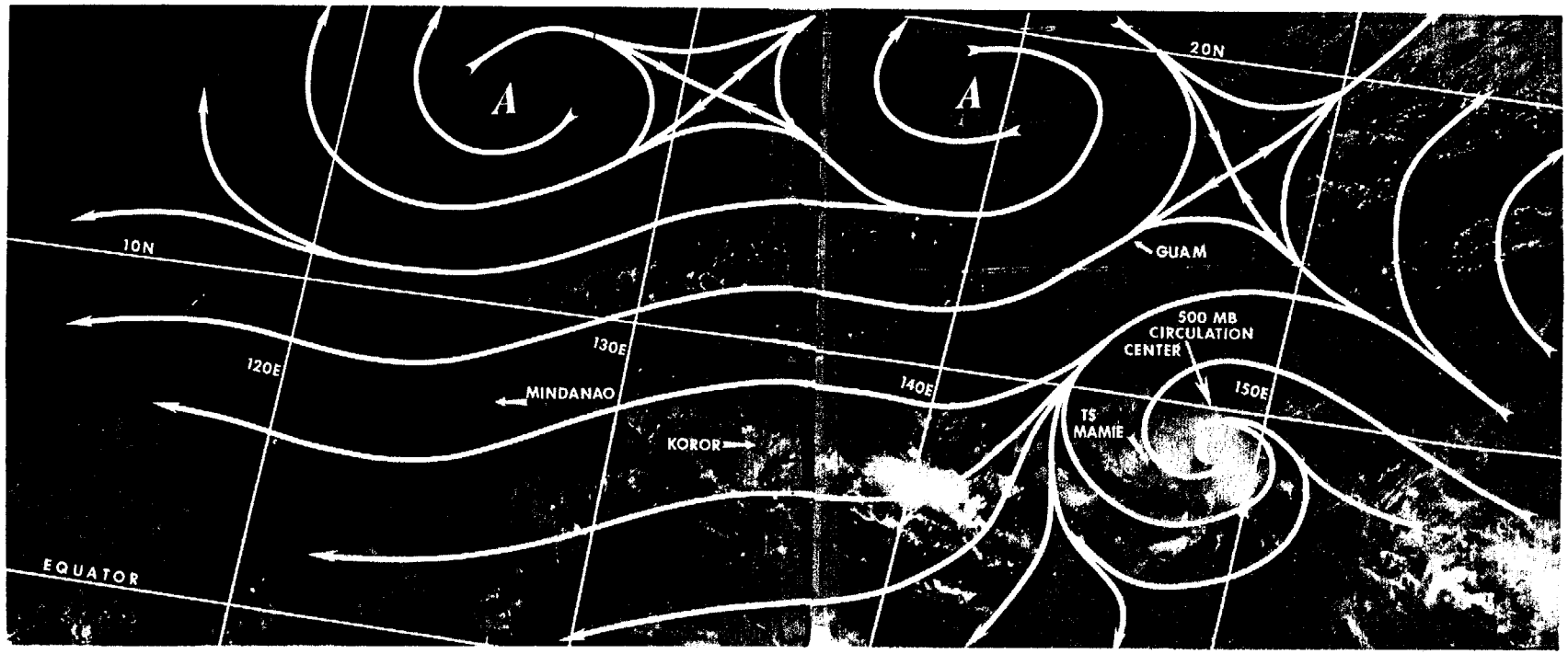

Figure 3-02-1. 500 mb streamline analysis for 150000Z March superimposed on a mosaic from visual satellite imagery. This figure depicts the steering influence of a strong subtropical ridge north of Tropical Storm Mamie. (150436Z and 150618Z March, NOAA 7 visual imagery).

On the second, and on subsequent reconnaissance aircraft missions, the Aerial Reconnaissance Weather Officers (ARWOs) observed an eyewall which was restricted to the lower levels. (Maximum observed height of the eyewall was near 10,000 ft (3048 m)). Due to Mamie's compactness and increasing vertical wind shear in the mid- and upper-tropospheric levels, the eyewall did not fully develop and extend to heights that could be observed on satellite imagery. This failure to develop in the vertical contributed to Mamie not reaching typhoon strength.

After tracking across the northern portion of Mindanao, Mamie entered the Sulu Sea with winds of 40 kt (21 m/sec) and was unable to reintensify despite surface conditions which were generally favorable for reintensification. On 21 March, as Mamie reached the South China Sea, a weakness in the subtropical ridge allowed a more northwestward track which was maintained until approximately 230000Z, when the ridge strengthened and Mamie resumed a westward movement. At 241200Z, Mamie made final landfall near Nha Trang, Vietnam and then dissipated in the mountainous region to the west.

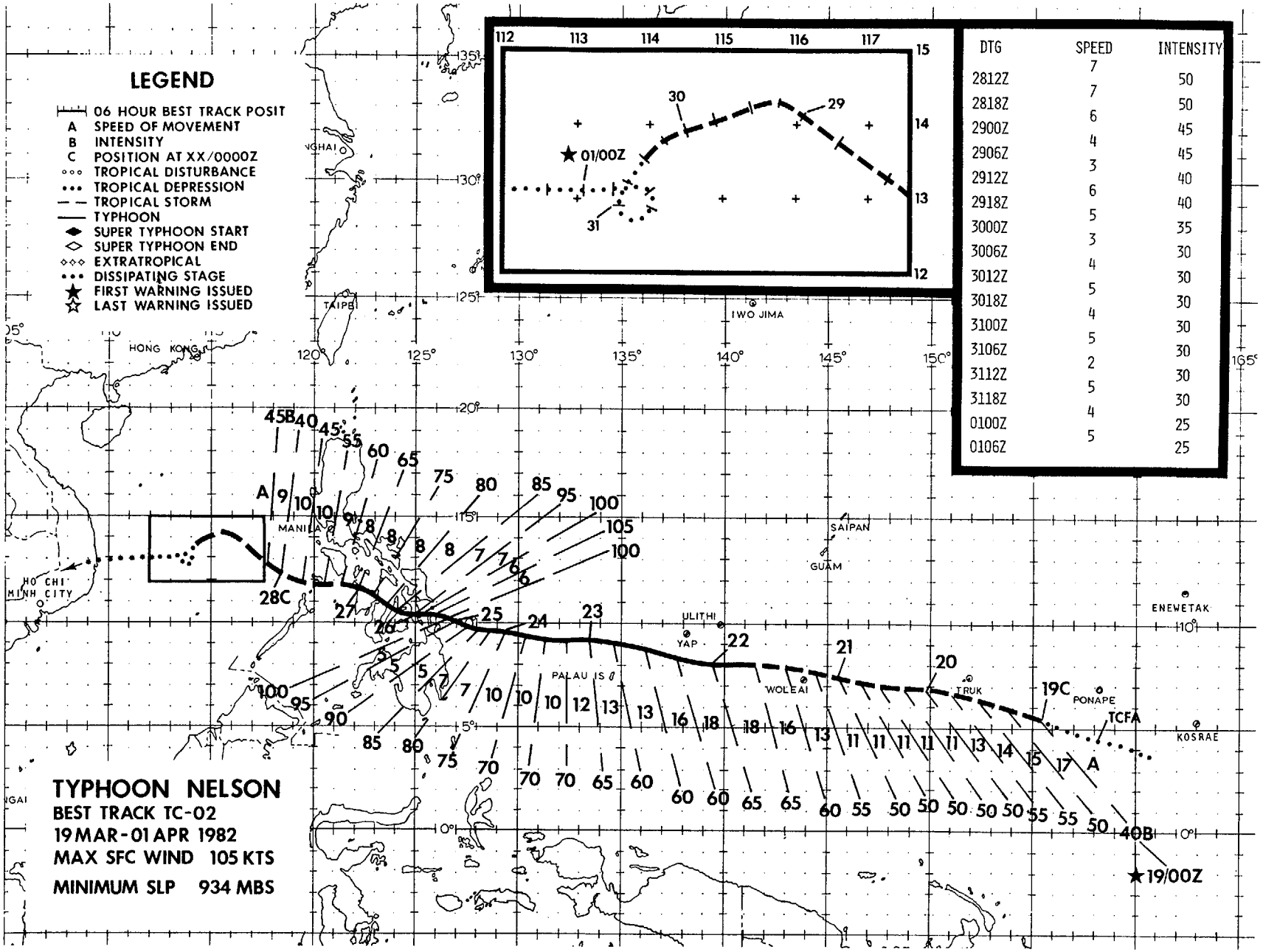

DTG	SPEED	INTENSITY
2812Z	7	50
2818Z	7	50
2900Z	6	45
2906Z	4	45
2912Z	3	40
2918Z	6	40
3000Z	5	35
3006Z	3	30
3012Z	4	30
3018Z	5	30
3100Z	4	30
3106Z	5	30
3112Z	2	30
3118Z	5	30
0100Z	4	25
0106Z	5	25

Typhoon Nelson was the second of three early season tropical cyclones in the western North Pacific which formed at very low latitudes southeast of Guam. Nelson, similar to Mamie (01), was a well-behaved tropical cyclone which developed and tracked westward, south of a strong mid-tropospheric ridge (centered near 15N 150E and extending west-northwest toward Taiwan).

In the initial stages of development, Nelson intensified rapidly from a weak tropical disturbance to a full-fledged tropical storm. In fact, the Tropical Cyclone Formation Alert, which was issued just 10 hours before the first warning, was preceded and followed by satellite fixes (180900Z and 181800Z) which described very little convective organization. However, at 190615Z, a reconnaissance aircraft reported flight level (1500 ft (457 m)) winds of 66 kt (34 m/sec), surface winds of 50 kt (26 m/sec), and an extrapolated sea level pressure of 993 mb.

Nelson's rapid development was in response to a very strong divergence field in the upper-troposphere located over the cyclone, where a 40 to 60 kt (21 to 31 m/sec) easterly jet branched to the northwest and southwest. However, while these strong easterlies remained near Nelson, further development was limited to minimal typhoon strength. During this entire period, Nelson moved rapidly westward at speeds reaching 18 kt (33 km/hr) on 22 April, after which a gradual slowing in forward speeds and further intensification followed. After maintaining intensities between 60 and 70 kt (31 to 36 m/sec) for 60 hours, a change in the upper air patterns allowed Nelson to deepen rapidly, reaching 100 kt (51 m/sec) within 24 hours.

At 231200Z, while Nelson was moving away from the westernmost extent of the upper-tropospheric ridge (Figure 3-02-1), nearby westerlies aloft provided a strong outflow channel to the north and northeast.

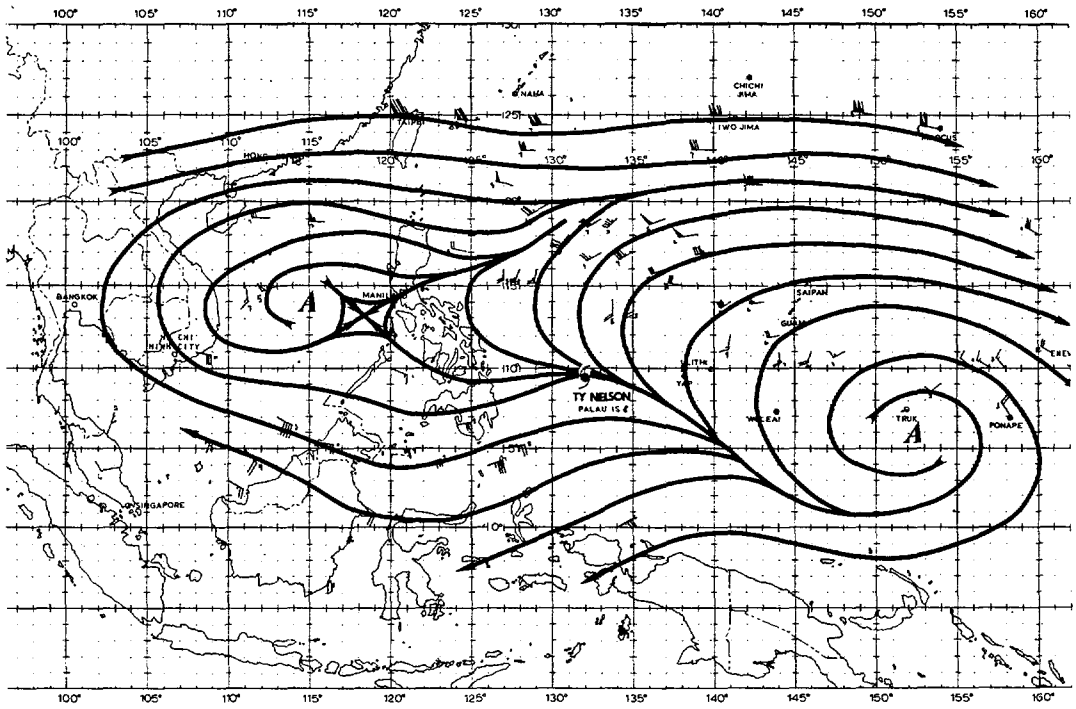

Figure 3-02-1. 200 mb analysis at 231200Z March. Note Typhoon Nelson's position just west of the westernmost portion of the ridge and the presence of a westerly current seven degrees north which will provide a good outflow channel.

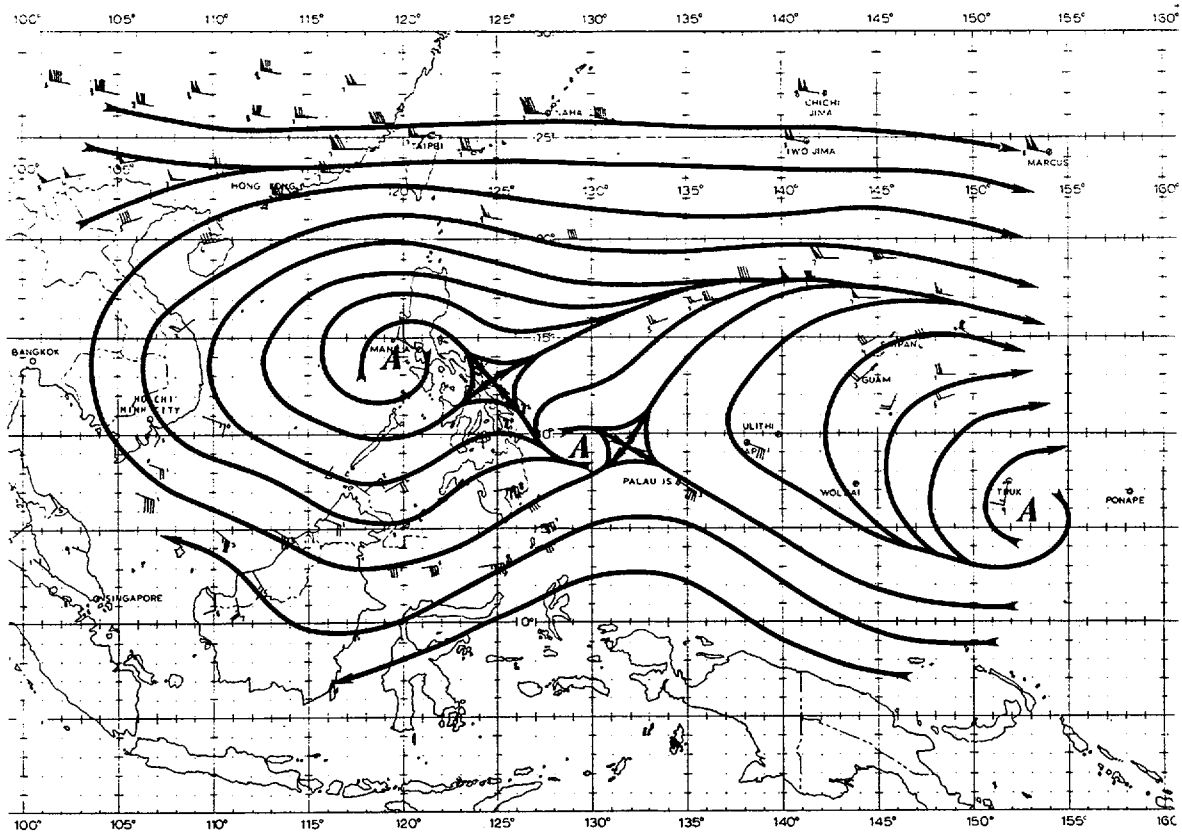

Figure 3-02-2. 200 mb analysis at 240000Z March. Within 12 hours an appreciable change in the upper-tropospheric levels has allowed the formation of an anticyclone aloft and the beginning of the good outflow channel into the westerlies.

As this occurred, an upper-level anticyclone was established (Figure 3-02-2) and intensified over Nelson; concurrently, Nelson responded and reached a maximum intensity of 105 kt (54 m/sec) at 251200Z (Figure 3-02-3).

On 27 March, a much weakened Tropical Storm Nelson entered the South China Sea after navigating through the south-central Philippines. On 28 March, Nelson briefly reintensified before weakening under the influence of vertical wind shear. Until 291200Z, the presence of a 500 mb short wave trough north of Nelson provided a favorable opportunity for recurvature toward the northeast. However, Nelson was quickly sheared and the low-level center meandered westward and eventually dissipated four days later. The fifty-third and final warning was issued at 010000Z April for Tropical Depression 02 (Nelson), approximately 240 nm (444 km) east of Nha Trang, Vietnam, near to the location where Tropical Storm Mamie (01) had made landfall one week earlier.

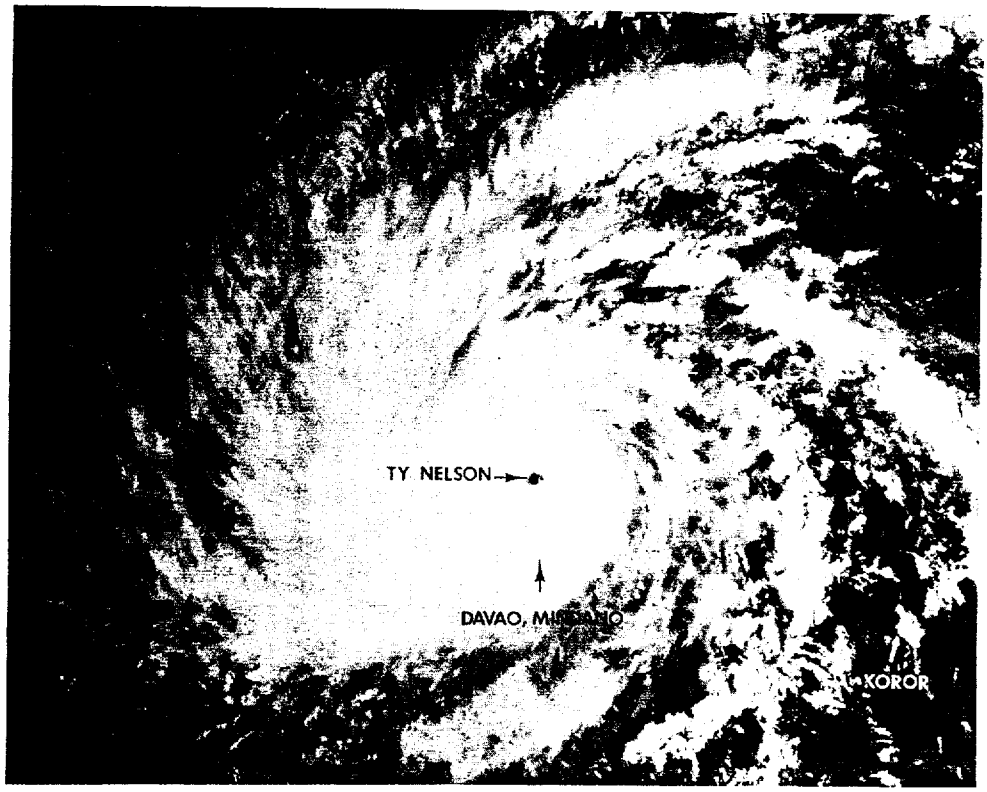

Figure 3-02-3. Typhoon Nelson near peak intensity, east of the Philippines. Note the anticyclonic flow aloft and the well-formed outflow channel to the north, 250601Z March. (NOAA 7 visual satellite imagery)

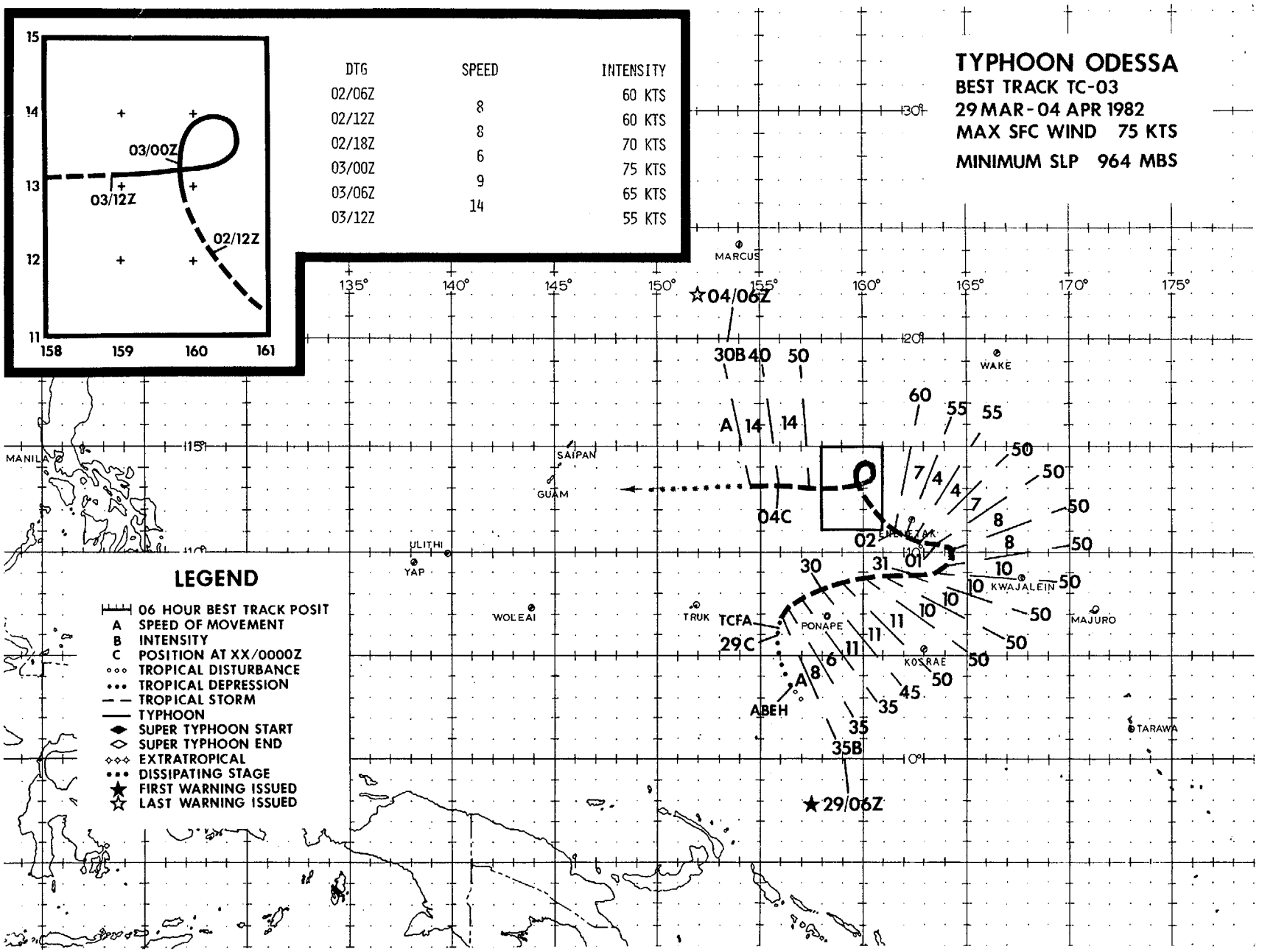
TYPHOON ODESSA
BEST TRACK TC-03
29 MAR - 04 APR 1982
MAX SFC WIND 75 KTS
MINIMUM SLP 964 MBS
DTG SPEED INTENSITY
02/06Z 60 KTS
02/12Z 8 60 KTS
02/18Z 8 70 KTS
03/00Z 6 75 KTS
03/06Z 9 65 KTS
03/12Z 14 55 KTS
03/00Z
03/12Z
02/12Z
LEGEND
06 HOUR BEST TRACK POSIT
A SPEED OF MOVEMENT
B INTENSITY
C POSITION AT XX/0000Z
TROPICAL DISTURBANCE
TROPICAL DEPRESSION
TROPICAL STORM
TYPHOON
SUPER TYPHOON START
SUPER TYPHOON END
EXTRATROPICAL
DISSIPATING STAGE
FIRST WARNING ISSUED
LAST WARNING ISSUED
☆04/06Z
★29/06Z
TCFA
ABEH
MARCUS
WAKE
SAIPAN
GUAM
MANILA
ULITHI
YAP
WOLEAI
TRUK
PONAPE
KOSRAE
KWAJALEIN
MAJURO
TARAWA

March is normally a relatively quiet month in the tropical western North Pacific, producing on the average less than one tropical cyclone per year. March 1982 was quite the contrary, with the genesis of three tropical cyclones taking place within a period of 13 days; 1967 was the most recent year with more than one tropical cyclone during March. Typhoon Nelson (02) and the subject of this report, Typhoon Odessa represent only the fifth and sixth typhoons to occur in March since the JTWC was established in 1959.

Just as March was a unique month in the level of tropical cyclone activity, Odessa was unique among the three tropical cyclones. As illustrated in Figure 3-03-1, tropical cyclones which develop near 160E tend to follow one of two climatological tracks: 60 percent move in a generally westward direction and 40 percent move in a generally northward direction. Although both Tropical Storm Mamie (01) and Typhoon Nelson (02) moved westward from this genesis area, Odessa's track defied climatology as it moved both eastward and westward across the area shown for northward-moving tropical cyclones.

Typhoon Odessa was initially detected as an area of loosely organized convection near 2N 159E on 26 March. In the following three days, a cloud system center emerged from these low-latitudes and moved northwestward. A Tropical Cyclone Formation Alert was issued at 290400Z upon receipt of reconnaissance aircraft data which indicated that a closed circulation had developed. As subsequent aircraft data and satellite imagery became available, it was evident that the circulation had rapidly organized and thus, at 290741Z, the initial warning was issued for Odessa with maximum surface winds of 35 kt (18 m/sec)

Much of the remaining discussion will concentrate on the meteorological factors which influenced Odessa's atypical track. To facilitate this discussion, Odessa's best track has been divided into four segments (Figure 3-03-2) representing the different track directions of the tropical cyclone. Each of these segments can be explained quite well in post-analysis when large-scale changes in the mid-latitudes at distances 600 to 1200 nm (1111 km to 2222 km) from Odessa are considered.

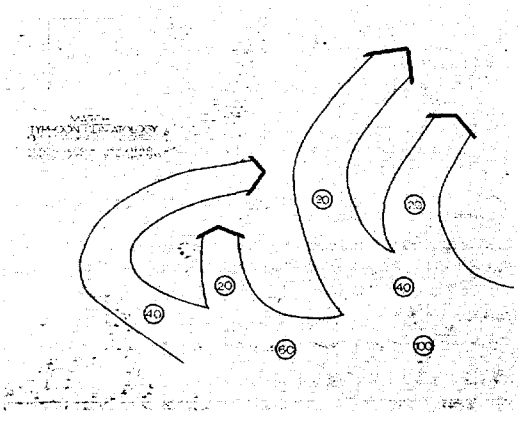

Figure 3-03-1. March Typhoon Climatology Tracks (JTWC Special Study 105-8 March 1970)

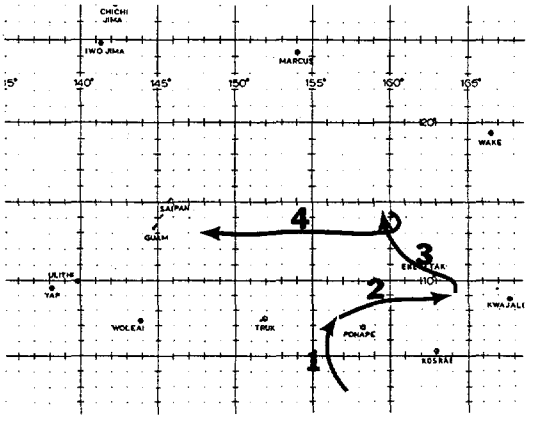

Figure 3-03-2. Typhoon Odessa's best track illustrating the four segments of Odessa's track as discussed in the text.

Odessa's initial movement to the northwest was in response to a weakening of the subtropical ridge northeast of Guam and the rapid cyclogenesis which was occurring southeast of Japan. The first three forecasts described a short-term northwestward movement followed by a more pronounced westward track. However, the continued deterioration of the subtropical ridge, north of Odessa, essentially removed any easterly steering current capable of driving Odessa westward. During the same period, a major high pressure system moved southeastward from Japan and strengthened the low-level northeasterly wind regime west of Odessa. Conventional surface data, at 300000Z, show this ridging extended deep into the tropics and created an effective block to any continued northwestward advance by Odessa (Figure 3-03-3). At mid-tropospheric levels, rawinsonde data from Truk (WMO 91334), Ponape (WMO 91348) and Kwajalein (WMO 91366) indicated that the base of a mid-latitude trough extended well into the tropics and south of Odessa. Although the axis of this trough was located well northeast of Odessa, between 160E and 165E (500 mb), its influence on Odessa's movement became obvious in the days that followed.

On 30 and 31 March, as Odessa tracked eastward at 10 to 11 kt (19 to 20 km/hr), the mid-latitude trough advanced more rapidly eastward and was located near 170E at 310000Z. Odessa, now 400 nm (741 km) west of the trough axis, began to slow and eventually turn toward the north. As Odessa approached 10N, it turned west-northwestward in response to a weak subtropical ridge filling in behind the mid-latitude trough

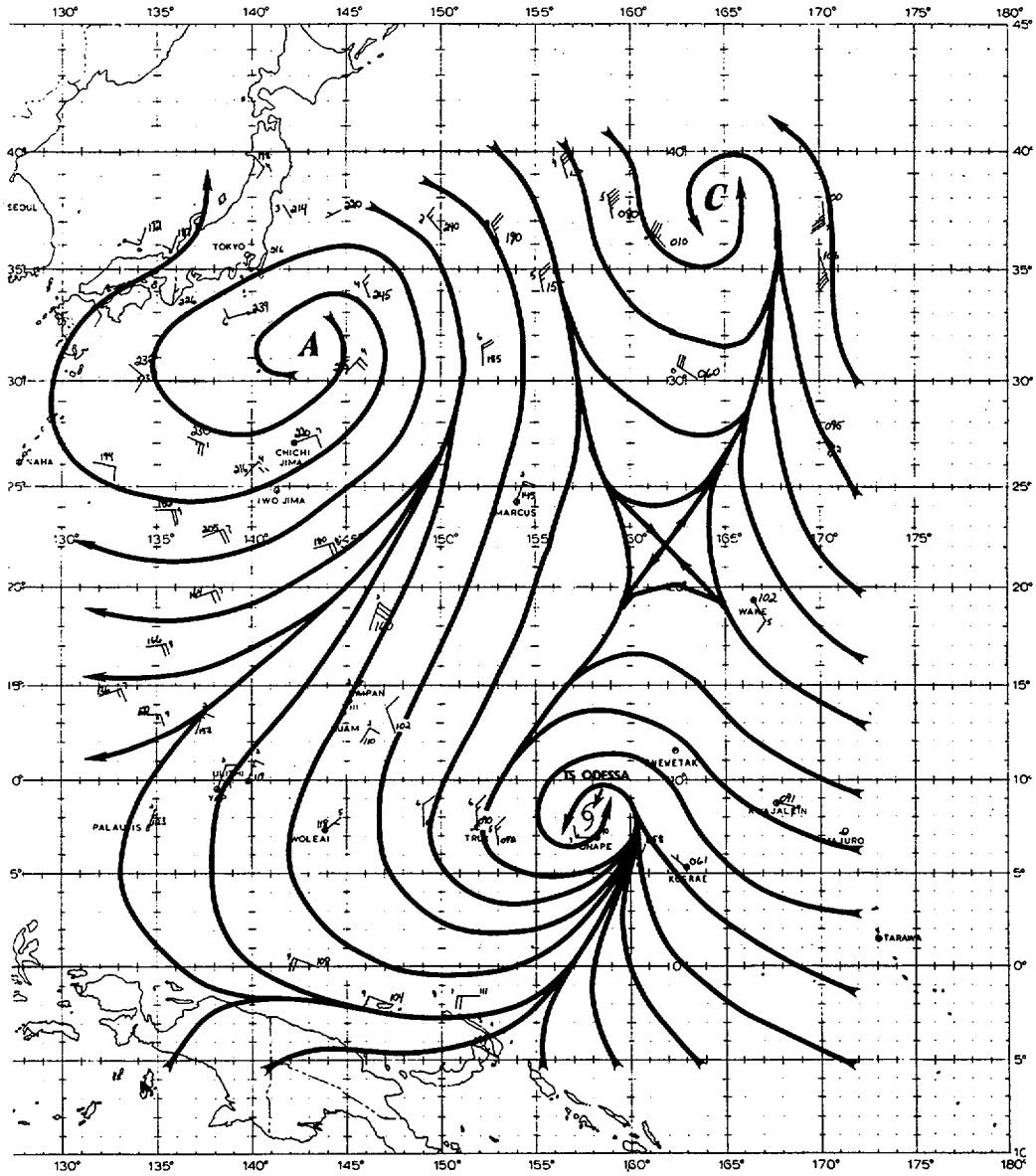

Figure 3-03-3. The 300000Z March 1982 surface/gradient level wind data and streamline analysis. Wind speeds are in knots.

(which had stalled near 175E). To this point, Odessa had maintained an intensity near 50 kt (26 m/sec) as westerlies restricted the development of the cyclone's circulation. With the subtropical ridge in place, Odessa was able to develop a closed circulation in the mid-tropospheric levels and a noticeable intensification trend began which culminated with a peak intensity of 75 kt (39 m/sec) at 030000Z (Figure 3-03-4 shows Odessa just prior to reaching typhoon strength).

Just as Odessa reached maximum intensity, the last major directional change commenced. On 3 April, Odessa was approaching a break in the subtropical ridge, along 158E. Forecasts described a track northward around the ridge axis and then northeastward toward Wake Island. However, strong mid- and upper-level southerly winds moved over Odessa and a rapid shearing of the major convective features to the northeast followed. At 030800Z, a reconnaissance aircraft located Odessa's low-level circulation center 90 nm (167 km) southwest of the closest convective activity. During the 24 hours that followed, Odessa weakened rapidly and was no longer detectable from satellite imagery after 040600Z.

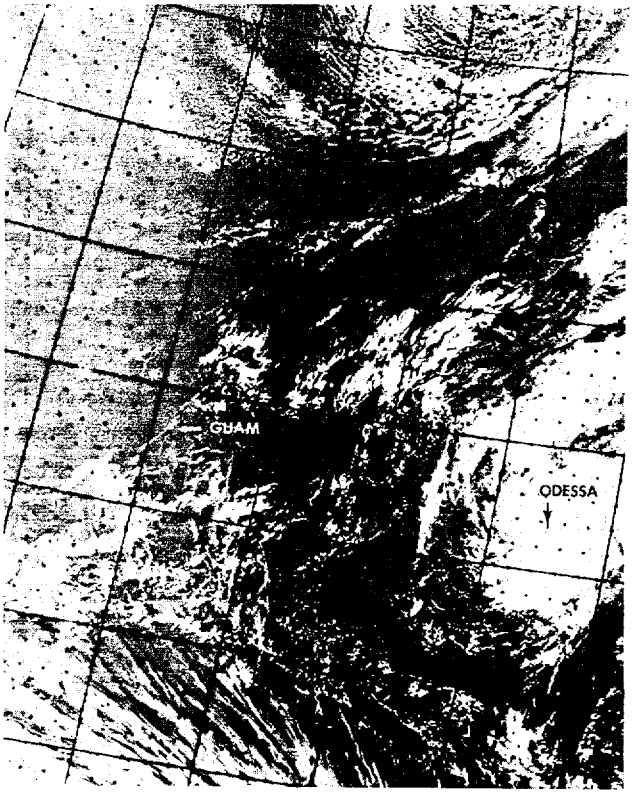

Figure 3-03-4. Tropical Storm Odessa, approximately 18 hours prior to reaching maximum intensity. At this time, Odessa was approximately 90 nm (167 km) west of Enewetak Atoll with maximum winds of 60 kt (31 m/sec). Note the cirrus streamers to the south, these originated from TC 17-82 (Bernie) in the Southern Hemisphere. Later, near 030000Z, Bernie's expansive development would increase the southerly winds moving toward Odessa and aid in the shearing process which led to Odessa's dissipation. 020425Z April (NOAA 7 visual imagery).

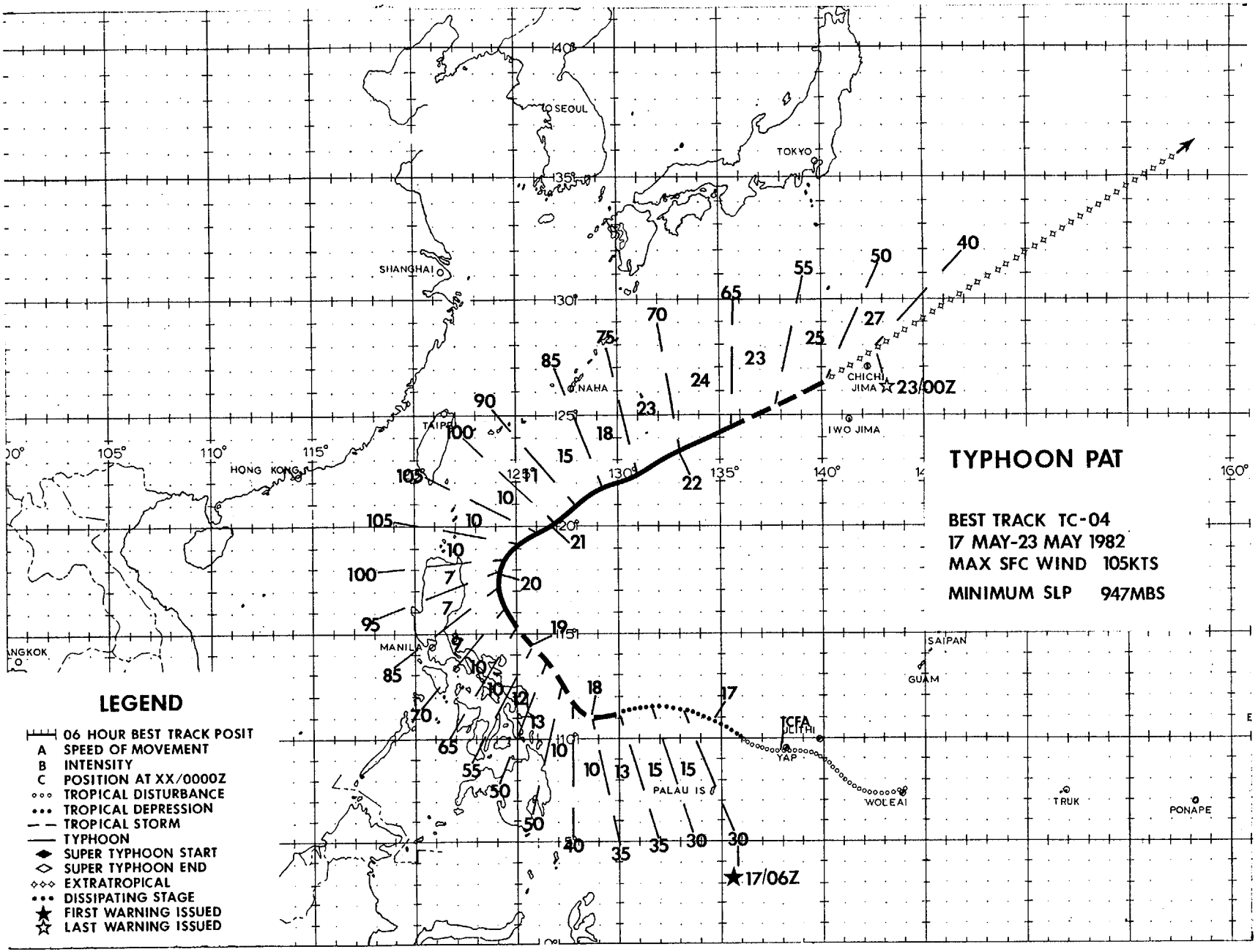
TYPHOON PAT
BEST TRACK TC-04
17 MAY-23 MAY 1982
MAX SFC WIND 105KTS
MINIMUM SLP 947MBS
LEGEND
06 HOUR BEST TRACK POSIT
A SPEED OF MOVEMENT
B INTENSITY
C POSITION AT XX/0000Z
TROPICAL DISTURBANCE
TROPICAL DEPRESSION
TROPICAL STORM
TYPHOON
SUPER TYPHOON START
SUPER TYPHOON END
EXTRATROPICAL
DISSIPATING STAGE
FIRST WARNING ISSUED
LAST WARNING ISSUED
SEOUL
TOKYO
SHANGHAI
NAHA
TAIPEI
HONG KONG
MANILA
IWO JIMA
CHICHI JIMA
23/00Z
SAIPAN
GUAM
TCFA
YAP
PALAU IS
WOLEAI
TRUK
PONAPE
17/06Z

The transition from the winter to the summer monsoon regime over the tropical western North Pacific can vary greatly from year to year. During this transition time (March through May), tropical cyclone activity can be very strong (six in 1980) or moderate (three in 1981). In May, 1982, there were several disturbances that developed in the near-equatorial trough and then dissipated without producing a significant tropical cyclone. During the third week of May, Typhoon Pat developed and became the only disturbance to reach warning status in the region between early April (Typhoon Odessa (03)) and late June (Typhoon Ruby (05)).

The disturbance that eventually produced Typhoon Pat was first detected as a mid-level circulation southwest of Guam. The 140000Z May 500 mb streamline analysis depicted a cyclonic circulation center near 8N 143E. Coincident with the analysis, satellite imagery indicated an area of centralized convection associated with the circulation. A Tropical Cyclone Formation Alert (TCFA) was issued at 140305Z when evidence of a strong upper-level circulation center was noticed on satellite imagery. Aircraft reconnaissance at 140600Z reported no evidence of a surface circulation but did observe an area of strong low-level convergence near the convective disturbance.

It wasn't until the disturbance began moving out of the near-equatorial trough that a low-level circulation could be located by reconnaissance aircraft. On 17 May, another aircraft investigation located a closed circulation at 1500 ft (472 m) but surface winds were too light to determine a surface circulation center. The first warning on Pat, as Tropical Depression 04, was issued at 170600Z when sustained increased convective organization was observed on satellite imagery.

The forecast movement for the first six warnings projected Pat to move westward with passage over the Philippines, south of Luzon. This scenario was based on the existence of a mid-level (500 mb) ridge centered over the western portion of the South China Sea which was forecast to build eastward thus blocking northward movement of Typhoon Pat. During the ensuing 24-hour period, little change was evident in the mid-level ridge north and northwest of Pat (Figure 3-04-1). The

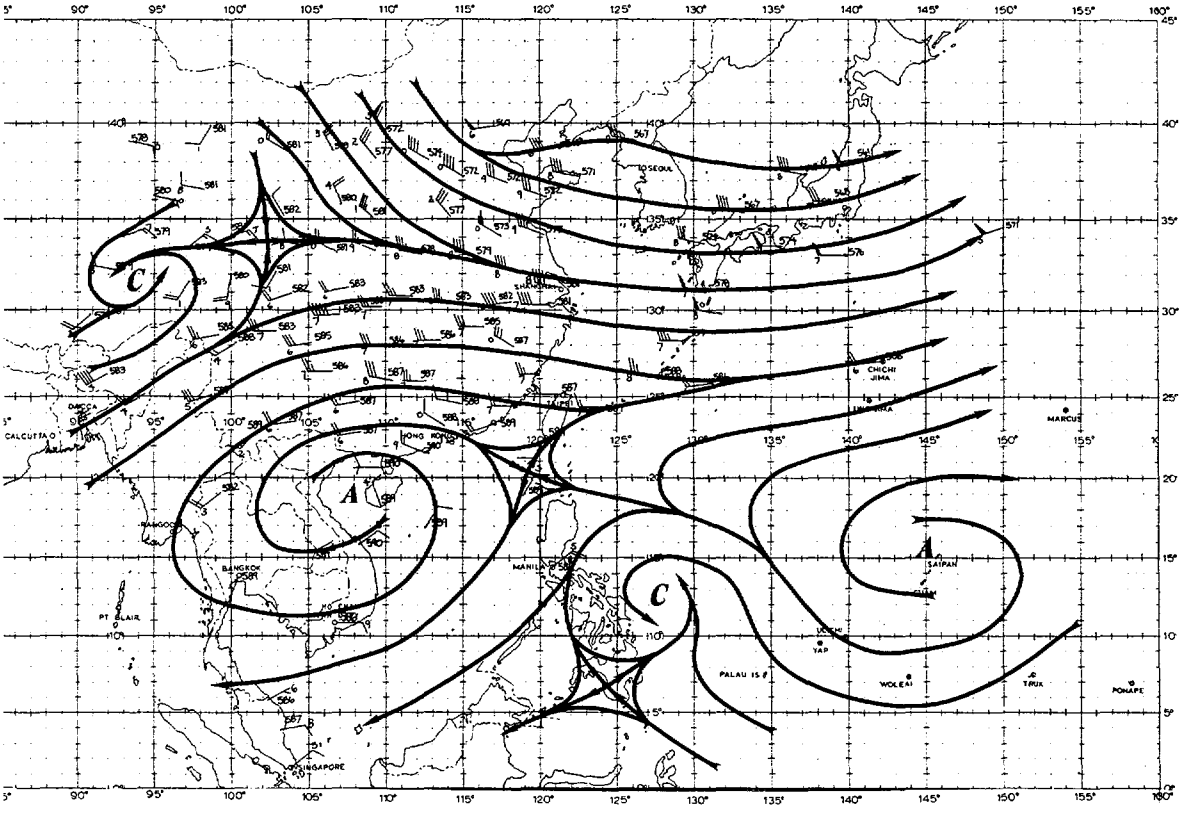

Figure 3-04-1. 500 mb streamline analysis at 181200Z May which shows Pat just south of an apparent weakness in the subtropical ridge. There had been no appreciable height-fall changes over a 24-hour period when Pat suddenly changed from a westward-moving to northward-moving tropical cyclone.

expected building of the ridge had not materialized; yet until 18 May, Pat persisted on its westward track. Then abruptly at 180600Z, Pat turned northward and paralleled the eastern portion of the Philippines for two days. Aircraft reconnaissance data at 180940Z provided the first indication of a possible track change, which was later confirmed by satellite fixes from Detachment 1, 1WW, Nimitz Hill, Guam and radar fixes from Cataduanes Island (WMO 98447). At 190000Z, upon evaluation of the fix data and a reevaluation of the westward track forecast scenario, JTWC changed the forecast track northward and toward eventual recurvature. From that point forward, Pat presented no further track forecasting problems.

Shortly after turning northward, Pat began to rapidly intensify, aided by a 200 mb wind maximum that had moved north of Pat and had enhanced outflow channels to the northeast. At 211200Z, Typhoon Pat reached its maximum intensity of 105 kt (54 m/sec) (Figure 3-04-2). This rapid intensification was not fully anticipated as Pat was forecast to only attain minimal typhoon strength. When aircraft reconnaissance data at 192233Z reported 95 kt (49 m/sec) surface winds, this new information was factored into the next forecast which then called for Pat to attain maximum intensity within the ensuing 12 to 18 hours. Fortunately, Pat's increased intensity did not bring any destructive winds to the Philippines, previously hit by Tropical Storm Mamie (01) and Typhoon Nelson (02), despite approaches as close as 90 nm (167 km) to Cataduanes Island and eastern Luzon.

As Typhoon Pat approached 20N, a track toward the northeast became increasingly favorable. In recurvature, Pat began to accelerate in response to increasing mid- and upper-level westerly steering currents. A new method for forecasting the acceleration of northward-moving tropical cyclones, developed by JTWC personnel during the past year, was used to predict the point of initial acceleration as well as the rate of acceleration; Typhoon Acceleration Prediction Technique (TAPT) (Weir, 1982), utilizes 200 mb analysis data to determine possible future acceleration. First used on the 191200Z analysis data, TAPT accurately predicted acceleration to begin near 19N and gave excellent guidance on the speed of movement to 24N, where Pat slowed its forward speed and weakened from the effects of vertical wind shear on the system's organization.

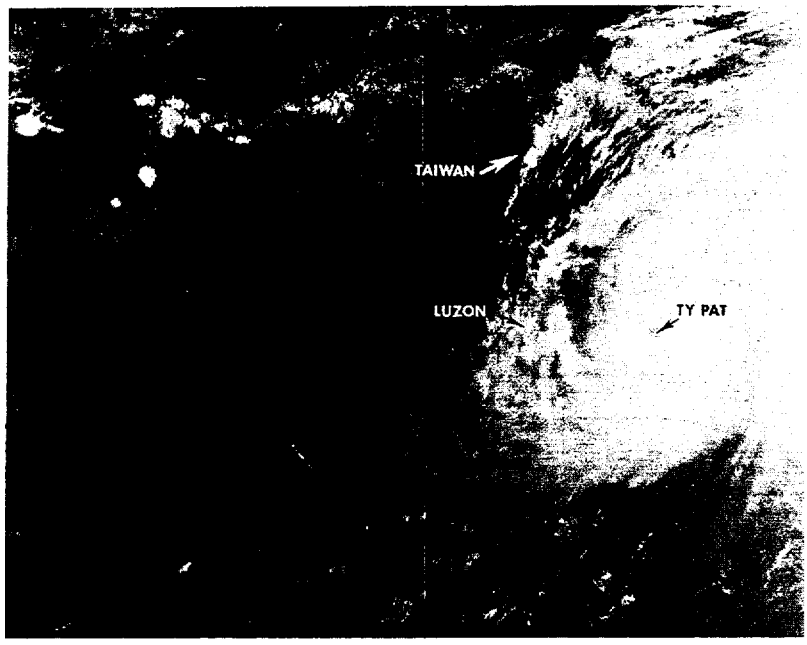

Figure 3-04-2. Typhoon Pat near maximum intensity of 105 kt (54 m/sec), 150 nm (278 km) east of Luzon, 200641Z May (NOAA 7 visual imagery).

On 22 May, as Typhoon Pat approached 24N, a weak frontal system (associated with an extratropical low east of Japan) was moving toward Pat and the first indications of Pat's eventual transition to an extratropical low were observed. Since 211600Z, there had been a marked decrease in Pat's deep-layer convection; additionally, aircraft reconnaissance data at 220955Z indicated that the central sea level pressure had risen to 988 mb. Although observed winds were still near typhoon strength, the maximum winds were observed at distances much further from the center than in previous missions. These expanding wind radii are frequently associated with tropical cyclones undergoing extratropical transition as the cyclone's energy source changes from latent heat release to a more baroclinic process. By 221200Z, synoptic data gave evidence of the incursion of cool, dry air into Pat's center and satellite imagery showed the system merging into a weak frontal boundary. Transition to an extratropical low was completed by 230000Z and this low gradually dissipated during the subsequent 24 hours as it was drawn into a stronger extratropical system, east of Japan.

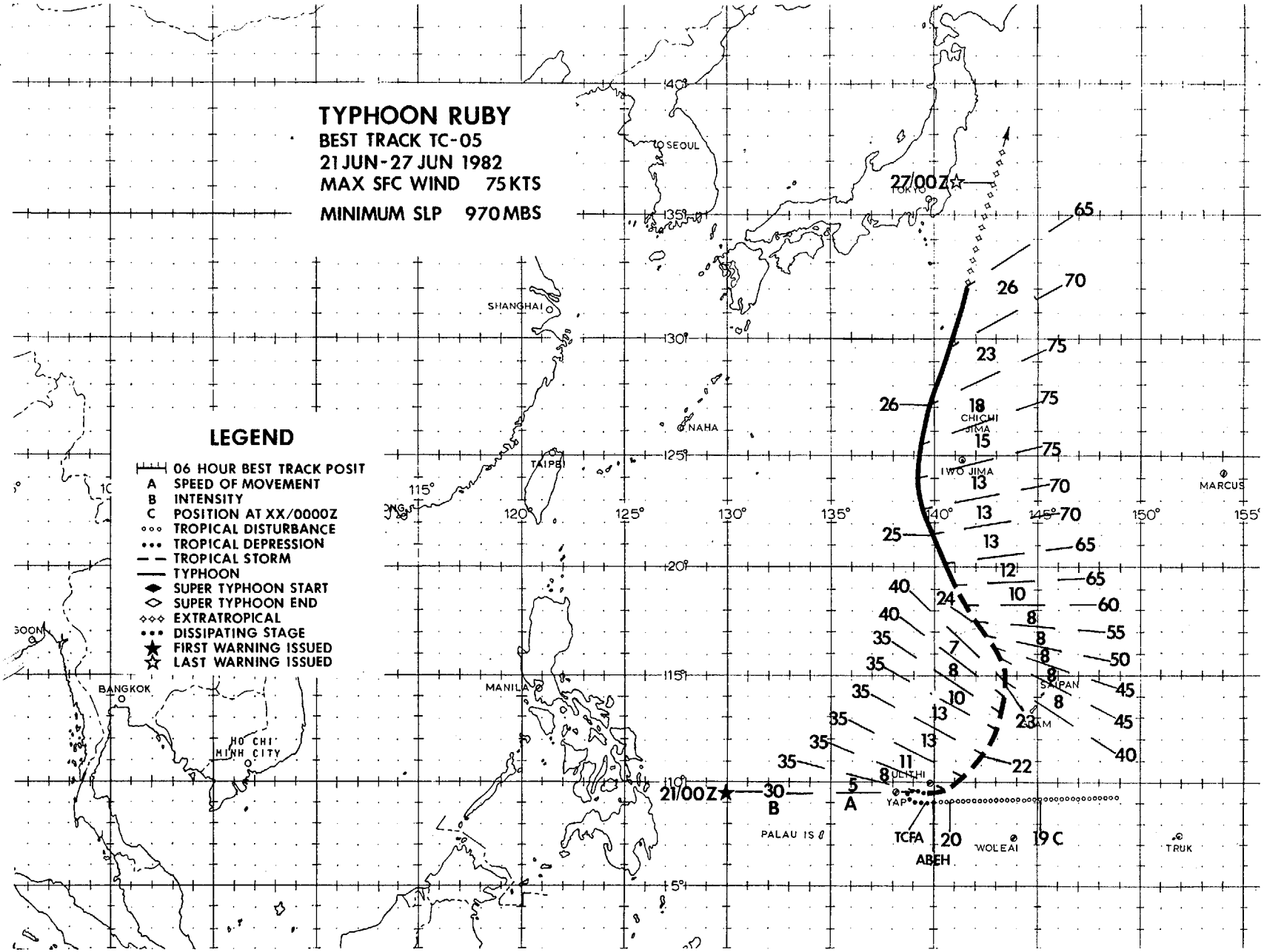
TYPHOON RUBY
BEST TRACK TC-05
21 JUN - 27 JUN 1982
MAX SFC WIND 75 KTS
MINIMUM SLP 970 MBS
LEGEND
06 HOUR BEST TRACK POSIT
A SPEED OF MOVEMENT
B INTENSITY
C POSITION AT XX/0000Z
TROPICAL DISTURBANCE
TROPICAL DEPRESSION
TROPICAL STORM
TYPHOON
SUPER TYPHOON START
SUPER TYPHOON END
EXTRATROPICAL
DISSIPATING STAGE
FIRST WARNING ISSUED
LAST WARNING ISSUED
TO SEOUL
TOKYO
SHANGHAI
NAHA
TAIPEI
BANGKOK
MANILA
HO CHI MINH CITY
IWO JIMA
CHICHI JIMA
MARCUS
SAIPAN
YAP
PALAU IS
WOLEAI
TRUK
ABEH
TCFA
27/00Z
21/00Z
115°
120°
125°
130°
135°
140°
145°
150°
155°
20°
15°
10°
5°

Typhoon Ruby developed from a convective disturbance which was initially detected southeast of Guam on 18 June. During the first ten days of Ruby's development, its track and eventual extratropical transition were dramatically affected by several events which can be traced to fairly rapid changes in the upper-troposphere. These events will be discussed individually as they occurred during Ruby's lifespan; however, collectively, they illustrate the need for a better understanding of the upper-troposphere and its effects on subsequent tropical cyclone development and movement.

Satellite imagery, on 18 June, located a weak convective disturbance 320 nm (593 km) southeast of Guam. During the next 24 hours, this disturbance was observed tracking westward to near 145E where it weakened significantly while an upper-level anticyclone, previously supporting the convection, receded to a position east of 150E. On 20 June, a cloud cluster developed near 9N 141E and continued moving westward, south of Ulithi Atoll (WMO 91203). A Tropical Cyclone Formation Alert was issued upon receipt of Ulithi's 200600Z surface observation which reported a six-hour pressure fall

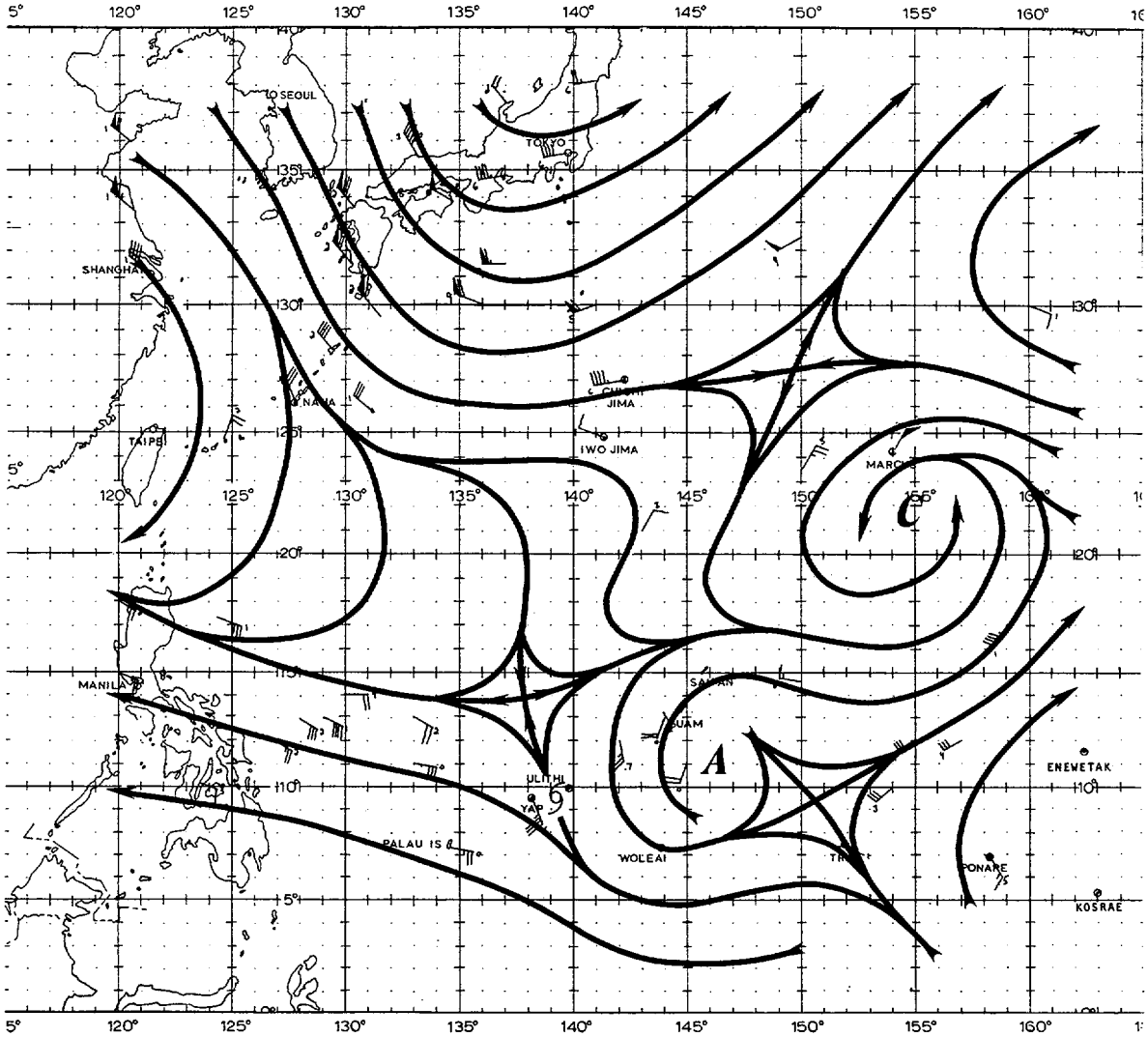

Figure 3-05-1. 210000Z June 1982, 200 mb streamline analysis. Ruby, positioned within a divergent southerly flow, was maintaining a central convective feature. To the north, a broad northerly flow was beginning to influence the near-storm environment. Wind speeds are in knots.

of 5 mb to 1004 mb, and a windshift from 030 degrees at 20 kt (10 m/sec) to 100 degrees at 25 kt (13 m/sec).

During the next 42 hours, satellite imagery and synoptic data indicated very little westward movement, with the system moving erratically between Yap and Ulithi. At 202339Z, the first aircraft reconnaissance mission into the system located a well-defined, very compact, 995 mb circulation center 45 nm (83 km) west-southwest of Ulithi. Based on these data, the first warning was issued for Tropical Storm Ruby at 210000Z with a forecast track toward the west-northwest. This forecast track was based on a very close agreement in most objective forecast aids. In fact, only the 700 mb and 850 mb steering aids, which indicated south-eastward low-level steering, did not support this initial forecast movement.

The apparent conflict between low-level and mid-level steering was seen as a reason for Ruby's erratic movement; but at that point, the long-term potential for a west-northwestward track looked good. At 210830Z, an aircraft fix located Ruby 35 nm (65 km) south of Ulithi; this fix was in good agreement with Ulithi's 210600Z observation. Unfortunately, the 210600Z observation would be the last received from Ulithi for 24 hours. During the next 18 hours, fix positions from infrared satellite imagery showed Ruby moving northward, then northwestward, passing over Ulithi. Without sufficient synoptic data to the contrary, the next few warnings followed these satellite positions and maintained the forecast track toward the west-northwest.

However, on this first day in warning status, the upper-level wind regime near Ruby was changing. As depicted in Figure 3-05-1,

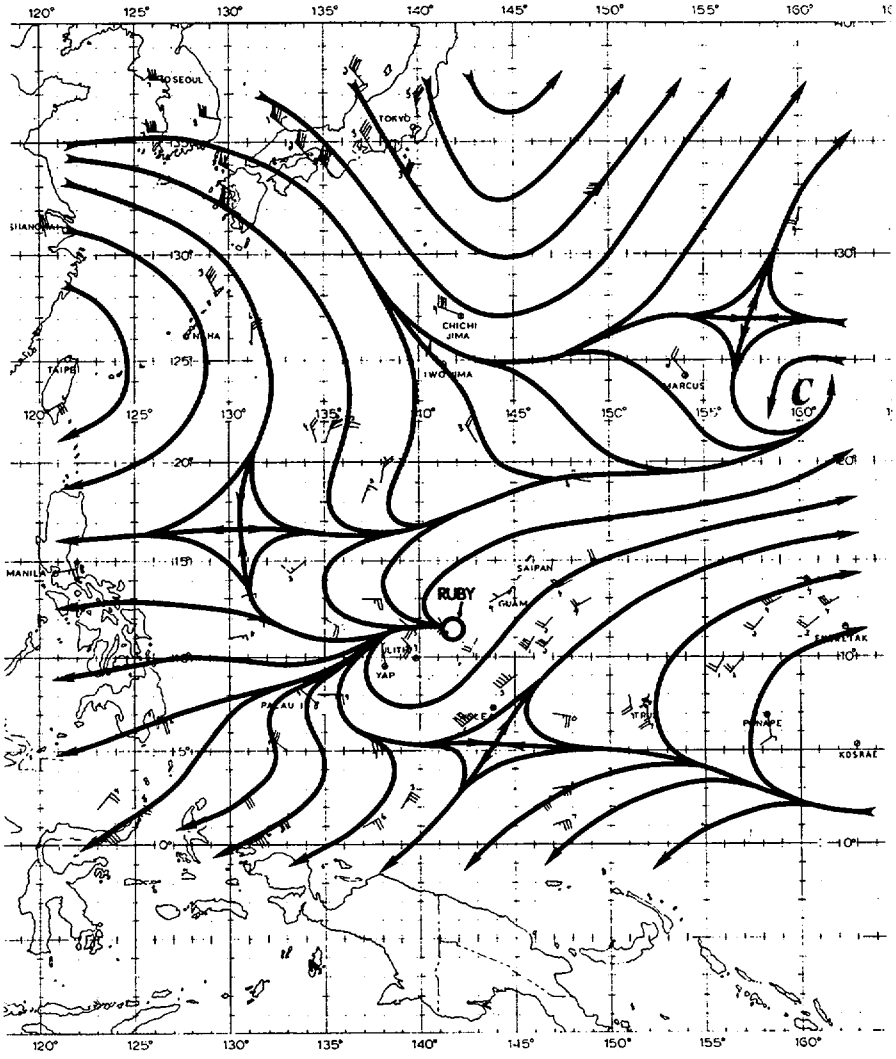

Figure 3-05-2. 220000Z June 1982, 200 mb streamline analysis. Considerable change has occurred in a 24-hour period. The northerly winds have penetrated to 10N, where the base of an upper-level trough formed. Coincident with this trough, a maximum cloud zone developed over the area south of Ruby's position and near-gale force winds were observed over a broad area at the surface and gradient levels near the upper-level trough/maximum cloud zone. Wind speeds are in knots.

the 200 mb winds at 210000Z were strongly divergent over Ruby but a broad mid-latitude trough, south of Japan, was introducing a significant northerly flow into the region. By 220000Z, the 200 mb winds (see Figure 3-05-2) had changed and an upper-level trough had set up south of 10N, and south of Ruby. While this process was underway, the objective forecast aids - especially the tropical cyclone models - were predicting a return to a westward track while analyses data were indicating a strengthening of the monsoon flow, located southeast and southwest of Ruby. When the first visual satellite imagery became available on 22 July, a low-level circulation center was seen embedded in a maximum cloud zone which had developed over the monsoon flow. This circulation, presumed to be Ruby, was located near 11N 142E, or more than 200 nm (370 km) from the 210000Z warning position. The 220000Z warning was immediately amended and a forecast track to the northeast, toward Guam, was issued. Interestingly, this amended warning had an exact 24-hour forecast position and only a 57 nm (106 km) error at 48-hours; but more importantly, a similar set of forecast errors could have been produced as early as 210600Z if the development of an upper-level trough and associated surge in the southwest monsoon could have been predicted from the 210000Z upper-wind flow analysis. This northeastward movement has become a familiar pattern in years past when developing tropical cyclones become involved with an intensifying southwest monsoon. For recent examples, refer to past ATCRs describing Tropical Depression 16/Typhoon Orchid (1980), Tropical Storm Thelma/Typhoon Vernon (1980), Tropical Depression 11/Tropical Storm Phyllis (1981), and Typhoon Gay (1981).

As Ruby moved northeastward toward Guam, its intensity remained near 35 kt (18 m/sec). During this period, much of Ruby's circulation pattern was involved with the monsoonal flow and the strongest winds were observed within the maximum cloud zone associated with this flow. Not until 23 June, when Ruby turned northward and became a separate entity from this maximum cloud zone, did its surface pressures fall and intensity increase.

Although the best track might suggest a rather steady increase in both Ruby's intensity and speed of movement from 23 through 25 June, these days were marked by often conflicting fix data. For example, the 240445Z visual satellite imagery (refer to Figure 3-05-3) indicated an exposed low-level circulation center near 19N 142E, while a

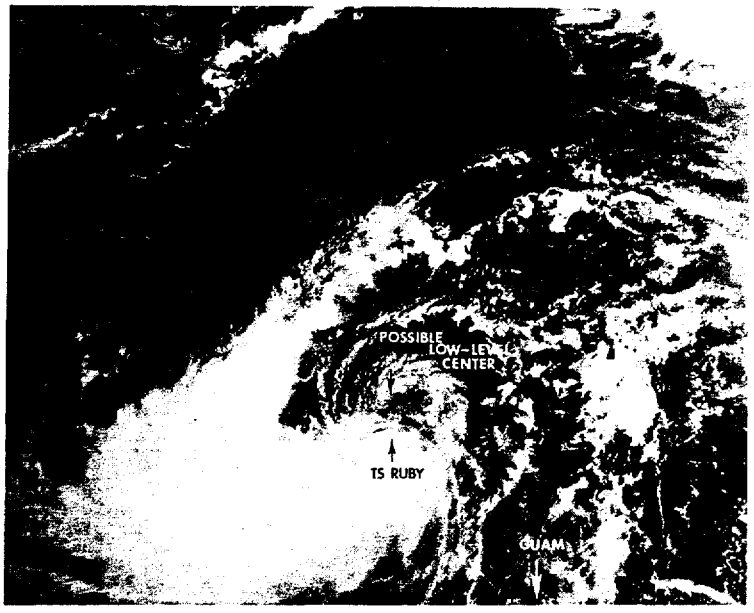

Figure 3-05-3. Visual satellite imagery suggested a low-level circulation center located in the northern periphery of the cloud system. This apparent low-level center was located well-north of a aircraft position received more than 3 hours later. 240445Z June 1982 (NOAA 7 visual satellite imagery).

reconnaissance aircraft surface/700 mb fix, at 240809Z, found a center nearly 60 nm (111 km) to the south. On 25 June, the 250630Z and 250911Z 700 mb aircraft fixes were positioned in a way to suggest either erratic movement or multiple circulation centers. These phenomena have been observed in other tropical cyclones which have emerged from an active monsoon flow. Typhoon Orchid (1980) had a sufficient amount of satellite, aircraft and radar fixes to suggest a high speed looping pattern over a 30-hour period. Ruby's intensity during this period was equally hard to determine. Intensity estimates derived from visual satellite imagery (Dvorak, 1973) and minimum sea level pressures (Atkinson and Holliday, 1977) were normally separated by 15 to 25 kt (8 to 13 m/sec), with the pressure consistently lower than expected during this period. In post-analysis, both the track and the intensity trend have been smoothed by a careful reevaluation of the data during this period.

As Ruby moved north-northwestward, the potential for recurvature, significant acceleration and extratropical transition became increasingly important. Based on a series of evaluations from the 240000Z, 241200Z and 250000Z 200 mb charts, 24N was consistently identified as the best latitude for initial acceleration into the mid-latitude westerlies (Typhoon Acceleration Prediction Technique (Weir, 1982)). A persistent and strong west-southwesterly 200 mb flow over Japan gave an indication for the potential of recurvature toward the northeast and, based on the mean latitudes of recent mid-latitude low pressure systems and ocean sea surface temperature fronts, 35N was deemed to be a favorable latitude for extratropical transition. Figure 3-05-4 depicts the 251200Z 200 mb flow with Typhoon Ruby near 24N. Within 18 hours, Ruby had assumed a north-northeastward track and accelerated to 23 kt (43 km/hr). The 260000Z 200 mb analysis (Figure 3-05-5)

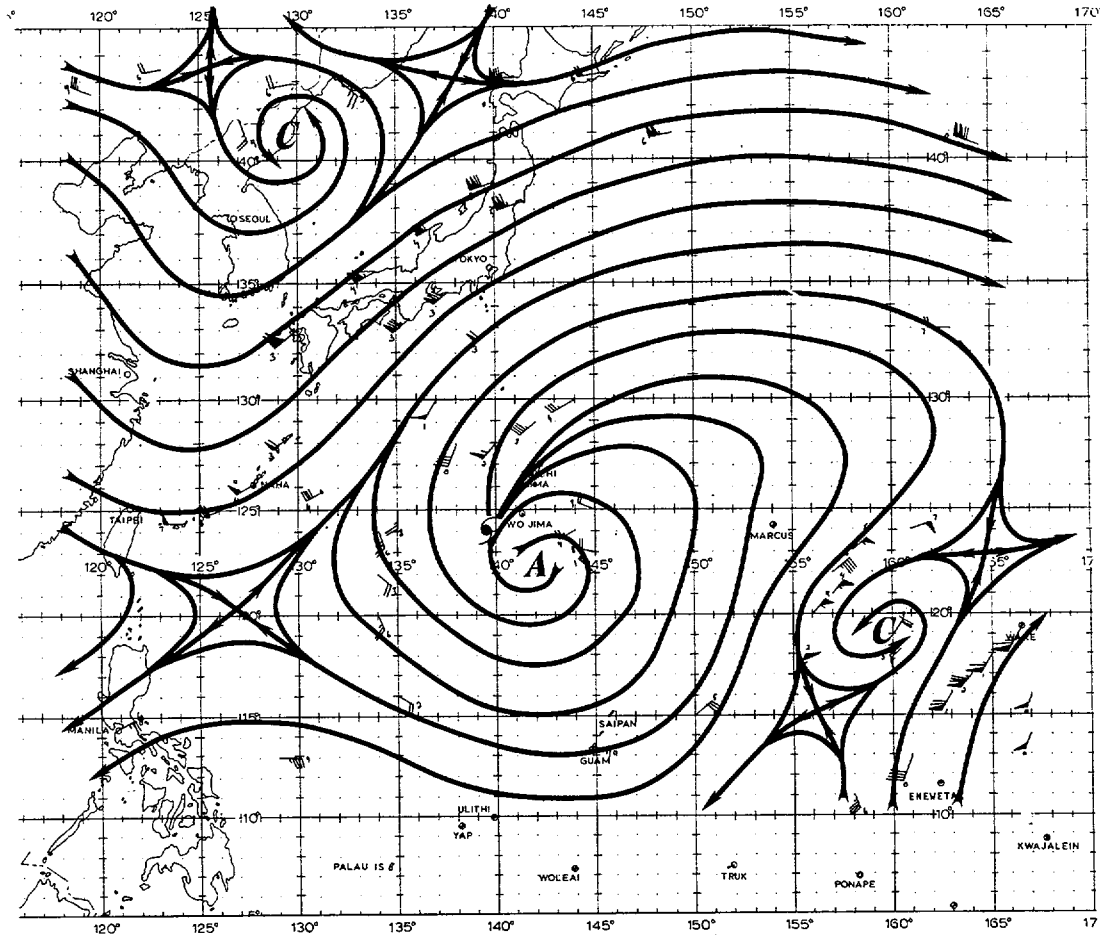

Figure 3-05-4. 251200Z June 1982, 200 mb streamline analysis. Typhoon Ruby was becoming involved with the upper-level mid-latitude westerlies. Wind speeds are in knots.

showed a dramatic change in the upper-wind pattern over Japan; 200 mb winds had become south-southeasterly and thus, signalled the potential for a more northward track. However, visual satellite fixes indicated a continuing tendency toward the northeast and the northeast forecast track was maintained. The 260602Z reconnaissance aircraft fix located Ruby's low-level circulation center 70 nm (130 km) west of the 260600Z warning position and these data, along with the 200 mb winds, dictated an amended warning toward the north-northeast and passing just east of northern Honshu.

A similar shift in the 200 mb flow also occurred with Typhoon Thad (August, 1981) and as Ruby approached the mid-latitude westerlies, the potential for such a shift was being closely monitored. Unlike Thad, Ruby quickly transitioned to an extratropical low and this movement and upper-wind shift may have been associated with that process more than any large-scale changes in the upper-troposphere.

The final tropical cyclone warning for Ruby was issued at 270000Z, after the 262149Z aircraft fix data indicated a cold core low was present at 700 mb. As an extratropical low, Ruby continued to move toward the north and rapidly occluded, becoming nearly stationary east of Hokkaido for several days thereafter.

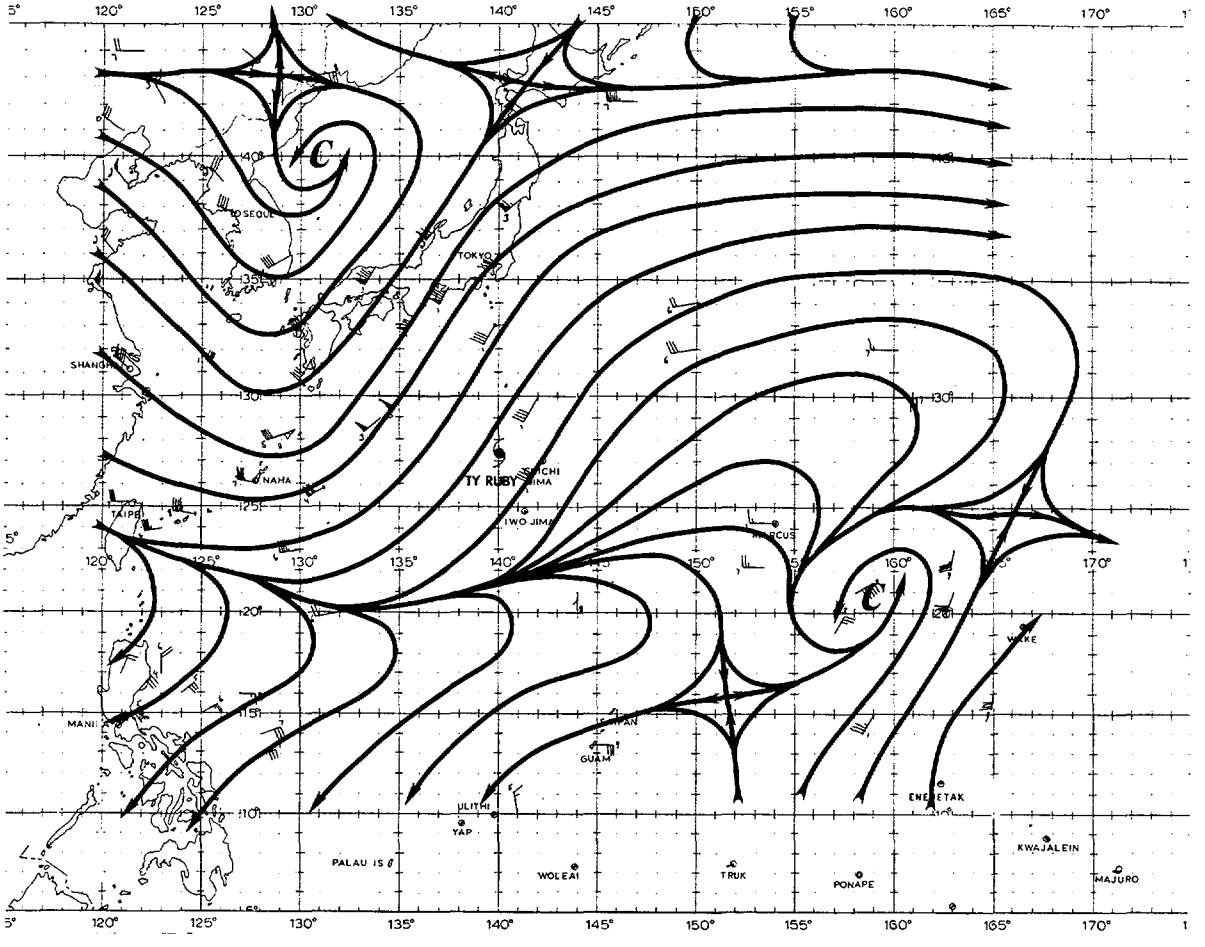

Figure 3-05-5. 260000Z June 1982, streamline analysis. Typhoon Ruby was well-embedded in the mid-latitude flow. Note the significant change in the 200 mb wind pattern over Japan in just 12 hours. This change, along with Ruby's rapid extratropical transition produced an extended north-northeastward movement and not the north-eastward track predicted earlier from the 200 mb flow depicted in Figure 3-05-4. Wind speeds are in knots.

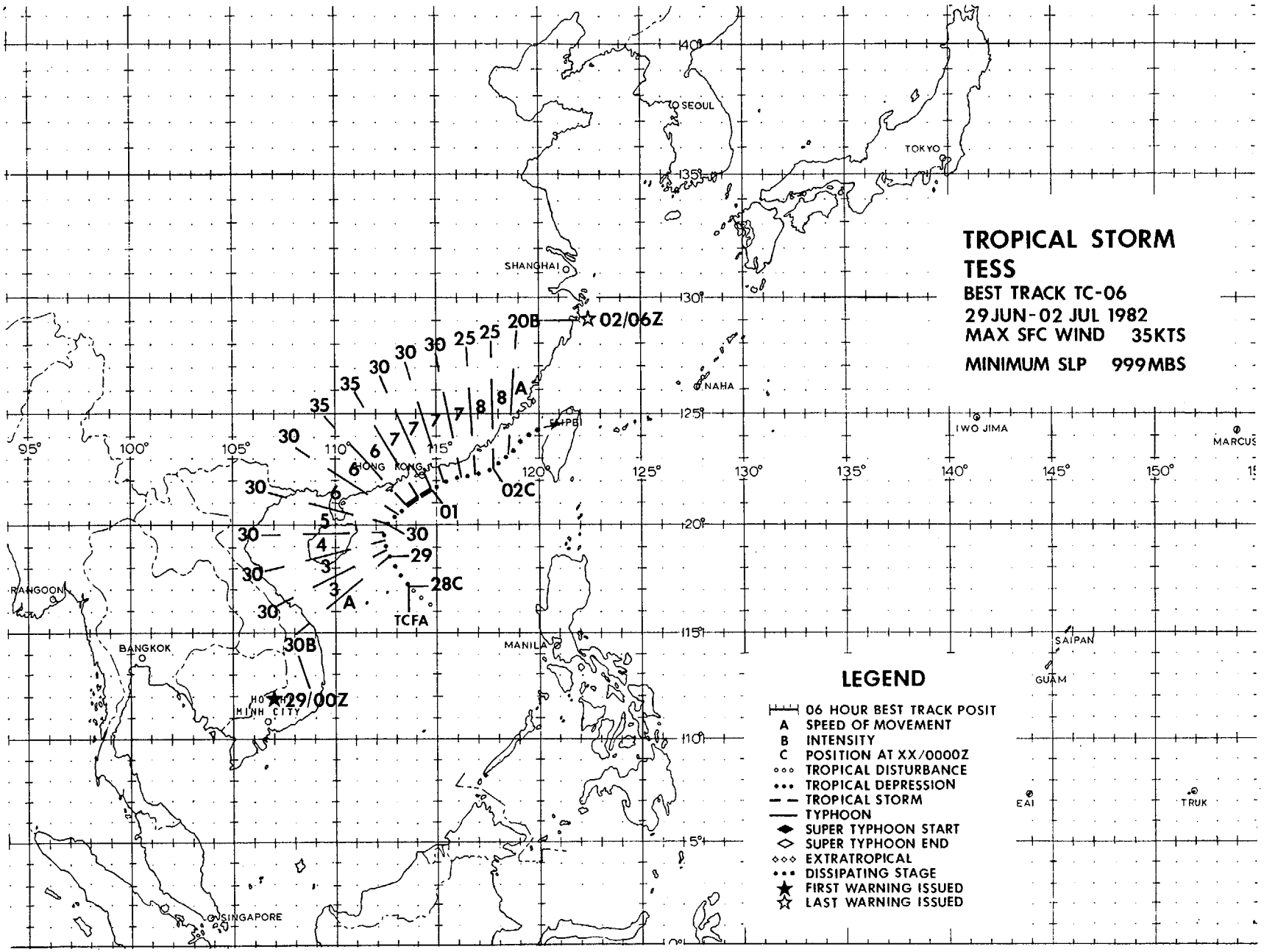
TROPICAL STORM
TESS
BEST TRACK TC-06
29JUN-02 JUL 1982
MAX SFC WIND 35KTS
MINIMUM SLP 999MBS
LEGEND
06 HOUR BEST TRACK POSIT
A SPEED OF MOVEMENT
B INTENSITY
C POSITION AT XX/0000Z
TROPICAL DISTURBANCE
TROPICAL DEPRESSION
TROPICAL STORM
TYPHOON
SUPER TYPHOON START
SUPER TYPHOON END
EXTRATROPICAL
DISSIPATING STAGE
FIRST WARNING ISSUED
LAST WARNING ISSUED
02/06Z
29/00Z
TCFA
SEOUL
TOKYO
SHANGHAI
NAHA
TAIPEI
HONG KONG
IWO JIMA
MARCUS
RANGOON
BANGKOK
MANILA
SAIPAN
GUAM
EAI
TRUK
SINGAPORE
HO CHI MINH CITY

The Tropical Storm Tess had its origins and much of its life cycle linked to a strong southwest monsoonal flow which was established over the South China Sea in late June. While low surface pressures and gale force winds generally prevailed over a majority of the region, a disturbance could not be detected until 27 June, when synoptic reports indicated the development of a weak low-level circulation. At the point of initial detection, the nearest area of significant convection was located more than 200 nm (370 km) to the northwest of the circulation. A Tropical Cyclone Formation Alert was issued at 272330Z when it had become apparent that a zone of lower surface pressures (< 1002 mb) was aligning itself in close proximity to the disturbance.

During the subsequent 24-hour period, there was an increase in convective activity within the formation alert area and satellite imagery suggested an increase in convective organization. Although still lacking evidence of vertical alignment, the trends toward lower surface pressures and increased convection prompted the issuance of the initial warning for Tropical Depression 06 at 290000Z.

From 28 to 30 June, Tropical Depression 06 tracked northward without any further evidence of convective organization. On 30 June, the depression turned east-northeastward and paralleled the coast of China. During this period, the southwest monsoon had abated somewhat and several weak circulations (eddies) became evident on satellite imagery (Figure 3-06-1). However, as the system passed south of Hong Kong, synoptic reports indicated that near-gale and gale force winds were present close to Tropical Depression 06. Thus, on the 010000Z July warning, Tropical Depression 06 was upgraded to Tropical Storm Tess. Post-analysis of this period indicates that Tess probably only attained tropical storm strength for a relatively short period (301200Z to 301800Z).

On 1 and 2 July, surface synoptic data indicated a marked decrease in wind velocities in the area and thereafter, the remants of Tess gradually dissipated as it approached the Formosa Strait.

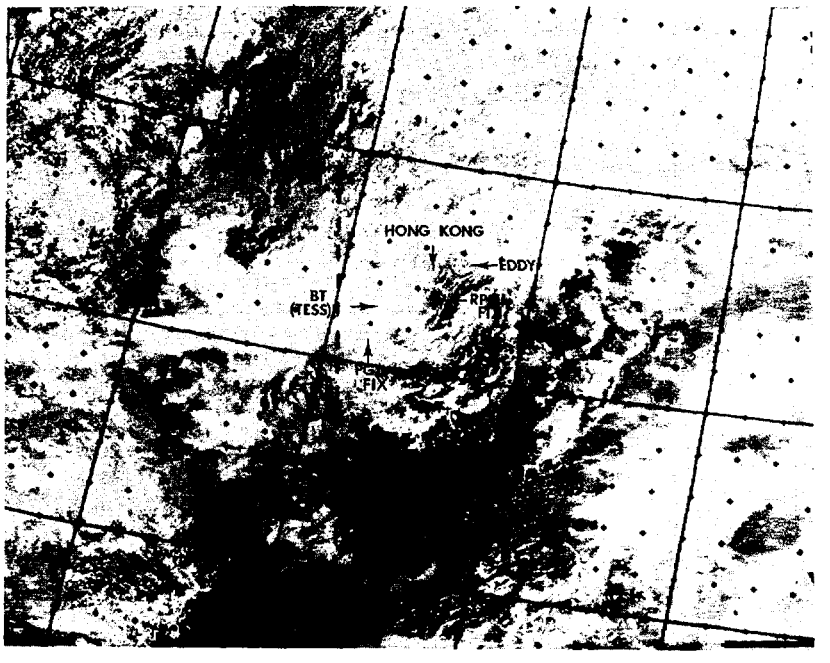

Figure 3-06-1. Satellite imagery shows several low-level eddies far removed from the central convective mass. Fix positions supplied from Detachment 5, 1WW, Clark AB, RP (RPMK) and from Detachment 1, 1WW, Nimitz Hill, Guam (PGTW) differ considerably in determining which eddy is the developing Tropical Storm Tess. The final best track position at fix time is shown as BT. 300656Z June (NOAA 7 visual imagery)

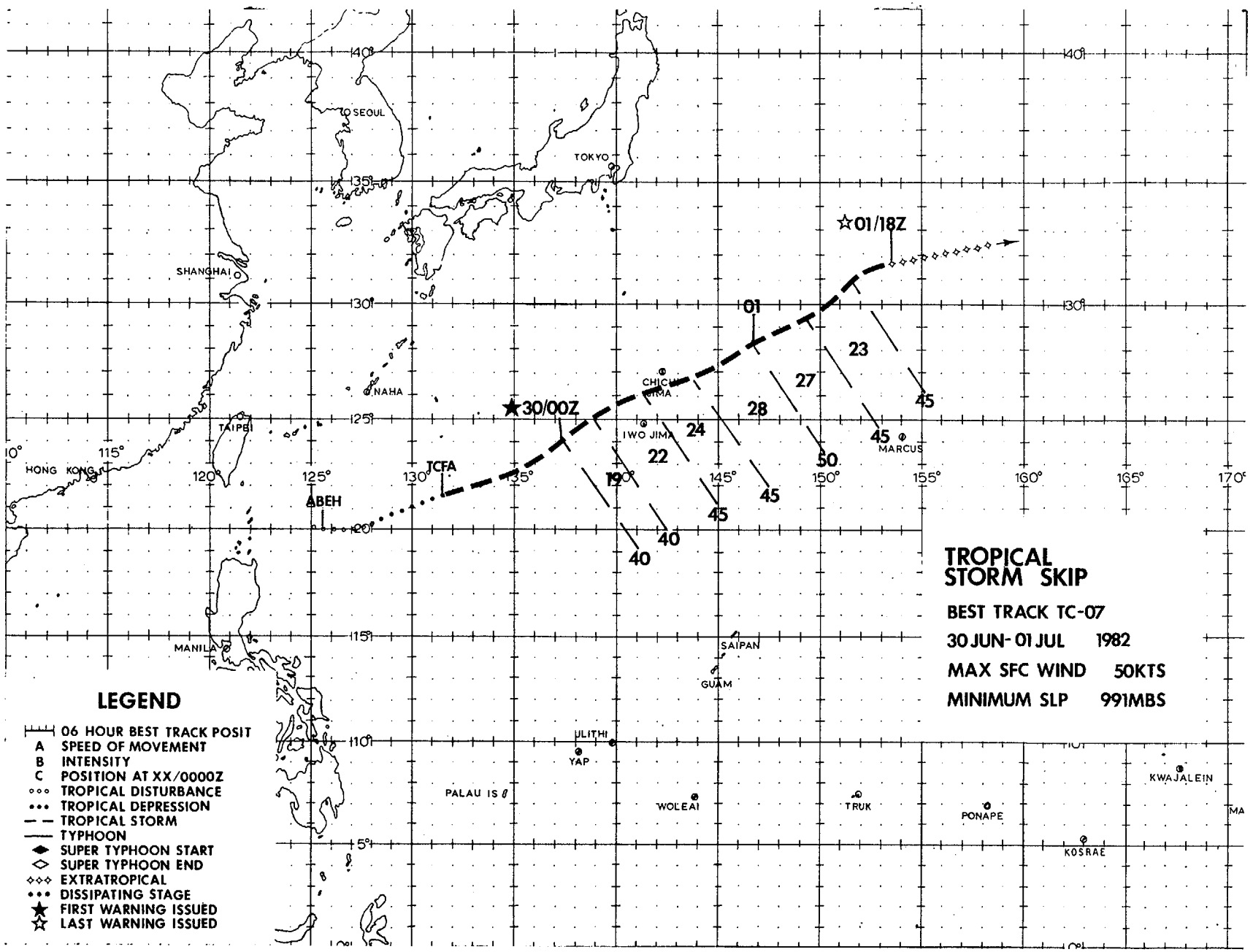
TROPICAL
STORM SKIP
BEST TRACK TC-07
30 JUN- 01 JUL 1982
MAX SFC WIND 50KTS
MINIMUM SLP 991MBS
LEGEND
06 HOUR BEST TRACK POSIT
A SPEED OF MOVEMENT
B INTENSITY
C POSITION AT XX/0000Z
TROPICAL DISTURBANCE
TROPICAL DEPRESSION
TROPICAL STORM
TYPHOON
SUPER TYPHOON START
SUPER TYPHOON END
EXTRATROPICAL
DISSIPATING STAGE
FIRST WARNING ISSUED
LAST WARNING ISSUED
☆01/18Z
★30/00Z
TCFA
ABEH
01
19
SEOUL
TOKYO
SHANGHAI
NAHA
TAIPEI
HONG KONG
CHICHI JIMA
IWO JIMA
MARCUS
MANILA
SAIPAN
GUAM
ULITHI
YAP
PALAU IS
WOLEAI
TRUK
PONAPE
KOSRAE
KWAJALEIN

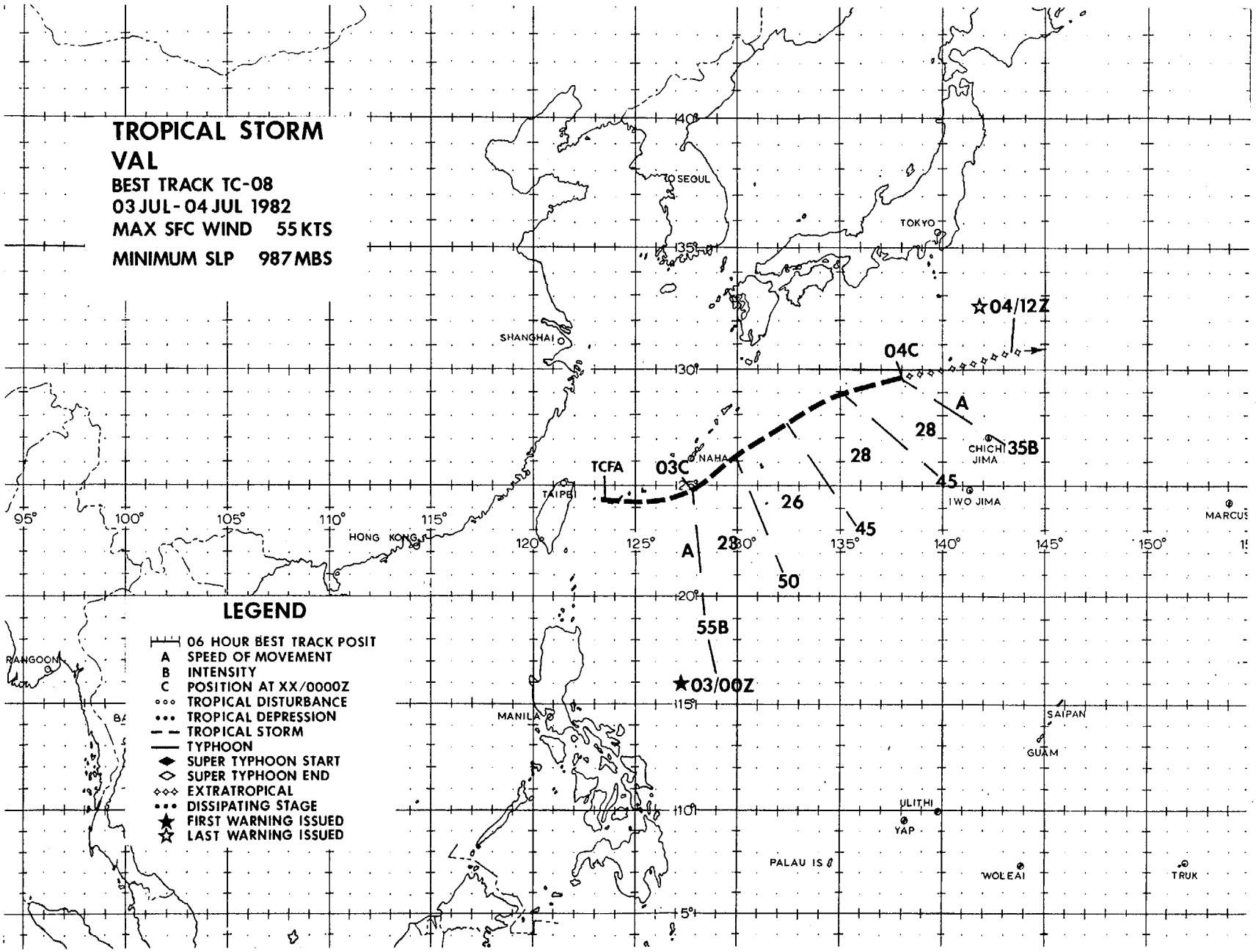
TROPICAL STORM
VAL
BEST TRACK TC-08
03 JUL - 04 JUL 1982
MAX SFC WIND 55 KTS
MINIMUM SLP 987 MBS
LEGEND
06 HOUR BEST TRACK POSIT
A SPEED OF MOVEMENT
B INTENSITY
C POSITION AT XX/0000Z
TROPICAL DISTURBANCE
TROPICAL DEPRESSION
TROPICAL STORM
TYPHOON
SUPER TYPHOON START
SUPER TYPHOON END
EXTRATROPICAL
DISSIPATING STAGE
FIRST WARNING ISSUED
LAST WARNING ISSUED
SEOUL
TOKYO
SHANGHAI
NAHA
TAIPEI
HONG KONG
RANGOON
MANILA
CHICHI JIMA
IWO JIMA
MARCUS
SAIPAN
GUAM
ULITHI
YAP
PALAU IS
WOLEAI
TRUK
TCFA
03C
04C
35B
55B
☆04/12Z
★03/00Z
A
28
45
26
50
95°
100°
105°
110°
115°
120°
125°
130°
135°
140°
145°
150°
40°
35°
30°
25°
20°
15°
10°
5°

Each tropical cyclone season sees a few circulations develop near the mid-latitudes which appear to have both tropical and extratropical characteristics. These "hybrid" or "subtropical" cyclones have long been known to the tropical forecaster. In particular, an article by Herbert and Poteat (1975) describes several distinguishing characteristics that allow differentiation between tropical and subtropical systems based upon satellite imagery (Table 3-07-1). The week between 23 June and 5 July saw two such circulations, Tropical Storms Skip and Val, develop southeast of Taiwan. During their existence each of these relatively small and compact systems were observed to have several characteristics associated with non-tropical cyclones, e.g. very little deep-layer convection near the surface center, displacement of convective features poleward and eastward of the system center, and each remained entirely enveloped within a larger cloud system associated with the mid-latitude westerlies. Conversely, both aircraft and satellite reconnaissance data indicated some typical tropical characteristics, i.e. a sharp pressure gradient near the center, surface winds in excess of 45 kt (23 m/sec), warm central temperatures, and a small but uniquely tropical upper-level anticyclonic outflow pattern.

The origin of the first circulation, Tropical Storm Skip, was more tropical in nature. The disturbance was first detected near 20N 124E on 26 June when surface synoptic data indicated the presence of a circulation that was subsequently apparent as an exposed low-level circulation on satellite imagery. Synoptically, a sharp trough existed between this area and Typhoon Ruby (05), which was in its initial phases of extratropical transition near 30N 130E. Although satellite imagery indicated that frontogenesis had begun, it is unclear from the available data just how far south along the trough the front could be identified. To the west, an active monsoon trough, which was soon to spawn Tropical Storm Tess (06) in the South China Sea, had also begun to push into the area. During the next three days, winds in excess of 15 to 20 kt (8 to 10 m/sec) could be detected in the monsoon flow south of the circulation; however, very little organized convection could be detected near the vortex. In the upper-troposphere, westerlies penetrated as far south as 25N (at 500 mb) and 20N (at 200 mb) as the result of deep troughing behind the now extratropical Ruby. By 29 June the 200 mb flow began to ridge strongly along the trough boundary and 60 to 70 kt (31 to 36 m/sec) westerly winds to the north were soon accompanied by 65 kt (33 m/sec) northeasterly winds south of the trough. This resulted in an extensive cloud band more than 500 nm (926 km) wide along this entire region. A Tropical Cyclone Formation Alert (TCFA) was issued at 290500Z when a small upper-level anticyclone appeared to be developing in the vicinity of the low-level circulation (Figure 3-07-1).

TABLE 3-07-1. SUBTROPICAL AND TROPICAL CYCLONES

A. DETERMINING TYPE

	SUBTROPICAL	TROPICAL
1. Main convection	Poleward & eastward from center	Equatorward & eastward from center
2. Cloud system size	Width 15° latitude or more	Width usually less than 10° latitude
3. Interaction with environment	Convective cloud system remains connected to other synoptic systems (Some cold lows excepted)	Cloud system becomes isolated

B. DETERMINING ORIGIN

1. Frontal band - typical cloud structure
2. East of upper trough - amorphous convective cloud mass
3. Cold low - circular cloud pattern with limited convection near center

(From Herbert and Poteat, 1975)

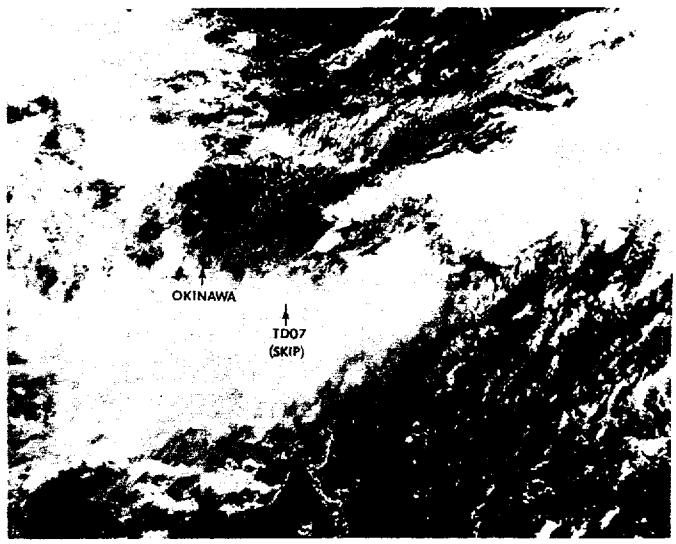

Figure 3-07-1. A developing low-level circulation can be detected within the confines of a broad large-scale cloud pattern. Weak upper-level outflow can be detected at 290526Z June (NOAA 7 visual imagery).

An aircraft investigative mission on 30 June located a 991 mb center with surface winds of 45 kt (23 m/sec), prompting the first warning to be issued at 300000Z. During the next 36 hours, Skip moved quickly northeastward along the frontal trough, averaging over 24 kt (44 km/hr), however its convection remained weak and generally restricted to within 120 nm (222 km) of its northern and eastern sides (Figure 3-07-2). Throughout Skip's lifetime, the Aerial Reconnaissance Weather Officers (ARWOs) consistently reported very little convection near the center, rather large light and variable wind centers, and an abundance of stratocumulus entrainment. By 011600Z July, all convection had dissipated from the vicinity of Skip's center and the upper-level anticyclone was no longer visible, indicating that the storm had completed its extratropical transition.

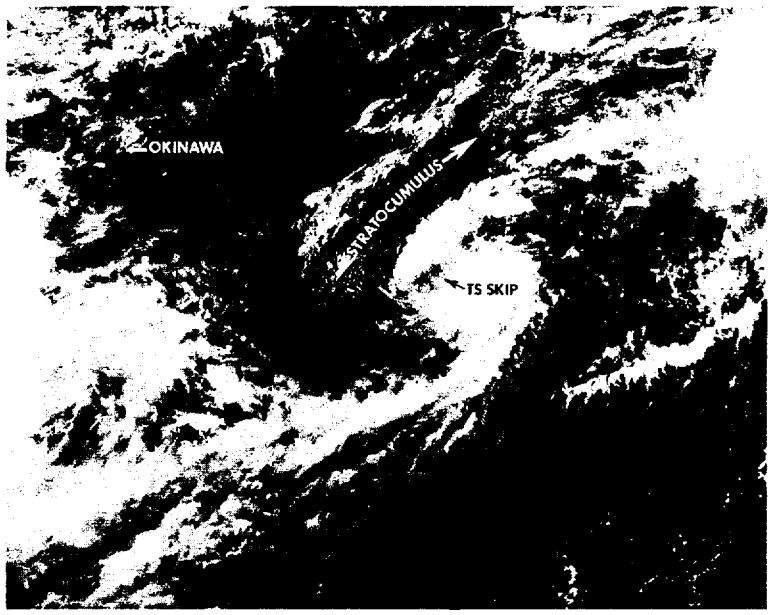

Figure 3-07-2. Tropical Storm Skip's exposed low-level circulation can be seen at 300514Z June to the south and west of its major convective area. Note the extent of stratocumulus to the north of this system. (NOAA 7 visual imagery).

As Skip was moving rapidly toward the northeast, a new circulation could be identified from 1 July synoptic data, just east of Taiwan. At this time, the frontal trough ran westward from Skip into the vicinity of northern Taiwan. Upper-level westerlies prevailed throughout the region although sharp ridging south of the 200 mb jet still maintained the large band of clouds. Isolated convection was present throughout this cloud mass, although none could be identified with the low-level circulation as it remained quasistationary. However, aircraft reconnaissance at 020115Z did identify a 995 mb center with winds up to 35 kt (18 m/sec) in the flow south of the circulation, thus a TCFA was issued. Convection finally began to develop near the circulation's center by 021200Z and, when the next aircraft mission found that the circulation had moved eastward and deepened to 987 mb, the first warning was issued at 030000Z. As was the case for Tropical Storm Skip, Val moved quickly northeastward along the trough, averaging over 26 kt (46 km/hr). Also like Skip, convection remained weakly organized and restricted to within 100 to 200 nm (185 to 370 km) of the system's center (mostly on the northern and eastern sides). As can be seen in Figure 3-07-3, Val still displayed its own individual outflow pattern despite being embedded within the larger cloud mass. By 040000Z, Val had lost all of its convection and could no longer be identified on satellite imagery as it completely merged into the frontal zone.

Both Tropical Storms Skip and Val contained many of the characteristics of sub-tropical cyclones identified in Table 3-07-1. Although monsoonal flow probably helped initiate Skip's low-level vortex, its further development and propagation can more likely be attributed to its position in relation to the eastern side of the upper trough. This is especially true of Val which formed farther north. Convection for both storms remained weak and unorganized and, partially due to strong westerly vertical shear, the low-level centers were often exposed with convection remaining poleward and eastward. Figures 3-07-2 and 3-07-3 show that each system did eventually become partially isolated from the dominance of the mid-latitude westerlies and displayed their own anticyclonic outflow pattern.

Re-analysis of synoptic and satellite data revealed that Skip and Val were not the only circulations to develop during this unique period. At 300000Z, Skip (located near 24N 137E) could be seen flanked by circulations (or frontal waves) at 34N 153E, 31N 143E and 20N 125E. Similar conditions occurred for Tropical Storm Val as well. On the synoptic-scale each was only a small part of an extensive mass of clouds along the eastern boundary of a very active mid-latitude upper-level trough.

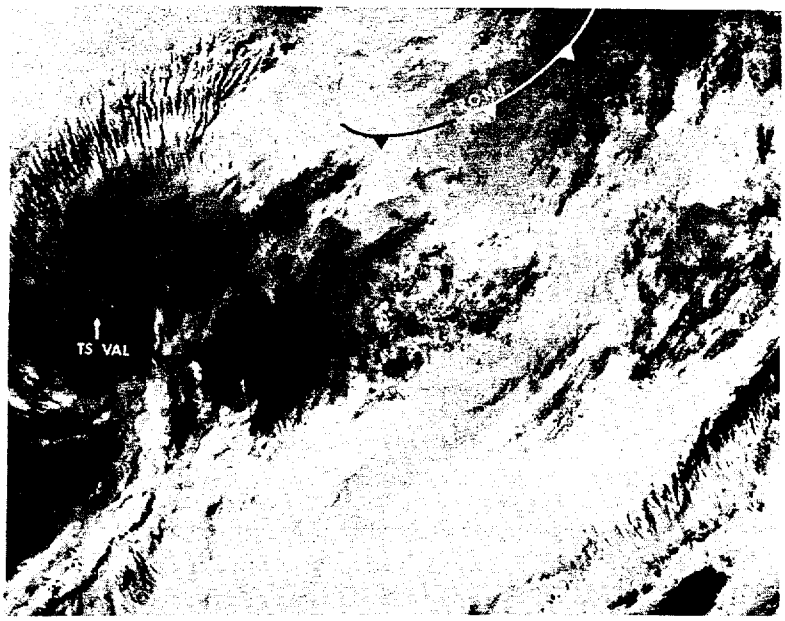

Figure 3-07-3. Tropical Storm Val's unorganized convection and outflow pattern can be seen with respect to larger frontal cloud mass pattern at 031723Z July. (NOAA 7 infrared imagery).

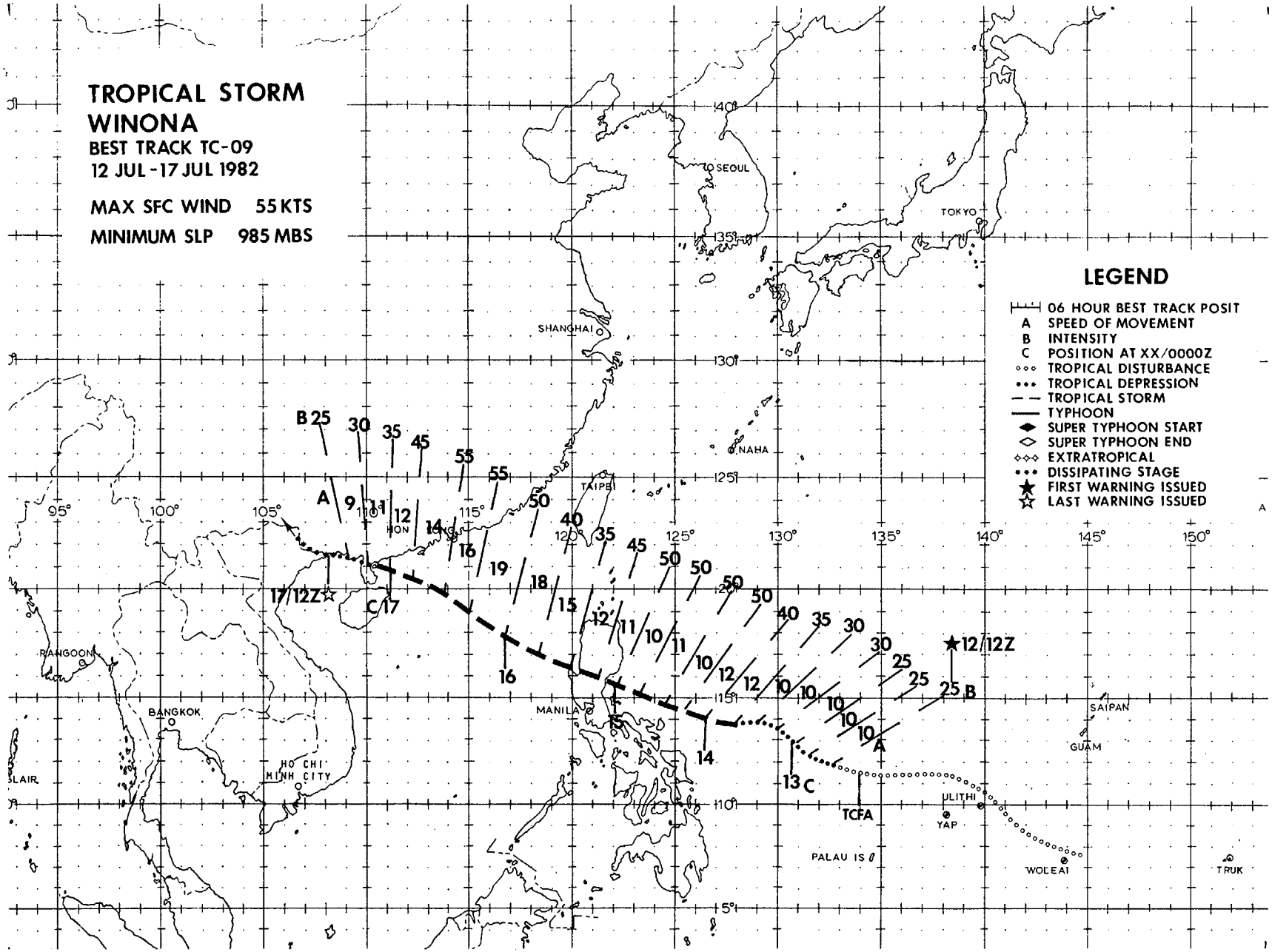
TROPICAL STORM
WINONA
BEST TRACK TC-09
12 JUL - 17 JUL 1982
MAX SFC WIND 55 KTS
MINIMUM SLP 985 MBS
LEGEND
06 HOUR BEST TRACK POSIT
A SPEED OF MOVEMENT
B INTENSITY
C POSITION AT XX/0000Z
TROPICAL DISTURBANCE
TROPICAL DEPRESSION
TROPICAL STORM
TYPHOON
SUPER TYPHOON START
SUPER TYPHOON END
EXTRATROPICAL
DISSIPATING STAGE
FIRST WARNING ISSUED
LAST WARNING ISSUED
SEOUL
TOKYO
SHANGHAI
NAHA
TAIPEI
HONG KONG
MANILA
RANGOON
BANGKOK
HO CHI MINH CITY
SAIPAN
GUAM
ULITHI
YAP
PALAU IS
WOLEAI
TRUK
17/12Z
12/12Z
TCFA
95°
100°
105°
115°
120°
125°
130°
135°
140°
145°
150°
40°
35°
30°
25°
15°
10°
5°

Tropical Storm Winona exemplifies tropical cyclone development without corresponding upper-level support. The presence of strong upper-level winds is often an inhibiting factor for significant tropical cyclone development. Based on JTWC's 200 mb synoptic data and streamline analyses, a strong subtropical ridge centered over central China was reinforcing strong upper-level winds over the Philippine Sea and South China Sea (See Figure 3-09-1). This situation persisted throughout Winona's warning period. The presence of 35 to 45 kt (17 to 23 m/sec) northeasterly winds in the upper-troposphere over Winona prevented the development of a strong anticyclonic outflow pattern and was a major factor in restricting further development to typhoon strength.

Winona's entire intensification process was slow. Between 10 and 12 July, three Tropical Cyclone Formation Alerts (TCFA) were issued as satellite imagery, synoptic and reconnaissance aircraft data revealed a persistent, but weak, disturbance moving westward through a primary tropical cyclone genesis region between Guam and the Republic of the Philippines. Reconnaissance aircraft investigative missions on the 10th and 11th found a weakly organized system with minimum sea level pressures of 1008 mb. At 121200Z, synoptic data gave the first indication that the disturbance was intensifying as gradient-level winds reported by Yap (WMO 91413) increased to 25 kt (13 m/sec). Simultaneously, the 200 mb streamline analysis indicated the development of a weak anti-

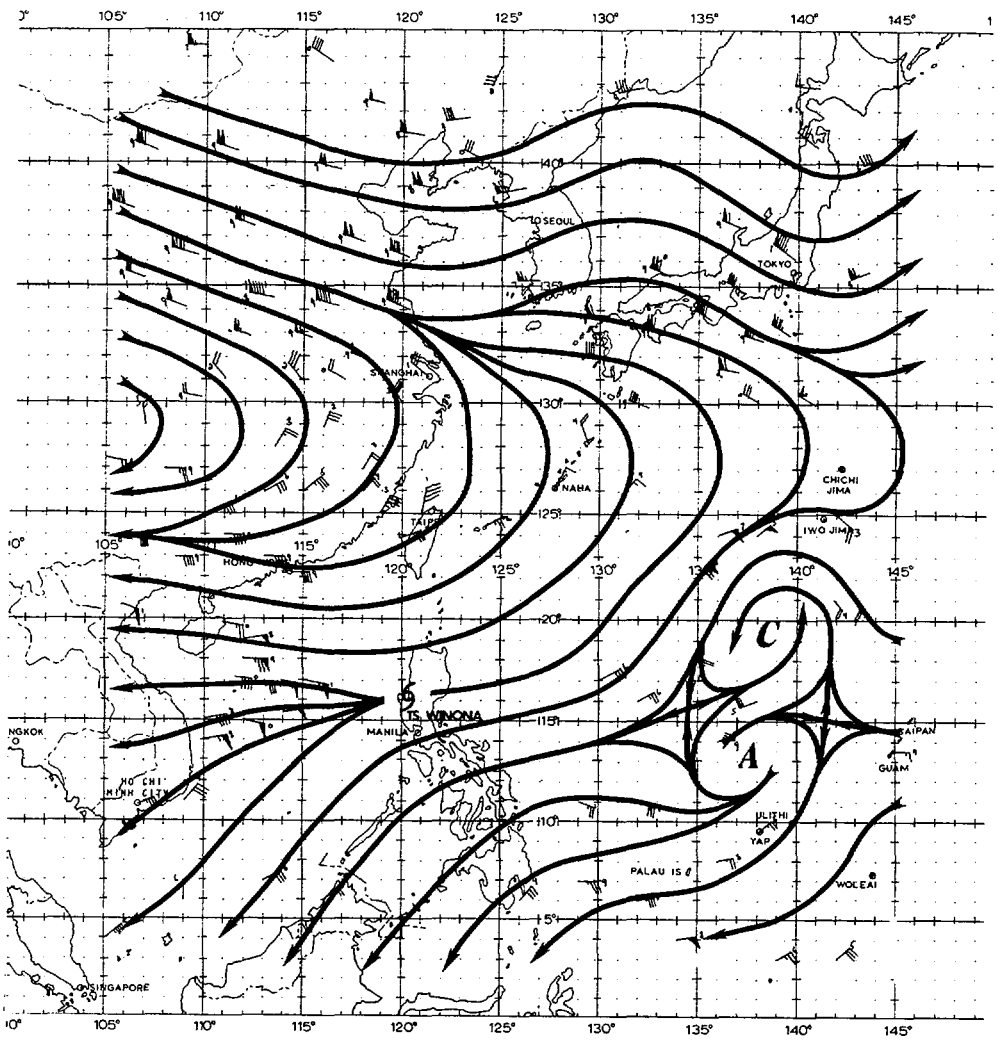

Figure 3-09-1. 200 mb streamline analysis at 151200Z July. Strong upper-level northeasterly winds prevent the development of outflow channels to the north.

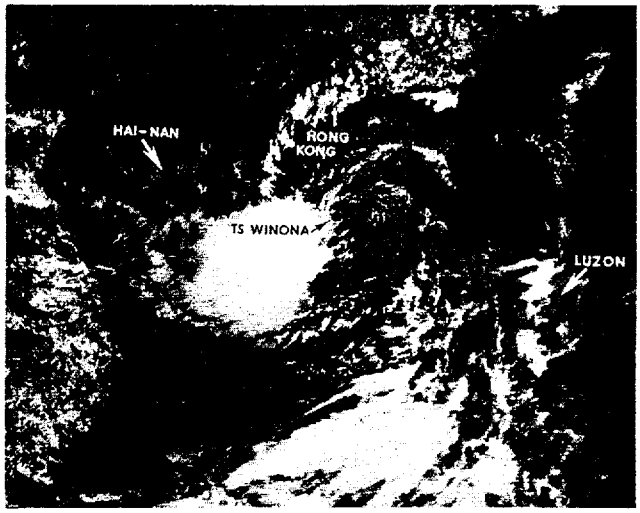

Figure 3-09-2. Tropical Storm Winona at 55 kt (28 m/sec) intensity, 400 nm (741 km) northwest of central Luzon. Even at maximum intensity, Winona's upper- and lower-level centers are not aligned due to the presence of strong upper-tropospheric winds. 160707Z (NOAA 7 visual imagery).

cyclone over the disturbance. This information, combined with increasing convection and organization (apparent on satellite imagery), prompted the issuance of the initial warning for Tropical Depression 09 at 121400Z. Subsequent aircraft reconnaissance at 130036Z confirmed JTWC's suspicions of intensification when it was reported that the minimum sea level pressure had dropped to 1000 mb.

From the initial warning, JTWC forecasts predicted that Winona would move into a region of strong upper-level winds which would inhibit its development. Thus, a maximum intensity of 50 kt (26 m/sec) was forecast prior to Winona's expected landfall upon central Luzon. Winona's intensity and movement were well-forecast during this period as it proceeded west-northwestward along the southern periphery of the subtropical ridge, centered along 25N.

By 140600Z, Winona reached the forecast 50 kt (26 m/sec) intensity which it maintained until landfall on Luzon at 150500Z. As Winona crossed central Luzon, it passed 35 nm (65 km) north of Clark AB, where maximum sustained winds recorded were 23 kt (12 m/sec) with peak gusts to 30 kt (15 m/sec). Reported damage to the surrounding region was estimated at $275,000 with 272 families left homeless as a result of severe flooding.

Winona entered the South China Sea as a minimal tropical storm, but upon reaching open waters, its convection increased and Winona reintensified to a peak intensity of 55 kt

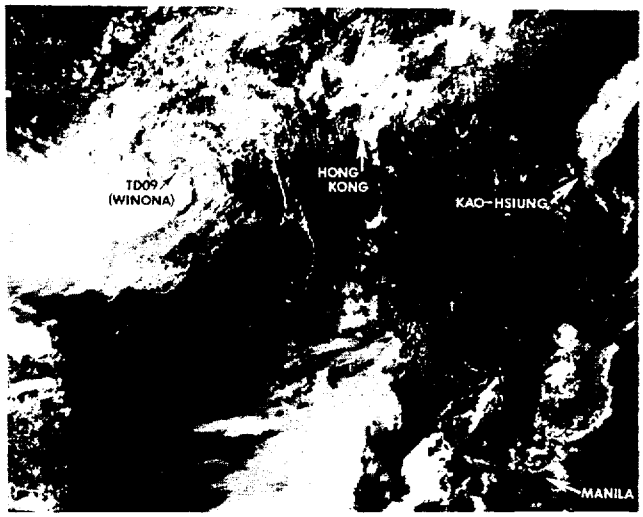

Figure 3-09-3. Winona after being downgraded to a tropical depression 210 nm (389 km) west-southwest of Hong Kong. Notice the persistent strong upper-level shear. 170655Z July (NOAA 7 visual imagery).

(28 m/sec) at 160600Z (Figure 3-09-2). This intensification occurred even though 40 kt (21 m/sec) 200 mb winds persisted over the area. However, based on limited 500 and 700 mb data, it appears that the strong winds did not extend into the mid-tropospheric levels. This situation allowed Winona's convection to develop well into the mid-tropospheric levels while the strong upper-level winds provided a sufficient outflow channel to the southwest.

Winona was forecast to move northward along the western periphery of the subtropical ridge upon entering the South China Sea. However, a 500 mb synoptic track completed by the 54th Weather Reconnaissance Squadron at 151200Z showed that a second ridge had developed east of Taiwan, resulting in a steering flow over the South China Sea toward the west-northwest. The 151800Z and subsequent forecasts reflected this new information and projected Winona on a west-northwestward track, with landfall expected southwest of Hong Kong.

After reaching maximum intensity on 16 July, Winona weakened as wind shear in the mid- and upper-layers increased. Winona became an exposed low-level system as its convective center was sheared to the southwest early on 17 July. By 170600Z, Winona was downgraded to a tropical depression as it passed 40 nm (74 km) north of Hai-Nan Island (See Figure 3-09-3). Further dissipation as a significant tropical cyclone occurred as it moved toward the China-Vietnam coastline on 18 July.

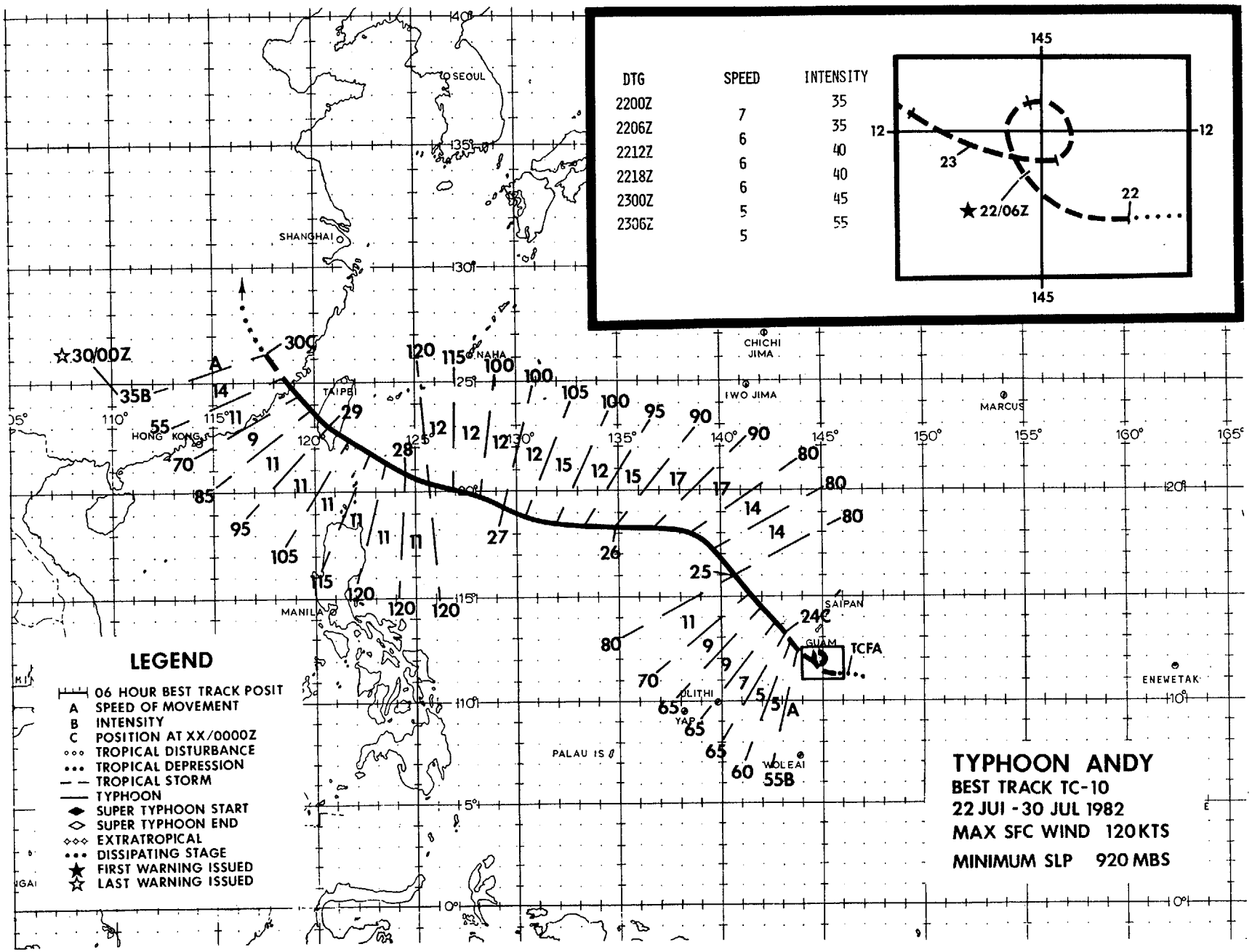
DTG
SPEED
INTENSITY
2200Z
7
35
2206Z
6
35
2212Z
6
40
2218Z
6
40
2300Z
5
45
2306Z
5
55
145
12
12
23
22
★22/06Z
145
☆30/00Z
A
35B
30
14
29
28
27
26
25
24
TCFA
SEOUL
SHANGHAI
NAHA
TAIPEI
HONG KONG
MANILA
CHICHI JIMA
IWO JIMA
MARCUS
SAIPAN
GUAM
ENEWETAK
ULITHI
YAP
PALAU IS
WOLEAI
55B
LEGEND
06 HOUR BEST TRACK POSIT
A SPEED OF MOVEMENT
B INTENSITY
C POSITION AT XX/0000Z
TROPICAL DISTURBANCE
TROPICAL DEPRESSION
TROPICAL STORM
TYPHOON
SUPER TYPHOON START
SUPER TYPHOON END
EXTRATROPICAL
DISSIPATING STAGE
FIRST WARNING ISSUED
LAST WARNING ISSUED
TYPHOON ANDY
BEST TRACK TC-10
22 JUI - 30 JUL 1982
MAX SFC WIND 120KTS
MINIMUM SLP 920 MBS

Andy formed on the northern edge of a zone of maximum cloudiness associated with the monsoon trough south of Guam. Prior to 22 July, the low-level westerlies were well established along 10N and extended eastward to the dateline. Satellite imagery on 20 July showed this maximum cloud zone had begun to segment. Within 24 hours the cloudiness consolidated into three distinct masses centered near 132E, 148E and 168E. Each cloud mass was poorly defined but had rudimentary banding features. The cloud system centers near 148E and 168E drifted westward, intensified, and became Typhoon Andy and Super Typhoon Bess (11) respectively. The cloud mass near 132E drifted westward and was disrupted by the combined effects of the rugged terrain over the Philippines and vertical wind shear from a tropical upper-tropospheric trough (TUTT).

A Tropical Cyclone Formation Alert (TCFA) was issued for the area south of Guam at 211900Z due to significant pressure falls (to below 1004 mb), increased convection, and convective organization. Aircraft reconnaissance at 220229Z located a small, tight circulation center with a minimum sea level pressure of 995 mb. These data, along with observed winds of 35 to 40 kt (18 to 21 m/sec) prompted the issuance of the first warning. Although intensification was evident from 20 to 24 July on satellite imagery, the cloud pattern remained poorly defined and the circulation center was difficult to position -- except for a brief period on 23 July, when the low-level center was visible on the satellite imagery. Aircraft reconnaissance was an invaluable asset during this period; no other reconnaissance platform was capable of following the low-level wind center, particularly since there was considerable interest on Guam as the fix data received implied an anticyclonic loop 35 nm (65 km) in diameter just 90 nm (167 km) south of the island.

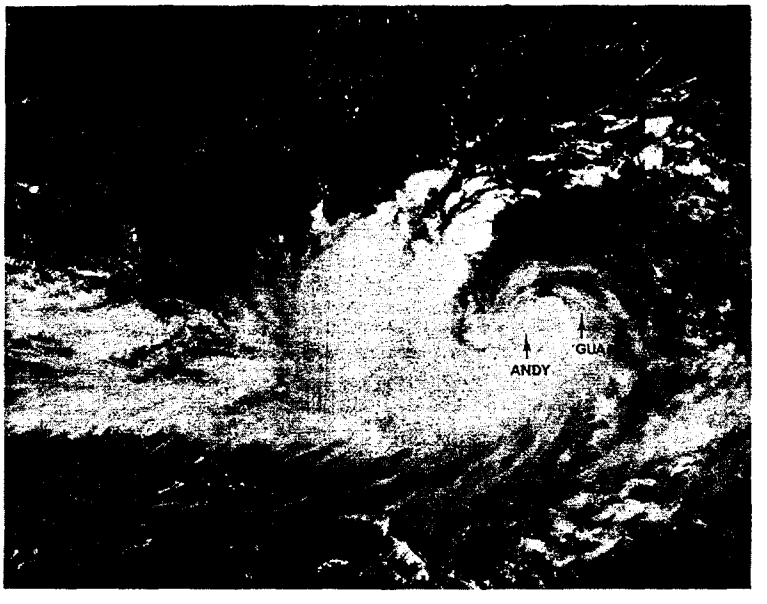

Figure 3-10-1. At 240530Z July Andy, shortly after reaching typhoon strength, is shown 125 nm (232 km) west of Guam (see arrow). During this time the strong south-westerly fetch south of Typhoon Andy brought phenomenal surf to Guam. (NOAA 7 visual imagery)

While Andy was undergoing the loop south of Guam, several meteorological factors were influencing the synoptic situation. Rawinsonde observations from Chichi Jima (WMO 47971) at 221200Z and 230000Z revealed 500 mb height falls of 10 to 20 meters. These falls indicated a weakening of the subtropical ridge north of Andy as well as a lessening of the steering current, factors probably accounting for Andy's lack of forward movement. In addition, reconnaissance aircraft consistently reported Andy's 700 mb center 10 to 20 nm (19 to 37 km) south of the surface center. This tilt, half of the diameter of the loop, suggests that Andy's actual movement during this period might have been virtually nil, and may have been more related to the fix accuracies and the internal dynamics of the developing tropical cyclone. However, for best track purposes, this period is described well by the loop.

After completing the loop, Andy accelerated to the northwest and intensified. In Andy's wake, Guam experienced phenomenal surf on exposed southern and western beaches as a strong southwesterly fetch was brought to bear on the island on 24 July (See Figure 3-10-1). Andy's northwestward track turned abruptly toward the west as the cyclone

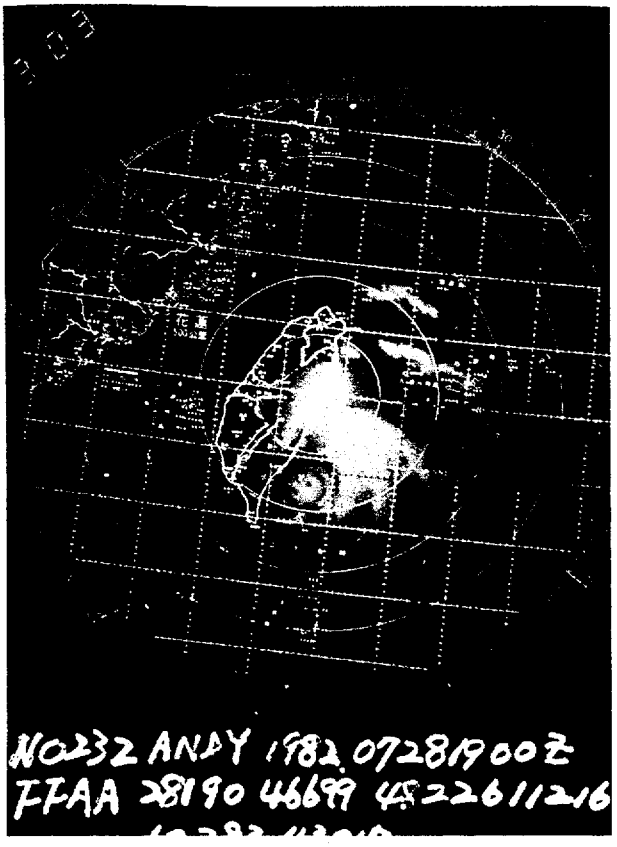

Figure 3-10-2. Typhoon Andy as seen by radar from Hua Lien (WMO 46699) at 281900Z July (Photograph courtesy of Central Weather Bureau, Taipei, Taiwan)

reached 18N on 25 July. This track change occurred while reported 500 mb heights rose at Chichi Jima, to the northeast of Andy. From this point onward, Andy remained equatorward of and parallelled the subtropical ridge axis.

While Andy was tracking westward, upper-level outflow channels to the east (south of the TUTT axis) and to the southwest (return flow from the monsoon over southeast Asia) provided a favorable environment for intensification. At 271800Z, Andy reached a maximum intensity of 120 kt (62 m/sec). Until making landfall upon the southern portion of Taiwan on 29 July (See Figure 3-10-2), Andy's intensity remained over 100 kt (51 m/sec). Taiwan experienced torrential rains from the typhoon's passage; especially hard hit was the eastern coastal area, where considerable damage from flooding was reported. Weakened from Taiwan's rugged terrain, Andy continued westward, across the Formosa Strait, and dissipated in the mountainous area of southeastern China on 30 July.

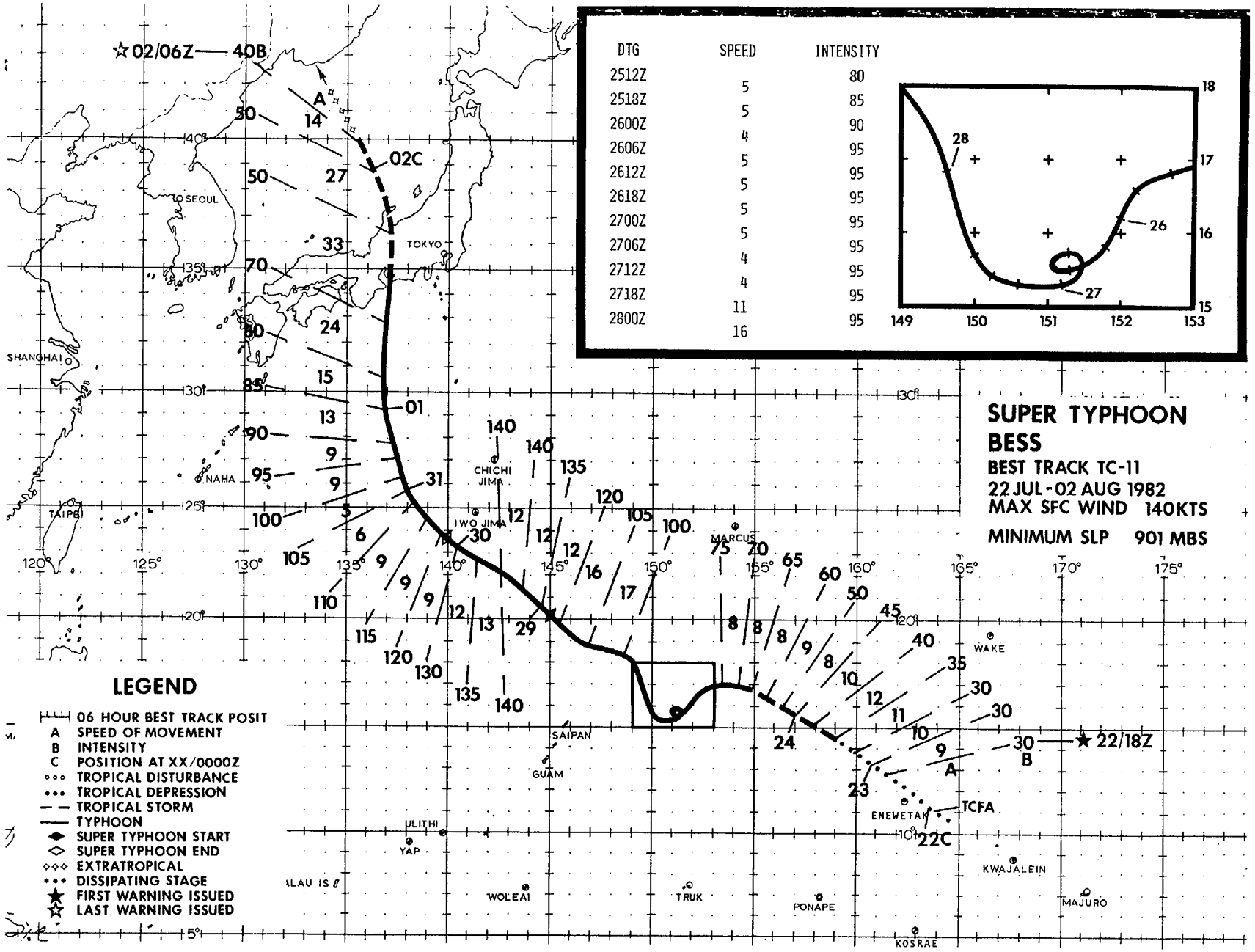

DTG	SPEED	INTENSITY
2512Z		80
2518Z	5	85
2600Z	5	90
2606Z	4	95
2612Z	5	95
2618Z	5	95
2700Z	5	95
2706Z	5	95
2712Z	4	95
2718Z	4	95
2800Z	11	95
	16	

SUPER TYPHOON BESS

BEST TRACK TC-11

22 JUL - 02 AUG 1982

MAX SFC WIND 140 KTS

MINIMUM SLP 901 MBS

Bess formed at the eastern end of a maximum cloud zone associated with the monsoon trough anchored south of Guam. By 21 July, this area of cloudiness had separated into three masses near 132E, 148E, and 168E. The two easternmost cloud masses continued to develop and became Typhoon Andy (10) and Super Typhoon Bess. The third area dissipated over the Philippine Islands.

A Tropical Cyclone Formation Alert was issued for an area near 11N 165E at 211900Z. Observations from Kwajalein (WMO 91336) and Ailinglaplap (WMO 91367) showed that sea level pressures had continued to fall in the region, and satellite imagery indicated increased convection and organization in the cloud system.

The first warning, with maximum winds of 30 kt (15 m/sec), was issued at 221800Z when the curvature of loosely organized cloud bands into the central cloud mass increased. Initial forecasts for Bess indicated a track toward the northwest, in response to an east-southeasterly flow at low- and mid-levels. Reconnaissance aircraft missions during the period 222200Z to 232200Z indicated that the surface and 700 mb centers were not well-aligned vertically. Once this feature was eliminated, Bess began to intensify and by 241800Z, it was upgraded to typhoon strength based upon satellite imagery which indicated a 30 nm (56 km) eye had developed.

Bess maintained its northwestward track for the first 48 hours in warning status. However, by 241800Z a noticeable decrease in the speed of movement was observed as Bess began to move toward the west-northwest. This change in motion was thought to be the result of westward building of the subtropical ridge to the north. Consequently, the forecast track was changed to a more westward heading. Contrary to JTWC expectations, Bess took a turn toward the southwest at 251200Z. Subsequent analysis of satellite imagery indicates that a short wave trough had just passed to the north of the circulation. The enhanced northwesterly flow behind this trough forced Bess toward the southwest. During this period, Bess slowed to 5 kt (9 km/hr) and completed a 20 nm (37 km) diameter cyclonic loop, while its intensity remained at 95 kt (49 m/sec). Further intensification did not occur and Bess remained on its southwestward track until another short wave trough moved eastward from Japan on 27 July. In response to this trough, Bess took a noticeable turn north-northwestward until 280600Z when Bess began moving toward the northwest along the southwestern extension of the subtropical ridge. While moving northwestward, a rapid intensification period began, culminating in the attainment of super typhoon strength and a peak intensity of 140 kt (72 m/sec) at 290600Z.

As Bess approached 25N, a decrease in forward movement was observed; numerical forecast fields and the JTWC 500 mb analysis of 30 June indicated a weakness forming in the subtropical ridge over the southern islands of Japan which would allow Bess to take a more northward track. As Bess entered the south-southeasterly flow associated with the western periphery of the subtropical ridge, interaction with the mid-latitude westerlies was expected to occur within 36 hours and Bess was forecast to recurve along the southern coast of Japan. Bess, however, maintained a northward track. The Typhoon Acceleration Prediction Technique TAPT (Weir, 1982) was employed, and correctly forecast significant acceleration commencing near 28N. From this latitude, Bess did begin to accelerate toward the north and eventually merged with a low pressure center in the Sea of Japan on 02 August.

Bess passed over the Araumi Peninsula on central Honshu where extensive damage and human suffering were reported. The greatest damage was caused by torrential rainfall which set off 1,557 landslides and flooded over 27,000 homes, leaving 25,000 persons homeless, and 59 dead. More than 25 ships ran aground or were lost, over 100 bridges were washed out, and nearly 300 acres (741 hectares) of farmland were flooded.

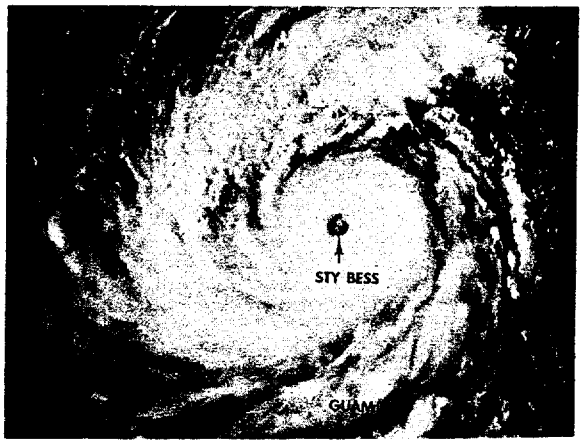

Figure 3-11-1. Super Typhoon Bess at maximum intensity. 290430Z August (NOAA 7 visual imagery).

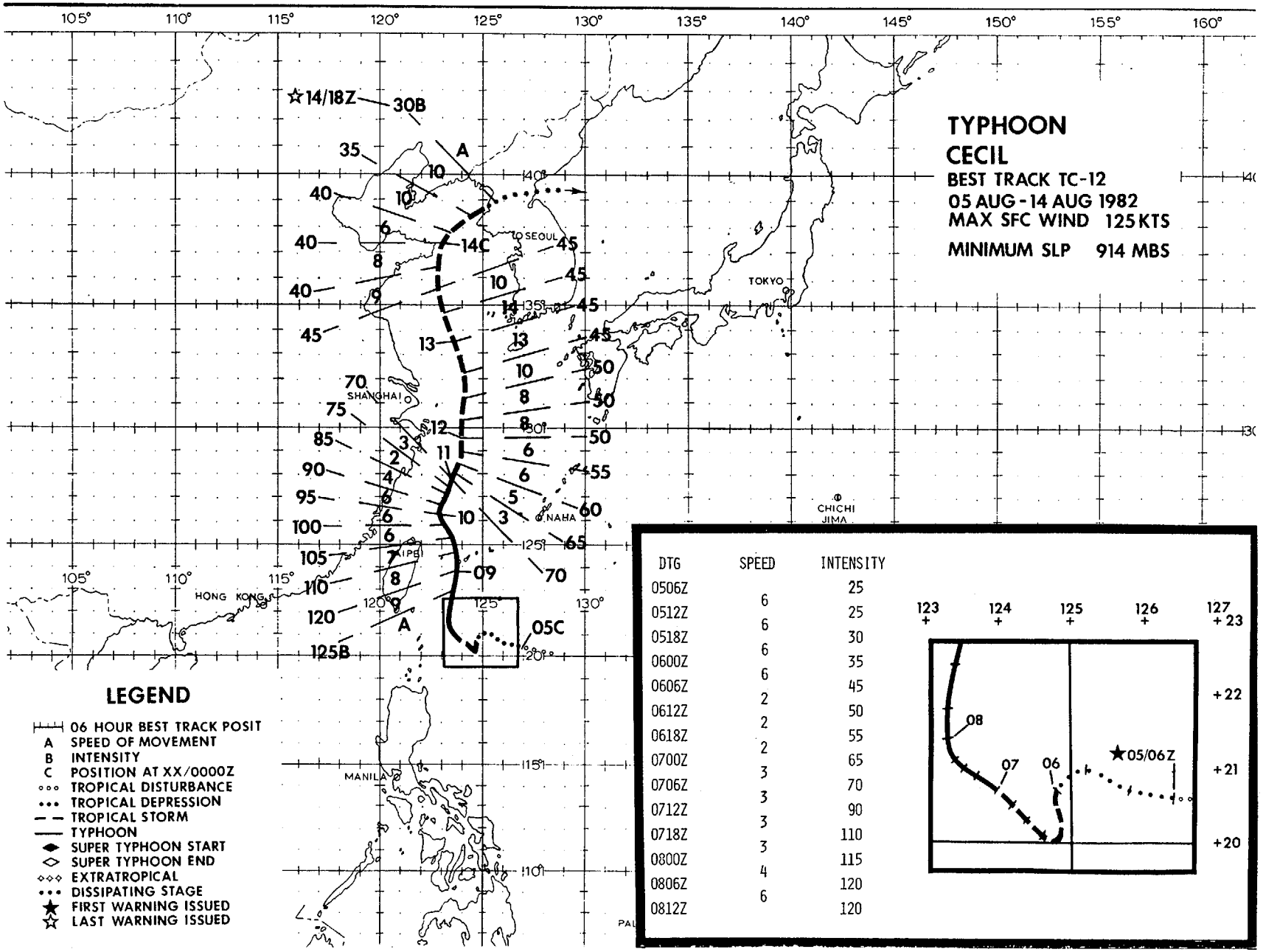
TYPHOON
CECIL
BEST TRACK TC-12
05 AUG - 14 AUG 1982
MAX SFC WIND 125 KTS
MINIMUM SLP 914 MBS
LEGEND
06 HOUR BEST TRACK POSIT
A SPEED OF MOVEMENT
B INTENSITY
C POSITION AT XX/0000Z
TROPICAL DISTURBANCE
TROPICAL DEPRESSION
TROPICAL STORM
TYPHOON
SUPER TYPHOON START
SUPER TYPHOON END
EXTRATROPICAL
DISSIPATING STAGE
FIRST WARNING ISSUED
LAST WARNING ISSUED
DTG SPEED INTENSITY
0506Z 25
0512Z 6 25
0518Z 6 30
0600Z 6 35
0606Z 6 45
0612Z 2 50
0618Z 2 55
0700Z 2 65
0706Z 3 70
0712Z 3 90
0718Z 3 110
0800Z 3 115
0806Z 4 120
0812Z 6 120
05/06Z
SEOUL
TOKYO
SHANGHAI
NAHA
CHICHI JIMA
HONG KONG
MANILA
IPEI

The tropical disturbance which later became Typhoon Cecil was first distinguishable as a low-level circulation about 250 nm (463 km) north of Truk (WMO 91334) on 31 July. This disturbance persisted as a closed circulation on the surface streamline analyses and as an area of enhanced convective activity on satellite imagery that travelled westward along the monsoon trough for the next four days. Although mentioned in four consecutive Significant Tropical Weather Advisories (ABEH PGTW), a Tropical Cyclone Formation Alert (TCFA) was not issued on the system during this period because a strong easterly flow at upper-levels was expected to inhibit development of the disturbance. Figure 3-12-1 is typical of the upper-level (200 mb) flow during this period. On 4 August, increased convective activity was apparent from satellite imagery, ship reports in the area indicated that central pressures had dropped to 1000-1003 mb and weakening of the upper-level easterlies was indicated by the 200 mb analysis data. When it became evident that the disturbance had indeed intensified, and that further intensification was likely, a TCFA was issued at 041400Z.

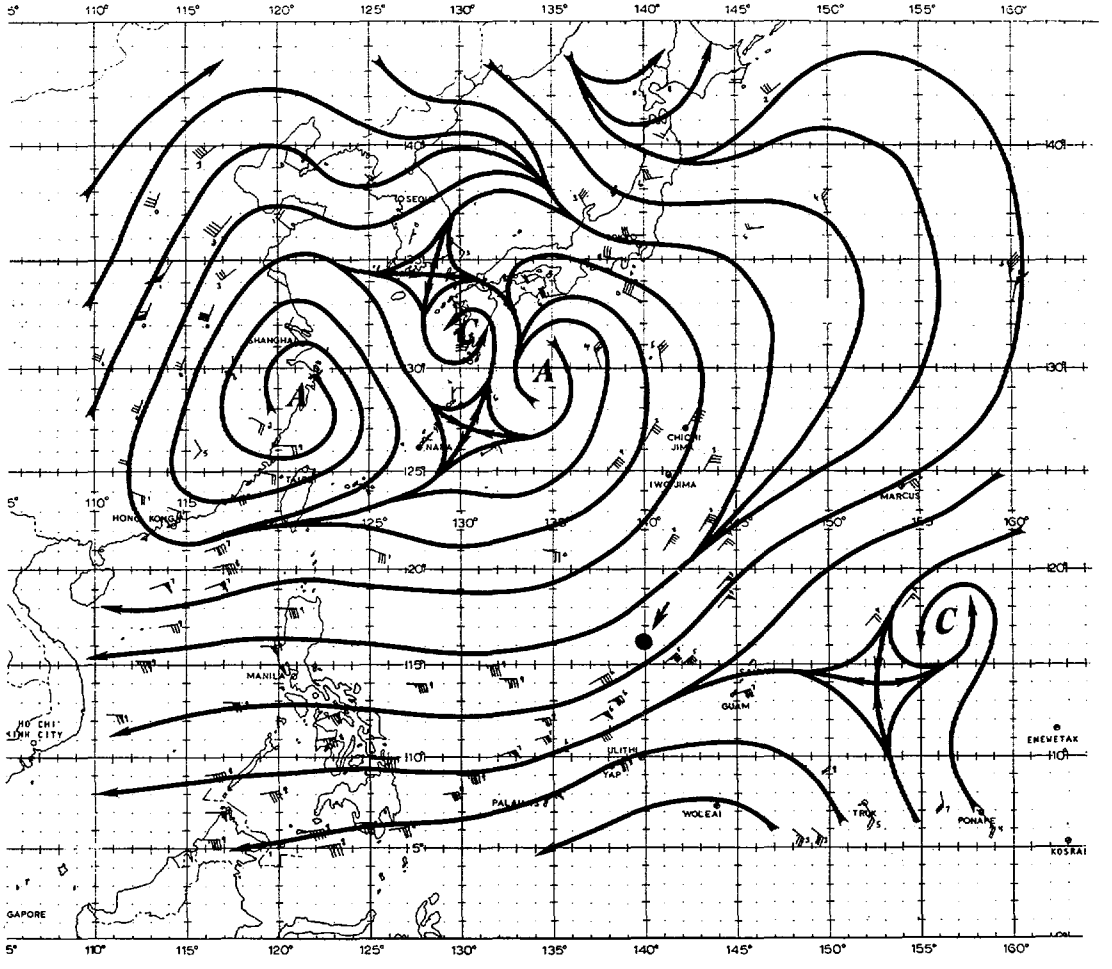

Figure 3-12-1. 030000Z August 200 mb streamline analysis. The location of the surface circulation is indicated by the dark circle.

Figure 3-12-2. 081838Z August (NOAA 7 infrared imagery).

The first warning on Tropical Depression 12 was issued at 050600Z after an aircraft reconnaissance mission observed sustained winds of 25 kt (13 m/sec) associated with the circulation. Tropical Depression 12 continued to track westward under the influence of easterly steering currents along the southern periphery of the subtropical ridge. Upgraded to tropical storm status on 6 August, Cecil turned southward, slowed to 3 kt (6 km/hr), and then turned northwestward. From 6 to 8 August, Cecil intensified from 35 kt (18 m/sec) to 115 kt (59 m/sec), reaching a peak intensity of 125 kt (64 m/sec) at 081800Z while located 120 nm (222 km) east of Taiwan (figures 3-12-2 and 3-12-3).

As Cecil approached Taiwan from the southeast, its track turned sharply northward until reaching 25N when Cecil once again assumed a more northwestward track. Although Cecil never approached closer than 80 nm (148 km) to Taiwan, heavy rains associated with its peripheral circulation touched off landslides which killed at least 19 people in Wu-Koo County, near Taipei.

On 10 August, Cecil turned toward the north-northeast and the combined effects of colder ocean temperatures, vertical wind shear, and cooler surrounding air began to take their toll. Within three days after reaching maximum intensity, Cecil was downgraded to a tropical storm.

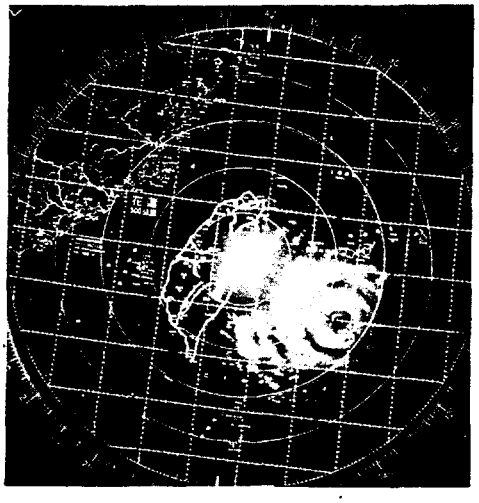

Figure 3-12-3. Typhoon Cecil as seen by radar from Hua Lien (WMO 46699) at 081900Z August (Photograph courtesy of the Central Weather Bureau, Taipei, Taiwan).

As a tropical storm, Cecil continued to move northward in response to steering from an extension of the subtropical ridge which had built northward into the Sea of Japan. The situation at 500 mb is illustrated by the 101200Z August 500 mb streamline analysis (Figure 3-12-4) which is typical of the mid-level synoptic pattern during Cecil's northward movement.

By 14 August, Cecil, located near 38N 124E, was beyond the northward influence of the subtropical ridge and entering an area of westerly flow. Cecil moved eastward in response to its new environment and made landfall on Korea with 35 kt (18 m/sec) winds. Although, at this time, Cecil was a weak storm in terms of wind intensity, there was a great deal of precipitation associated with the circulation. Heaviest rains, 21.2 inches (55 cm), were recorded in Sanchong, resulting in severe flooding which left 35 dead, 28 missing, and 42 injured in addition to an estimated 30 million dollars in property damage. Cecil's circulation was unable to reorganize after crossing the Korean peninsula and dissipated in the Sea of Japan on 15 August.

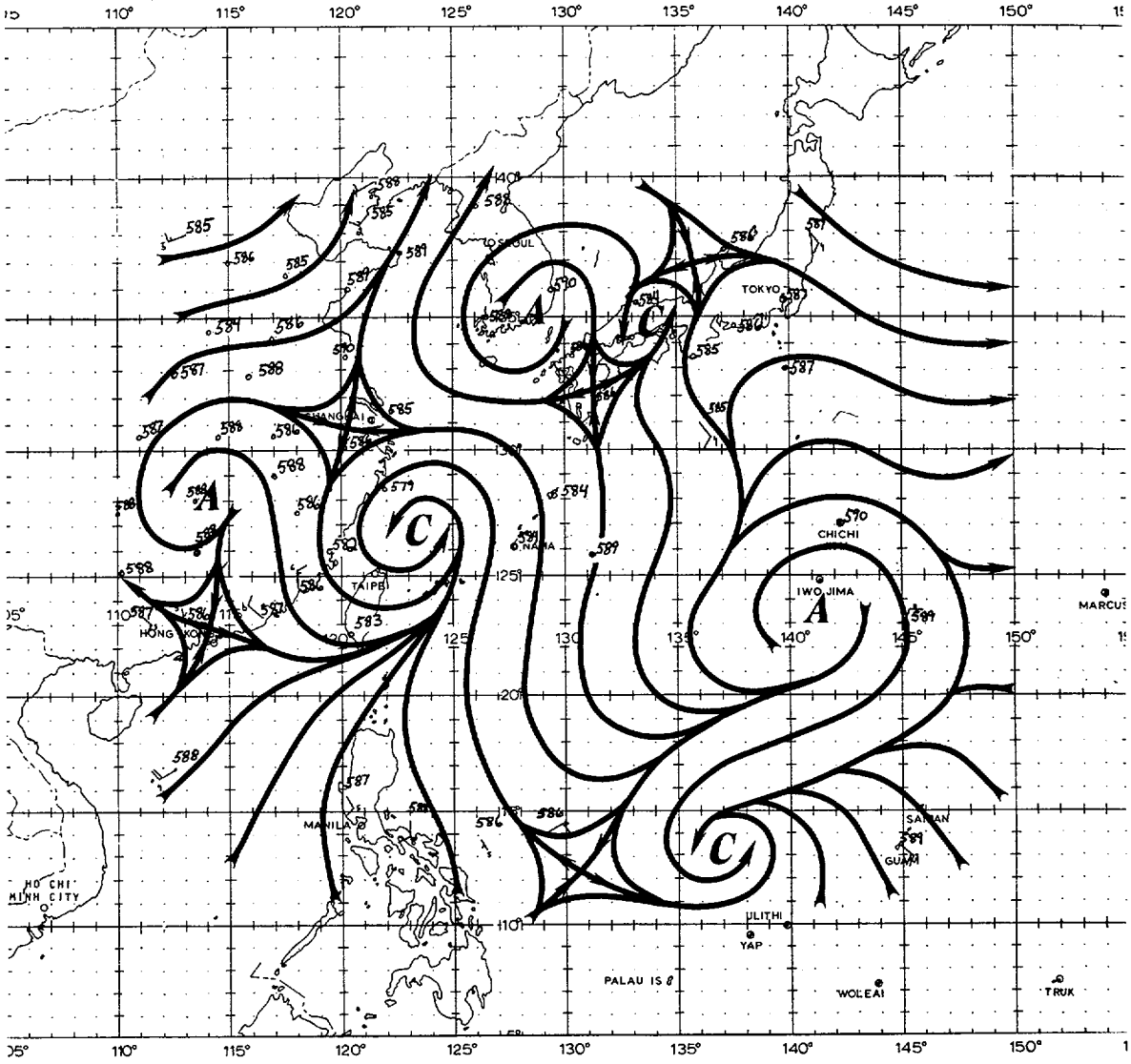

Figure 3-12-4. 101200Z August 500 mb streamline analysis.

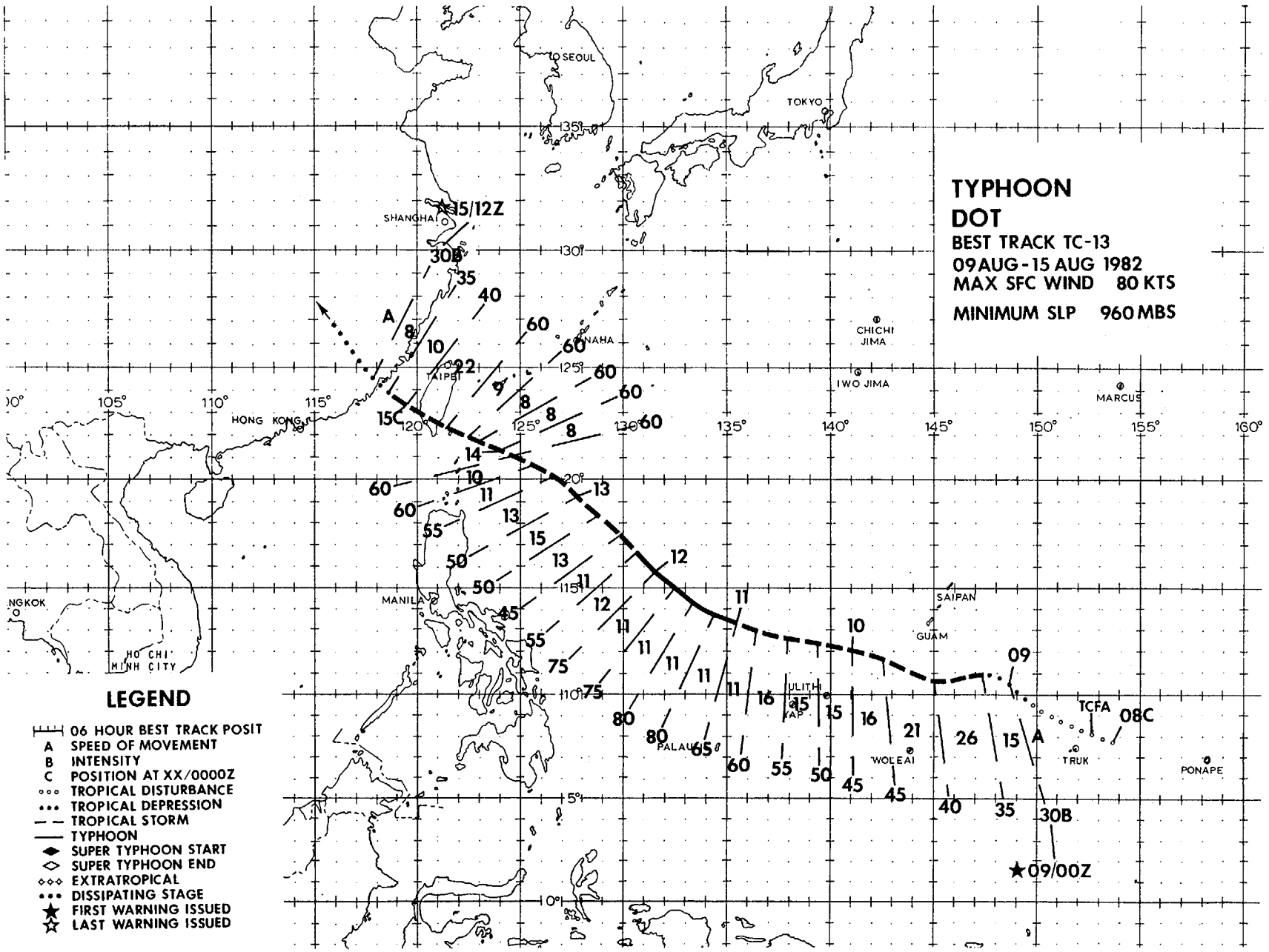
TYPHOON
DOT
BEST TRACK TC-13
09AUG-15 AUG 1982
MAX SFC WIND 80 KTS
MINIMUM SLP 960 MBS
LEGEND
06 HOUR BEST TRACK POSIT
A SPEED OF MOVEMENT
B INTENSITY
C POSITION AT XX/0000Z
TROPICAL DISTURBANCE
TROPICAL DEPRESSION
TROPICAL STORM
TYPHOON
SUPER TYPHOON START
SUPER TYPHOON END
EXTRATROPICAL
DISSIPATING STAGE
FIRST WARNING ISSUED
LAST WARNING ISSUED
15/12Z
09/00Z
TCFA
08C
SEOUL
TOKYO
SHANGHAI
TAIPEI
NAHA
CHICHI JIMA
IWO JIMA
MARCUS
HONG KONG
MANILA
SAIPAN
GUAM
TRUK
PONAPE
WOLEAI
PALAU
ULITHI
HO CHI MINH CITY
105°
110°
115°
120°
125°
130°
135°
140°
145°
150°
155°
160°
30°
25°
20°
15°
10°
5°

The origins of Typhoon Dot can be traced back to a weak surface circulation located near Kwajelein (WMO 91366) on the 5th of August. Surface winds associated with this circulation were 5 to 10 kt (3 to 5 m/sec) and the minimum surface pressure was 1008 mb. Over the next two days, as the circulation drifted northwestward, it remained fairly weak with loosely organized convection and light winds. On 8 August, a reconnaissance aircraft mission into the area showed that the circulation had maximum sustained winds of 20 kt (10 m/sec) but that the surface circulation was still very broad with relatively unorganized convection. However, satellite imagery and 200 mb data indicated that an upper-level anticyclone was present in the area, although not vertically aligned with the surface center. A Tropical Cyclone Formation Alert (TCFA) was issued at 080500Z based upon the persistence of the system and the presence of upper-level conditions that could lead to intensification of the disturbance. The initial warning on Tropical Depression 13 was issued at 090000Z when satellite imagery indicated that the cloud pattern associated with the developing depression was becoming more organized along with increased convective activity.

A reconnaissance aircraft mission at 090118Z observed surface winds of 35 kt (18 m/sec) and an extrapolated minimum sea level pressure of 1003 mb. Based on these data, Tropical Depression 13 was upgraded to Tropical Storm Dot at 090600Z. During this period, the subtropical ridge was well established to the north of the system; thus Dot was forecast to track westward and to continue to intensify. Dot lived up to these expectations, moving westward and reaching typhoon strength on 11 August. However, after reaching a maximum intensity of 80 kt (41 m/sec), Dot began to weaken as upper-level outflow channels became restricted due to interaction with Typhoon Cecil (12) located to the northwest. This interaction is easily seen on satellite imagery (Figure 3-13-1 shows the early stages of this interaction); at this time, Cecil was located northeast of Taiwan with maximum winds of 90 kt (46 m/sec) and Tropical Storm Dot, with maximum sustained winds of 50 kt (26 m/sec), was rapidly intensifying and would achieve maximum sustained winds of 80 kt (41 m/sec) on the following day. Although there was some interference in the upper-level outflow between the two cyclones, Dot's outflow channels to the northeast and southwest were well established. Figure 3-13-2 shows the relationship between the two cyclones two and one-half days later. Although the satellite pass was not optimally located, features of interest are readily observable, i.e., Dot's outflow channels to the north were completely cut off by the strong northeasterly winds associated with Cecil's outflow. The 200 mb analysis for

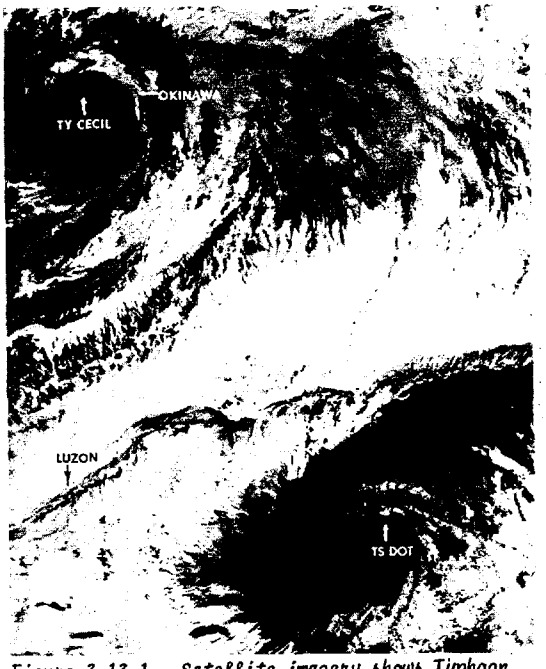

Figure 3-13-1. Satellite imagery shows Typhoon Cecil at the upper left and Tropical Storm Dot at the lower right. 1005292 August (NOAA 7 infrared imagery).

Figure 3-13-2. Satellite imagery shows Tropical Storm Cecil at the upper left and Tropical Storm Dot at the lower left. 121750Z August (NOAA 7 infrared imagery).

this period (Figure 3-13-3) shows that flow was unidirectional over Dot, with no indication of an anticyclone at that level.

As the distance between Cecil and Dot increased over the next few days, Dot regained intensity, reaching maximum sustained winds of 60 kt (31 m/sec) on the 13th. Figure 3-13-4 shows the relationship between Dot's intensity and the separation between the two cyclones. The data indicate a correlation between separation and Dot's intensity once the separation distance fell below 1000 nm (1852 km).

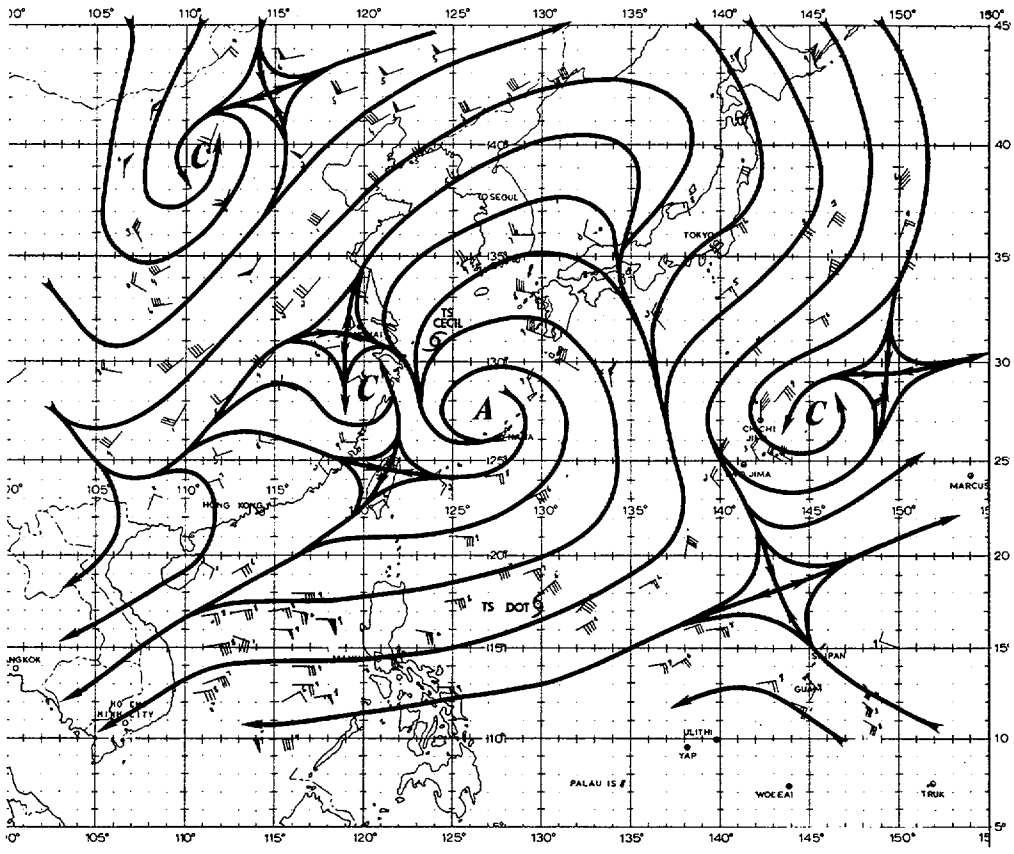

Figure 3-13-3. 121200Z 200 mb analysis with surface position of Tropical Storms Cecil and Dot superimposed.

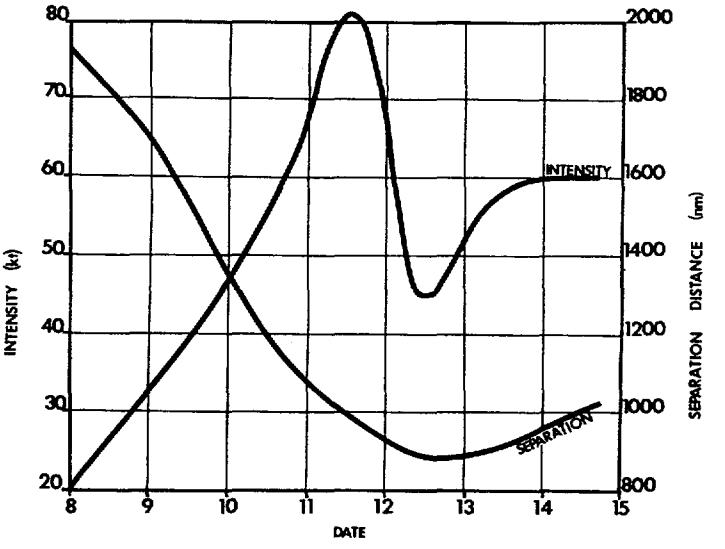

Figure 3-13-4. Variation in intensity as a function of time and separation between Dot and Cecil.

As Dot continued westward along the southern periphery of the subtropical ridge, several forecasts were issued indicating Dot would follow Cecil and turn toward the north prior to reaching Taiwan. However, the subtropical ridge was reestablished in the region to the north of Taiwan after Cecil's passage; subsiding air between the two tropical cyclones probably contributed to the ridging in this area, thereby causing Dot to continue its movement westward toward Taiwan. Although Dot's passage over Taiwan was rapid, the rugged topography of the island had a devastating effect on Dot's low-level circulation. Figure 3-13-5 shows Dot as a well-organized tropical storm with maximum sustained winds of 60 kt (31 m/sec) prior to landfall. Figure 3-13-6 shows Dot 12 hours later in the Formosa Strait, barely distinguishable as a tropical storm. Dot never recovered from the effects of this crossing and dissipated less than a day later over the mountainous regions of eastern China.

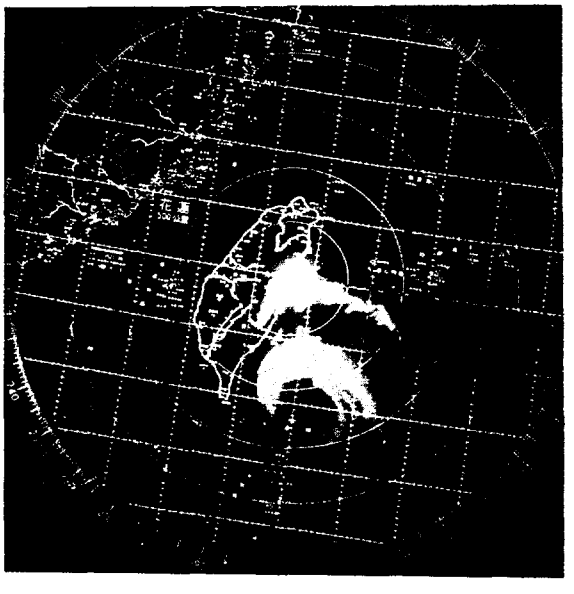

Figure 3-13-5. Tropical Storm Dot was approaching Taiwan from the southeast, as seen by radar from Hua Lien (WMO 46699) at 1414007 August (Photograph courtesy of the Central Weather Bureau, Taipei, Taiwan).

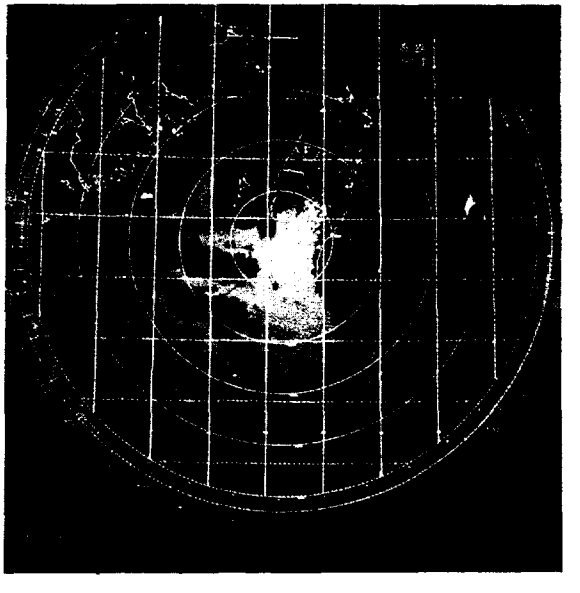

Figure 3-13-6. Tropical Storm Dot, located in the Formosa Strait after crossing southern Taiwan, as seen by radar from Kao-hsiung (WMO 46744) at 1502007 August (Photograph courtesy of the Central Weather Bureau, Taipei, Taiwan).

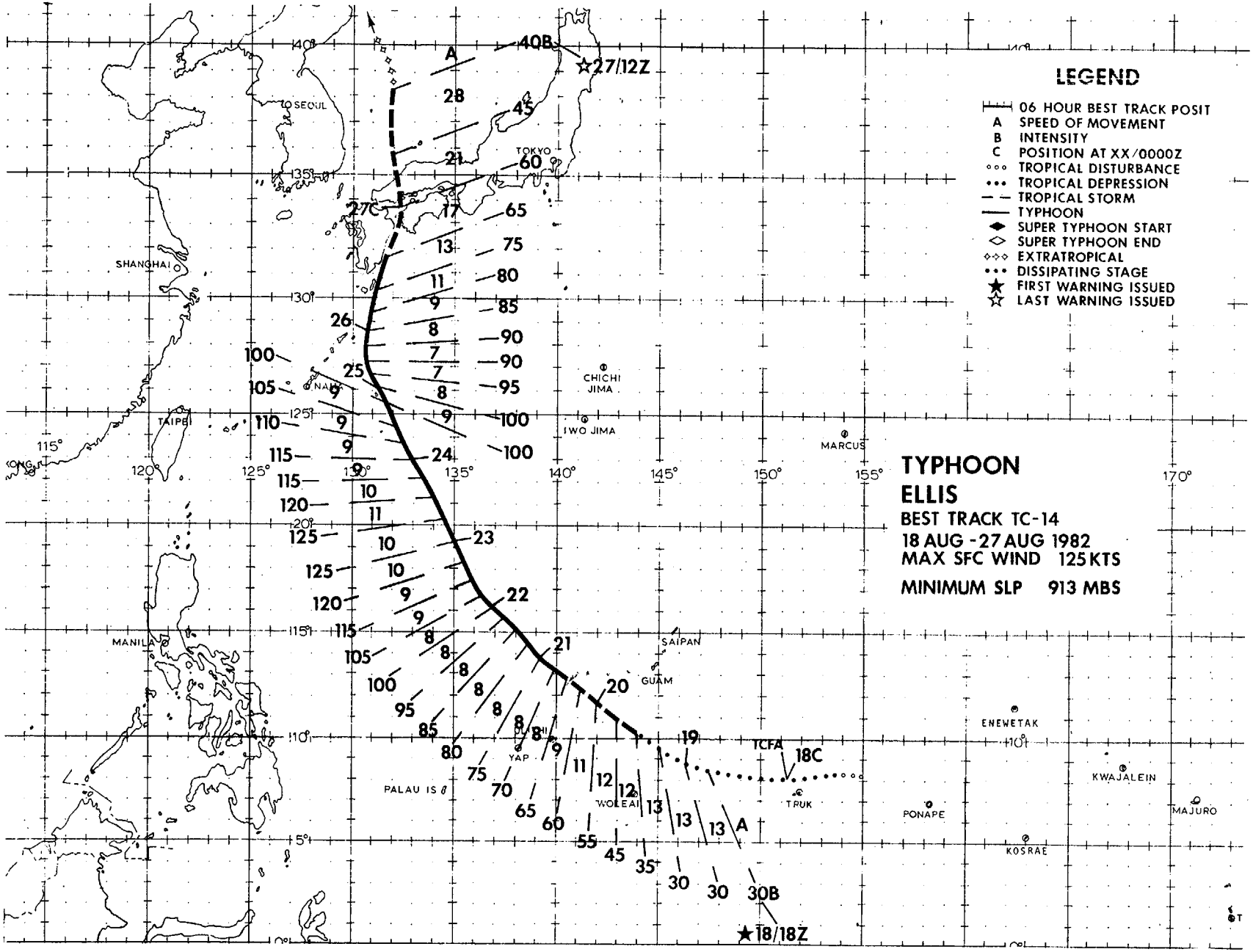
LEGEND
06 HOUR BEST TRACK POSIT
A SPEED OF MOVEMENT
B INTENSITY
C POSITION AT XX/0000Z
TROPICAL DISTURBANCE
TROPICAL DEPRESSION
TROPICAL STORM
TYPHOON
SUPER TYPHOON START
SUPER TYPHOON END
EXTRATROPICAL
DISSIPATING STAGE
FIRST WARNING ISSUED
LAST WARNING ISSUED
TYPHOON
ELLIS
BEST TRACK TC-14
18 AUG - 27 AUG 1982
MAX SFC WIND 125 KTS
MINIMUM SLP 913 MBS
☆27/12Z
★18/18Z
TCFA
SEOUL
TOKYO
SHANGHAI
TAIPEI
MANILA
CHICHI JIMA
IWO JIMA
MARCUS
SAIPAN
GUAM
YAP
PALAU IS
WOLEAI
TRUK
PONAPE
ENEWETAK
KWAJALEIN
MAJURO
KOSRAE

Typhoon Ellis developed from a disturbance that was first detected within the monsoon trough south of Ponape on 15 August. From initial detection to the issuance of a Tropical Cyclone Formation Alert (TCFA) on 18 August, the disturbance slowly acquired convective organization. Once organized, development was quite rapid, with Ellis reaching a peak intensity of 125 kt (64 m/sec) on 23 August.

The TCFA was issued at 180100Z when satellite imagery identified a cloud mass near 8N 151E that had acquired an upper-level outflow channel to the southwest. At 180402Z, the initial reconnaissance aircraft mission located a 20 kt (10 m/sec) circulation center 85 nm (157 km) northwest of Truk Atoll. During the next 24 hours, satellite imagery provided fix positions on the convective center that showed movement toward the west-northwest at speeds approaching 16 kt (30 km/hr).

Based on continued convective organization, the first warning was issued for Tropical Depression 14 at 181800Z. At 191108Z, data from the second reconnaissance aircraft mission indicated maximum winds of 35 kt (18 m/sec) were present and, at 191200Z, Tropical Depression 14 was upgraded to Tropical Storm Ellis. On the 19th Ellis began tracking more northwestward in response to weaker steering currents south of 15N. From the first warning until the seventh warning (200600Z) the forecast scenario anticipated an initial jog to the northwest then, as Ellis began interacting with the subtropical ridge, it would return to a more westward heading. However, a deep mid-latitude trough (near 40N 115E at 200000Z) began to weaken the subtropical ridge southwest of Japan and the anticipated westward movement never materialized. By 201200Z, the effects of this mid-latitude trough on the strength of the subtropical ridge became evident and the forecast track was shifted toward the northwest.

On 20 August, satellite imagery (Figure 3-14-1) indicated the development of a banding-type eye. Ellis was upgraded to typhoon strength at 210000Z when both

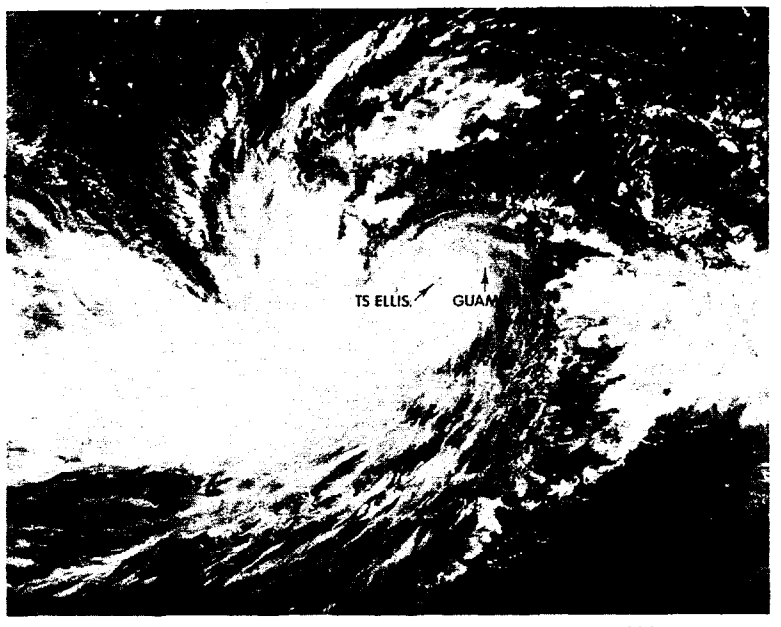

Figure 3-14-1. As an intense tropical storm, Ellis was exhibiting a strong southwest upper-level outflow pattern during a period when a banding-type eye was forming. 200510Z August (NOAA 7 visual imagery).

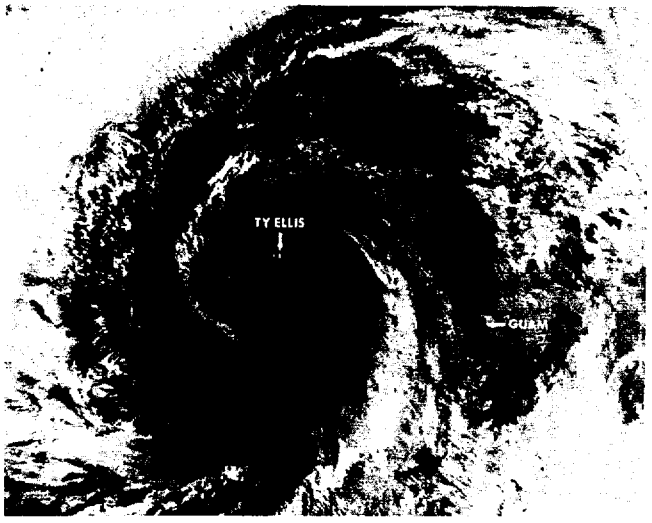

Figure 3-14-2. Typhoon Ellis, with strong upper-level outflow to the east and the southwest, was nearing a peak intensity of 125 kt (64 m/sec) at 221730Z August (NOAA 7 infrared imagery).

aircraft and satellite data supported an intensity greater than minimum typhoon strength (64 kt (33 m/sec)). In the following days, Ellis continued to develop rapidly, passing 100 kt (51 m/sec) intensity on 22 August and peaking at 125 kt (64 m/sec) on 23 August. Figure 3-14-2 shows Ellis just seven hours prior to reaching its maximum intensity.

By 230000Z, significant height falls were evident in the mid-tropospheric levels along the Ryukyu Islands, northwest of Ellis. The mid-latitude trough which had previously influenced Ellis's northwestward track was moving into the Yellow Sea. A day earlier, Ellis had shifted to a north-northwestward track as the subtropical ridge continued to weaken south of Japan. Interestingly, the 14 warnings issued from 221800Z to 260000Z consistently identified Ellis track within 30 nm (56 km) of the eventual best track up to 29N. During this period, both the analyses and numerical forecast fields maintained a very good relationship between the mid-latitude trough near Korea and the subtropical ridge, east of Japan.

As Ellis moved east of Okinawa on 25 August (Figure 3-14-3) its movement shifted toward the north. As early as 240000Z, JTWC forecasts began to anticipate this movement

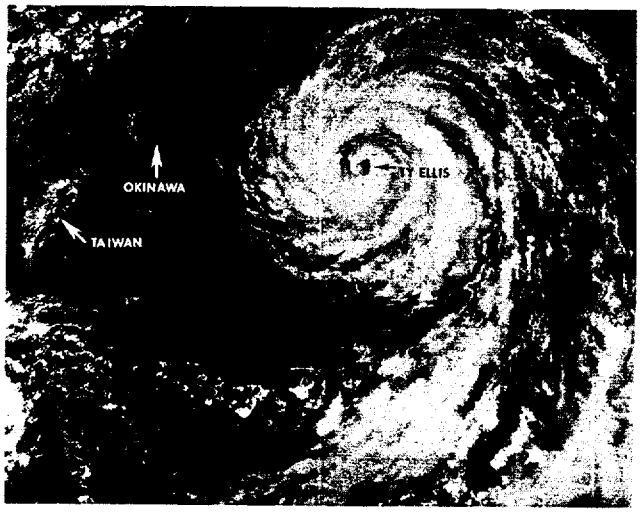

Figure 3-14-3. Typhoon Ellis, located 140 nm (259 km) east of Okinawa, was approaching the mid-latitude westerlies and subsequent acceleration toward the north. 250551Z August (NOAA 7 visual imagery).

as well as significant acceleration as Ellis approached 28N, based on guidance from the Typhoon Acceleration Prediction Technique (TAPT) (Weir, 1982). Unfortunately Ellis slowed to 7 kt (13 km/hr) while approaching 28N and the early acceleration forecasts became premature in the timing of the initial acceleration. However, as Ellis crossed 28N, the predicted acceleration occurred and the speeds attained were very close to those predicted by TAPT.

Once the acceleration was underway, Ellis commenced a more rapid weakening trend as the combined effects of increasing vertical wind shear and interaction with the topography of Kyushu, Skikoku and western Honshu reduced Ellis to an estimated 45 kt (23 m/sec) intensity as it entered the Sea of Japan.

Ellis moved toward the north-northeast on 26 August and passed along Kyushu's eastern coastline and then just west of Hiroshima on 27 August. This jog to the north-northeast was costly for the region, as torrential rains (as much as 28 inches (71 cm) in 24 hours), flooding, landslides, and high winds brought much of southwestern Japan to a virtual standstill. Having left much of its fury behind, Ellis entered the Sea of Japan on 27 August and rapidly transitioned into an extratropical low pressure system which would later move northwestward, passing 120 nm (222 km) west of Vladivostok, USSR.

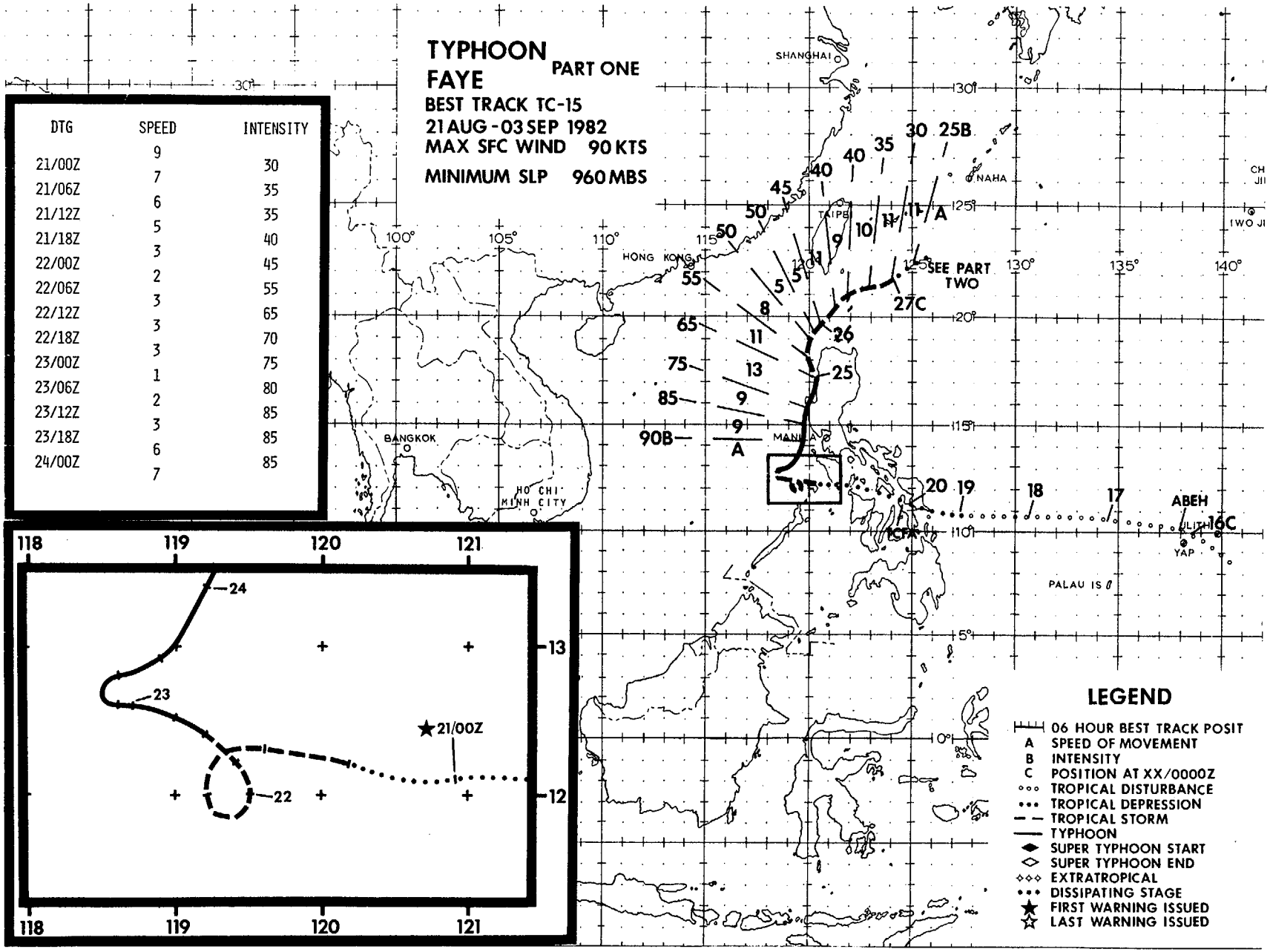
TYPHOON
FAYE
PART ONE
BEST TRACK TC-15
21 AUG - 03 SEP 1982
MAX SFC WIND 90 KTS
MINIMUM SLP 960 MBS
DTG SPEED INTENSITY
21/00Z 9 30
21/06Z 7 35
21/12Z 6 35
21/18Z 5 40
22/00Z 3 45
22/06Z 2 55
22/12Z 3 65
22/18Z 3 70
23/00Z 3 75
23/06Z 1 80
23/12Z 2 85
23/18Z 3 85
24/00Z 6 85
7
SHANGHAI
NAHA
TAIPEI
HONG KONG
BANGKOK
HO CHI MINH CITY
MANILA
YAP
PALAU IS
ABEH
SEE PART TWO
21/00Z
LEGEND
06 HOUR BEST TRACK POSIT
A SPEED OF MOVEMENT
B INTENSITY
C POSITION AT XX/0000Z
TROPICAL DISTURBANCE
TROPICAL DEPRESSION
TROPICAL STORM
TYPHOON
SUPER TYPHOON START
SUPER TYPHOON END
EXTRATROPICAL
DISSIPATING STAGE
FIRST WARNING ISSUED
LAST WARNING ISSUED

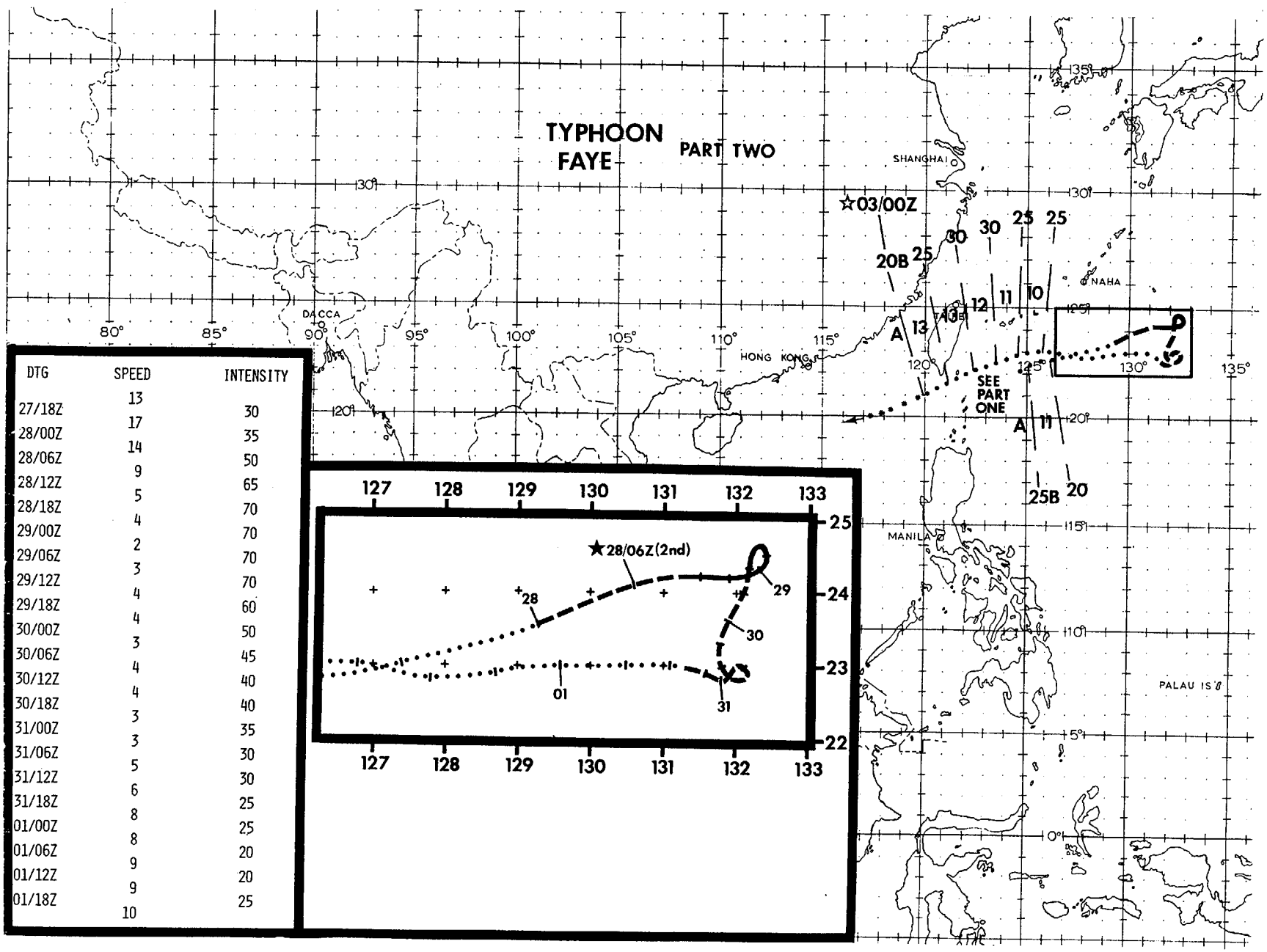

DTG	SPEED	INTENSITY
27/18Z	13	30
28/00Z	17	35
28/06Z	14	50
28/12Z	9	65
28/18Z	5	70
29/00Z	4	70
29/06Z	2	70
29/12Z	3	70
29/18Z	4	60
30/00Z	4	50
30/06Z	3	45
30/12Z	4	40
30/18Z	4	40
31/00Z	3	35
31/06Z	3	30
31/12Z	5	30
31/18Z	6	25
01/00Z	8	25
01/06Z	8	20
01/12Z	9	20
01/18Z	9	25
	10	

Typhoon Faye (15) proved to be one of the more difficult tropical cyclones to forecast during the 1982 season (Figure 3-15-1). With forecast errors of 142, 384, and 629 nm (263, 711, and 1182 km) for 24, 48, and 72 hours, respectively, the forecast history for Typhoon Faye is a good example of what can happen when there is confusion in understanding the effect that the large-scale flow field and other larger tropical cyclones can have on a very small but intense cyclone. In this report the life history of Typhoon Faye is depicted in table form with seven segments (Table 3-15-1). For each segment, key events along with the basic forecast philosophy and prognostic reasoning are described. A brief post-analysis description is then presented in order to compare the actual events of the tropical cyclone and the synoptic situation. In this presentation it will be evident how a basically sound and logical forecast can go astray when all the "facts" are not completely understood. Furthermore, an attempt has been made in this table to describe for the reader the basic forecast/thought process at the JTWC. Figures 3-15-2 to 3-15-7 depict several events along Typhoon Faye's track.

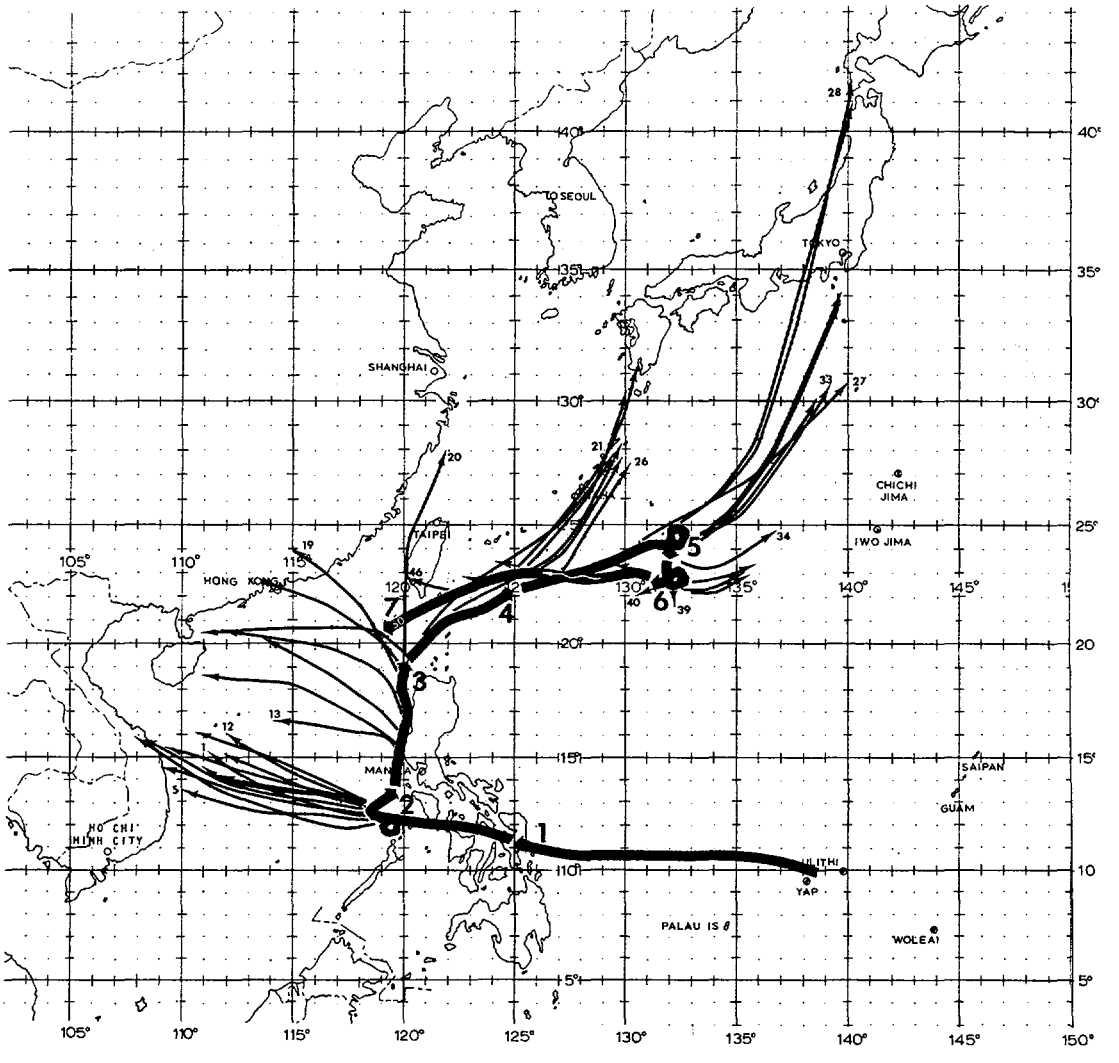

Figure 3-15-1. JTWC Windshield-wiper Chart. This chart depicts the forecast track for each warning issued for Faye. Ideally, in a well-handled forecast situation, there is not a "windshield-wiper" (back and forth) effect but a superposition of one forecast track upon another. Forecast segments will be described in Table 3-15-1.

TABLE 3-15-1

Segment	Time Period (Warnings) *Events	Prognostic Reasoning	Post-analysis Discussion
1	16/00Z - 20/00Z Aug (none) *Weak disturbance moves westward in the Philippine Sea toward the southern Philippines *Monitoring disturbance for indication of convective development	Although an exposed low-level circulation could be identified on satellite imagery as well as on synoptic data, little development was expected due to the proximity of the Philippines and the dominance of the flow pattern around Typhoon Ellis (14) near Guam.	Little difference from prog reasoning. An upper-level anticyclone did develop over the area when an upper trough moved between the system and Ellis; however, convection remained unorganized due to orographic influences from the Philippines.
2	20/00Z - 24/00Z Aug (#1 - #12) *System organizes in the South China Sea *Tropical Cyclone Formation Alert at 200203Z *1st warning at 210000Z in South China Sea *Upgrading to tropical storm status at 210600Z *Upgrading to typhoon status at 221200Z	Movement: Subtropical ridge in the vicinity of Hong Kong was forecast by the FNOC models to persist and strengthen during the forecast period. This would cause the system to slowly increase its forward speed toward the west-northwest. All objective aids predicted a west to northwest movement. Intensification: Dominance of both the upper- and lower-level flow by Ellis in the Philippine Sea, as well as slight northerly shear from the 200 mb ridge over China, was expected to prevent much intensification.	Movement: The dominance of Ellis, as well as the slow encroachment of a frontal zone from central China, prevented much building of the ridge over Hong Kong resulting in weak steering flow near Faye - especially in the lower layers. Faye showed little trend in movement until a frontal/shear zone reached southeastern China on 23-24 Aug (height falls were seen at 500 and 700 mb throughout region). Intensification: Although the adverse vertical shear had an effect on the cyclone, it resulted in a small, restricted system rather than a weak one. A small TUTT cell which was analyzed near Hai-nan Island on 22 Aug appeared to aid Faye's upper-level outflow toward the northeast.
3	24/00Z - 25/18Z Aug (#13 - #19) *System continues northward *System reaches greatest strength (90 kt (46 m/sec)) at 240600Z *System reaches Luzon at 241800Z with significant damage to Wallace Air Station at 242200Z with gusts up to 100 kt (51 m/sec) *Downgrading to tropical storm status at 250000Z	Movement: A persistent northward movement was expected during the initial 24 hours with a more climatological northwestward track in the outlook period. Although the daily analysis indicated that the subtropical ridge over China was moving north and weakening, FNOC prog series continued to call for a gradual strengthening of the ridge with time. Further support of this prognosis was seen in the expected quick movement of Ellis toward the north. Since Ellis was dominating the subtropical regions between 20-30N, its acceleration to the north and out of the subtropics, would allow for the eventual reintensification of the ridge. Finally, a forecast of westward movement continued to be predicted because of two primary reasons: the hesitation to break from the forecast philosophy maintained through the first 19 forecasts and the almost total lack of climatological tracks eastward of the South China Sea. Intensification: Little change from the forecast reasoning in Segment 2. Although northeasterly vertical shear from Ellis continued to dominate, it was now generally thought that Faye would remain strong in spite of the adverse synoptic environment. Only after Faye made landfall on Luzon was a gradual weakening trend predicted.	Movement: Inspite of predictions to the contrary by the FNOC prog series, the ridge over southern China continued to retreat northward and weaken as strong troughing dominated the region between Ellis and Faye. This resulted in an almost due northward movement of Faye. Toward the end of this period, low- to mid-level westerly flow began to strengthen in the Luzon Strait while Ellis slowed its forward speed to 7 kt (13 km/hr) just east of Okinawa. Intensification: Faye continued to intensify until its circulation pattern began to interact with the mountainous terrain of western Luzon. Once landfall was made at 241800Z, a steady deterioration was observed as Faye had trouble maintaining good vertical alignment. The cause of this poor alignment appeared to come equally from the orographic effects of Luzon and the strong vertical shear north of Luzon initiated by Ellis's outflow pattern.

Segment	Time Period (Warnings) *Events	Prognostic Reasoning	Post-analysis Discussion
4	25/18Z - 27/06Z Aug (#20 - #26) *System begins to move northeastward at 251800Z *Initial final warning at 270600Z	Movement: Once Faye began to move northeastward at 11 kt (20 km/hr) along the low-level flow induced by Ellis, it was assumed that it would continue this motion until it reached Japan as FNOC prog series maintained a trough in this region throughout the period. Intensification: It was believed that if Faye could maintain its vortex, slow reintensification was possible once the strong shear from Ellis subsided. This scenario was abandoned for gradual dissipation when aircraft missions continued to show a weakening trend.	Movement: Initial northeast movement was well predicted; however, toward the end of the period the low-level flow began to split in the vicinity of Faye with a portion of the flow moving northward into the trough and the other portion moving east-southeastward toward the newly developed Tropical Storm Gordon (16). Faye began to follow this more eastward track near the end of the period. Intensification: Upper-level shear from the remains of Ellis continued to hamper Faye's efforts to reintensify. This adverse environmental effect reduced Faye to an exposed low-level circulation with only a few isolated convective cells.
5	27/06Z - 29/18Z Aug (#27 - #33) *System continues on a east-northeastward track *System reintensifies to tropical storm status at 280000Z *JTWC resumes warning status at 280600Z *System intensifies to typhoon strength at 280900Z *System weakens to tropical storm strength at 291500Z	Movement: After Ellis moved north of Japan, the long wave trough was positioned over western Japan and the Sea of Japan. Since FNOC Progs predicted little change in pattern, a forecast track toward the northeast appeared the most logical. This was also supported by the CYCLOPS steering aids and the dynamic models. The JTWC TAPT technique - which keys on the 200 mb flow - predicted rapid acceleration toward the northeast north of 25N was likely. The direction of movement was predicted along the 500 mb flow. Intensification: Wind intensities were forecast based on persistence in the near term and gradual weakening with increasing latitude in the outlook period.	Movement: Although the upper trough remained over Japan as predicted, Faye perhaps due to its small size, failed to entrain into this flow or move north of 25N. Instead it appeared to be trapped within the low-level trough between Faye and Gordon and after 281800Z it became quasi-stationary. This resulted in very large forecast errors for this period. Intensification: Once Faye moved out of the strong shearing environment, rapid intensification occurred. Faye went from a weak tropical depression to a typhoon in 27 hours. This reintensification was not well predicted nor was its extremely small size (smaller than that observed in the South China Sea). Aircraft at this time measured maximum surface winds of 70 kt (36 m/sec) out to only 10 nm (19 km) from the center and 30 kt (15 m/sec) winds out to 60 nm (111 km).

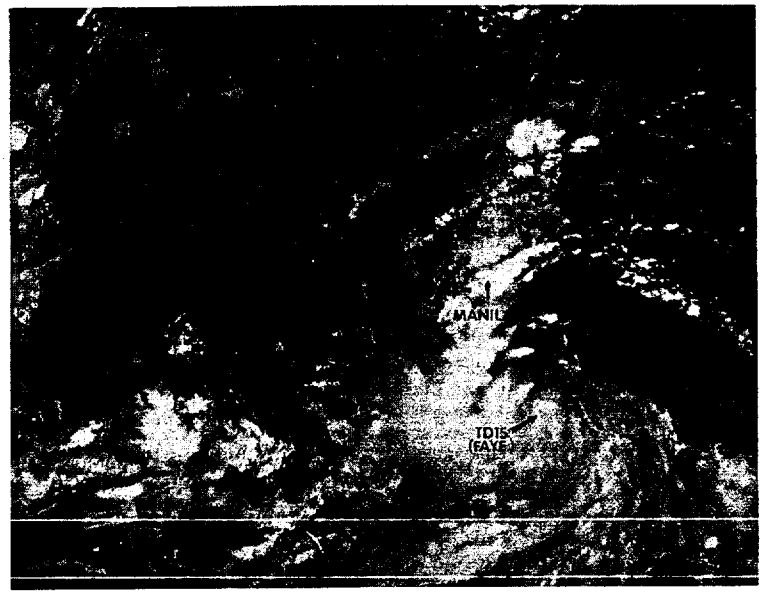

Figure 3-15-2. (Segment 1) Faye, as a tropical depression, crossing the southern Philippines. Although wind speeds were generally less than 25 kt (13 m/sec), widespread damage to property and agriculture was reported by Philippine newspapers due to flooding. 200652Z August (NOAA 7 visual imagery).

Segment	Time Period (Warnings) *Events	Prognostic Reasoning	Post-analysis Discussion
6	29/18Z - 31/06Z Aug (#34 - #39) *System shows little trend in movement and continues to weaken	Movement: Since it was apparent that Faye was not responding to the mid-latitude trough to the north, it was forecast to move eastward with the low-level flow directed toward Typhoon Gordon (16). Initially, movement was expected to be slow since the analysis fields indicated weak steering flow within the trough between Faye and Gordon. Once Gordon moved north, stronger westerlies were expected to accelerate Faye's low-level circulation eastward. Intensification: Dissipation was expected within 24 to 48 hours due to the proximity of Faye to Gordon's strong upper-level outflow pattern.	Movement: During this period, Gordon failed to maintain a steady northward motion. Instead, Gordon slowed its forward speed to 5 kt (9 km/hr). This, in turn, resulted in extremely weak steering flow at all levels around Faye. Toward the end of the period, a ridging pattern began developing over western Japan resulting in a slight increase in northerly and then northeasterly flow. Faye began to move slowly southwestward in response to this flow. Intensification: Although Faye continued to weaken as predicted, the cause was not from Gordon's upper-level wind pattern but from the movement of an upper trough from China to a position over Faye. This resulted in Faye being stripped of its convection, leaving an exposed low-level circulation.
7	31/06Z Aug - 03/06Z Sep (#40 - #50) *System weakens to a tropical depression at 310600Z *System drifts westward for three days as an exposed low-level circulation *Final warning issued by JTWC for Faye at 030000Z *System dissipates in the South China Sea at 030600Z	Movement: With the ridge well established north of the system and over western Japan, a predicted westward movement appeared to be best. Intensification: Aircraft reconaissance indicated that Faye's central pressure had risen to 999 mb and so each warning during this period predicted dissipation within 24 hours.	Movement: Forecast track was fairly accurate although Faye's increase in forward speed to 13 kt (24 km/hr) was not anticipated. Intensification: Although its wind intensities were only 20-30 kt (10-15 m/sec), Faye managed to survive as a low-level circulation much longer than predicted. Final dissipation did not occur until Faye's exposed low-level circulation became entrained into the monsoon circulation that was to become Typhoon Hope (17) in the South China Sea.

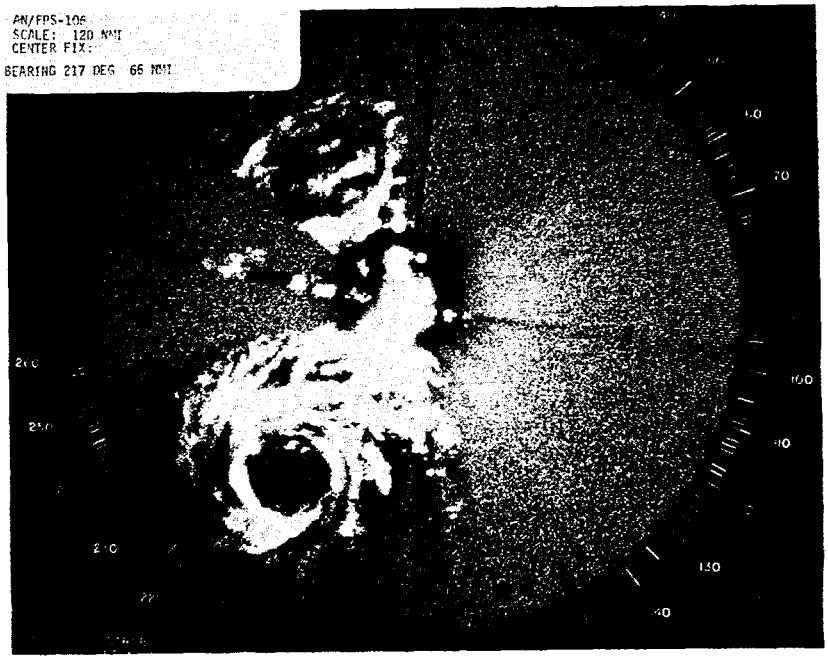

Figure 3-15-3. (Segment 3) The "eye" of Typhoon Faye as seen by radar 66 nm (122 km) southwest of Subic Bay at 240358Z August. (Photograph courtesy of NOCF, Cubi Pt, Republic of the Philippines)

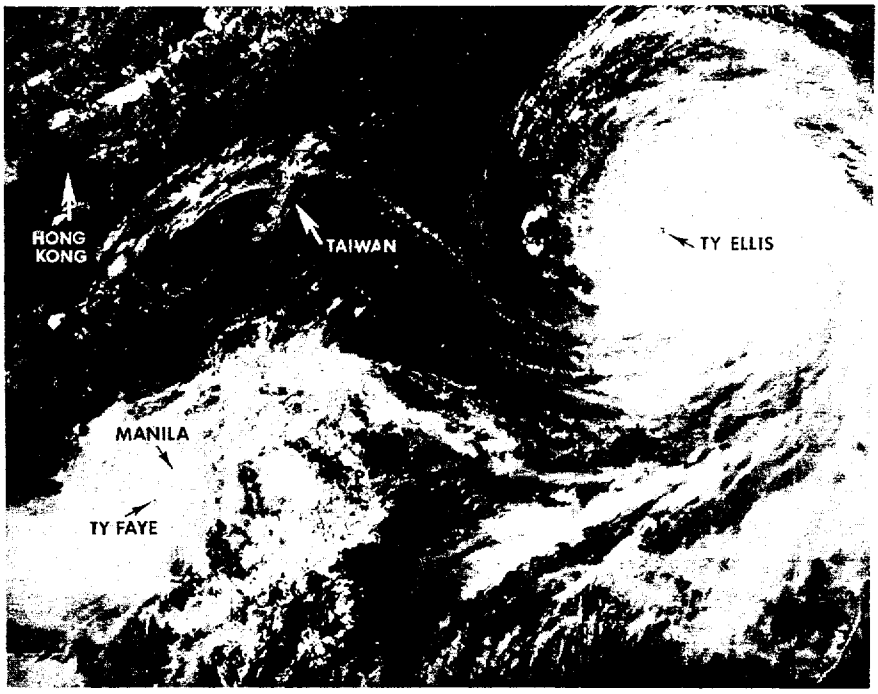

Figure 3-15-4. (Segment 3) Typhoon Faye at full strength, 90 kt (46 m/sec), just south of Luzon. The much larger Typhoon Ellis, 110 kt (57 m/sec), can be seen 925 nm (1713 km) northeast of Faye. 240603Z August (NOAA 7 visual imagery)

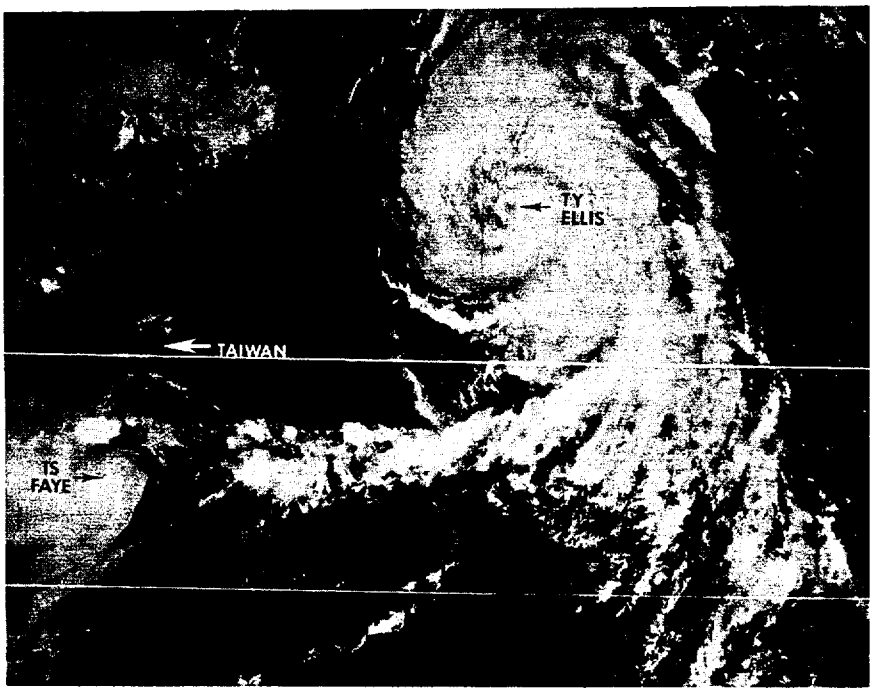

Figure 3-15-5. (Segment 4) Tropical Storm Faye just south of Taiwan weakening rapidly at 260539Z August as it moves under the strong upper-level outflow of Typhoon Ellis. (NOAA 7 visual imagery)

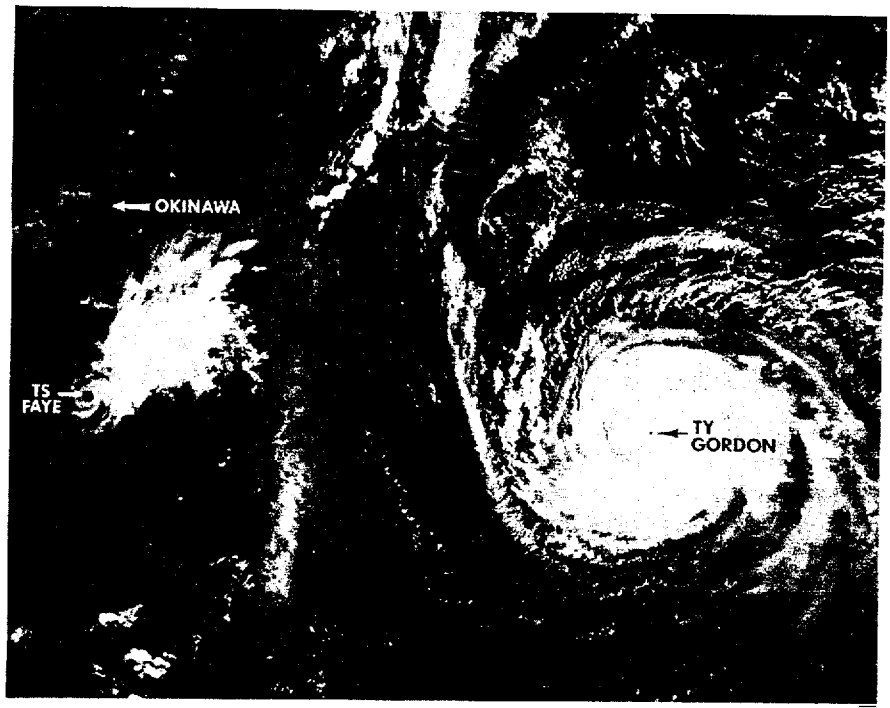

Figure 3-15-6. (Segment 6) Tropical Storm Faye, 50 kt (26 m/sec), once again being dwarfed by another tropical cyclone (Typhoon Gordon, 100 kt (51 m/sec)) at 300451Z August (NOAA 7 visual imagery)

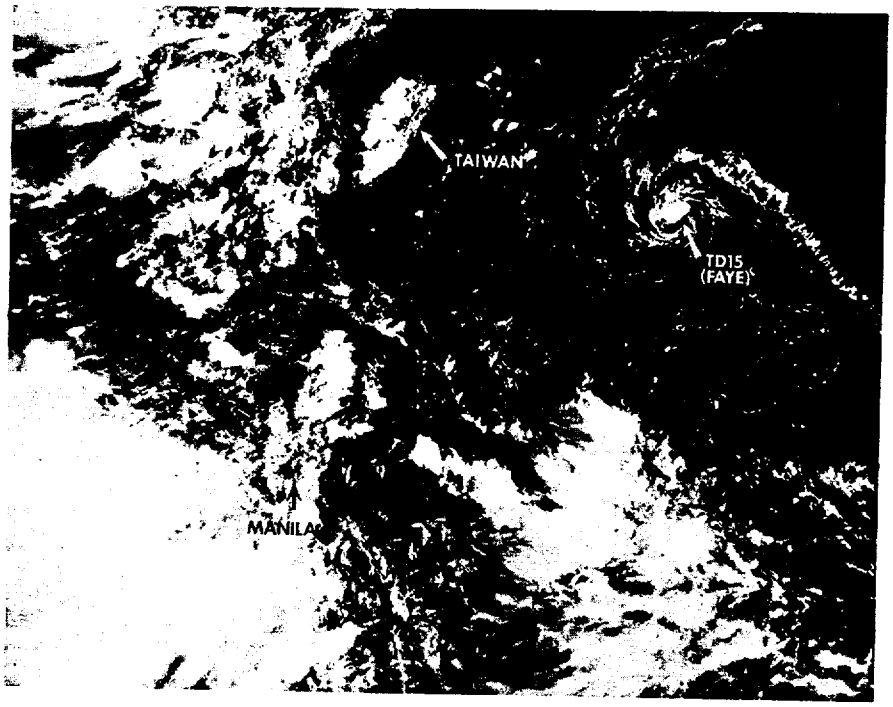

Figure 3-15-7. (Segment 7) An exposed low-level circulation can be seen just east of Taiwan as the remains of Typhoon Faye at 010608Z September. This weak circulation persisted for over three days. (NOAA 7 visual imagery)

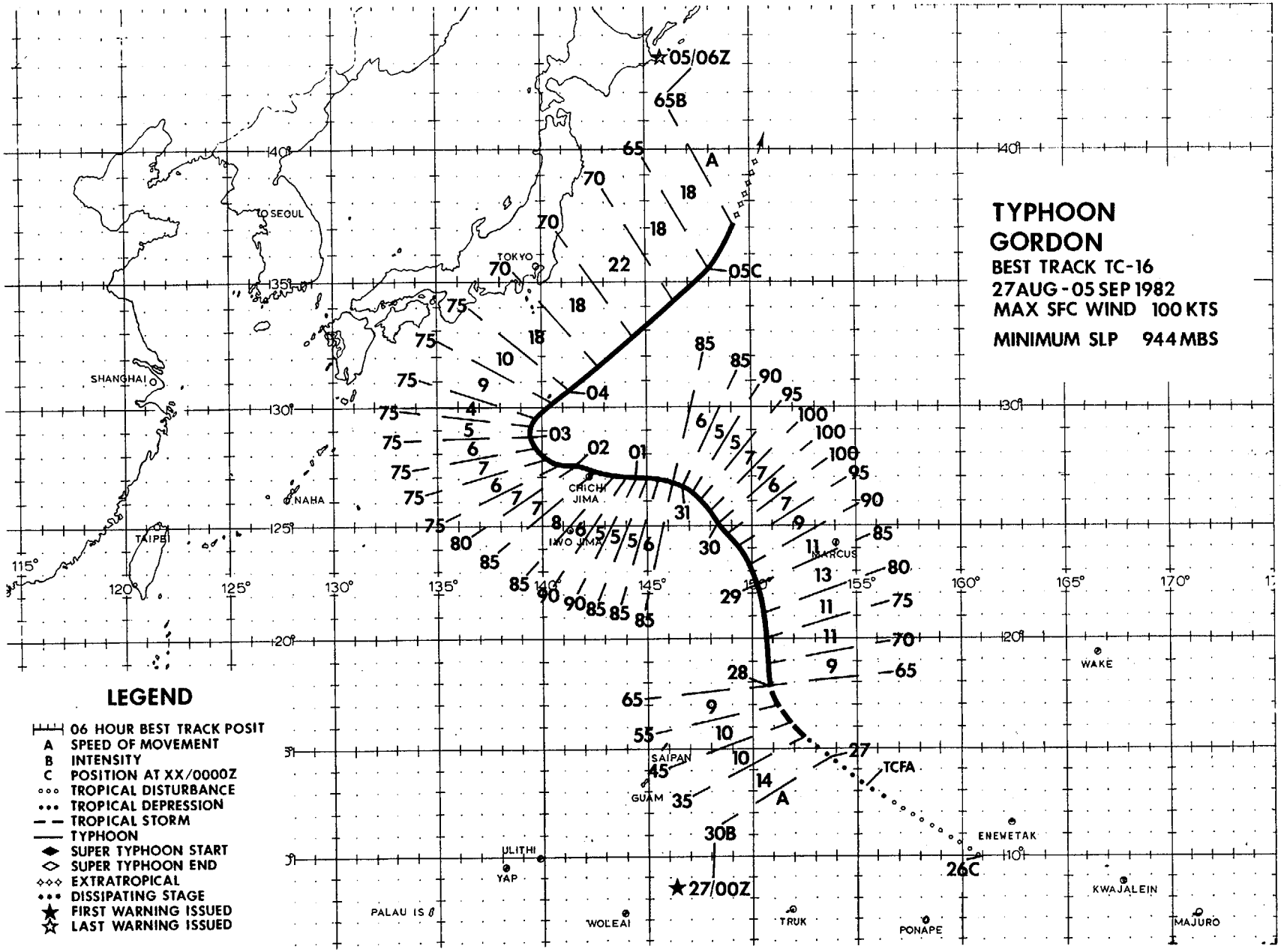
TYPHOON
GORDON
BEST TRACK TC-16
27AUG - 05 SEP 1982
MAX SFC WIND 100 KTS
MINIMUM SLP 944 MBS
LEGEND
06 HOUR BEST TRACK POSIT
A SPEED OF MOVEMENT
B INTENSITY
C POSITION AT XX/0000Z
TROPICAL DISTURBANCE
TROPICAL DEPRESSION
TROPICAL STORM
TYPHOON
SUPER TYPHOON START
SUPER TYPHOON END
EXTRATROPICAL
DISSIPATING STAGE
FIRST WARNING ISSUED
LAST WARNING ISSUED
05/06Z
05C
27/00Z
26C
TCFA
SEOUL
TOKYO
SHANGHAI
NAHA
TAIPEI
CHICHI JIMA
IWO JIMA
MARCUS
WAKE
SAIPAN
GUAM
ENEWETAK
ULITHI
YAP
PALAU IS
WOLEAI
TRUK
PONAPE
KWAJALEIN
MAJURO

Typhoon Gordon developed rapidly from a disturbance which was initially detected while it was embedded in an elongated monsoon trough along 8N between 145E and 175E. Within 48 hours of its initial detection, Gordon reached typhoon strength and eventually proved to be one of the most difficult typhoons of the season for JTWC forecasters.

On 25 August, a surface circulation was detected near 8N 163E associated with an area of strong, yet unorganized convection. During the ensuing 24 hours little increase in convective organization was noted on satellite imagery; however, an upper-tropospheric pattern existed nearby that was conducive for further development. Analysis data indicated that outflow channels were readily available via an upper-level anticyclone centered near 10N 167E, further enhanced by a tropical upper-tropospheric trough (TUTT) north of Guam.

Rapid development did not occur until the upper-level anticyclone moved over the surface circulation. A TUTT cell located northwest of the disturbance enabled outflow channels to remain open to all quadrants and resulted in a significant increase in convection on 26 August. A Tropical Cyclone Formation Alert (TCFA) was issued at 261500Z during this burst in convective activity and organization. Synoptic data from Truk Atoll (WMO 91334) and Ponape (WMO 91348) at 261200Z also indicated intensification was occurring as gradient level winds increased to near 30 kt (15 m/sec) at both reporting stations.

A reconnaissance aircraft investigative mission at 262347Z was able to fix a circulation center near 14.5N 154E with associated surface winds of 30 kt (15 m/sec) and a 1001 mb sea level pressure. These data preceded the issuance of the first warning for Tropical Depression 16 at 270100Z. One day later, at 272335Z, reconnaissance aircraft data showed Gordon's central sea level pressure had dropped to 977 mb and surface winds of 65 kt (33 m/sec) were observed in the north semicircle. During this period of intensification, Gordon was upgraded to tropical storm status at 270600Z and typhoon status at 280000Z based on reported aircraft data and steadily increasing cloud system organization. At 291800Z, four days after initial detection, Gordon's rapid intensification ended at 100 kt (51 m/sec) (See Figure 3-16-1).

The forecasts issued by JTWC during Gordon's developing stages anticipated a northwestward movement toward a weakness in the subtropical ridge located near 20N 150E. These forecasts anticipated recurvature to occur as Gordon moved north of the ridge axis along 23N and came under the influence of an advancing mid-latitude trough. In response to this synoptic situation, Gordon's forward speed slowed as it approached the ridge axis on 28 August; however, the mid-latitude trough continued its eastward movement and by 29 August, its effects on Gordon's movement were no longer evident. Following the passage of this trough, the subtropical ridge was re-established north of Gordon and in response, Gordon resumed a northwestward track along the ridge's southwestern periphery. Forecasts issued on 29 and 30 August reflected Gordon's continued northwestward movement followed by a northward movement and acceleration toward Japan.

By 31 August, a different forecast scenario was gaining strength. At 310000Z, 500 mb and 700 mb height rises were observed over southern Honshu and north of Gordon, indicating the approaching short wave trough was weakening or moving more northeastward than previously forecast. During this period, Gordon, with 90 kt (46 m/sec) surface winds, was advecting large amounts of warm, moist air from the tropics and thereby strengthening the ridge to the northeast. This strengthening of the ridge, combined with changes in the short wave trough, forced Gordon toward

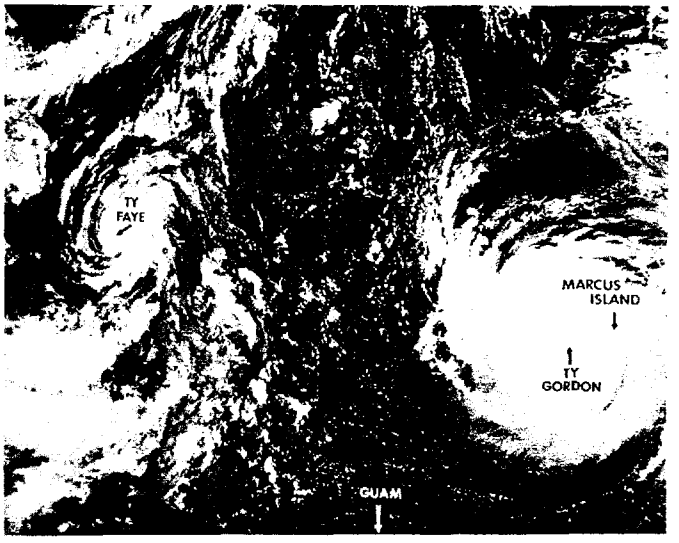

Figure 3-16-1. Typhoon Gordon near maximum intensity of 100 kt (51 m/sec) 640 nm (1185 km) northeast of Guam. Typhoon Faye is also seen in this picture south of Okinawa. 290502Z August (NOAA 7 visual imagery).

a more westward track which was maintained until late on 2 September.

In response to numerical forecast fields which showed a low- to mid-level ridge near Korea building eastward over Japan, JTWC forecasts on 2 September began forecasting a continued westward movement along the southern periphery of the two ridges. By 030000Z, a conflicting forecast scenario began to develop. It was observed that 500 mb and 700 mb heights were falling over southern Honshu, indicating that the short wave trough, located over Hokkaido, was deepening once again. However, the numerical forecast fields provided by Fleet Numerical Oceanography Command (FNOC), Monterey, CA, did not reflect this tendency and continued to build the ridge behind the short wave trough and to the north of Gordon's track. At this time, two opposing forecasts were considered possible: one reflecting the westward track below the ridge; the other, indicating a sharp recurvature and acceleration toward the northeast in response to the deepening trough. JTWC chose to maintain the westward prediction as the FNOC forecast fields appeared to be a meteorologically sound solution to the synoptic situation. Concurrently, an intensive meteorological watch was instituted whereby conventional analysis data and satellite imagery were closely monitored for indication of any changes which would mandate a change from the westward-moving forecast scenario.

On 3 September, Gordon slowed to 4 kt (7 km/hr) from 7 kt (13 km/hr) and took an increasingly more northward course. This movement, combined with the continued 500 mb and 700 mb height falls over Honshu prompted JTWC to abandon the westward forecast at 031200Z, and adopt a forecast toward sharp recurvature and acceleration to the northeast.

Subsequent to the change in the JTWC forecast toward recurvature, the FNOC forecast fields, produced from the 031200Z data base, changed significantly and supported the recurvature scenario. Had the numerical forecast series indicated this trend earlier and not persisted in building the low- to mid-level ridge eastward from Korea, the recurvature track would have been adopted much earlier or perhaps not even abandoned on 2 September. This forecast situation emphasizes the difficulty in issuing credible forecasts when there exists a conflict between the observed short-term changes in the analysis data and the numerically forecast changes beyond the analysis period. There are no easy answers in there situations and unfortunately, in similar future forecast situations, JTWC and its customers may well have to deal with alternating guidance from both analysis and forecast fields.

On 3 and 4 September, Gordon did sharply recurve to the east-northeast as it became embedded in the mid-latitude westerlies along the southeastern periphery of the short wave trough. A fairly rapid acclera-tion to 22 kt (41 km/hr) was observed prior to extratropical transition near 37N at 050600Z. As Gordon recurved, it passed 260 nm (482 km) southeast of Tokyo. The U.S. Naval Oceanography Command Facility at Yokosuka, Japan, reported maximum sustained winds of 32 kt (16 m/sec) with a maximum gust of 44 kt (23 m/sec) during the period, 3 to 4 September. Fortunately, despite some difficult forecast situations, Gordon did not strike any major land mass and there was no significant damage to military or civilian interests in Japan.

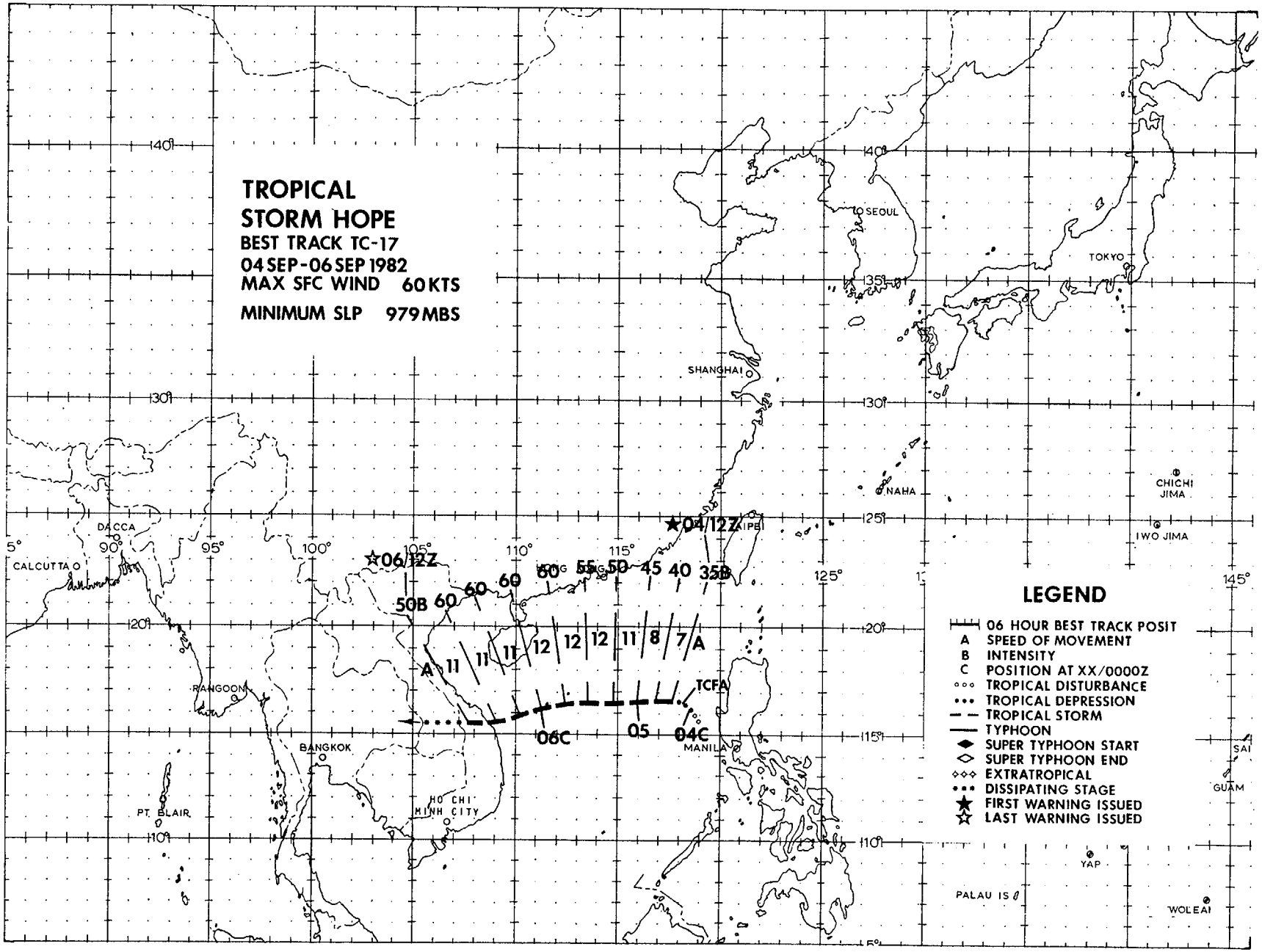
TROPICAL
STORM HOPE
BEST TRACK TC-17
04 SEP-06 SEP 1982
MAX SFC WIND 60 KTS
MINIMUM SLP 979 MBS
SEOUL
TOKYO
SHANGHAI
NAHA
CHICHI JIMA
IWO JIMA
DACCA
CALCUTTA
RANGOON
BANGKOK
PT. BLAIR
HO CHI MINH CITY
MANILA
GUAM
YAP
PALAU IS
WOLEAI
☆06/12Z
★04/12Z
50B 60 60 60 60 55 50 45 40 35B
A 11 11 11 12 12 12 11 8 7/A
TCFA
06C
05
04C
LEGEND
06 HOUR BEST TRACK POSIT
A SPEED OF MOVEMENT
B INTENSITY
C POSITION AT XX/0000Z
TROPICAL DISTURBANCE
TROPICAL DEPRESSION
TROPICAL STORM
TYPHOON
SUPER TYPHOON START
SUPER TYPHOON END
EXTRATROPICAL
DISSIPATING STAGE
FIRST WARNING ISSUED
LAST WARNING ISSUED

Tropical Storm Hope developed from a monsoon depression which formed on 3 September along the northern edge of a strong southwest monsoon flow (25 to 30 kt (13 to 15 m/sec)) that was present over the southern portion of the South China Sea. During the formative stages of this rapidly deepening monsoon depression, shipboard synoptic observations provided essential data which enabled the JTWC to closely monitor the system's development.

At 040345Z, a Tropical Cyclone Formation Alert was issued for an area west of central Luzon when shipboard observations revealed surface pressures had dropped to at least 1002 mb near the depression's center. The 041200Z synoptic data, indicating improved organization in the low-level wind flow, prompted the first warning which was issued at 041500Z. In support of the first two warnings, satellite fix positions - based on a poorly-defined cloud signature - and surface observations did not correlate very well on the system's center. Thus, when a resources permitting aircraft reconnaissance mission at 042357Z located Hope well southwest of the previous warning position, with maximum winds of 45 kt (23 m/sec) and a 994 mb central sea level pressure, the tropical cyclone was relocated and upgraded to tropical storm status on the 050000Z warning.

During the first 30 hours in warning status, Hope intensified to a peak of 60 kt (31 m/sec) which was maintained until landfall. On 6 September, Hope slammed into the coast of Vietnam, 25 nm (46 km) south of Da Nang, and subsequently dissipated over the mountainous terrain of Vietnam and Laos. Accompanying Hope's demise over Southeast Asia, widespread flooding was reported in Vietnam and northeastern Thailand, resulting in several thousand people fleeing their homes and extensive damage to the season's rice crop.

From the first warning, JTWC forecasts continued to anticipate that Hope would slow its forward movement, or move towards the west-northwest and slow. Hope, however, accelerated towards the west-southwest, paralleling the subtropical ridge axis to the north, and the expected forecast movement was never realized.

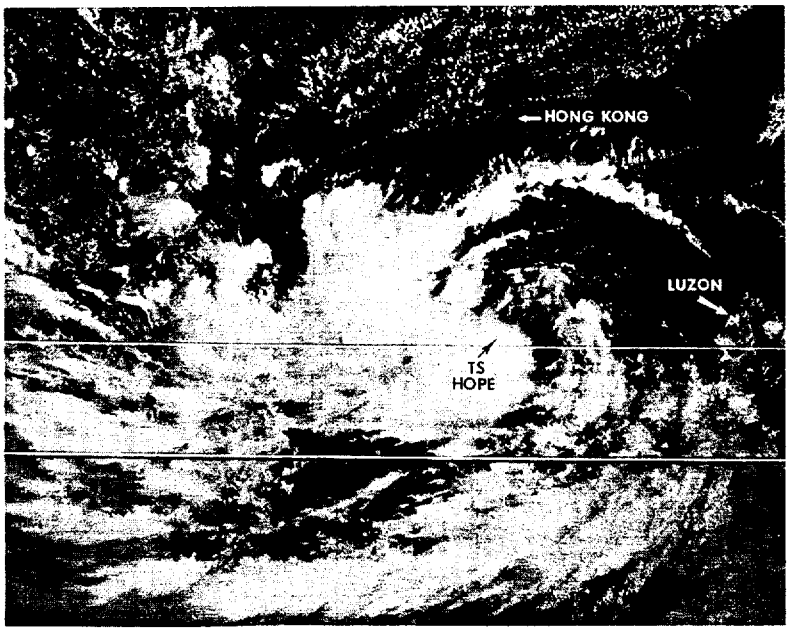

Figure 3-17-1. Tropical Storm Hope near 50 kt (26 m/sec) intensity in the central South China Sea. 050700Z September (NOAA 7 visual imagery).

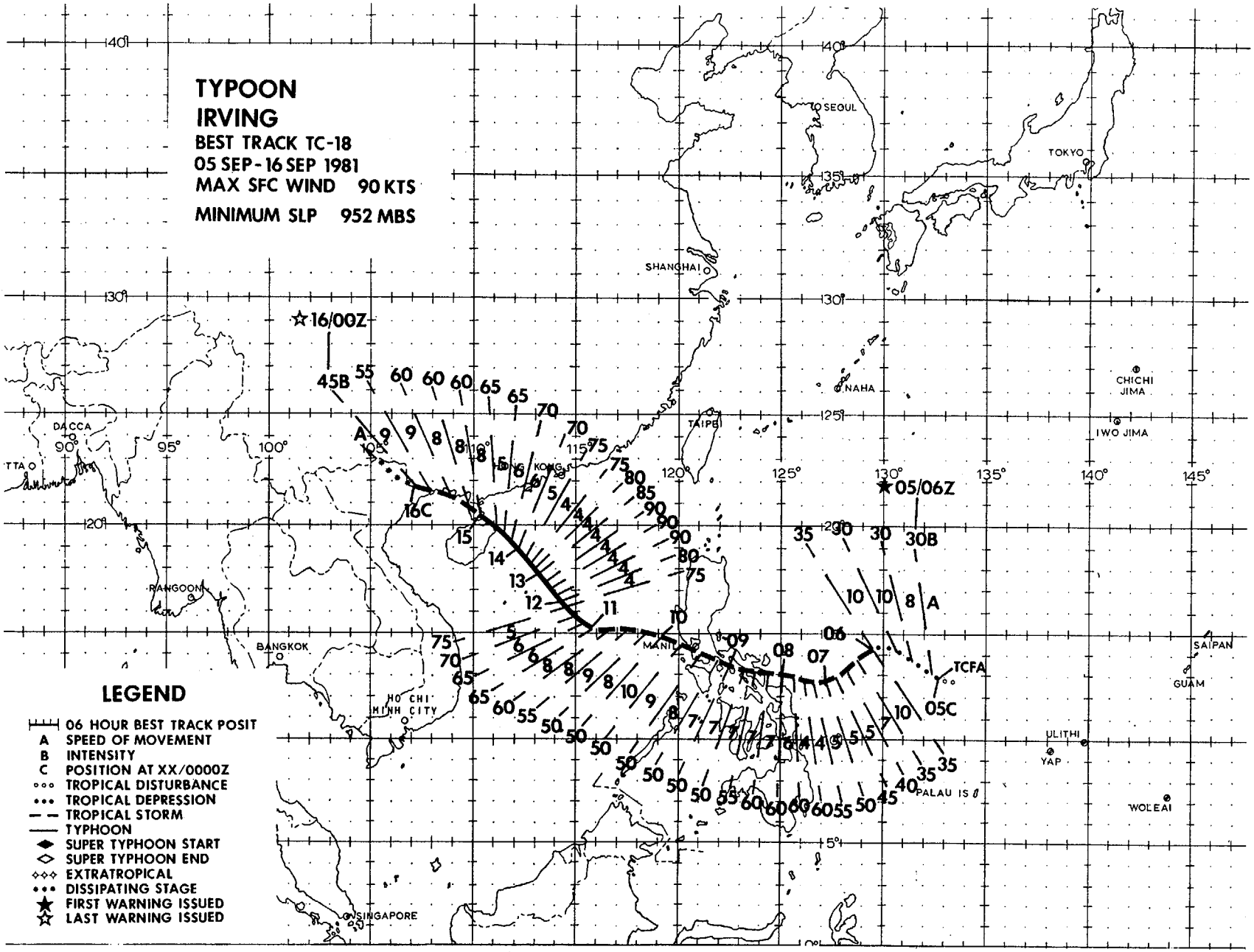
TYPOON
IRVING
BEST TRACK TC-18
05 SEP - 16 SEP 1981
MAX SFC WIND 90 KTS
MINIMUM SLP 952 MBS
16/00Z
05/06Z
TCFA
LEGEND
06 HOUR BEST TRACK POSIT
A SPEED OF MOVEMENT
B INTENSITY
C POSITION AT XX/0000Z
TROPICAL DISTURBANCE
TROPICAL DEPRESSION
TROPICAL STORM
TYPHOON
SUPER TYPHOON START
SUPER TYPHOON END
EXTRATROPICAL
DISSIPATING STAGE
FIRST WARNING ISSUED
LAST WARNING ISSUED
SEOUL
TOKYO
SHANGHAI
NAHA
TAIPEI
HONG KONG
CHICHI JIMA
IWO JIMA
DACCA
RANGOON
BANGKOK
MANILA
HO CHI MINH CITY
SINGAPORE
SAIPAN
GUAM
ULITHI
YAP
PALAU IS
WOLEAI

Typhoon Irving developed within an area of unorganized convection associated with an active monsoon trough anchored south of Guam in early September. Surface pressures throughout the region between 125E to 165E and 8N to 13N were below 1004 mb, and the southwest monsoon flow averaged 20 kt (10 m/sec) over much of the region. By 040300Z, a low-level circulation was evident on visual satellite imagery near 11N 130E, although nearby convection had decreased during the preceding 12 hours. During this period, another tropical cyclone was developing in the monsoon trough near 12N 147E (Typhoon Judy (19)). The passage of Typhoon Gordon (16) east of Japan re-established a low-level easterly flow to the north of both of the developing systems; thus increasing the potential for further development.

As the circulation near 130E (Irving) developed, an increase in cloud organization was seen on satellite imagery which led to the issuance of a Tropical Cyclone Formation Alert at 050000Z. An immediate, abbreviated warning bulletin for Tropical Depression 18 was issued by JTWC at 050855Z, when reconnaissance aircraft closed off a surface circulation with observed winds near 30 kt (15 m/sec). Based on continued convective organization, Tropical Depression 18 was upgraded to Tropical Storm Irving at 051800Z.

Early in its development, Irving was characterized as an exposed low-level circulation center to the east of the most active convection region of the disturbance. Visual satellite imagery and aircraft reconnaissance data enabled JTWC to follow the surface center, rather than the upper-level (convective) center, as Irving moved across the Philippine Sea.

From 6 to 8 September Irving remained equatorward of a strengthening subtropical ridge and maintained a westward track across the Philippine Sea. Irving made landfall at 080900Z, on the southern tip of Luzon (Figure 3-18-1). Maximum winds at landfall were 60 kt (31 m/sec). Thereafter, Irving assumed a more northwestward path (of least resistance) through the Sibuyan Sea

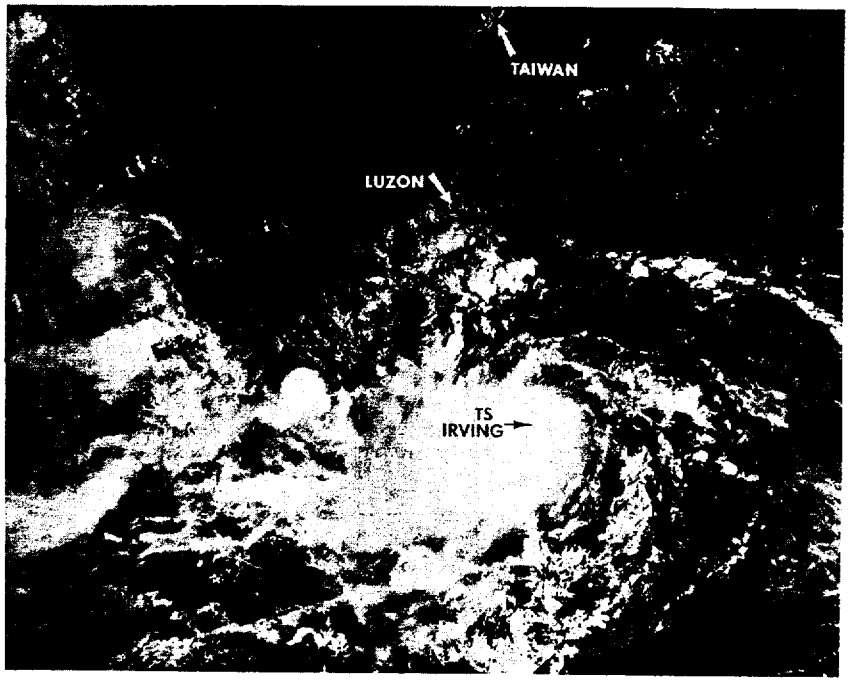

Figure 3-18-1. Tropical Storm Irving near landfall south of Luzon. 081616Z September (NOAA 7 visual imagery)

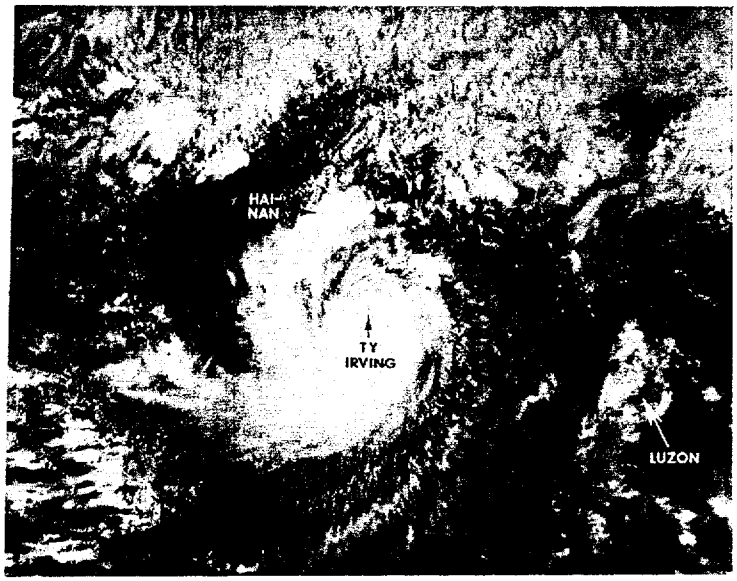

Figure 3-18-2. Typhoon Irving near maximum intensity in the South China Sea. 130706Z September (NOAA 7 visual imagery)

and remained over a marine pathway between the islands of the central Philippines. During this period, Irving maintained much of its intensity although some convective organization was lost. Irving entered the open waters of the South China Sea, 27 nm (50 km) southwest of Cubi Point Naval Air Station at 091700Z. NAS Cubi reported sustained winds of 46 kt (24 m/sec) with a peak gust of 64 kt (33 m/sec) during Irving's transit of the region.

As Irving moved into the South China Sea, a return to a more westward track and gradual intensification were forecast, with the subtropical ridge anticipated to maintain itself north of Irving's track throughout most of the period. A more northwestward track became probable based upon analyses of 500 and 700 mb heights at 110000Z that indicated height falls at both levels were occurring over China. Irving, sensing this developing weakness in the subtropical ridge, maintained

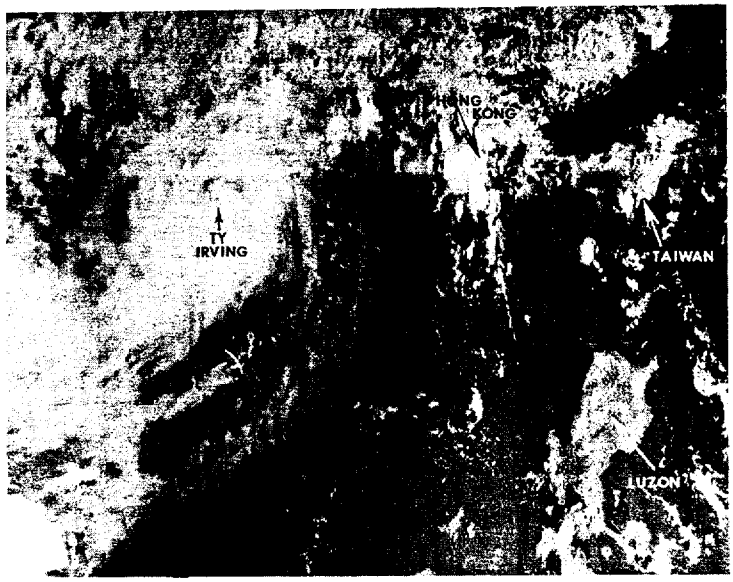

Figure 3-18-3. Typhoon Irving approaching mainland China. 150643Z September (NOAA 7 visual imagery)

a slow, northwestward movement until 141200Z, when a slight acceleration began. Aircraft reconnaissance at 120630Z reported a maximum observed surface wind of 90 kt (46 m/sec), well above the 50 to 65 kt (26 to 33 m/sec) range previously forecast. Figure 3-18-2 shows Irving near peak intensity. The aircraft data also indicated that Irving had a very tight circulation, with the radius of 50 kt (26 m/sec) winds within 60 nm (111 km) of the center during this period of maximum intensity. Radar observations, as well as synoptic reports from the Paracel Islands (WMO 59981 and 59985) were very useful in accurately determining Irving's position and intensity during the period 12-13 September when reconnaissance aircraft fix missions could no longer be flown.

On 15 September, as the system began to interact with Hai-nan Island and the coast of China, Irving was downgraded to tropical storm strength (Figure 3-18-3). Irving made landfall 110 nm (204 km) northeast of Hanoi at 151800Z, and thereafter rapidly dissipated over the mountainous area of Vietnam.

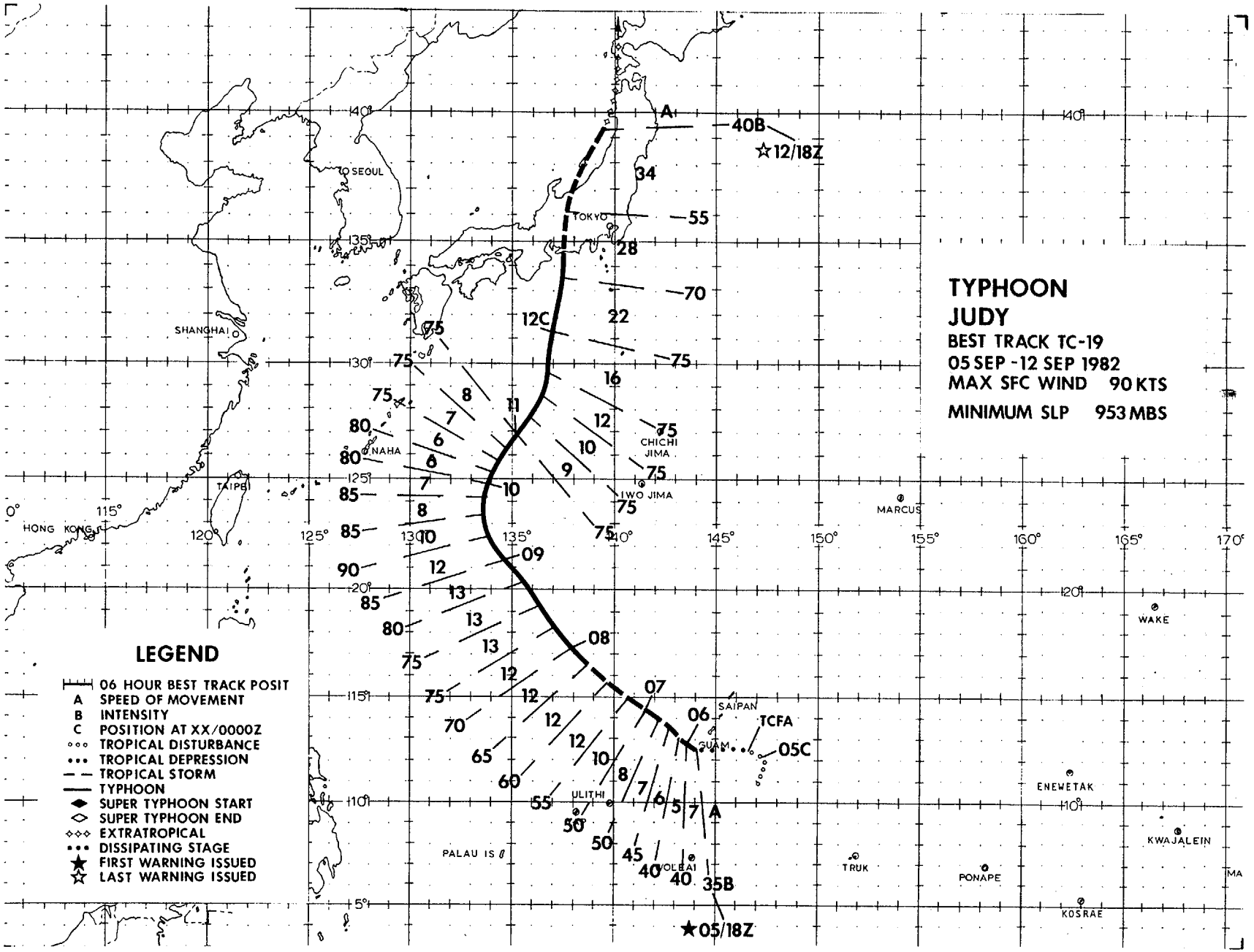
TYPHOON
JUDY
BEST TRACK TC-19
05 SEP - 12 SEP 1982
MAX SFC WIND 90 KTS
MINIMUM SLP 953 MBS
LEGEND
06 HOUR BEST TRACK POSIT
A SPEED OF MOVEMENT
B INTENSITY
C POSITION AT XX/0000Z
TROPICAL DISTURBANCE
TROPICAL DEPRESSION
TROPICAL STORM
TYPHOON
SUPER TYPHOON START
SUPER TYPHOON END
EXTRATROPICAL
DISSIPATING STAGE
FIRST WARNING ISSUED
LAST WARNING ISSUED
SEOUL
TOKYO
SHANGHAI
NAHA
TAIPEI
HONG KONG
CHICHI JIMA
IWO JIMA
MARCUS
SAIPAN
GUAM
TCFA
05C
ULITHI
PALAU IS
WOLEAI
TRUK
PONAPE
KOSRAE
ENEWETAK
WAKE
KWAJALEIN
40B
12/18Z
35B
05/18Z

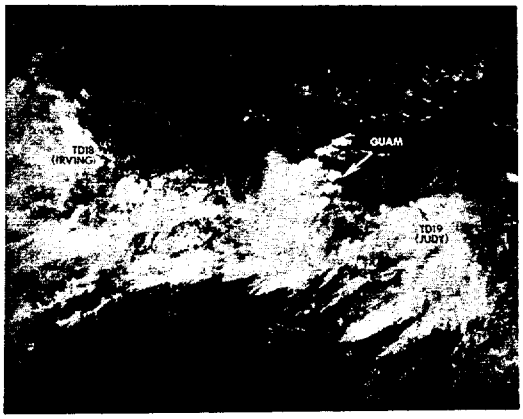

Figure 3-19-1. 050520Z September (NOAA 7 visual imagery).

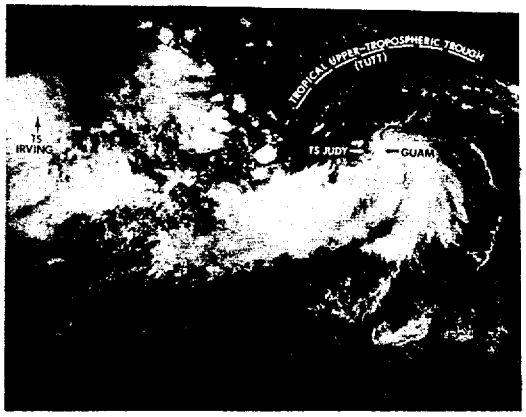

Figure 3-19-2. 060508Z September (NOAA 7 visual imagery).

Typhoon Judy, along with Typhoon Irving (18) developed within a very active monsoon trough that dominated the low-latitudes of the western North Pacific during the first week of September. At 041200Z, synoptic data indicated low-level winds were beginning to organize around the disturbances which later became Judy and Irving. This apparent organization prompted the reissuance of the Significant Tropical Weather Advisory (ABEH PGTW) at 041600Z which discussed each of these systems for the first time. The relatively continuous maximum cloud zone that spawned these two typhoons is shown in Figure 3-19-1, at about the time that a Tropical Cyclone Formation Alert was issued for Judy and the initial warning was issued for Tropical Depression 18 (Irving).

During the ensuing 24-hour period, Judy rapidly organized while Irving slowly intensified. It was during this period that satellite imagery showed the maximum cloud zone segmenting around the two systems (Figure 3-19-2). The first warning for Tropical Depression 19 was issued at 051600Z when satellite imagery indicated a progressive development of cloud features around the system. The first reconnaissance aircraft mission for Judy was conducted at 052239Z and reported 45 kt (23 m/sec) surface winds and a 994 mb minimum sea level pressure. Based on these data, Tropical Depression 19 was upgraded to Tropical Storm Judy on the 060000Z warning.

Initial forecasts for Judy anticipated a movement toward the west-northwest as the numerical forecast series built the subtropical ridge from 150E toward 130E along 25N. However, the subtropical ridge did not build from east to west but built northward along 150E instead. This change in ridge orientation, along with the eastward progression of a short wave trough over Asia, permitted Judy to track northwestward toward eventual recurvature east of Okinawa.

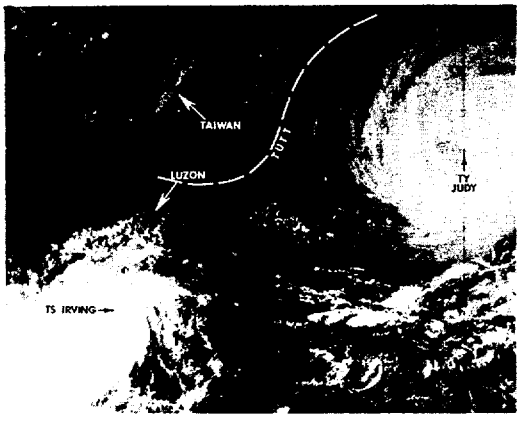

Figure 3-19-3. 090613Z September (NOAA 7 visual imagery).

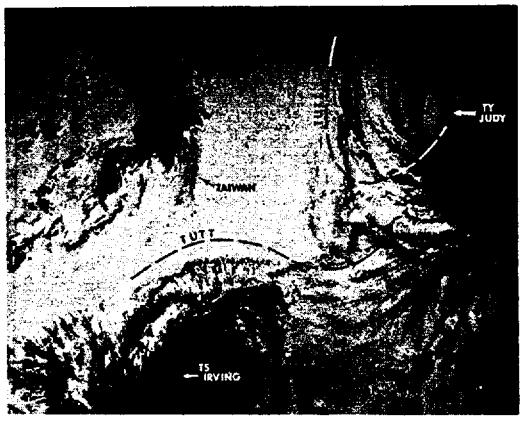

Figure 3-19-4. 091858Z September (NOAA 7 infrared imagery).

From 6 to 9 September, Judy developed at a fairly steady rate (15 to 20 kt (8 to 10 m/sec) per day) and reached a peak intensity of 90 kt (46 m/sec) on 9 September. This period of intensification was aided by a tropical upper-tropospheric trough (TUTT) that was located to the north and northwest of Judy through most of this period.

On 8 and 9 September, 200 mb data and satellite imageries suggested that Judy's upper-level circulation was moving into a region previously occupied by the TUTT. As depicted in Figure 3-19-3, the TUTT axis was contorted northward around the periphery of the advancing Judy. By 091858Z (Figure 3-19-4), satellite imagery revealed that the west quadrant was virtually devoid of deep-layer convection and Judy's center had expanded to more than 90 nm (167 km) in diameter. During this period, Judy exhibited a reversal in sea level pressure tendency and subsequent reintensification was not observed. Based on the interpretation of available data, it appears that at the mid- and upper-tropospheric levels, Judy may have ingested the remnants of the TUTT; and this entrainment of cooler air at these levels may have accounted for the changes in Judy's intensity trend and the resultant satellite signature that were observed on 9 September.

Prior to 081800Z, JTWC forecast tracks predicted that Judy would progress slowly toward the north in the 48- to 72-hour period with a close approach to Okinawa expected. However, with the issuance of warning number 13 at 081800Z, a significant change toward the north and recurvature toward eastern Honshu was forecast. This change in the forecast was prompted by the 081200Z 500 mb and 200 mb analyses data which showed a deeper penetration of a mid-latitude trough, south of Korea, than was previously anticipated.

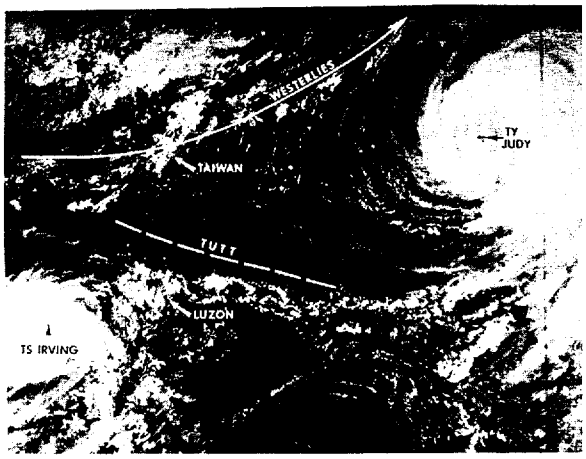

Figure 3-19-5. 100601Z September (NOAA 7 visual imagery)

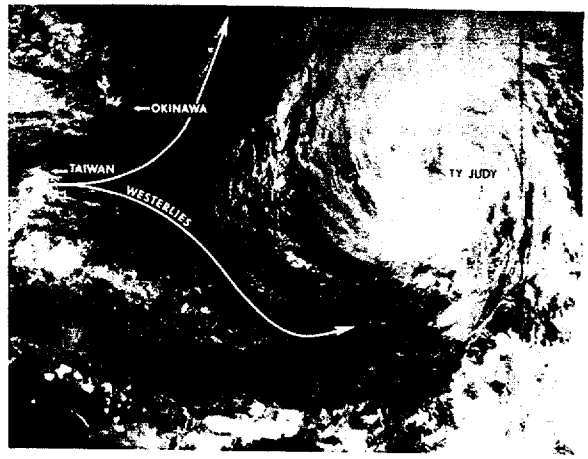

Figure 3-19-6. 110549Z September (NOAA 7 visual imagery)

On 10 September, Judy was moving slowly (6 to 7 kt (11 to 13 km/hr)) toward the north-northeast; satellite imagery (Figure 3-19-5) shows the cloud signature returning to a more circular appearance. Presumably, the interaction with the TUTT had ceased and the mid- and upper-levels were returning to a more typical environment for a mature typhoon.

Judy accelerated toward Japan on the 11th; this movement had been expected as early as 9 September (near 24N) but was delayed until the influence of low-level steering became favorable for a sustained northward movement. A low-level anti-cyclone, centered near 45N 120E, had been exerting a relatively strong north to northeast flow over the Sea of Japan southward to 27N. On 11 September, this anticyclone began to weaken and its influence on the region north of Judy abated. In response, Judy accelerated from 8 kt (15 km/hr) at 110000Z to well over 25 kt (46 km/hr) before it struck Japan 38 hours later. Figure 3-19-6 shows Judy as this acceleration began.

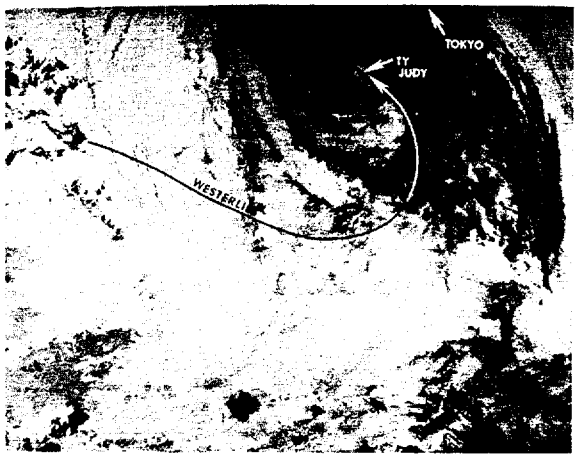

Figure 3-19-7. 111834Z September (NOAA 7 infrared imagery)

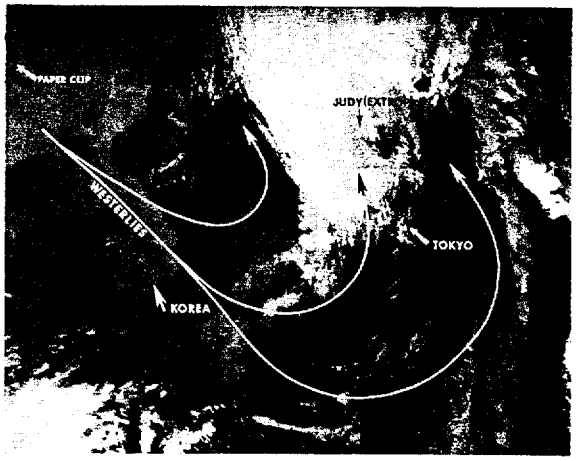

Figure 3-19-8. 121810Z September (NOAA 7 infrared imagery).

As Judy approached 30N, strong upper-level winds from the south-southwest began exerting considerable pressure on Judy. As seen in Figure 3-19-7, convective activity was eroding on the southwestern periphery of Judy's center. This process preceded and accompanied Judy through its extratropical transition (Figure 3-19-8).

At 120800Z, Judy made landfall upon Omaezaki Point in Shizuoka Prefecture, southeast of Nagoya. Judy moved rapidly over the mountainous region of central Honshu and entered the eastern portion of the Sea of Japan where extratropical transition followed. In its wake, Judy left at least 25 dead and the accompanying torrential rains and floods damaged more than 61,000 houses, washed out sections of 956 highways and swept away 46 bridges in an area stretching from Osaka in the south, to Hokkaido in the north.

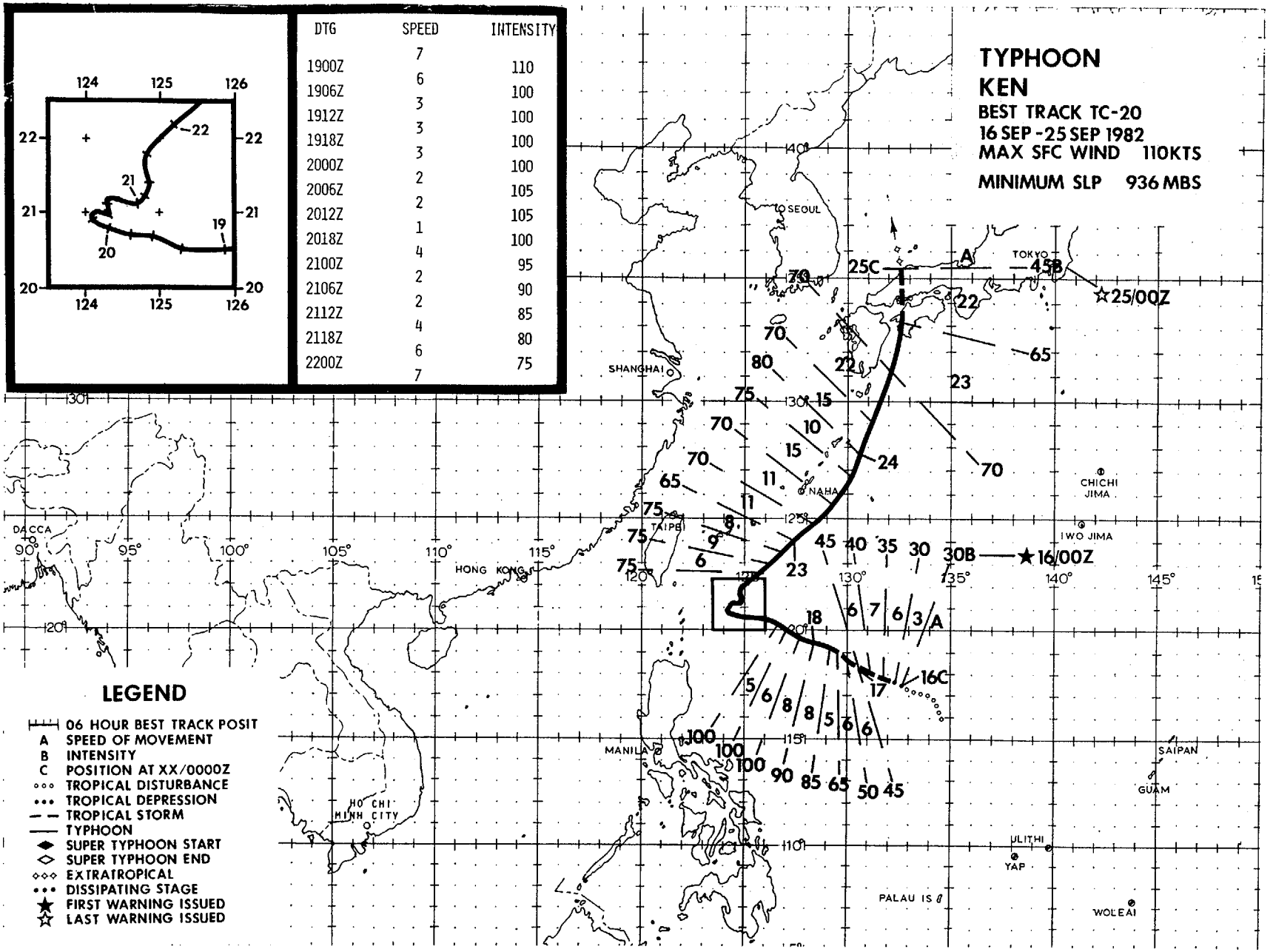
TYPHOON
KEN
BEST TRACK TC-20
16 SEP - 25 SEP 1982
MAX SFC WIND 110KTS
MINIMUM SLP 936 MBS
DTG SPEED INTENSITY
1900Z 7 110
1906Z 6 100
1912Z 3 100
1918Z 3 100
2000Z 3 100
2006Z 2 105
2012Z 2 105
2018Z 1 100
2100Z 4 95
2106Z 2 90
2112Z 2 85
2118Z 4 80
2200Z 6 75
☆25/00Z
★16/00Z
LEGEND
06 HOUR BEST TRACK POSIT
A SPEED OF MOVEMENT
B INTENSITY
C POSITION AT XX/0000Z
TROPICAL DISTURBANCE
TROPICAL DEPRESSION
TROPICAL STORM
TYPHOON
SUPER TYPHOON START
SUPER TYPHOON END
EXTRATROPICAL
DISSIPATING STAGE
FIRST WARNING ISSUED
LAST WARNING ISSUED
SEOUL
TOKYO
SHANGHAI
NAHA
TAIPEI
HONG KONG
MANILA
DACCA
HO CHI MINH CITY
CHICHI JIMA
IWO JIMA
SAIPAN
GUAM
ULITHI
YAP
PALAU IS
WOLEAI

Typhoon Ken formed in mid-September in the western portion of an elongated monsoon trough in the Philippine Sea. Satellite imagery on 14 and 15 September showed a persistent convective disturbance near 17N 134E with evidence of upper- and lower-level circulation centers. A reconnaissance aircraft mission early on 16 September closed off a surface circulation near 18N 133E, with 10 to 35 kt (5 to 18 m/sec) winds and a minimum sea level pressure of 1003 mb. Based on this information, JTWC elected to forgo the issuance of a Tropical Cyclone Formation Alert and, at 160300Z, the initial warning was issued on Ken as Tropical Depression 20.

Ken was upgraded to tropical storm status on the 161200Z warning after aircraft reconnaissance reported a 999 mb central pressure and sustained winds of 35 kt (18 m/sec). Initial warnings for Ken anticipated movement toward the west, passing near the northern tip of Luzon within 72 hours. These forecasts were based on the apparent strength of the mid-level steering flow along the southern periphery of the subtropical ridge which was centered between Taiwan and Okinawa. Thirty-three hours after the initial warning was issued, Ken was upgraded to typhoon status when aircraft reconnaissance data showed a central pressure of 976 mb, equivalent to an intensity of 65 kt (33 m/sec) (Atkinson and Holliday, 1977). Ken underwent a rapid intensification during the following 24 to 36 hours, with its intensity surpassing 100 kt (51 m/sec) on 18 September. Up to this point in its development Ken was characterized as a compact system; for example, aircraft data at 180600Z indicated a 938 mb central pressure in a 10 nm (19 km) diameter eye with a maximum surface wind of 100 kt (51 m/sec) located within a band of maximum winds only 15 nm (28 km) from the center.

Ken moved much slower than anticipated, and toward the west-northwest, for the first four days in warning status. During this period, a gradual but significant change in the subtropical ridge was taking place; by 19 September the ridge had retrograded southwestward and strengthened over southern China and the northern portion of the South China Sea. JTWC forecasts during this period expected this slow movement to be short-lived based on a forecast strengthening of the ridge north of Ken and a corresponding weakening of the ridge over the South China Sea which would allow Ken to resume its movement westward. This forecast scenario never materialized and, aided by analysis and prognostic fields from the 191200Z data base which provided indications that westward movement was not likely to occur, JTWC forecast tracks turned toward the north commencing with the 200000Z warning. Some of the indicators which prompted JTWC to change the forecast track were: the numerical forecast fields were starting to show a persistent break in the ridge north of Ken vice a strengthening of the ridge; the dynamic tropical cyclone models (OTCM, NTCM) began to consistently forecast a northward movement; and analysis data began to show significant height falls at the 700 mb level were starting to occur north of the ridge over southern Japan.

Despite all the signs predicting a northward movement, Ken eventually became quasi-stationary on 20 September (Figure 3-20-1 shows Ken at its westernmost position) and the character of the associated circulation pattern began to change dramatically; aircraft reconnaissance missions found the center expanding, with the strongest wind bands moving away from the center. The diameter and character of the eye (when observed) was also changing from mission to mission. A possible explanation of what

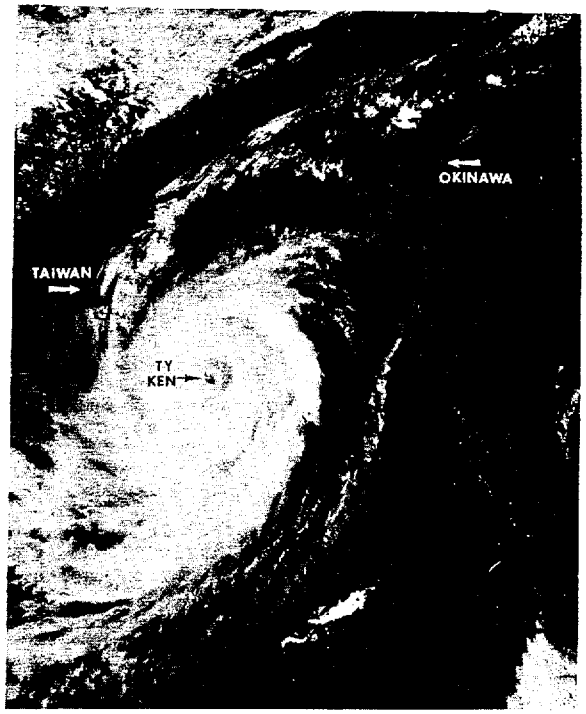

Figure 3-20-1. Typhoon Ken, at its westernmost position and just beginning a period of very little movement. Note the strong banding toward Ken's center. Within the next two days, much of this center would erode, leaving a nearly cloud-free area 60 nm (111 km) in diameter. 200542Z September (NOAA 7 visual imagery provided by Det 4, 1WW Clark AB RP).

caused Ken to undergo such drastic changes could be the interaction with mid-latitude westerlies advecting much cooler air into Ken's center, thus accounting for formation of the large cloud-free center. The 201200Z 500 mb analysis (Figure 3-20-2) shows the winds from the west moving into Ken's circulation about the time that these changes began. However, this does not explain why Ken's eye dissipated and then reformed within the otherwise cloud-free center, unless the westerlies were diverted from the center for short periods of time, allowing warm, moist air to reenter the center and assist in the reformation of the eye.

Ken's eye was last observed at 212011Z during a double-fix aircraft mission. On the first penetration, the mission Aerial Reconnaissance Weather Officer (ARWO) indicated the eye was 7 nm (13 km) in diameter but on the second penetration, at 212327Z, the ARWO reported "... the eye was so large we couldn't even pick it up on our radar ..."[1]. Further, the band of maximum winds were observed some 60 to 95 nm (111 to 176 km) from Ken's center.

On 21 September, satellite imagery and upper air analysis data indicated the trough north of the subtropical ridge had begun to

[1] Candis L. Weatherford, Capt, USAF, mission ARWO.

deepen. In response, Ken began to move erratically toward the northeast and by 211800Z was on a steady course toward Okinawa. The possibility of significant acceleration was examined as continued interaction with the mid-latitude westerlies seemed likely. A recently developed JTWC forecast aid, TAPT (Weir, 1982), indicated Ken might undergo acceleration near 25N. Indeed, as Ken approached 26N, its forward speed began to increase and acceleration continued until landfall on the island of Shikoku, Japan. During this acceleration period Ken passed 78 nm (143 km) southeast of Okinawa; maximum winds recorded at Kadena AB were 35 kt (18 m/sec) at 230955Z and a peak gust of 58 kt (30 m/sec) at 231135Z. Ken also brought a significant, and much needed, rainfall to Okinawa; 11.09 inches (28.2 cm) were recorded at Kadena on 23 September.

Once past Okinawa, Ken began to gradually weaken under strong mid- and upper-level westerlies. Aircraft reconnaissance missions continued to find the belt of maximum surface winds moving farther away from the center with every fix. Satellite imagery showed a steady decline in convection as Ken continued to move toward Japan. Ken made landfall upon Shikoku at 241700Z, crossed the inland sea, and then moved through western Honshu into the Sea of Japan where it became extratropical at 250000Z.

Ken was the fourth typhoon of the season to hit the main islands of Japan; it brought torrential rains and high winds, which triggered mudslides that flooded or wrecked thousands of homes and paralyzed both air and ground transportation. Reports from the region indicated that a peak gust of 114 kt (59 m/sec) was recorded on Shikoku during Ken's passage along with 8.7 inches (22.1 cm) of rain over one six-hour period.

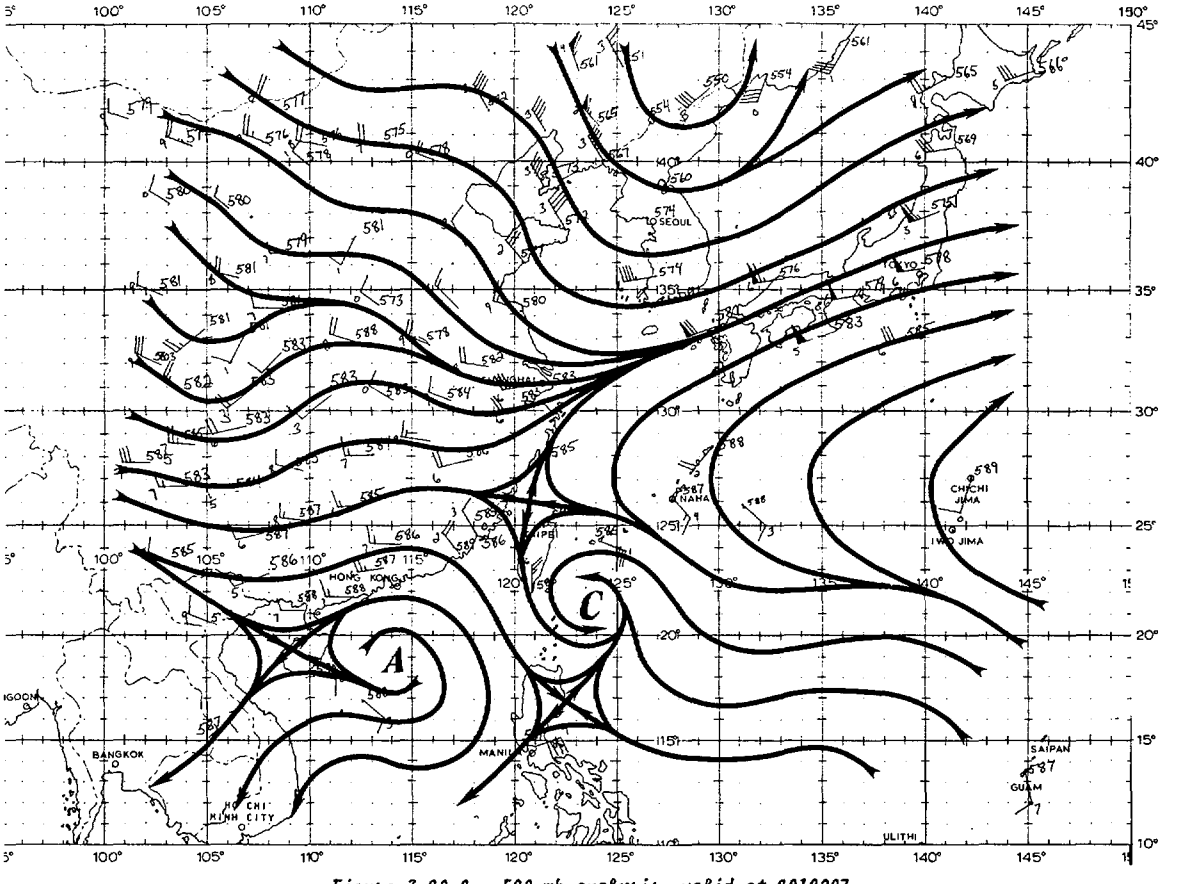

Figure 3-20-2. 500 mb analysis, valid at 201200Z. The strength of the subtropical ridge over China had diminished during the previous 12-hour period. This process allowed mid-latitude westerlies to move further southward and become involved with Ken's circulation pattern. The break in the east-west extension of the ridge, north of Ken, can also be seen. Wind speeds are in knots.

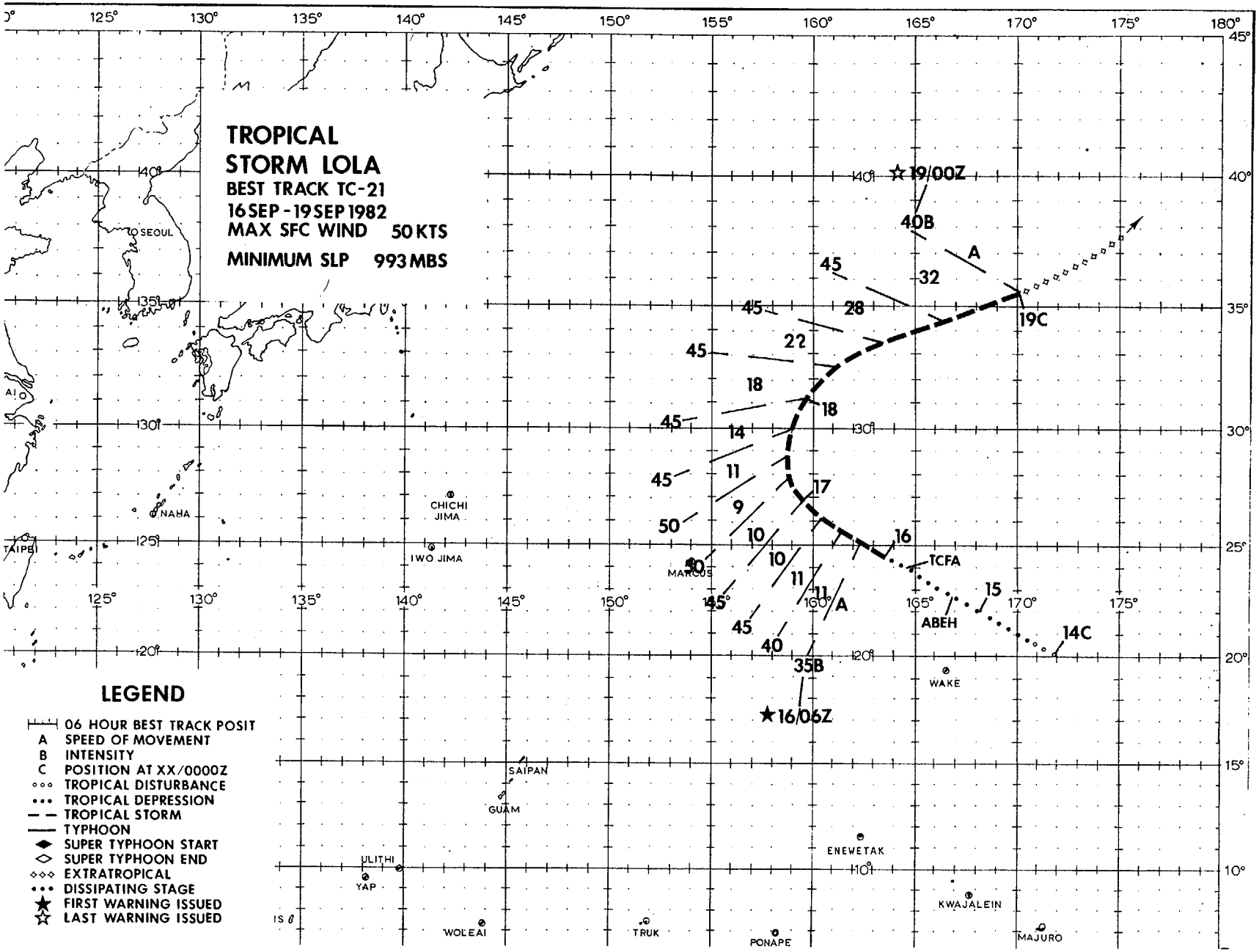
TROPICAL
STORM LOLA
BEST TRACK TC-21
16 SEP - 19 SEP 1982
MAX SFC WIND 50 KTS
MINIMUM SLP 993 MBS
☆19/00Z
40B
A
45
32
45
28
19C
45
22
18
18
45
14
45
11
17
9
50
10
16
TCFA
10
10
11
11
A
45
45
40
15
ABEH
14C
35B
★16/06Z
SEOUL
NAHA
TAIPEI
CHICHI JIMA
IWO JIMA
MARCUS
WAKE
SAIPAN
GUAM
ULITHI
YAP
WOLEAI
TRUK
PONAPE
ENEWETAK
KWAJALEIN
MAJURO
LEGEND
06 HOUR BEST TRACK POSIT
A SPEED OF MOVEMENT
B INTENSITY
C POSITION AT XX/0000Z
TROPICAL DISTURBANCE
TROPICAL DEPRESSION
TROPICAL STORM
TYPHOON
SUPER TYPHOON START
SUPER TYPHOON END
EXTRATROPICAL
DISSIPATING STAGE
FIRST WARNING ISSUED
LAST WARNING ISSUED

Tropical Storm Lola was the third tropical cyclone of the season to form in the subtropical latitudes of the western North Pacific Ocean. Typical of tropical cyclones that form north of 20N in the mid- and late summer, Lola's formation was aided by its proximity to a tropical upper tropospheric trough (TUTT) cell (Sadler, 1976) and remained a small, compact tropical cyclone during its lifetime. Due to Lola's remote location, no successful reconnaissance aircraft missions were flown and all fix positions and intensity estimates were based on analyses from satellite imagery.

Lola was first detected on satellite imagery as a weakly organized band of convection near the dateline on 13 September. By 140000Z, this convection had moved westward to within 600 nm (1111 km) of a well-defined TUTT cell that was located in the vicinity of Wake Island (WMO 91245). During the ensuing 24 hours, the upper-tropospheric divergence fields appeared to increase in the area and a small anticyclone was soon detected on satellite imagery over the disturbance. During the same period, a low-level shear line from a cold front moved to within 200 nm (370 km), north of the convective disturbance. This shear line appeared to aid the development of the low-level circulation center, as cumulus lines could be detected spiraling into the system's center from the north as early as 150000Z.

Convection remained weak and variable over the next 18 hours; however, at 151829Z a Tropical Cyclone Formation Alert was issued when upper-level outflow increased around the system. During the next 12 hours, convective organization increased and at 160600Z, the first warning was issued for Tropical Storm Lola when the intensity estimate from analysis of visual satellite imagery indicated the likelihood of 35 kt (18 m/sec) surface winds near Lola's center.

Lola's eventual recurvature around a mid-tropospheric anticyclone was well forecast due, in part, to good agreement from the very first forecast with the CYCLOPS steering aids and the One-Way Interactive Tropical Cyclone Model (OTCM).

As Lola approached 30N on 17 September, acceleration toward the northeast began in advance of a newly formed cold front which was moving toward Lola from the northwest. Extratropical transition was completed by 190000Z when Lola became totally entrained into the frontal system.

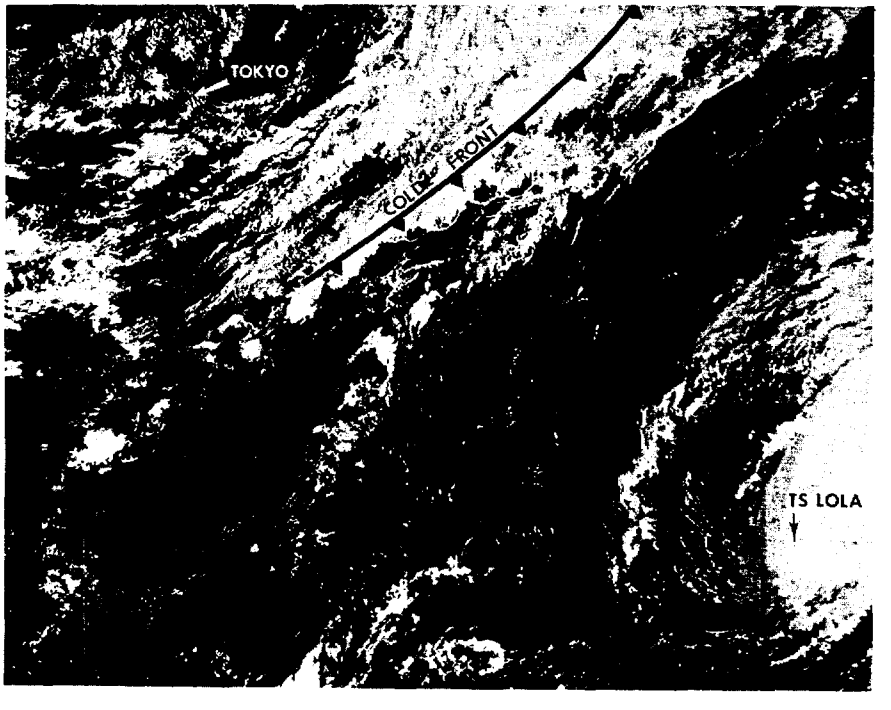

Figure 3-21-1. Tropical Storm Lola at the point of recurvature as a cold front approaches from the northwest. 170436Z September (NOAA 7 visual imagery).

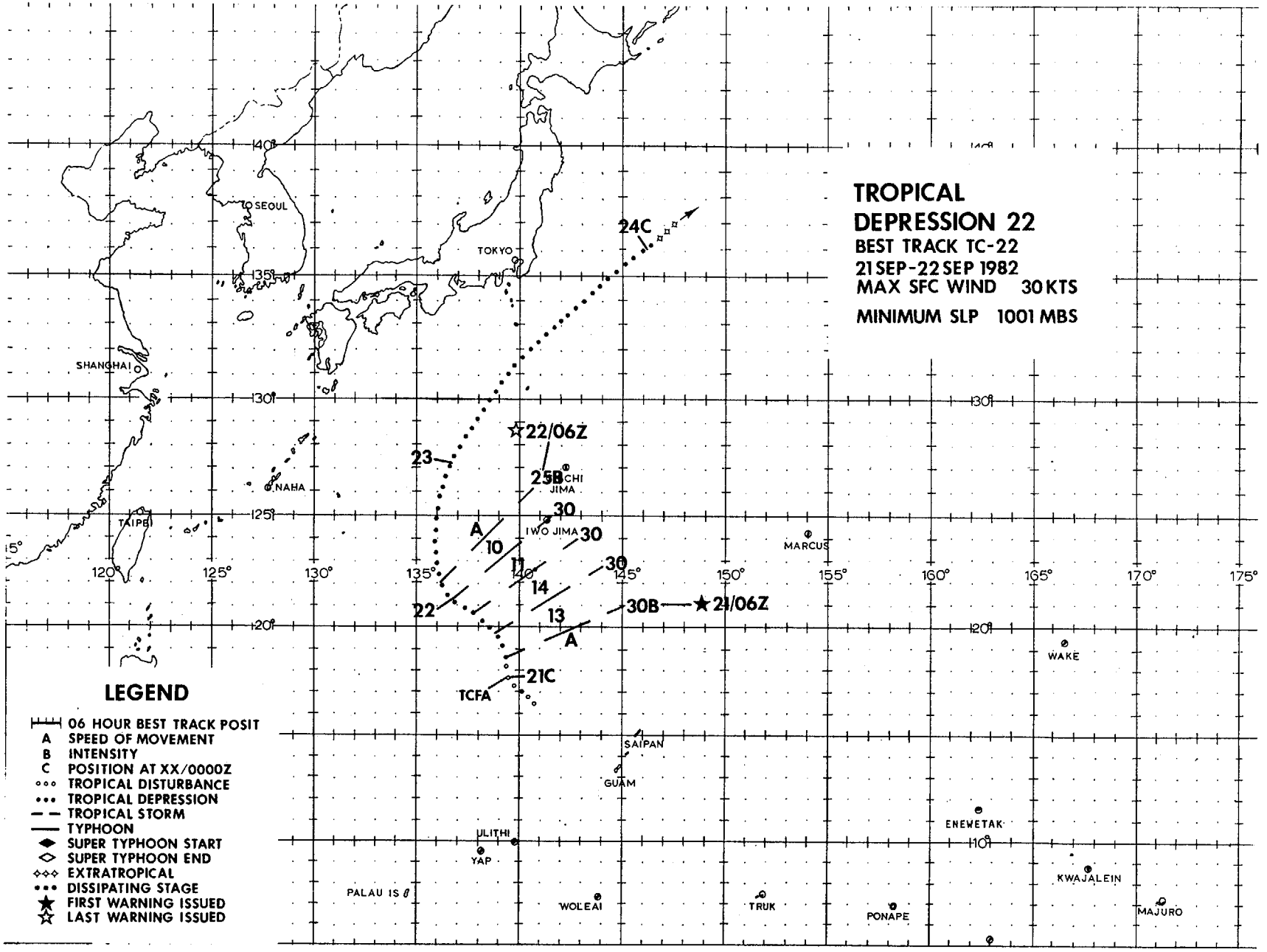
TROPICAL
DEPRESSION 22
BEST TRACK TC-22
21 SEP-22 SEP 1982
MAX SFC WIND 30 KTS
MINIMUM SLP 1001 MBS
LEGEND
06 HOUR BEST TRACK POSIT
A SPEED OF MOVEMENT
B INTENSITY
C POSITION AT XX/0000Z
TROPICAL DISTURBANCE
TROPICAL DEPRESSION
TROPICAL STORM
TYPHOON
SUPER TYPHOON START
SUPER TYPHOON END
EXTRATROPICAL
DISSIPATING STAGE
FIRST WARNING ISSUED
LAST WARNING ISSUED
TO SEOUL
TOKYO
SHANGHAI
NAHA
TAIPEI
IWO JIMA
MARCUS
SAIPAN
GUAM
ULITHI
YAP
PALAU IS
WOLEAI
TRUK
PONAPE
ENEWETAK
WAKE
KWAJALEIN
MAJURO
24C
22/06Z
25B
30
30
30
30B
21/06Z
23
22
21C
TCFA
A
10
11
14
13
A
140°
145°
150°
155°
160°
165°
170°
175°
135°
130°
125°
120°
15°
140
135
130
125
120
110

Tropical Depression 22 began its brief existence as a significant tropical cyclone in the wake of Typhoon Ken (20). An exposed low-level circulation, with convection displaced well west-southwest of the circulation center, was a persistent feature of this system throughout its lifetime as it was apparently dominated by Typhoon Ken's upper-level outflow.

The first aircraft investigative mission flown on 20 September closed a surface circulation with 15 kt (8 m/sec) winds and a central sea level pressure of 1002 mb. The mission Aerial Reconnaissance Weather Officer reported no mid- or upper-level cloud features associated with the low-level center. A second investigative flight on 21 September reported winds had increased to 20 kt (10 m/sec) near the circulation center, while winds of 30 kt (15 m/sec) were evident 70 nm (130 km) south of the center. Convection was displaced 90 nm (167 km) west-southwest of the low-level center but was increasing in intensity. This information prompted the issuance of a Tropical Cyclone Formation Alert (TCFA) at 210123Z.

Subsequent synoptic data carried a growing number of reports of 30 kt (15 m/sec) winds in the alert area, plus visual satellite imagery at 210300Z depicted a strengthening of the low-level circulation. Based on these factors, the first warning was issued on Tropical Depression 22 at 210600Z calling for movement toward the northwest. At this time Typhoon Ken was 900 nm (1667 km) to the west-northwest but minimal interaction was expected. However, Ken's outflow pattern was expected to inhibit rapid development of Tropical Depression 22. Therefore intensification to only 55 kt (28 m/sec) was forecast by the end of 72 hours. (See Figure 3-22-1).

During the ensuing 24-hour period aircraft and satellite data showed no indication of vertical development. Synoptic data at 220000Z indicated that surface winds had weakened to 20 kt (10 m/sec) and surface pressures had not changed from the previous 1002 mb level. Because Tropical Depression 22 was continuing to move more rapidly toward the north-northeast, little opportunity for further development was expected. Additionally, satellite imagery continued to show a weakening of the low-level circulation, thus warnings were suspended at 220700Z.

After dissipating as a significant tropical cyclone, a weak convective disturbance persisted and began accelerating northeastward. This disturbance did maintain enough integrity to induce the development of a small extratropical system upon merging with a frontal zone southeast of Japan on 24 September.

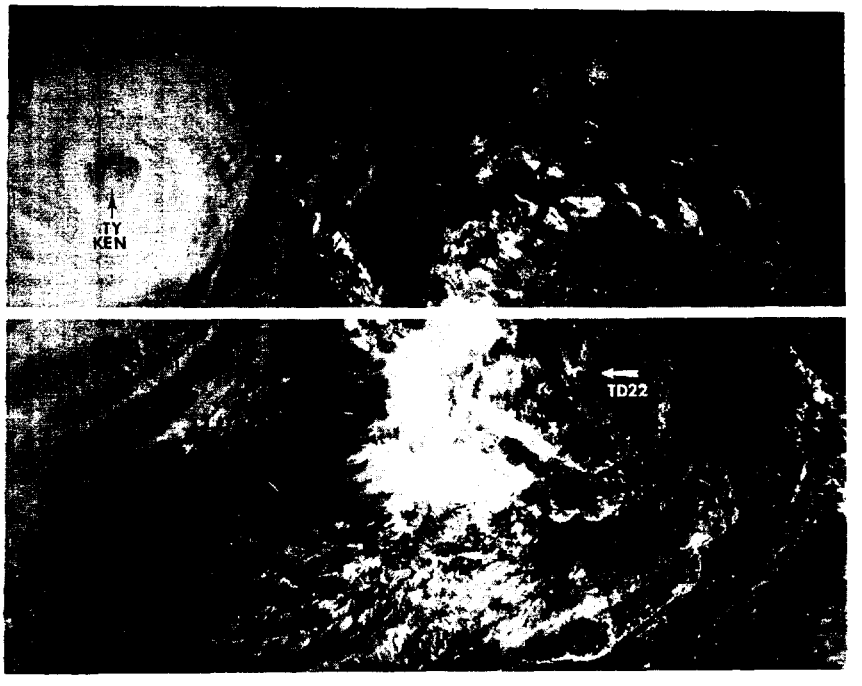

Figure 3-22-1. Tropical Depression 22 at 30 kt (15 m/sec) intensity as an exposed low-level circulation. Convection is displaced to the west-southwest. Typhoon Ken can be seen 900 nm (1667 km) to the northwest. 210529Z September (NOAA 7 visual imagery).

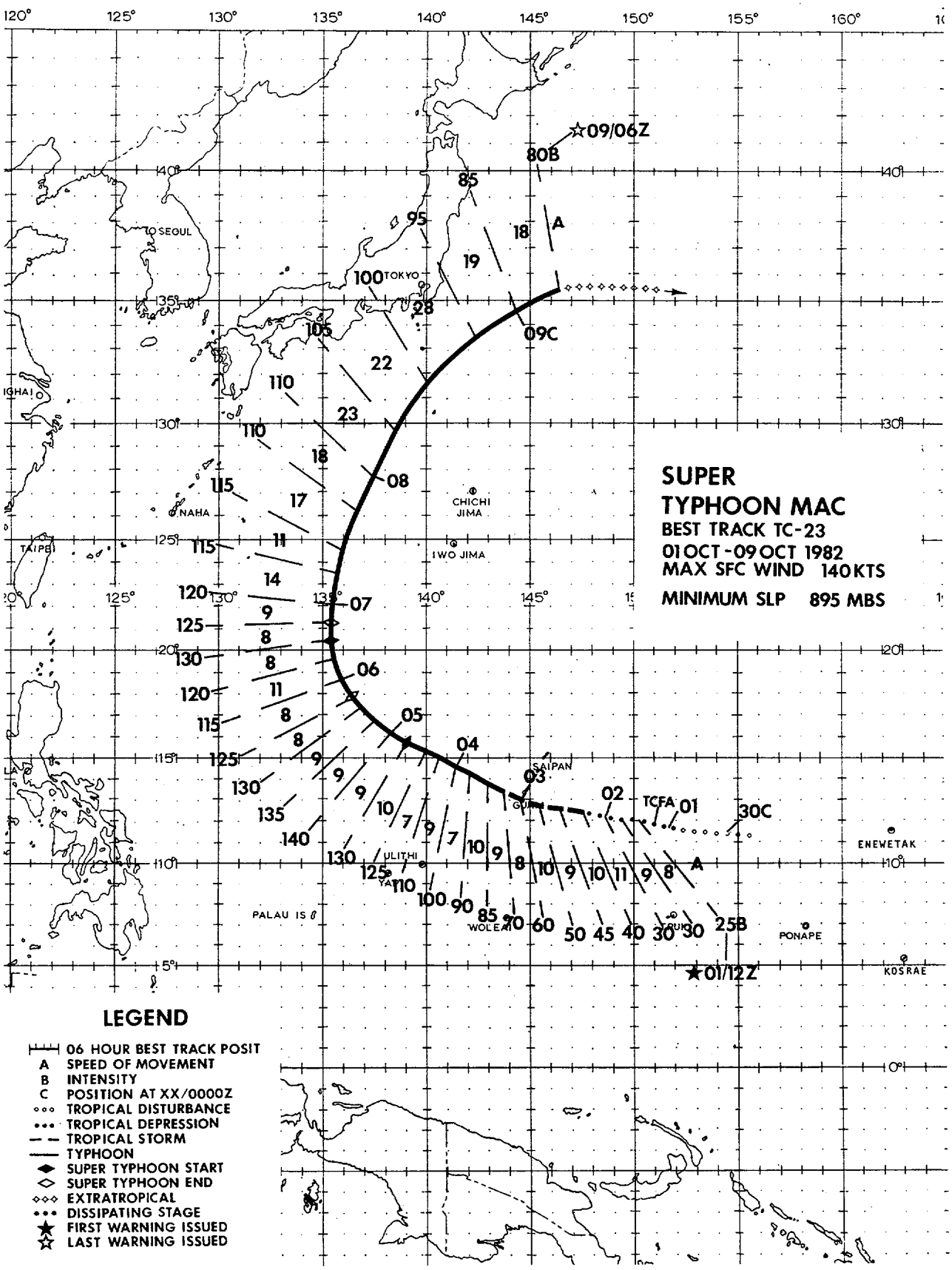
SUPER
TYPHOON MAC
BEST TRACK TC-23
01 OCT - 09 OCT 1982
MAX SFC WIND 140 KTS
MINIMUM SLP 895 MBS
LEGEND
06 HOUR BEST TRACK POSIT
A SPEED OF MOVEMENT
B INTENSITY
C POSITION AT XX/0000Z
TROPICAL DISTURBANCE
TROPICAL DEPRESSION
TROPICAL STORM
TYPHOON
SUPER TYPHOON START
SUPER TYPHOON END
EXTRATROPICAL
DISSIPATING STAGE
FIRST WARNING ISSUED
LAST WARNING ISSUED
☆09/06Z
★01/12Z
TCFA
SEOUL
TOKYO
NAHA
CHICHI JIMA
IWO JIMA
SAIPAN
GUAM
ULITHI
WOLEAI
PALAU IS
ENEWETAK
PONAPE
KOSRAE
TAIPEI

Super Typhoon Mac was spawned to the east of Ponape (WMO 91348) in an area which had been under close scrutiny by the Joint Typhoon Warning Center for several days. A persistent surface circulation, with an associated upper-level anticyclone, was closely monitored beginning on 28 September. No signs of significant development were evident until satellite imagery on 1 October revealed that the convective pattern was more conducive to intensification and the upper-level outflow signature was supportive of sustained further growth of the disturbance. Based upon this evidence, a Tropical Cyclone Formation Alert was issued at 010635Z. Further intensification was rapid; the first warning on Tropical Depression 23 was issued at 011200Z after nearby shipboard observations indicated that the surface pressure was as low as 1003 mb and that surface winds had risen to 25 kt (13 m/sec).

Because of Tropical Depression 23's location (near 12N 150E), it became apparent that the system presented a significant threat to the island of Guam. During its formative stages, Mac had moved somewhat erratically but had tracked generally west-northwestward under the influence of steering currents associated with the southern periphery of the subtropical ridge. Initially, numerical forecast fields indicated there would be no change in this steering flow over the next three days and Mac was predicted to continue on a west-northwest course. During this period, rapid intensification was expected due to favorable upper- and lower-level conditions: the relatively small upper-level anticyclone over the system was in close proximity to strong upper-level outflow channels; and at the surface, there was a massive area of inflow from the west with virtually no competition from other circulation centers in the area (Figure 3-23-1).

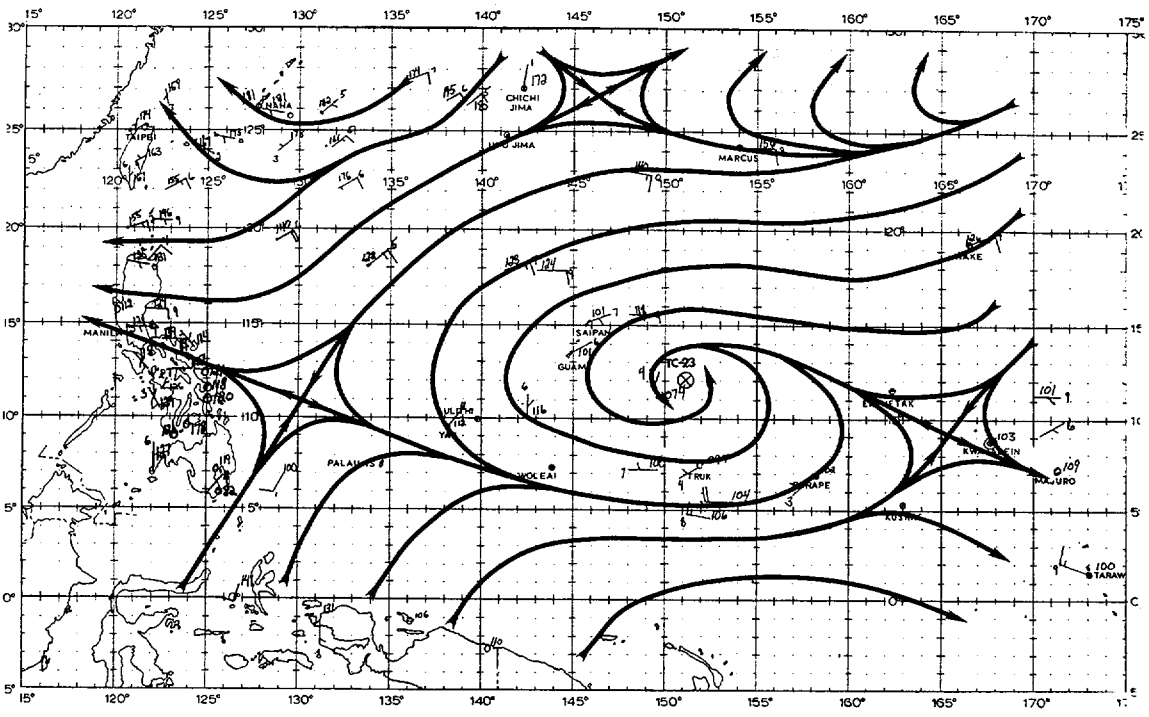

Figure 3-23-1. 011200Z October surface analysis. Wind speeds are in knots.

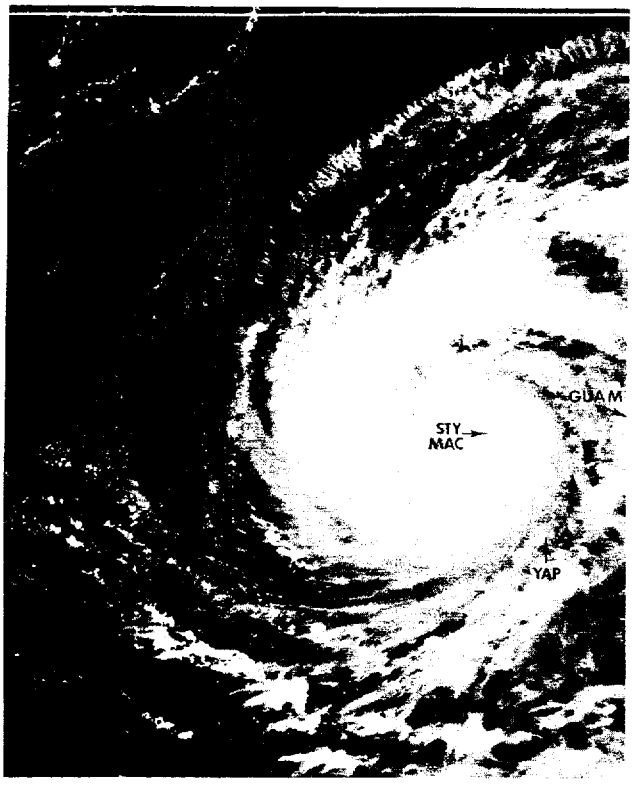

Figure 3-23-2. Super Typhoon Mac is shown 11 hours after maximum intensity, 050640Z October (NOAA 7 visual imagery).

Initial forecasts proved accurate as Mac passed 10 nm (19 km) southwest of Guam at 030000Z. Although maximum sustained winds within Mac were estimated to be 60 kt (31 m/sec) at closest point of approach to Guam, the highest sustained winds recorded at Nimitz Hill (24 nm (44 km) from Mac's center) were just 30 kt (15 m/sec). Guam experienced little structural or equipment damage because of the fortunate combination of adequate advance warning and preparation, and the compact wind radii associated with Mac. However, crop damage was extensive in the southern part of the island due to the heavy rains and relatively high winds experienced there; the Government of Guam Department of Agriculture estimated damages at 1.5 million dollars.

Mac continued to intensify rapidly after passing Guam. In two days, from the 3rd to the 5th, Mac more than doubled its intensity from 60 kt (31 m/sec) to 140 kt (72 m/sec) (Figure 3-23-2). Figure 3-23-3 shows the trends of various meteorological parameters over Mac's lifetime. The 700 mb data and minimum sea level pressure (MSLP) were derived from reconnaissance aircraft data. Items of particular note include: the dewpoint depression of 28°C, one of the largest ever recorded in a tropical cyclone; the redevelopment to super typhoon strength, only the sixth recorded instance since 1958; the correspondence of the MSLP trends and intensity peaks; and the relatively smooth intensity trend as presented by Dvorak analyses.

During its period of rapid intensification, Mac began to assume a more northwestward track in response to a developing weakness in the subtropical ridge near the Ryukyu Islands. On 5 and 6 October, after having attained super typhoon strength, Mac turned sharply north-northeastward and accelerated. Beginning with forecasts issued on 4 October, which keyed on the break in the subtropical ridge, JTWC anticipated this movement quite well. Because of a deep westerly flow which extended well to the south of the main islands of Japan, Mac never posed a threat to Japan even though it appeared to be right on course toward Tokyo until 8 October.

Once embedded in the mid-latitude westerly flow, Mac accelerated to a maximum forward speed of 28 kt (52 km/hr) but lost little of its intensity. Two days after its recurvature, Mac's intensity had dropped only 30 kt (15 m/sec), i.e. from 125 to 95 kt (64 to 49 m/sec); although Mac remained intense, it rapidly lost its tropical characteristics and transitioned into an extratropical system on 9 October.

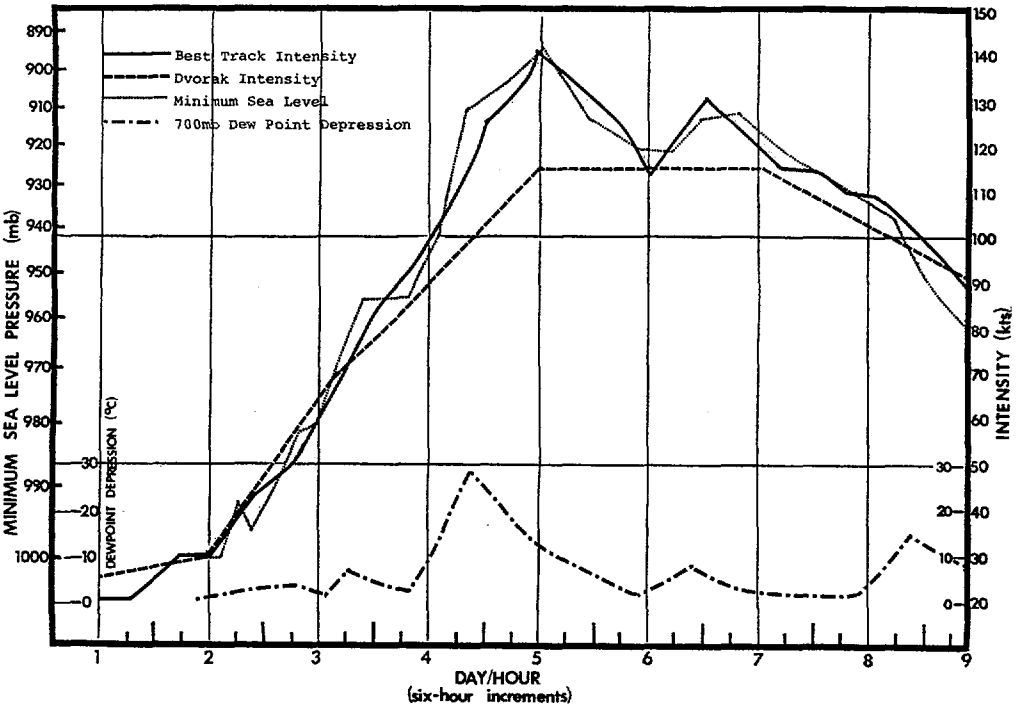

Figure 3-23-3. Comparisons of best track intensities, Dvorak intensity estimates, minimum sea level pressures, and 700 mb dewpoint depressions for the first eight days of Mac's existence.

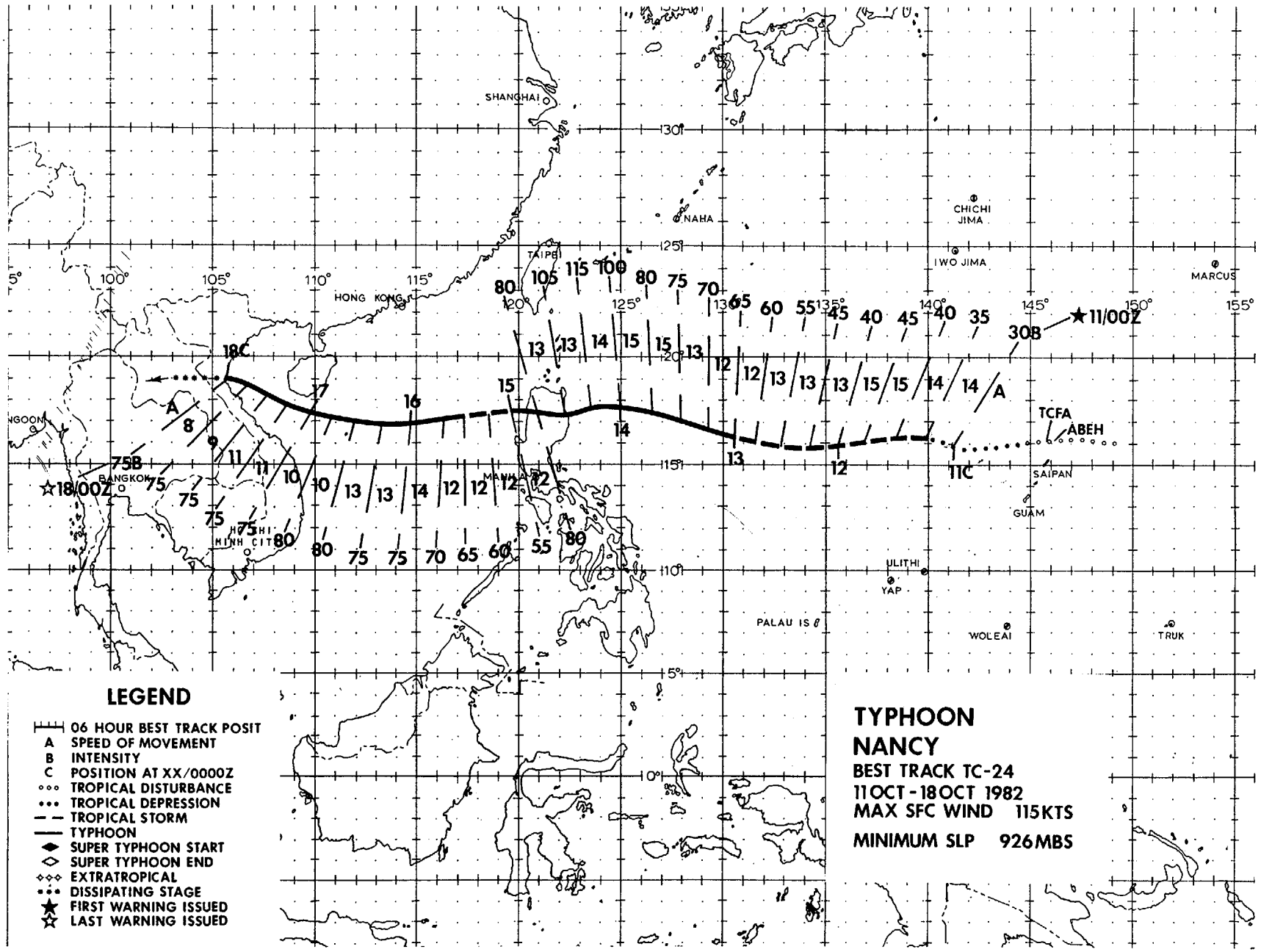
SHANGHAI
NAHA
TAIPEI
HONG KONG
CHICHI JIMA
IWO JIMA
MARCUS
BANGKOK
MANILA
HO CHI MINH CITY
SAIPAN
GUAM
ULITHI
YAP
PALAU IS
WOLEAI
TRUK
TCFA
ABEH
☆18/00Z
★11/00Z
18C
11C
30B
75B
100°
105°
110°
115°
120°
125°
130°
135°
140°
145°
150°
155°
25°
20°
15°
10°
5°
LEGEND
06 HOUR BEST TRACK POSIT
A SPEED OF MOVEMENT
B INTENSITY
C POSITION AT XX/0000Z
TROPICAL DISTURBANCE
TROPICAL DEPRESSION
TROPICAL STORM
TYPHOON
SUPER TYPHOON START
SUPER TYPHOON END
EXTRATROPICAL
DISSIPATING STAGE
FIRST WARNING ISSUED
LAST WARNING ISSUED
TYPHOON
NANCY
BEST TRACK TC-24
11OCT-18OCT 1982
MAX SFC WIND 115KTS
MINIMUM SLP 926MBS

A large area of weakly organized convection consolidated into a single mass on 8 October near 17N 158E in a region made favorable for cyclogenesis by the divergence aloft near an upper cold low. This convection was strong enough to become separate from the surrounding cloudiness lying south of an upper cold low embedded within a tropical upper-tropospheric trough (TUTT). Sustained surface pressure falls, however, weren't realized as this convective area degenerated later that day into a random pattern of cloudiness. The upper cold low continued to drift westward and was located near 148E on 10 October. This time the conditions were right for cyclogenesis — the upper-level divergence coupled with a pre-existing low-level cyclonic circulation and a tropical depression formed in the enhanced cloudiness just south of the TUTT. This cloudiness was separate and distinct from the routinely observed maximum cloud zone, which lay to the south, between 7N and 10N.

A Tropical Cyclone Formation Alert was issued at 100730Z for the area 200 nm (370 km) north of Guam due to the 1005 mb surface pressures and the significant

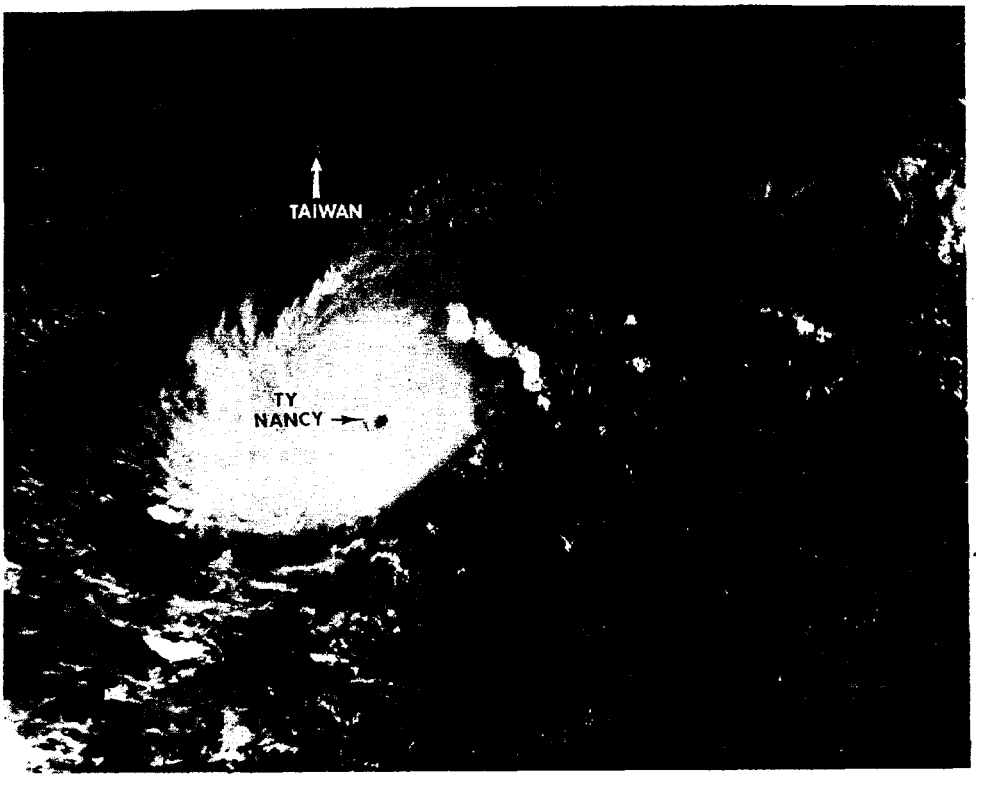

Figure 3-24-1. 140556Z October NOAA 7 visual imagery shows Typhoon Nancy at its peak intensity of 115 kt (59 m/sec) and approximately six hours away from landfall on northern Luzon. Note the island of Taiwan can be seen to the north of Nancy's cloud shields.

increase of cloud pattern organization. Again, because of the sparse conventional data, satellite images had been the key indicator of cyclogenesis and aircraft reconnaissance could not be scheduled to investigate the area until the following day.

The initial reconnaissance aircraft located a closed circulation and surface winds of 25 kt (13 m/sec) which prompted the first warning at 110200Z. Upgrading from tropical depression to tropical storm status followed within six hours, when the follow-on aircraft fix found 35 kt (18 m/sec) winds and a minimum sea level pressure of 999 mb. Nancy stabilized at moderate tropical storm strength and maintained a westward track for the next 24 hours.

Much of Nancy's early warning period was marked by several changes in the basic forecast track. The first four warnings anticipated that Nancy would track northward toward recurvature; however, due in part to the strengthening of the low-level easterly winds north of Nancy, this forecast movement did not occur and Nancy moved rapidly westward with the low-level steering flow. The next four warnings anticipated a west-northwestward movement and through the Bashi Channel, north of Luzon. This track was abandoned at 130000Z when analysis and numerical prognostic data showed evidence that a mid-latitude trough would deepen south of Korea and lessen the influence of the low-level steering on Nancy. Thus until 140600Z (warning 14), the JTWC forecasts showed a pronounced northwestward track toward Taiwan and mainland China. On 14 October, as it became evident that the forecast weakening of the low-level steering current would not materialize, the JTWC forecasts turned toward the west-southwest.

During this period of changing forecast scenarios, Nancy began to intensify. On 13

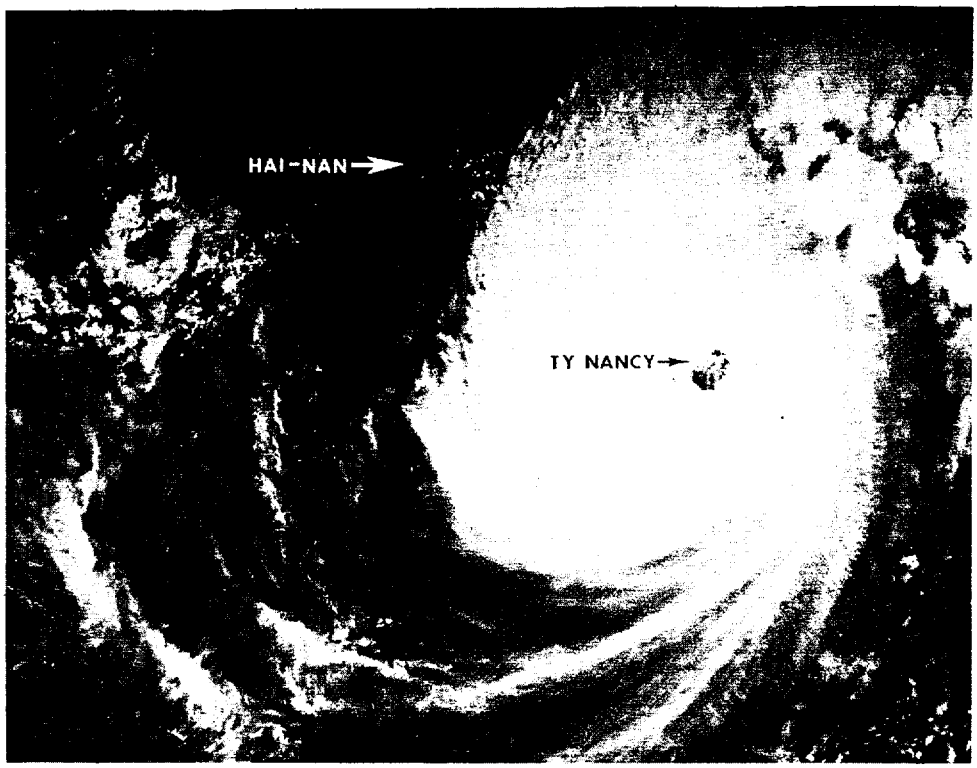

Figure 3-24-2. Typhoon Nancy was located near 17.0N 113.8E or 210 nm (389 km) east-southeast of the island of Hai-Nan at 160714Z October. Hai-Nan island was located on the northwestern edge of Nancy's cirrus cloud cover. Note the fair weather as indicated by the small, fair weather cumulus over the island and coastal areas of Vietnam, in sharp contrast to the approaching typhoon. (NOAA 7 visual imagery).

October, Nancy attained typhoon strength and then rapidly deepened to a peak intensity of 115 kt (59 m/sec) just six hours prior to landfall on northeastern Luzon. Nancy was reduced to tropical storm strength by a rugged overland transit, but was quick to regain typhoon strength upon reaching the open waters of the South China Sea. Nancy was the most intense typhoon to strike the Republic of the Philippines this year; in its wake, Nancy left at least 110 dead, 12,000 people homeless, and caused an estimated 46 million dollars damage.

The presence of a continuing strong mid- and upper-level circulation pattern made Nancy's reintensification in the South China Sea possible. At 161200Z, Nancy reached a second peak intensity of 80 kt (41 m/sec) as it passed just north of the Paracel Islands (WMO 59981). The influence of a subtropical ridge over southern China and the continuing presence of of the low-level northeasterly (monsoon) flow across the South China Sea kept Nancy on a westward track until it approached Hai-Nan Island late on 16 October. From near Hai-Nan until landfall, Nancy maintained a slower, northwestward track along the southern periphery of the subtropical ridge.

On 18 October, Nancy crossed the coast of Vietnam 15 nm (38 km) north of the city of Vinh (18.7N 105.7E) in the Nghe Tinh province, causing at least 71 deaths, leaving 194,200 people homeless, and devasting 185 square miles (48,000 hectares) of winter rice crops that were ready for harvest. Later satellite imagery (at 180600Z) indicated that Nancy's central convection had dissipated over the mountains of Vietnam.

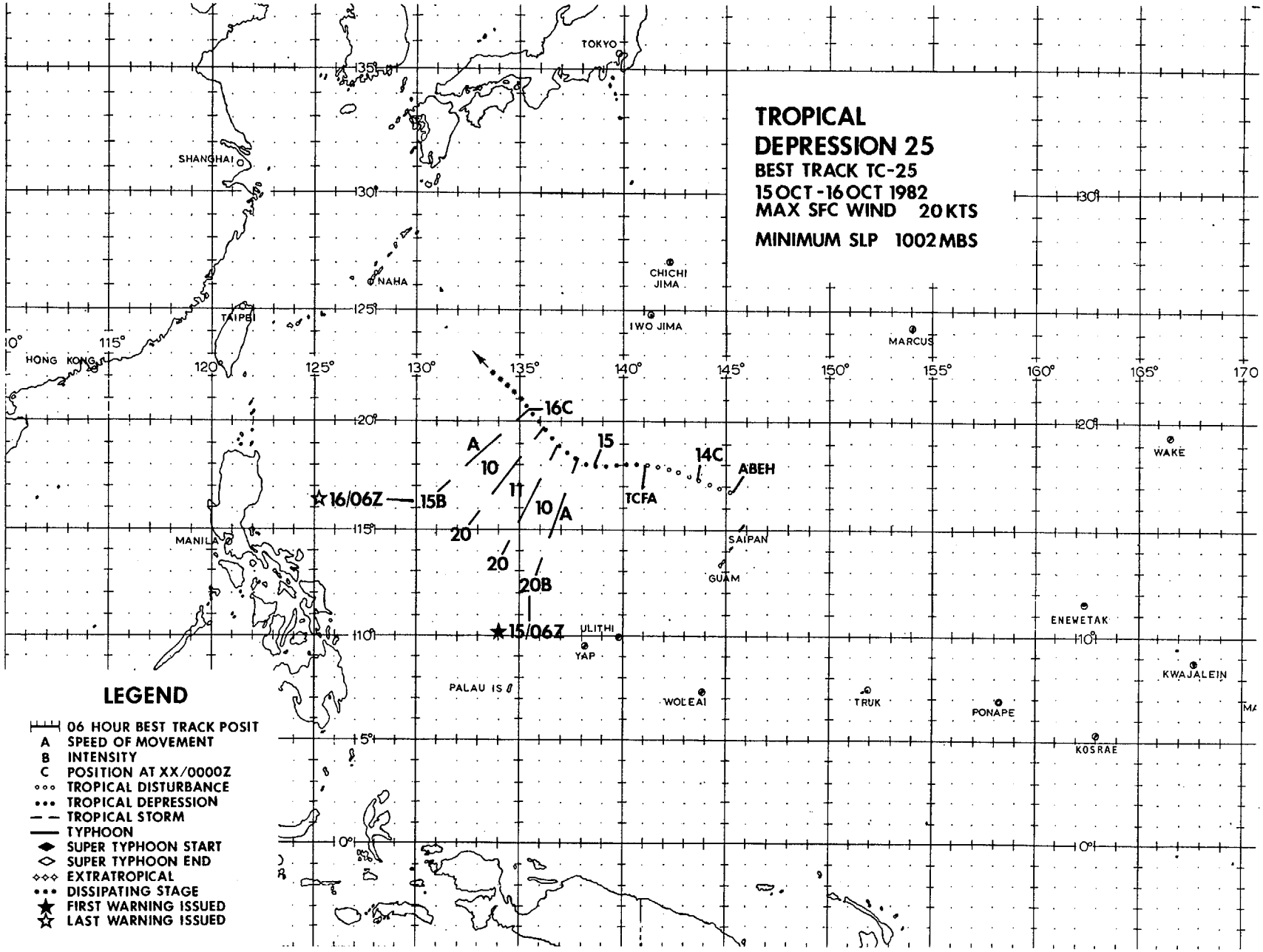
TROPICAL
DEPRESSION 25
BEST TRACK TC-25
15 OCT - 16 OCT 1982
MAX SFC WIND 20 KTS
MINIMUM SLP 1002 MBS
TOKYO
SHANGHAI
NAHA
CHICHI JIMA
IWO JIMA
MARCUS
TAIPEI
HONG KONG
WAKE
16C
15
14C
ABEH
TCFA
☆16/06Z
15B
A
10
11
10/A
20
20
20B
★15/06Z
MANILA
SAIPAN
GUAM
ULITHI
YAP
PALAU IS
WOLEAI
TRUK
PONAPE
ENEWETAK
KWAJALEIN
KOSRAE
LEGEND
06 HOUR BEST TRACK POSIT
A SPEED OF MOVEMENT
B INTENSITY
C POSITION AT XX/0000Z
TROPICAL DISTURBANCE
TROPICAL DEPRESSION
TROPICAL STORM
TYPHOON
SUPER TYPHOON START
SUPER TYPHOON END
EXTRATROPICAL
DISSIPATING STAGE
FIRST WARNING ISSUED
LAST WARNING ISSUED

On 14 October, surface observations indicated a weak circulation center near 18N 141E. Satellite analysis of the area revealed the presence of an upper-level anticyclone with potential to enhance the ventilation of the surface system. Expecting further development once the system attained vertical alignment, JTWC issued a Tropical Cyclone Formation Alert (TCFA) at 141200Z.

Aircraft reconnaissance at 142336Z located a weak surface circulation near 18N 139E, with central pressures estimated to be near 1006 mb. The initial warning on Tropical Depression 25 was issued after 150000Z satellite imagery showed the convective area near the center was becoming more organized.

Subsequent aircraft reconnaissance of the system at 150900Z reported maximum winds less than 10 kt (5 m/sec), and the circulation center could not be fixed by either winds or pressures. Satellite imagery indicated that the convection associated with the system had greatly weakened, and the overall organization had decreased. The subsequent warning, at 151200Z, anticipated further weakening of Tropical Depression 25 and the forecast period was shortened to 24 hours. On the following day, visual satellite imagery at 160000Z, with corroborative synoptic data, indicated that Tropical Depression 25 had become a fully exposed low-level circulation with no associated major convection. Thus, the final warning on Tropical Depression 25 was issued at 160600Z.

For the next 48 hours, this exposed low-level circulation remained evident on visual satellite imagery, as it progressed to the northwest. Re-development of some convective banding, curving into the system was observed on 18 October. The development of a weak anticyclonic pattern aloft prompted the issuance of a TCFA for the area, near 21N 134E, at 180800Z. A low-level aircraft investigative mission was conducted at 190200Z, but was unable to locate a closed circulation center.

Early on 19 October, when the remains of Tropical Depression 25 were entrained into the expanding low-level inflow pattern associated with Typhoon Owen (26), the TCFA was cancelled.

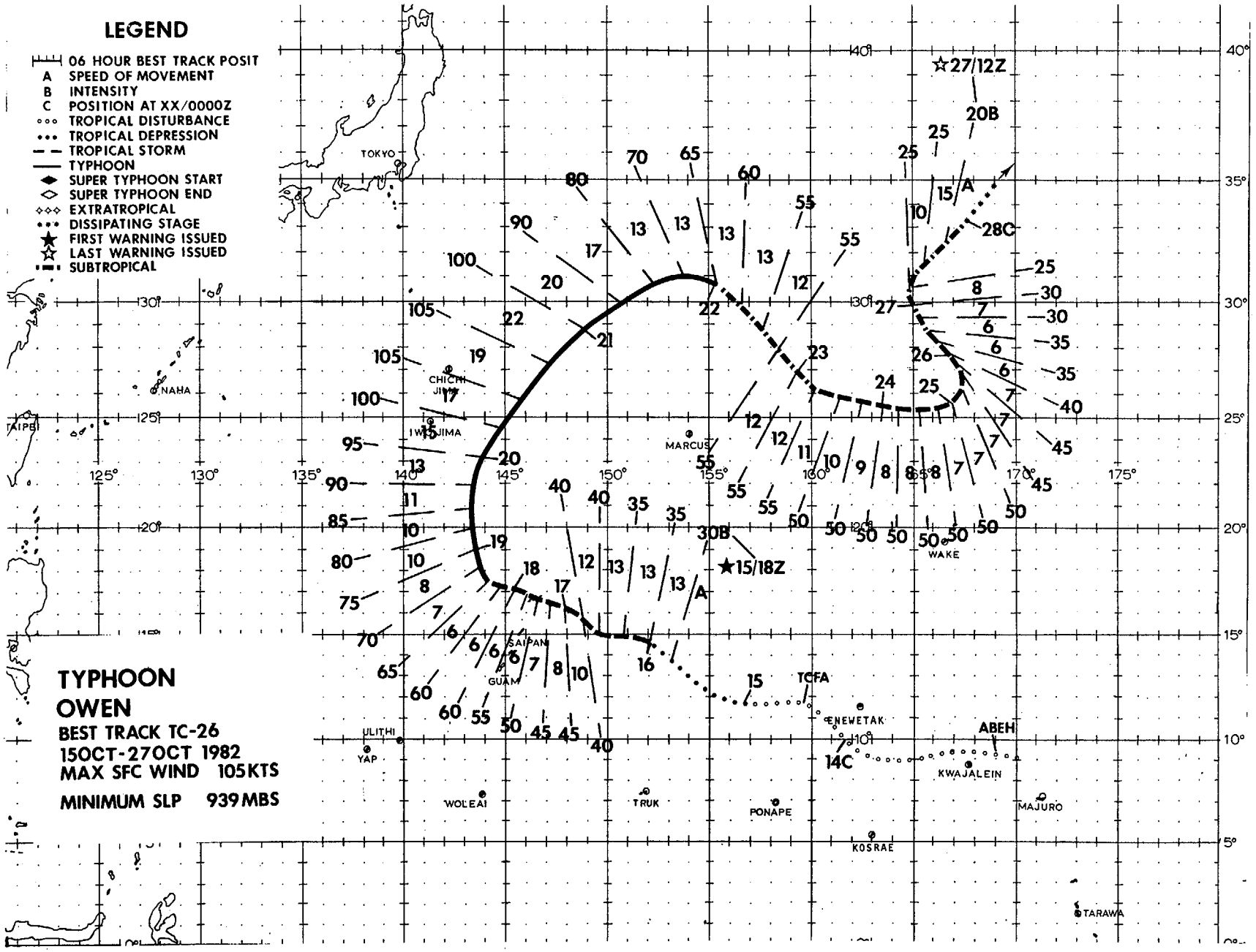
LEGEND
06 HOUR BEST TRACK POSIT
A SPEED OF MOVEMENT
B INTENSITY
C POSITION AT XX/0000Z
TROPICAL DISTURBANCE
TROPICAL DEPRESSION
TROPICAL STORM
TYPHOON
SUPER TYPHOON START
SUPER TYPHOON END
EXTRATROPICAL
DISSIPATING STAGE
FIRST WARNING ISSUED
LAST WARNING ISSUED
SUBTROPICAL
TYPHOON
OWEN
BEST TRACK TC-26
150CT-270CT 1982
MAX SFC WIND 105KTS
MINIMUM SLP 939MBS
☆27/12Z
20B
28C
30B
★15/18Z
14C
TCFA
TOKYO
NAHA
TAIPEI
CHICHI JIMA
IWO JIMA
MARCUS
WAKE
SAIPAN
GUAM
ULITHI
YAP
WOLEAI
TRUK
PONAPE
KOSRAE
ENEWETAK
KWAJALEIN
MAJURO
ABEH
TARAWA

Typhoon Owen culminated an active 14-week period (22 July through 27 October) during which 17 tropical cyclones reached warning status in the western North Pacific. During this period, only 10 calendar days did not have at least one tropical cyclone in warning status, with five days (26 to 30 September) the longest period without warnings. So obvious was the cessation of this period that four weeks elapsed between the final warning on Owen and the initial warning on the next tropical cyclone, Pamela (27).

Owen developed from a disturbance which was first detected on 13 October east of Kwajalein Atoll. On 14 October increased convective organization became evident on satellite imagery and, at 141200Z, a Tropical Cyclone Formation Alert was issued. During the subsequent 36-hour period, the disturbance slowly organized, e.g. a reconnaissance aircraft investigative mission conducted on 14 October located a weak surface circulation approximately 100 nm (185 km) east of the convective center. However, by 151800Z the convective features were indicative of a system of sufficient intensity to warrant transition to warning status, thus the initial warning was issued for Tropical Depression 26.

During the first 24 hours in warning status, positioning from aircraft and satellite data became more consistent, e.g. the 152317Z aircraft fix was located approximately 90 nm (167 km) east of the 160000Z satellite fix; by 162100Z the difference was less than 20 nm (37 km). As Figure 3-26-1 depicts, a strong upper-level tilt to the south was evident, but low-level cumulus cloud lines, detected north of the main convective mass, provided evidence of Owen's continued organization. Owen is another example of non-vertical alignment of developing tropical cyclones (Huntley and Diercks, 1981). Such systems normally become better aligned as they mature and Owen was no exception; on 18 and 19 October, the tilt became less evident and Owen responded by attaining typhoon strength at 181200Z and developing a banding-type eye on 19 October.

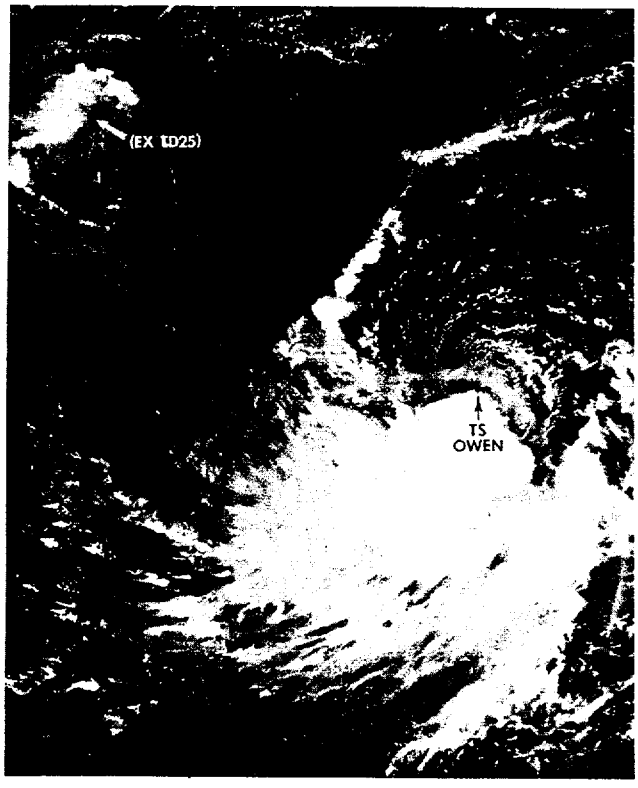

Figure 3-26-1. Low-level cumulus cloud lines can be seen entering Owen's center while the main convective features are displaced equatorward of the low-level center. Strong upper-level northeasterly winds are providing a unidirectional outflow channel toward the southwest. 170520Z October (NOAA 7 visual imagery).

While Owen was aligning in the vertical, it also began to slow its forward movement appreciably, from 13 to 6 kt (24 to 11 km/hr). Track forecasts (describing a west-northwest movement) were adequate until the system reached 17.5N 144E at 181200Z, when Owen turned sharply northward. Although most forecasts up to this point had anticipated an eventual northward movement, none fully anticipated the extent of Owen's turn on 18 October. This movement can be related to the development of a blocking high east of Japan. (Actually, the FNOC prognostic series more than adequately forecast this development, but an extension of the mid-tropospheric (500 mb) subtropical ridge north of Owen and westward to 135E was seen by forecasters as an inhibiting factor to more significant northward movement). The development of the block increased the south-to-north flow in the mid-levels, leading to an erosion of the subtropical ridge north of Owen and thus, allowed the typhoon to move northward.

From 19 to 21 October, Owen accelerated northward toward an anticipated extratropical transition, reaching a peak intensity of 105 kt (54 m/sec) (Figure 3-26-2). Speed of movement forecasts during this period were quite good and fully anticipated Owen's acceleration from 10 to 22 kt (19 to 41 km/hr). However, the track forecasts did not fair as well, primarily due to the conflicting options presented by the flow around the block. Figure 3-26-3 shows the configuration of the mid-tropospheric (500 mb) flow near the block on 20 October, as well as the various forecast tracks issued (from 190000Z to 210000Z) and Owen's eventual best track. As can be seen, forecasts 14 through 17 tended toward the east (south of the blocking high), forecasts 18 and 19 anticipated that Owen would move northward toward an occluded low near Kamchatka, and forecasts 20 through 22 seemed to split the difference. On 21 October, Owen's anticipated extratropical transition was well underway; its associated convective features

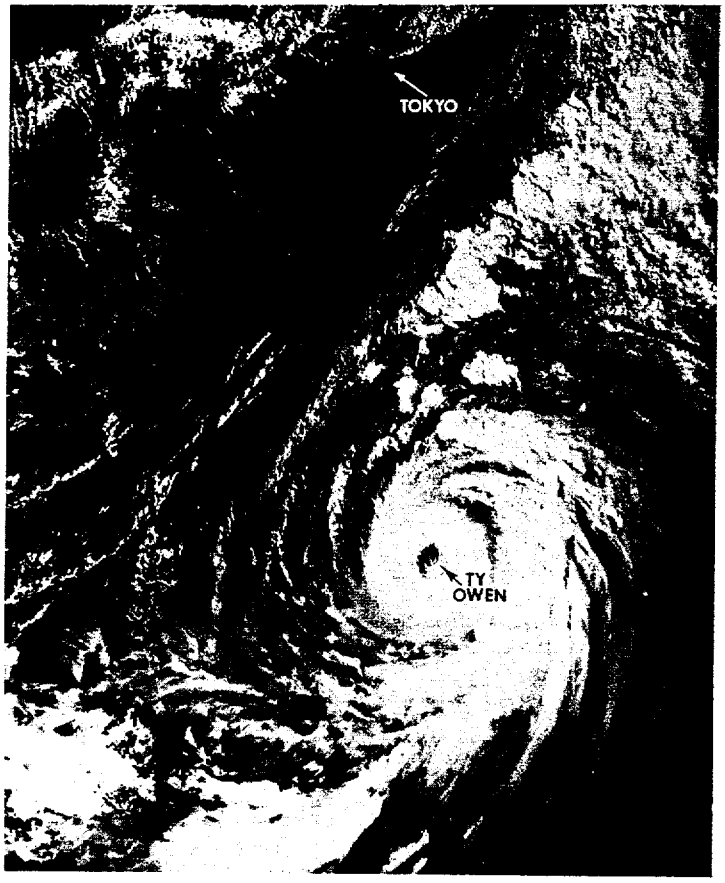

Figure 3-26-2. Typhoon Owen near maximum intensity, 710 nm (1315 km) south-southeast of Tokyo, Japan at 200443Z October (NOAA 7 visual imagery)

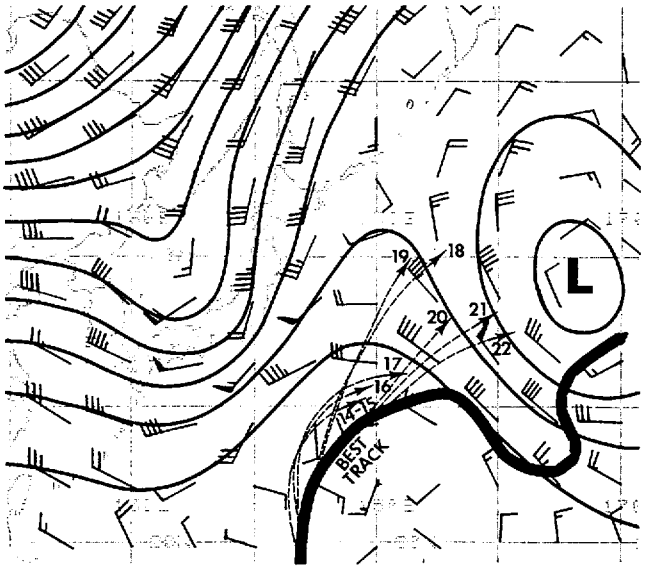

Figure 3-26-3. FNOC 500 mb analysis at 200000Z October with warnings 14 through 22 and Owen's best track superimposed. Wind speeds in knots.

were being sheared northward (away from the surface center), low-level inflow from the mid-latitudes dominated Owen's surface circulation pattern, and aircraft reports showed the band of maximum winds moving further from the center (135 nm (232 km) at 210704Z).

Numbered tropical cyclone warnings ended at 220000Z when satellite imagery indicated that Owen had transitioned to an extra-tropical low. During the next two days, extratropical gale warnings were issued by the NOCC Operations Department as the system tracked southeastward and south of the blocking high. On 23 October an increase in convective activity was noted equatorward of the system center (Figure 3-26-4) and during the next 24 hours it was closely monitored for possible reclassification as "tropical" vice "extratropical" or "sub-tropical" cyclone. The decision to redesignate Owen as a tropical cyclone occurred on 24 October when the convection began to reorganize around the system's center.

For the next 24 hours, Owen tracked eastward and maintained an estimated 50 kt (26 m/sec) intensity. Satellite fixes on 25 October began to indicate a pronounced northward track and a steady decrease in convective activity. From 25 to 27 October, the block, which had dominated the region for more than one week, began to break down and move eastward toward the International Dateline. As Owen moved north-northwestward then northeastward, it slowly weakened and dissipated in the warm sector of an advancing frontal system. The final tropical cyclone warning was issued for Owen (as Tropical Depression 26) at 271200Z some 1400 nm (2593 km) north of its point of initial detection after completing a track in excess of 3600 nm (6668 km).

Figure 3-26-4. At 240355Z October, a significant increase in convection is evident near the system's center; at the time Owen was in warning status as an extratropical low (NOAA 7 visual imagery).

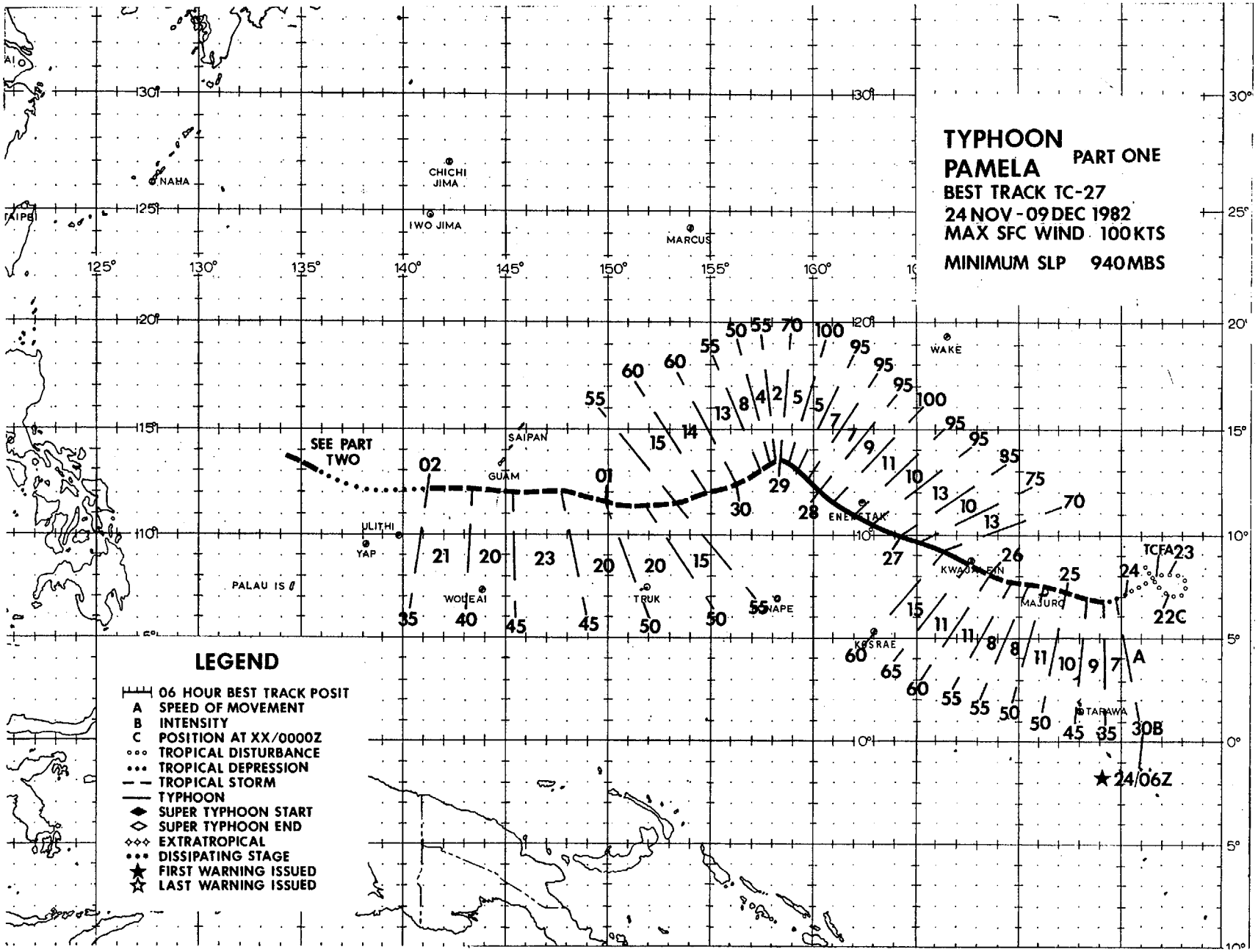
TYPHOON
PAMELA
PART ONE
BEST TRACK TC-27
24 NOV - 09 DEC 1982
MAX SFC WIND 100 KTS
MINIMUM SLP 940 MBS
LEGEND
06 HOUR BEST TRACK POSIT
A SPEED OF MOVEMENT
B INTENSITY
C POSITION AT XX/0000Z
TROPICAL DISTURBANCE
TROPICAL DEPRESSION
TROPICAL STORM
TYPHOON
SUPER TYPHOON START
SUPER TYPHOON END
EXTRATROPICAL
DISSIPATING STAGE
FIRST WARNING ISSUED
LAST WARNING ISSUED
SEE PART TWO
NAHA
CHICHI JIMA
IWO JIMA
MARCUS
WAKE
SAIPAN
GUAM
ULITHI
YAP
PALAU IS
WOLEAI
TRUK
NAPE
KWAJALEIN
MAJURO
KOSRAE
TCFA
★24/06Z

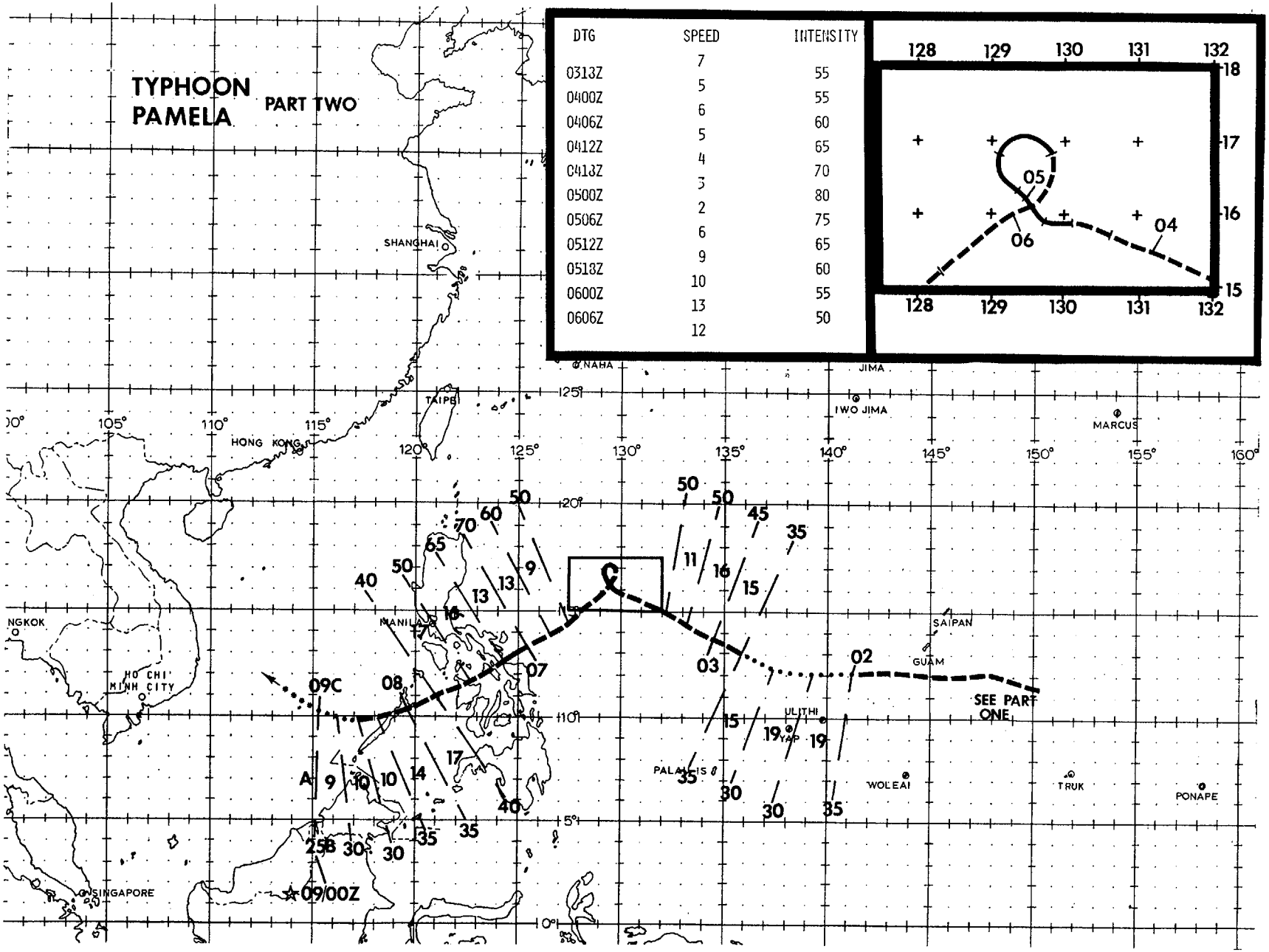
TYPHOON
PAMELA
PART TWO
DTG SPEED INTENSITY
0313Z 7 55
0400Z 5 55
0406Z 6 60
0412Z 5 60
0418Z 4 65
0500Z 3 70
0506Z 2 80
0512Z 6 75
0518Z 9 65
0600Z 10 60
0606Z 13 55
12 50
128 129 130 131 132
18 17 16 15
05 04 06
SHANGHAI
NAHA
IWO JIMA
MARCUS
TAIPEI
HONG KONG
MANILA
SAIPAN
GUAM
ULITHI
YAP
PALAU IS
WOLEAI
TRUK
PONAPE
HO CHI MINH CITY
SINGAPORE
09C 08 07 03 02
SEE PART ONE
09/00Z
105° 110° 115° 120° 125° 130° 135° 140° 145° 150° 155° 160°
25 20 15 10 5° 0°

Typhoon Pamela, the 27th significant tropical cyclone of the season, formed east of the Marshall Islands on 24 November. Uncommon for a late season tropical cyclone, Pamela went on to become the longest running, in terms of time and distance, tropical cyclone of the year before dissipating in the South China Sea on 9 December. During its active warning period, Pamela was upgraded to typhoon status on four distinct occasions (reduced to three in post-analysis), a very rare phenomenon.

Development was first observed on 21 November with the formation of an upper-level anticyclone which had some convective activity along its northern outflow band. Visual satellite imagery on 22 November showed a low-level circulation was present near 6N 177E. During the next 48 hours, this disturbance lingered in the region east of 175E with convective activity fluctuating near the center; however, a slow increase in organization, conducive to further development, was observed.

The slow development of this disturbance is attributed to the proximity of Hurricane Iwa (04C) in the eastern North Pacific. As Iwa moved northeastward and passed the Hawaiian Islands, the disturbance (Pamela) began moving westward. A noticeable increase in convection was observed, leading to the issuance of a Tropical Cyclone Formation Alert at 230600Z for an area east of Majuro Atoll. The system further organized, thus prompting the initial warning on Tropical Depression 27 at 240600Z. When the system developed a central convective feature, accompanied by a well-defined upper-level outflow pattern, it was upgraded to Tropical Storm Pamela at 241200Z.

The first several warnings called for movement toward the west-northwest with gradual intensification. These warnings were based on a forecast weakening of the subtropical ridge northwest of the system under the influence of a mid-latitude trough moving eastward from Japan. Indeed, Pamela moved west-northwestward through the Marshall Islands in the ensuing 84 hours. Satellite and aircraft reconnaissance data confirmed the gradual intensification of the system, with Pamela attaining typhoon status at 260600Z while passing approximately 60 nm (111 km) south-southeast of Kwajelein Atoll. By the time Pamela passed 35 nm (65 km) southwest of Enewetak Atoll at 271200Z, its intensity was estimated (from aircraft data) to be 95 kt (49 m/sec) (Figure 3-27-1). Initial reports from the Marshall Islands indicated moderate to severe damage to buildings and crops from those islands affected by Pamela's passage, but there were no reports of loss of life.

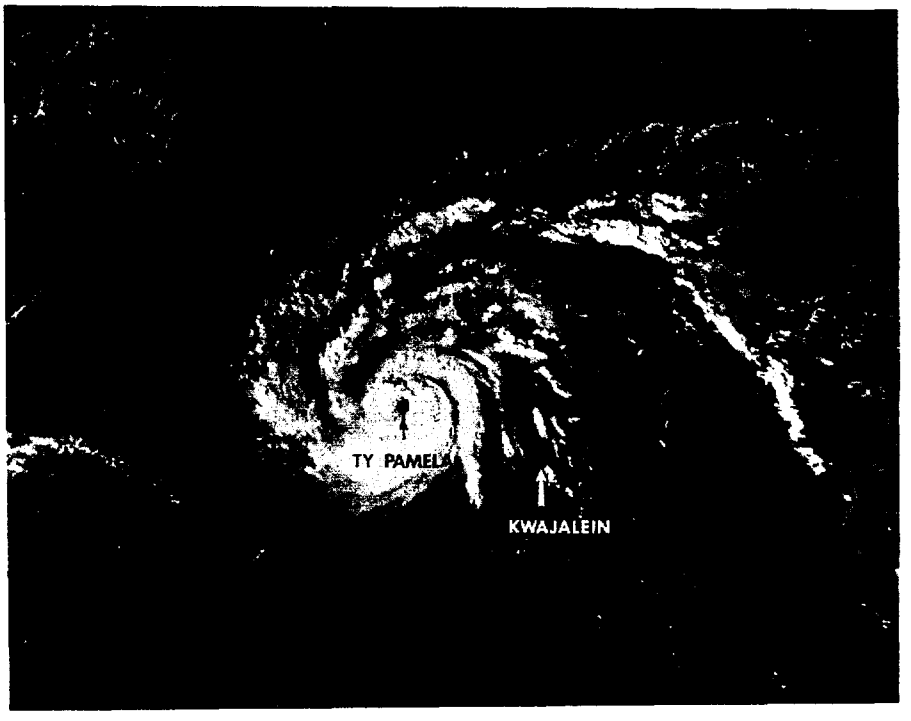

Figure 3-27-1. Typhoon Pamela, 15 hours prior to reaching maximum intensity of 100 kts (51 m/sec), 270348Z November (NOAA 7 visual imagery).

Once past the Marshall Islands, Pamela's forward speed began to slow as the system started to come under the influence of a mid-latitude trough passing to the north. As Pamela approached 19N it began to rapidly weaken as it encountered a mid- to upper-level shear zone associated with the trough. Evidence of the rapidity with which Pamela weakened is seen in the aircraft reconnaissance data. At 282105Z, a central pressure of 950 mb and an observed 100 kt (51 m/sec) surface wind were reported. A second reconnaissance mission about nine and one-half hours later (at 290640Z) reported a 979 mb central pressure and observed surface winds of only 50 kt (26 m/sec). This second report necessitated the downgrading of Pamela to tropical storm status on the subsequent warning. A much-weakened Pamela then moved toward the southwest and began to accelerate after breaking away from the effects of the trough and shear zone. This movement was in response to a strong northeast monsoonal flow which was present in the wake of the eastward-moving mid-latitude trough.

Commencing with the 291800Z warning, Pamela was forecast to reintensify and move westward along the southern periphery of the subtropical ridge, eventually passing near the island of Guam. The residents of Guam, remembering the devastation caused by Super Typhoon Pamela (May, 1976), had been nervously watching "Pamela's" progress since its designation while still some 1800 nm (3335 km) east of Guam. Needless-to-say, island residents began to prepare for a possible repeat of the conditions associated with Pamela's 1976 namesake.

Pamela continued to accelerate toward the southwest until 301200Z when it began to move westward. During this period, Pamela continued to weaken; instead of gaining the expected mid- and upper-level support for reintensification, Pamela remained disorganized and the anticapted intensification did not materialize. The 011200Z December 500 mb analysis, for example, did not show any mid-tropospheric circulation center near Pamela's low-level vortex.

Although Pamela was still weakening, it was considered a potentially dangerous tropical cyclone. At 011200Z, Pamela was located 90 nm (169 km) southeast of Guam and was moving westward at 23 kt (42 km/hr); its closest point of approach (to Guam) came two hours later with the maximum recorded wind (gust) of 40 kt (21 m/sec), far below the 138 kt (71 m/sec) gust observed during Super Typhoon Pamela in 1976.

At 011532Z, a reconnaissance aircraft was able to locate Pamela's 700 mb center 90 nm (169 km) southwest of Guam. Data from this fix indicated that Pamela's intensity had decreased to 49 kt (21 m/sec). The same aircraft was tasked to provide another fix of the 700 mb center at 011800Z but was unable to close off the circulation (the surface center was not observable due to darkness). The mission Aerial Reconnaissance Weather Officer (ARWO) felt that the 700 mb center had dissipated into a trough, providing further evidence that Pamela was continuing its weakening trend. A "resources permitting" "first-light" aircraft fix was requested for 012200Z. The aircraft orbited south of the main convection until daybreak; then, responding to a satellite position provided to JTWC by Det 1, 1WW, the aircraft was able to locate the surface center at 012150Z with an estimated 35 kt (19 m/sec) intensity.

During the next 24 hours, Pamela continued to move westward and weaken. Satellite imagery (Figure 3-27-2) and aircraft reconnaissance data revealed that Pamela had become a tropical depression by 020600Z. During this period, JTWC was forecasting Pamela to dissipate as a significant tropical cyclone over water within 48 hours.

Pamela, again as Tropical Depression 27, started to slow its forward speed and began to move toward the northwest, responding to another mid-latitude trough moving off the coast of Asia. Once this northwest movement began, indications that Pamela might reintensify became evident. First, the 021200Z 500 mb analysis suggested that a mid-tropospheric circulation had reformed; and second, aircraft reconnaissance at 022126Z was once again able to close off a 700 mb center with data indicating that an intensity of 35 kt (18 m/sec) had been reached. Later reconnaissance aircraft missions showed that Pamela was continuing its reintensification and it passed from tropical storm status to typhoon status (again) at 041200Z. During this period of reintensification, Pamela reached a maximum intensity of 80 kt (41 m/sec) while concurrently slowing to a minimum speed of 2 kt (4 km/hr) at 050000Z (Figure 3-27-3).

JTWC objective forecast aids and FNOC prognostic fields began to indicate the potential for recurvature once Pamela approached the axis of the (mid-tropospheric) subtropical ridge, near 17N. The 040000Z warning was the first to reflect a recurvature scenario. The numerical prognostic

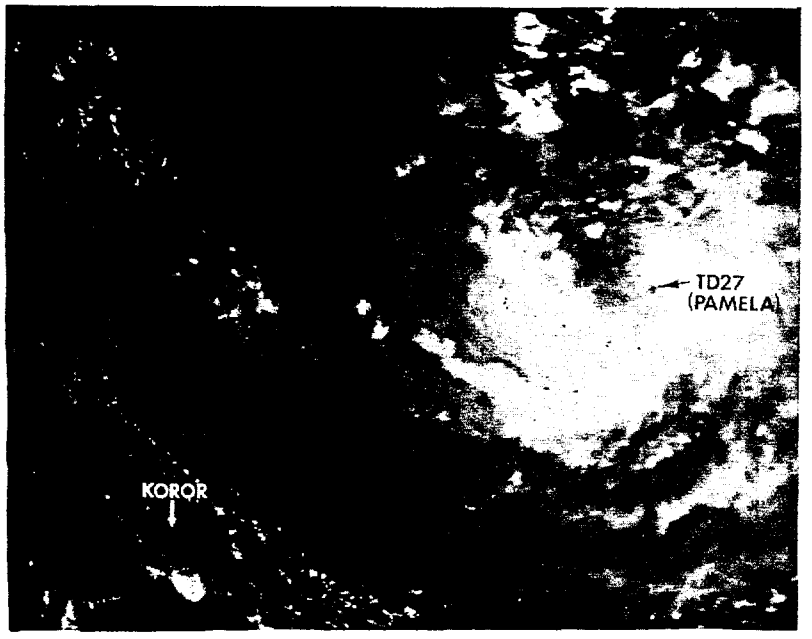

Figure 3-27-2. Pamela, now Tropical Depression 27, with estimated intensity of 30 kts (15 m/sec). 0?0611Z December (NOAA 7 visual imagery).

fields, from which this scenario was derived, forecast the subtropical ridge to weaken at all levels as a mid-latitude trough deepened in the East China Sea. This meteorological situation would allow Pamela to recurve toward the northeast, accelerate, and undergo an extratropical transition. However, the low-level (850 mb and below) ridge did not weaken as indicated by the prognostic series, and Pamela went on to complete a small anticyclonic loop and moved southwestward toward the Philippines. Early in the loop, Pamela began to interact with the mid-latitude westerlies and once again the effect of increased vertical wind shear weakened Pamela from 80 kt (41 m/sec) to 50 kt (26 m/sec) over a 30-hour period. However, as Pamela moved southwestward, the subtropical ridge to the north began to strengthen at all levels, allowing Pamela to reintensify to a typhoon for the third time. Pamela reached a maximum intensity of 70 kt (36 m/sec) about six hours prior to entering the islands of the central Philippines.

As Pamela moved through the Philippines and weakened, Tropical Depression 28 (Roger) formed in the Philippine Sea. The combined effects of interaction with the topography of the islands and a shift in the low-level wind regime toward Roger caused Pamela to weaken rapidly and eventually brought on its dissipation over the South China Sea.

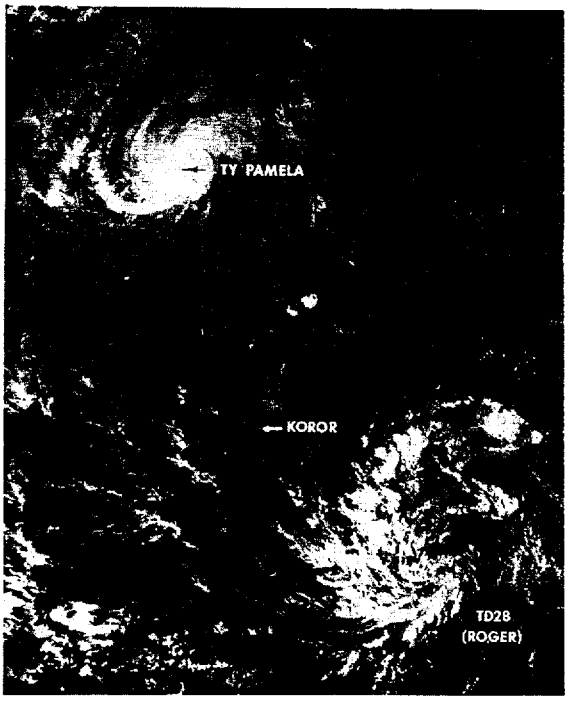

Figure 3-27-3. Typhoon Pamela, nearly six hours after attaining a second maximum intensity of 80 kts (41 m/sec). To the south, this imagery also shows Tyhpoon Roger in its formative stages. 0505342 December (NOAA 7 visual imagery).

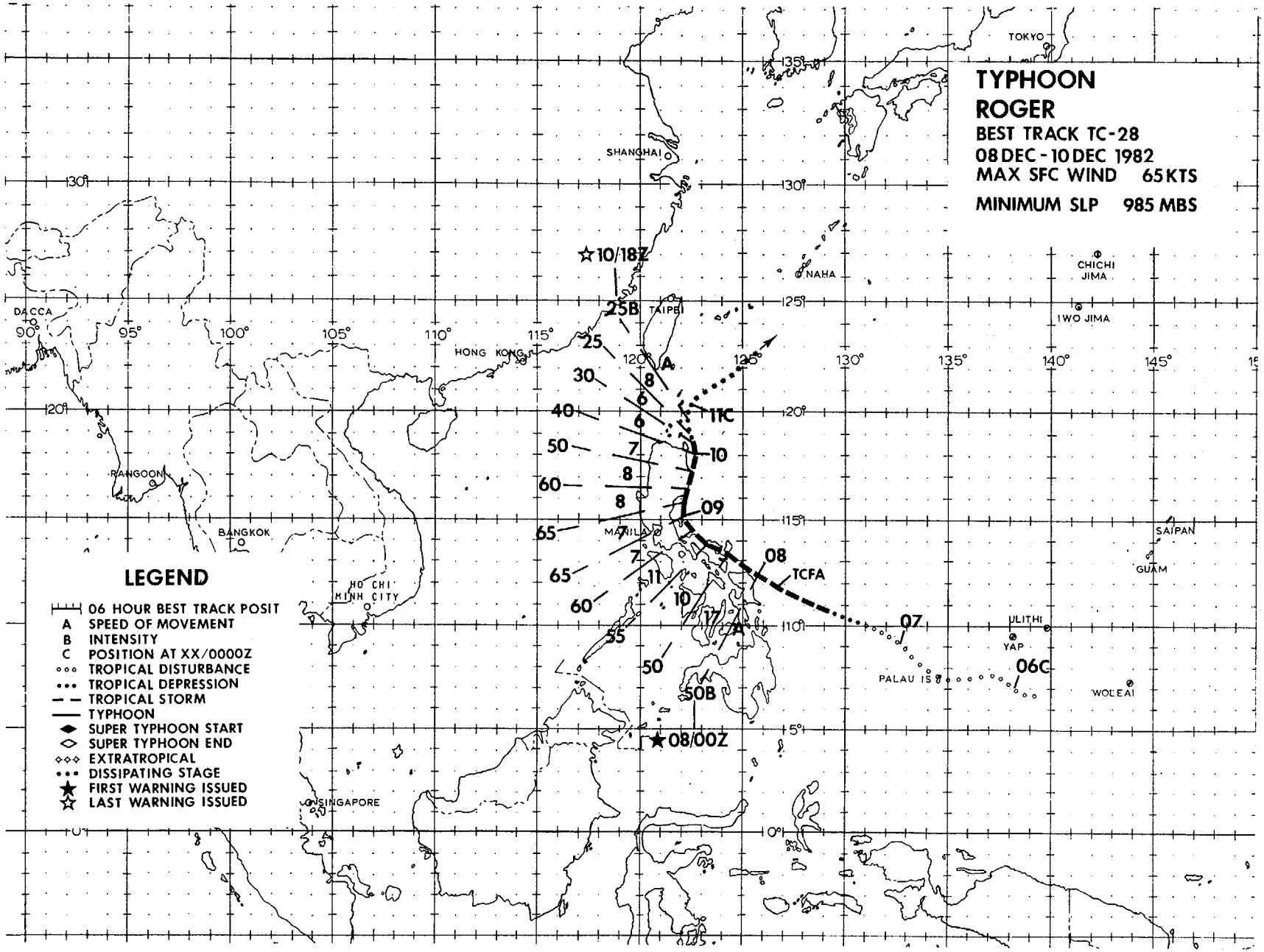
TYPHOON
ROGER
BEST TRACK TC-28
08 DEC - 10 DEC 1982
MAX SFC WIND 65 KTS
MINIMUM SLP 985 MBS
LEGEND
06 HOUR BEST TRACK POSIT
A SPEED OF MOVEMENT
B INTENSITY
C POSITION AT XX/0000Z
TROPICAL DISTURBANCE
TROPICAL DEPRESSION
TROPICAL STORM
TYPHOON
SUPER TYPHOON START
SUPER TYPHOON END
EXTRATROPICAL
DISSIPATING STAGE
FIRST WARNING ISSUED
LAST WARNING ISSUED
10/18Z
25B
25
30
40
50
60
65
65
60
55
50
50B
08/00Z
11C
10
09
08
TCFA
07
06C
TOKYO
SHANGHAI
NAHA
CHICHI JIMA
IWO JIMA
TAIPEI
HONG KONG
DACCA
RANGOON
BANGKOK
MANILA
HO CHI MINH CITY
SINGAPORE
SAIPAN
GUAM
ULITHI
YAP
PALAU IS
WOLEAI

Roger was particularly interesting in that it followed closely on the heels of Typhoon Pamela (27). Both systems remained south of the subtropical ridge axis, moved to a mid-tropospheric neutral point near northern Luzon and were profoundly affected by the passage of a mid-latitude trough. In sharp contrast to Pamela, which was a long-lived, significant tropical cyclone, Roger remained an incipient circulation for four days, and required three Tropical Cyclone Formation Alerts (TCFA) before attaining warning status on 7 December.

The first hint of formation occurred at 030600Z when a large area of convection appeared in an upper-level divergence pattern 1200 nm (2222 km) southeast of Typhoon Pamela. This pattern persisted aloft and drifted west-northwestward at 240 nm (444 km) per day. The low-level circulation center was displaced 150 nm (278 km) south of the cloud system center. This incongruity, or tilt, was present until 7 December and was, most probably, responsible for the long period of slow development.

The persistent convection feeding an outflow pattern aloft developed into a cloud system center, which prompted a TCFA at 042000Z and its reissuance for relocation at 050800Z. Development was arrested late on 5 December and the TCFA was cancelled at 060600Z. The upper-level mechanism (troughing off Asia) that was inhibiting Roger's development (in addition to contributing to its vertical tilt) was also affecting Pamela. During this period, Pamela slowed its forward motion, weakened, and changed course from the northwest to the southwest along the periphery of the northeast monsoon. By 061600Z Pamela and (formative) Roger had approached to within 600 nm (1111 km) of each other.

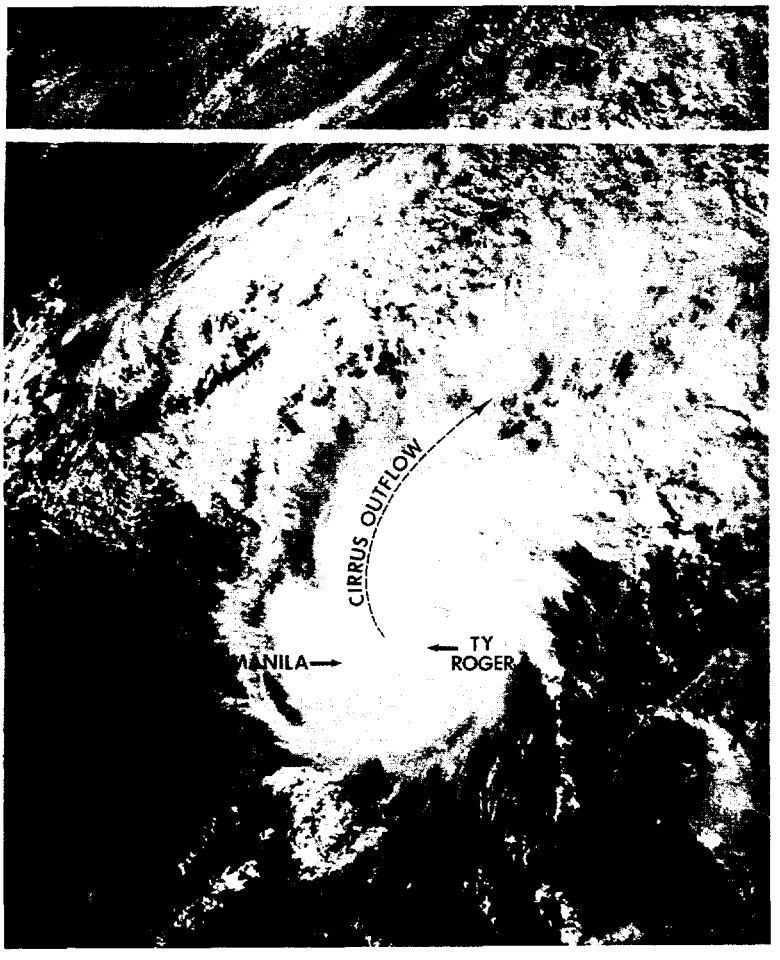

Figure 3-28-1. Expanded visual data of Roger just after reaching typhoon strength off the east coast of Luzon. The extensive low-level cloud deck to the north and northwest of the typhoon's cirrus outflow is embedded in the northeast monsoon. 090627Z December (NOAA 7 visual imagery)

During the next 24 hours the conditions for tropical cyclone development were favorable. Rawinsonde data from southwestern Taiwan (Tung-Chiang, Taiwan (WMO 46747)) indicated a 40 m height rise at 500 mb and reduced vertical wind shear. While Pamela moved into the central Philippines and weakened, Roger remained over water and underwent rapid intensification. The low-level wind circulation center and the cloud system center became vertically aligned and Roger gained tropical storm strength at 071200Z. Because of the sparse conventional data and the system's small maximum wind radius, the Joint Typhoon Warning Center could not verify the change in vertical alignment. As a reconnaissance aircraft deployed, a TCFA was issued at 072000Z. The first fix from the aircraft indicated a small, tight, 50 kt (26 m/sec) circulation with a minimum central pressure of 1002 mb, which prompted the initial warning at 080000Z.

Roger continued to move toward the northwest along the coast of the Philippines and intensified to typhoon strength at 090000Z. At 091200Z the 500 mb heights to the north at Tung-Chiang (WMO 46747) began to fall due to an approaching mid-latitude trough; the 700 mb flow had changed from northerly to southerly and the low-level northeast monsoonal flow weakened. Roger weakened to tropical storm intensity and moved northward along the east coast of northern Luzon. Satellite imagery revealed that a long cirrus plume was developing from Roger and streaming northeastward as the vertical shear increased aloft.

Increasing vertical shear, the approaching trough, and southerly low-level steering flow hinted at both recurvature (with sudden acceleration) and rapid shearing. Because of Roger's close proximity to land, aircraft reconnaissance was unable to monitor which scenario was taking place and, as a result, satellite data became the major input to the warnings. This posed a problem for the satellite analysts who could only position the top of the cloud system, which was becoming featureless and shearing off to the east. By 100600Z the cloud system center had been poorly organized for 12 hours and the apparent location of the low-level circulation center was highly suspect. Fortunately, by this time Roger had sufficient land clearance for the aircraft to be used. The fix located a greatly weakened center just off the northeastern tip of Luzon. These data required amendment of the 100600Z warning; downgrading Roger to a tropical depression, and relocating the circulation center 80 nm (148 km) to the northwest. The increasing vertical shear caused by the mid-latitude trough dropping southeastward across mainland China had disrupted the vertical linkage between the upper- and lower-level circulations and displaced the convection to the southeast.

The remains of the system were monitored for regeneration until 101800Z when the final warning was issued. The exposed low-level center continued to track northeastward for a day and was ingested into the frontogenic zone east of Taiwan.

2. NORTH INDIAN OCEAN TROPICAL CYCLONES

The 1982 North Indian Ocean tropical cyclone season was near normal. Five tropical cyclones reached warning status, two developed during the spring (monsoon) transition season and three developed during the fall transition season. One tropical cyclone developed in the Arabian Sea and the remaining four tropical cyclones developed in the Bay of Bengal. Tables 3-6 through 3-8 provide a summary of North Indian Ocean tropical cyclones, Tropical Cyclone Formation Alerts and Warnings.

TABLE 3-6. NORTH INDIAN OCEAN

1982 SIGNIFICANT TROPICAL CYCLONES

TROPICAL CYCLONE	PERIOD OF WARNING	CALENDAR DAYS OF WARNING	NUMBER OF WARNINGS ISSUED	MAXIMUM SURFACE WIND (KT)	ESTIMATED MSLP (MB)	BEST TRACK DISTANCE TRAVELED (NM)
1. TC 20-82	2 MAY - 5 MAY	4	14	125	914	1135
2. TC 22-82	2 JUN - 4 JUN	3	8	55	983	482
3. TC 23-82	14 OCT - 16 OCT	3	9	50	986	681
4. TC 24-82	17 OCT - 19 OCT	3	7	50	987	389
5. TC 25-82	5 NOV - 9 NOV	5	17	90	952	949
	1982 TOTALS:	18	55*			

* IN ADDITON, TWO AMENDED WARNINGS WERE ISSUED DURING 1982

TABLE 3-7.

1982 SIGNIFICANT TROPICAL CYCLONES

NORTH INDIAN OCEAN	JAN	FEB	MAR	APR	MAY	JUN	JUL	AUG	SEP	OCT	NOV	DEC	TOTAL
ALL TROPICAL CYCLONES	0	0	0	0	1	1	0	0	0	2	1	0	5
1975-1981													
AVERAGE	.1	-	-	.1	.7	.4	-	-	.4	.9	1.4	.4	4.6
CASES	1	0	0	1	5	3	0	0	3	6	10	3	32

FORMATION ALERTS: Five of the nine Formation Alert Events developed into significant tropical cyclones.

WARNINGS:

Number of warning days:	18
Number of warning days with two tropical cyclones in region:	0
Number of warning days with three or more tropical cyclones in region:	0

TABLE 3-8.

FREQUENCY OF TROPICAL CYCLONES BY MONTH AND YEAR

YEAR	JAN	FEB	MAR	APR	MAY	JUN	JUL	AUG	SEP	OCT	NOV	DEC	TOTAL
1971*	-	-	-	-	-	0	0	0	0	1	1	0	2
1972*	0	0	0	1	0	0	0	0	2	0	1	0	4
1973*	0	0	0	0	0	0	0	0	0	1	2	1	4
1974*	0	0	0	0	0	0	0	0	0	0	1	0	1
1975	1	0	0	0	2	0	0	0	0	1	2	0	6
1976	0	0	0	1	0	1	0	0	1	1	0	1	5
1977	0	0	0	0	1	1	0	0	0	1	2	0	5
1978	0	0	0	0	1	0	0	0	0	1	2	0	4
1979	0	0	0	0	1	1	0	0	2	1	2	0	7
1980	0	0	0	0	0	0	0	0	0	0	1	1	2
1981	0	0	0	0	0	0	0	0	0	1	1	1	3
1982	0	0	0	0	1	1	0	0	0	2	1	0	5
1975-1982													
AVERAGE	.1	-	-	.1	.8	.5	-	-	.4	1.0	1.4	.4	4.6
CASES	1	0	0	1	6	4	0	0	3	8	11	3	37

* JTWC warning responsibility began on 4 June 1971 for the Bay of Bengal, east of 90E. As directed by CINCPAC, JTWC issued warnings only for those tropical cyclones that developed or tracked through that portion of the Bay of Bengal. Commencing with the 1975 tropical cyclone season, JTWC's area of responsibility was extended westward to include the western portion of the Bay of Bengal and the entire Arabian Sea.

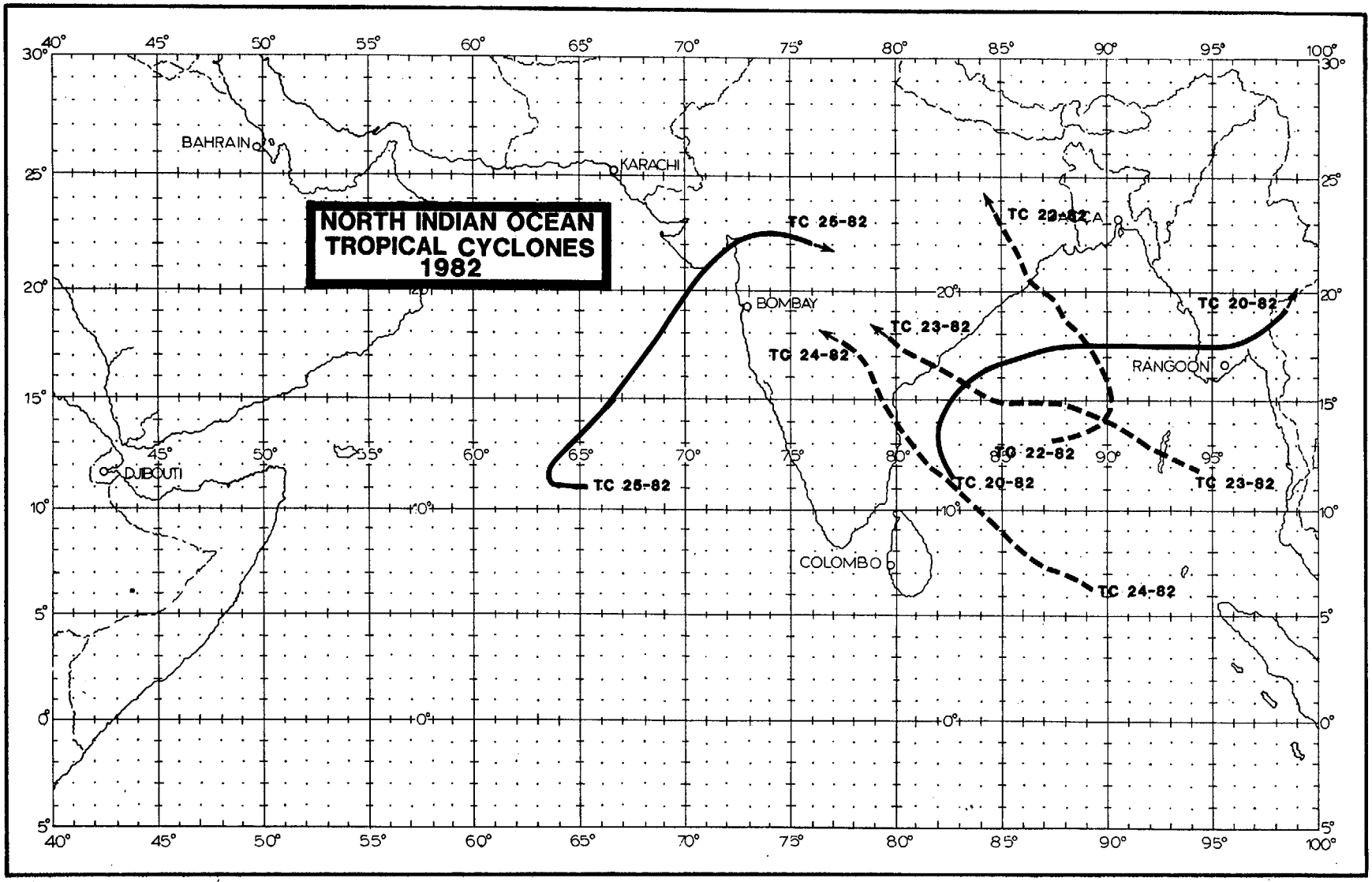

FWC/JTWC GUAM 3142/62 (NEW 2-76)

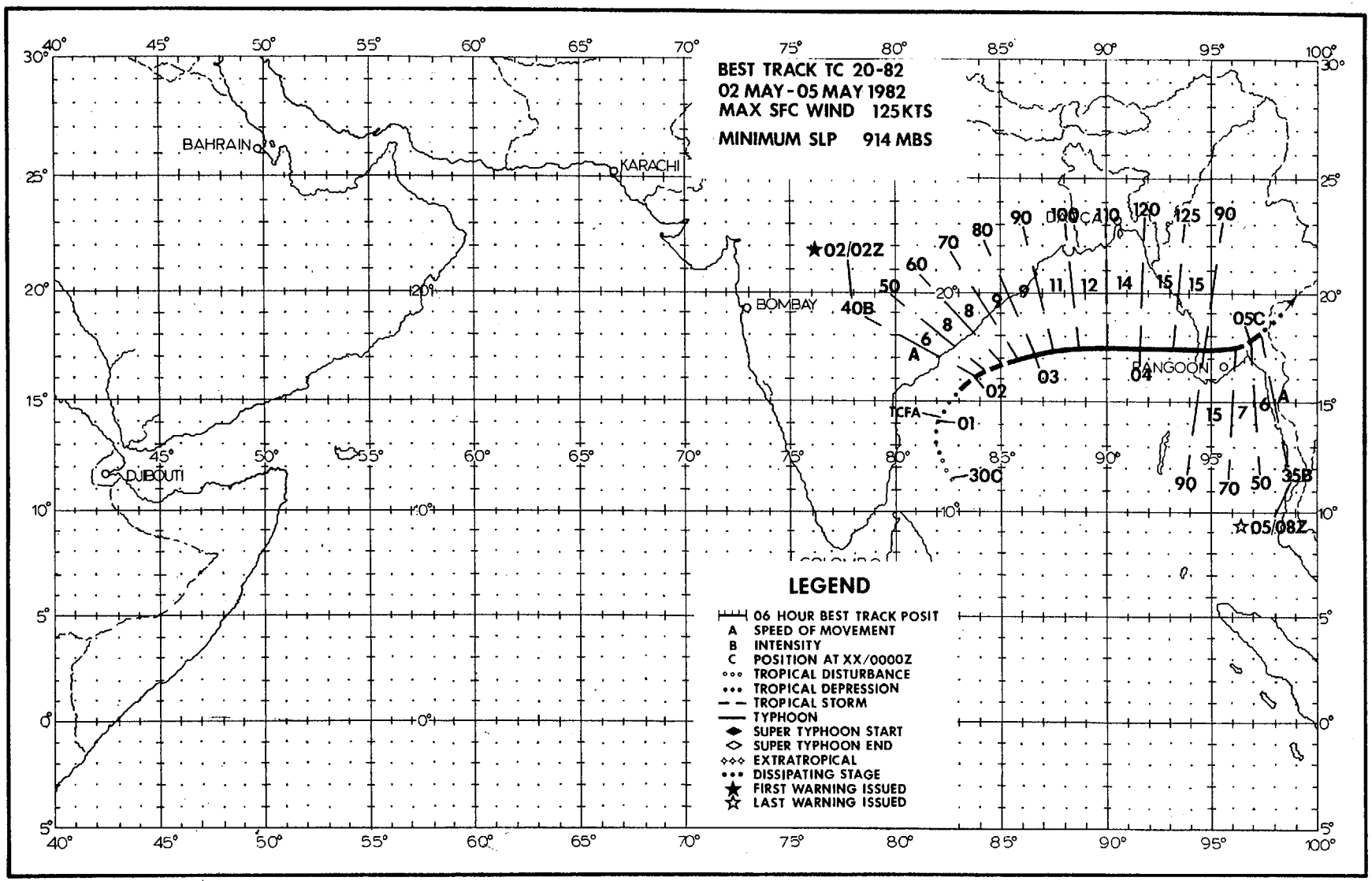

FWC/JTWC GUAM 3142/62 (NEW 2-76)

During late April, the monsoon trough was anchored in the latitudes south of Sri Lanka and extended eastward into the central portion of the Bay of Bengal. On 26 April, an area of convection associated with this trough became suspect and was discussed in the Significant Tropical Weather Advisory (ABEH PGTW); however, center fixes from satellite data were not available until 30 April when an upper-level circulation center was analyzed over the convection. On 1 May, a Tropical Cyclone Formation Alert was issued as a central dense overcast (CDO) formed over the system.

During this period, there was some concern about the actual intensity of the system at the surface. Surface observations from India, Sri Lanka, and throughout the Bay of Bengal indicated light and variable winds close to the developing system and the strongest winds (15 to 20 kt (8 to 10 m/sec)) far removed from the convection. Additionally, satellite fixes lacked continuity in tracking the system and the possibility that a significant surface circulation had not yet established itself seemed very realistic. However, NOAA 7 satellite imagery at 012132Z, received and analyzed at Air Force Global Weather Central (AFGWC), indicated a substantial increase in the system's convective organization, which prompted the issuance of the first warning for Tropical Cyclone 20-82 at 020200Z. From the initial warning position 440 nm (815 km) north-northeast of Sri Lanka, Tropical Cyclone 20-82 moved northeastward, remaining approximately 120 nm (222 km) east of India. Fix positions remained somewhat erratic in the early stages but improved when satellite imagery (021327Z NOAA 7) indicated that an eye had developed. The appearance of the eye also laid to rest any lingering doubts as to whether Tropical Cyclone 20-82 had developed into a significant tropical cyclone.

Track forecasts for Tropical Cyclone 20-82 were very good. From the first warning, Tropical Cyclone 20-82 was expected to move northeastward and turn more eastward with time. As Tropical Cyclone 20-82 approached 18N, it's movement became virtually eastward across the Bay of Bengal until landfall. While crossing the Bay of Bengal, Tropical Cyclone 20-82 continued to intensify and reached an estimated maximum intensity of 125 kt (64 m/sec) just prior to landfall. Best track intensities were based almost exclusively on Dvorak intensity estimates received from AFGWC and from Detachment 1,1WW, Nimitz Hill, Guam. However, despite the absence of verifying synoptic reports, satellite imagery (Figure 3-29-1) and later, casualty reports from Burma were convincing evidence that Tropical Cyclone 20-82 was a very intense (although quite compact) tropical cyclone.

The value of the meteorological satellite, especially in data sparse regions, has once again proven itself. In the era prior to the availability of imagery from satellites, Tropical Cyclone 20-82 would have been an undetected storm of great intensity that would strike without warning. A news release from Rangoon, Burma on 6 May, reported 7,000 homes destroyed in one township, and 85% of the homes and buildings in another township had their roofs blown away. Elsewhere, along Tropical Cyclone 20-82's path, schools, industries and hospitals were damaged or destroyed. Yet despite this extensive destruction, there were just five deaths reported in a region of the world where loss of human life is frequently in the hundreds from the effects of tropical cyclones.

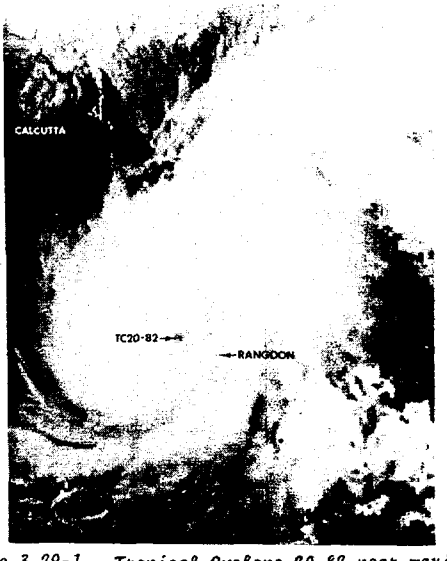

Figure 3-29-1. Tropical Cyclone 20-82 near maximum intensity, just west of Burma, 050423Z May. (NOAA 7 visual satellite imagery from AFGWC, Offutt, AFB, Nebraska)

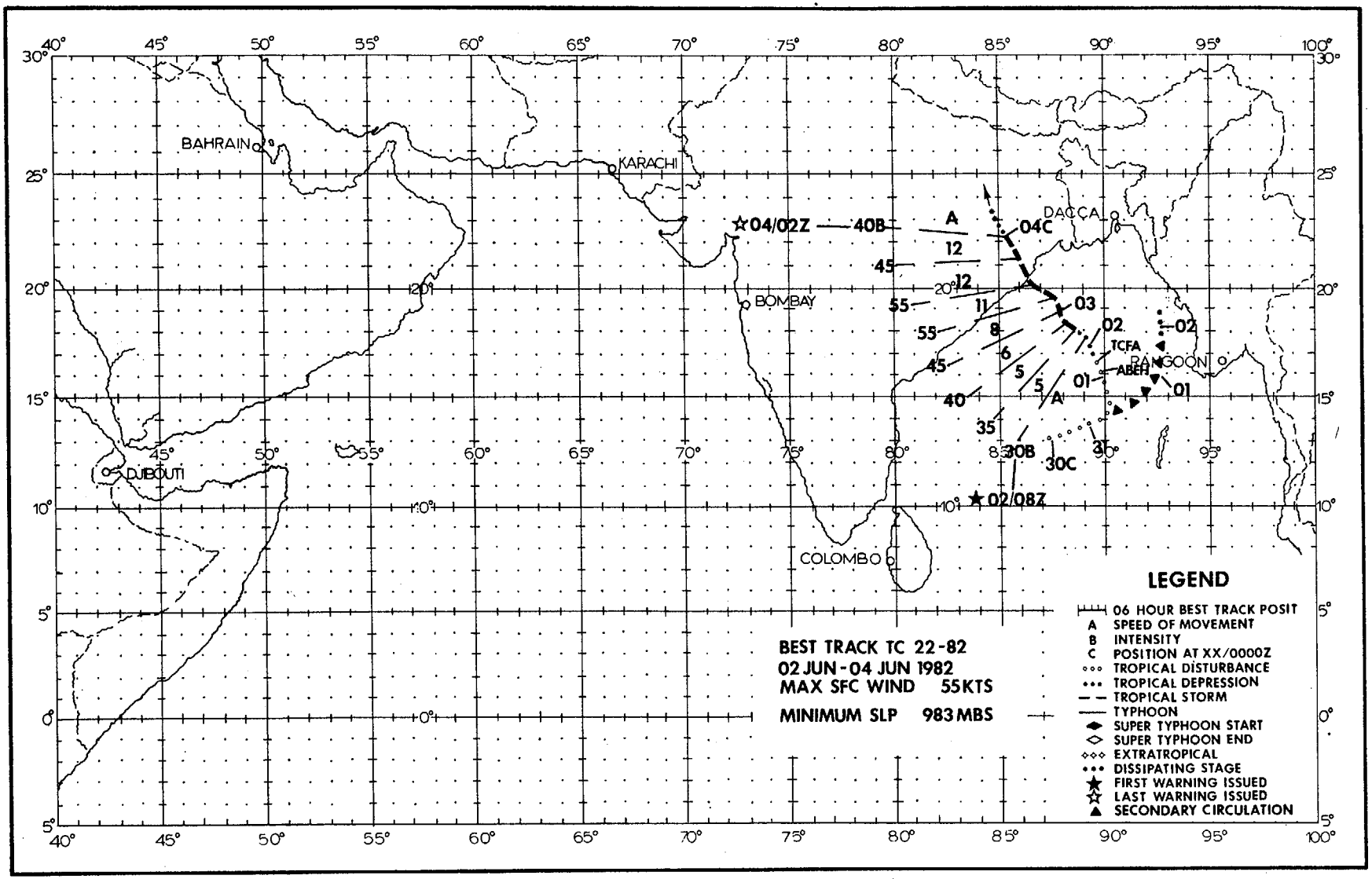

FWC/JTWC GUAM 3142/62 (NEW 2-76)

Tropical Cyclone 22-82 was the second significant tropical cyclone to develop in the Bay of Bengal during the spring (monsoon) transition season. During the last week of May, there was considerable convective activity over the central Bay of Bengal, resulting in two Tropical Cyclone Formation Alerts (TCFA) that were issued for a disturbance which tracked northeastward and moved into Burma on 29 May.

At 290000Z, a new convective area could be detected on satellite imagery moving out of a monsoon cloud band near 9N in the central Bay. During the ensuing three days, the convective area drifted northward with little evidence of a closed surface circulation. The synoptic environment in the Bay of Bengal at this time was dominated by strong (30 to 40 kt (15 to 21 m/sec)) westerly flow south of 9N, and by a 996 mb heat low over northern India.

By 010600Z June, the convective mass became more organized as an upper-level anticyclone could be analyzed from synoptic data, while visual satellite imagery revealed an exposed low-level circulation some 120 nm (222 km) to the northeast of the convective area. During the next 12 hours, satellite imagery indicated continued convective organization and at 011835Z, a TCFA was issued with the stipulation that the potential for significant tropical cyclone development was good, provided that either the low-level and upper-level features became better aligned or a new circulation developed under the convection. By 020800Z, when satellite data suggested that the latter case had occurred (the convective system had continued to develop and the exposed low-level circulation could no longer be detected on visual imagery), the first warning was issued for Tropical Cyclone 22-82.

During its short lifetime, Tropical Cyclone 22-82 followed a fairly straight, and climatological, northwestward track. Initially moving at 5 kt (9 km/hr), Tropical Cyclone 22-82 steadily increased it forward speed to 12 kt (22 km/hr) and intensified until making landfall at 031400Z. Satellite data from Air Force Global Weather Central (AFGWC) (Figure 3-30-1) and radar reports received at the Indian regional forecast center, indicated that Tropical Cyclone 22-82 was developing an eye when landfall was made just north of Paradip, 150 nm (278 km) southeast of Calcutta. In the coastal districts near Paradip and Orissa, where the tropical cyclone hit hardest, casuality reports indicated that more than 140 people were killed and more than 500,000 homes were destroyed. After landfall, Tropical Cyclone 22-82 rapidly dissipated as it tracked into the extreme southern portion of the Ganges River Valley.

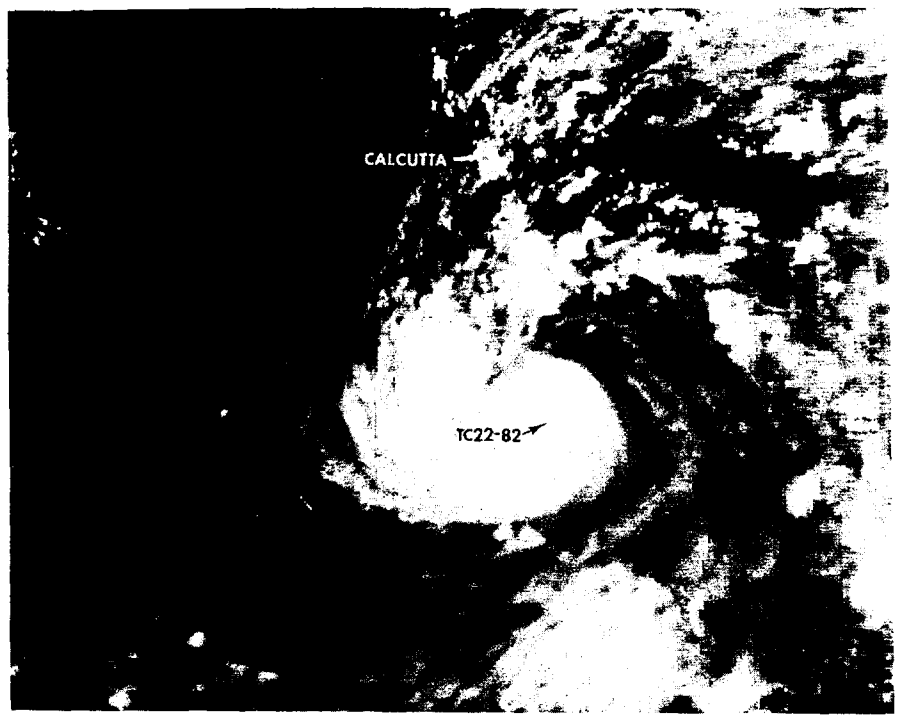

Figure 3-30-1. Tropical Cyclone 22-82 about five hours prior to landfall with an irregular 15 nm (28 km) eye near the center of the central dense overcast, 030858Z June (NOAA 7 visual satellite imagery from AFGWC, Offutt AFB, Nebraska).

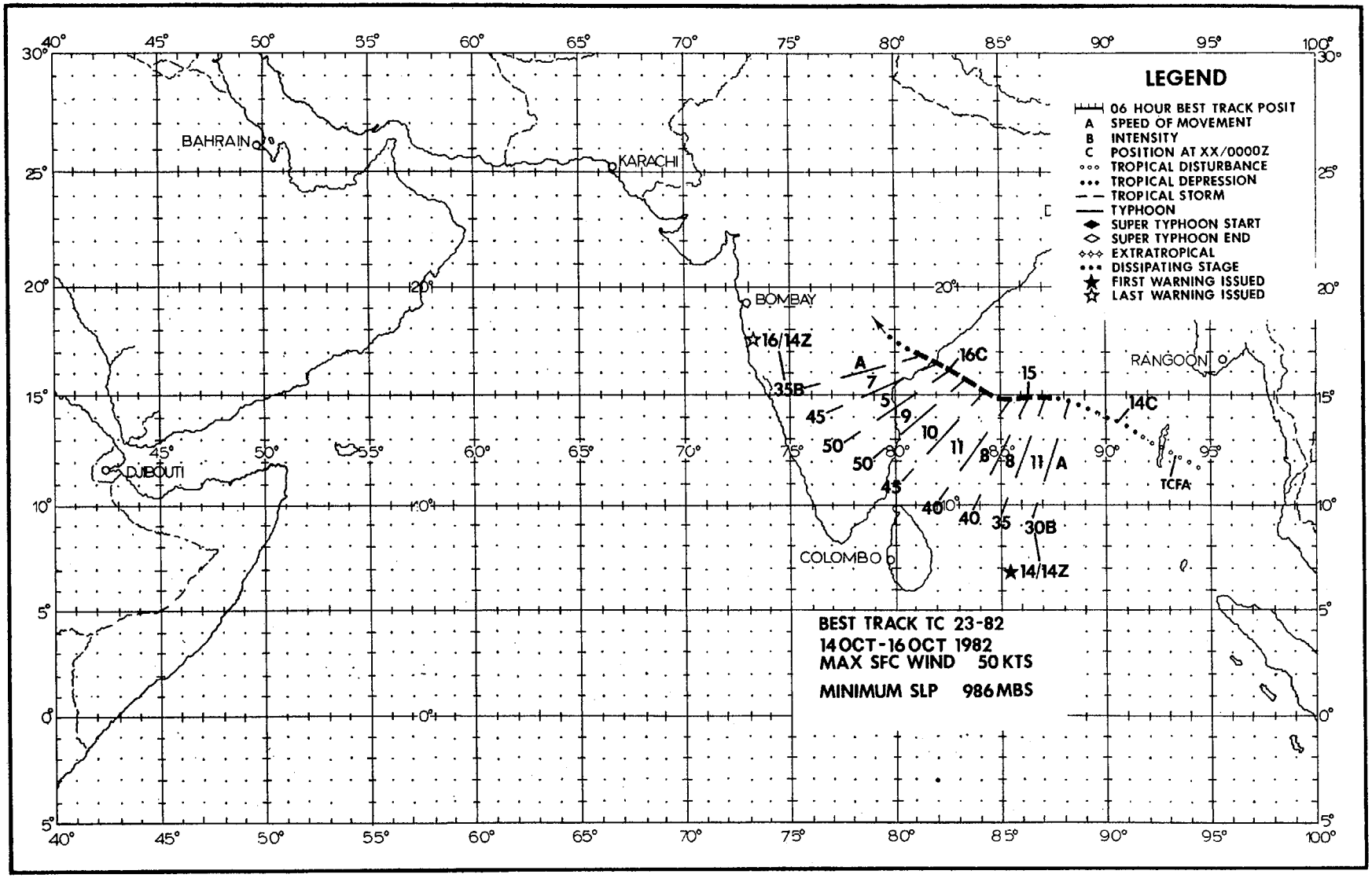

FWC/JTWC GUAM 3142/62 (NEW 2-76)

The initial stages of Tropical Cyclone 23-82's development were characterized by a persistent upper-level anticyclone and a weak surface disturbance associated with a broad area of convection. Initially detected on 9 October, JTWC tracked a westward-moving surface circulation from the Gulf of Thailand across the Malay Peninsula. Little development was evident from synoptic or satellite data as the system entered the southern Bay of Bengal. On 13 October, convection began to increase and show signs of organization while the system moved west of the Andaman Islands. A Tropical Cyclone Formation Alert was issued at 130600Z when satellite imagery revealed that the system's convection had organized under a more distinctly defined upper-level anticyclone. Late on 14 October satellite imagery showed that a strong central convective feature had developed and that upper-level outflow had increased. Based on these data, and the expectation of further development, the initial warning was issued at 141400Z for Tropical Cyclone 23-82.

The forecast tracks issued throughout Tropical Cyclone 23-82's lifespan anticipated movement toward the west-northwest in response to a mid-level steering current induced by a subtropical ridge centered over Burma. Tropical Cyclone 23-82 proved to be a "well-behaved" system and followed the forecast track toward the east coast of India. While in warning status Tropical Cyclone 23-82 gradually intensified and reached a peak intensity of 50 kt (26 m/sec) six hours prior to landfall. At approximately 161200Z, Tropical Cyclone 23-82 passed 35 nm (65 km) south of Kakinada, India (WMO 43189) with observed maximum sustained winds of 20 kt (10 m/sec). From Kakinada, Tropical Cyclone 23-82 proceeded inland and gradually dissipated.

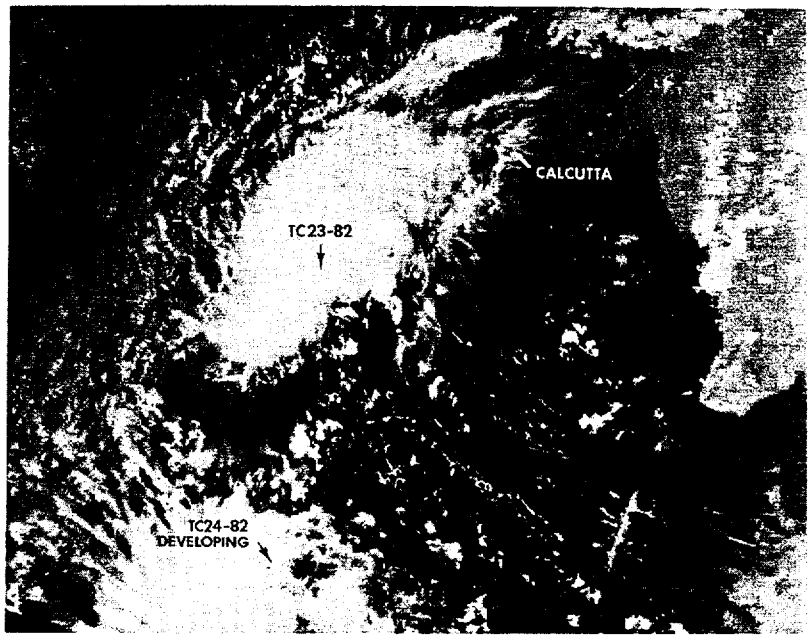

Figure 3-31-1. Tropical Cyclone 23-82 near landfall along the east coast of India with surface winds near 45 kt (23 m/sec). Tropical Cyclone 24-82 can be seen in its formative stages near Sri Lanka, 160856Z October (NOAA 7 visual imagery from AFGWC Offutt AFB, Nebraska).

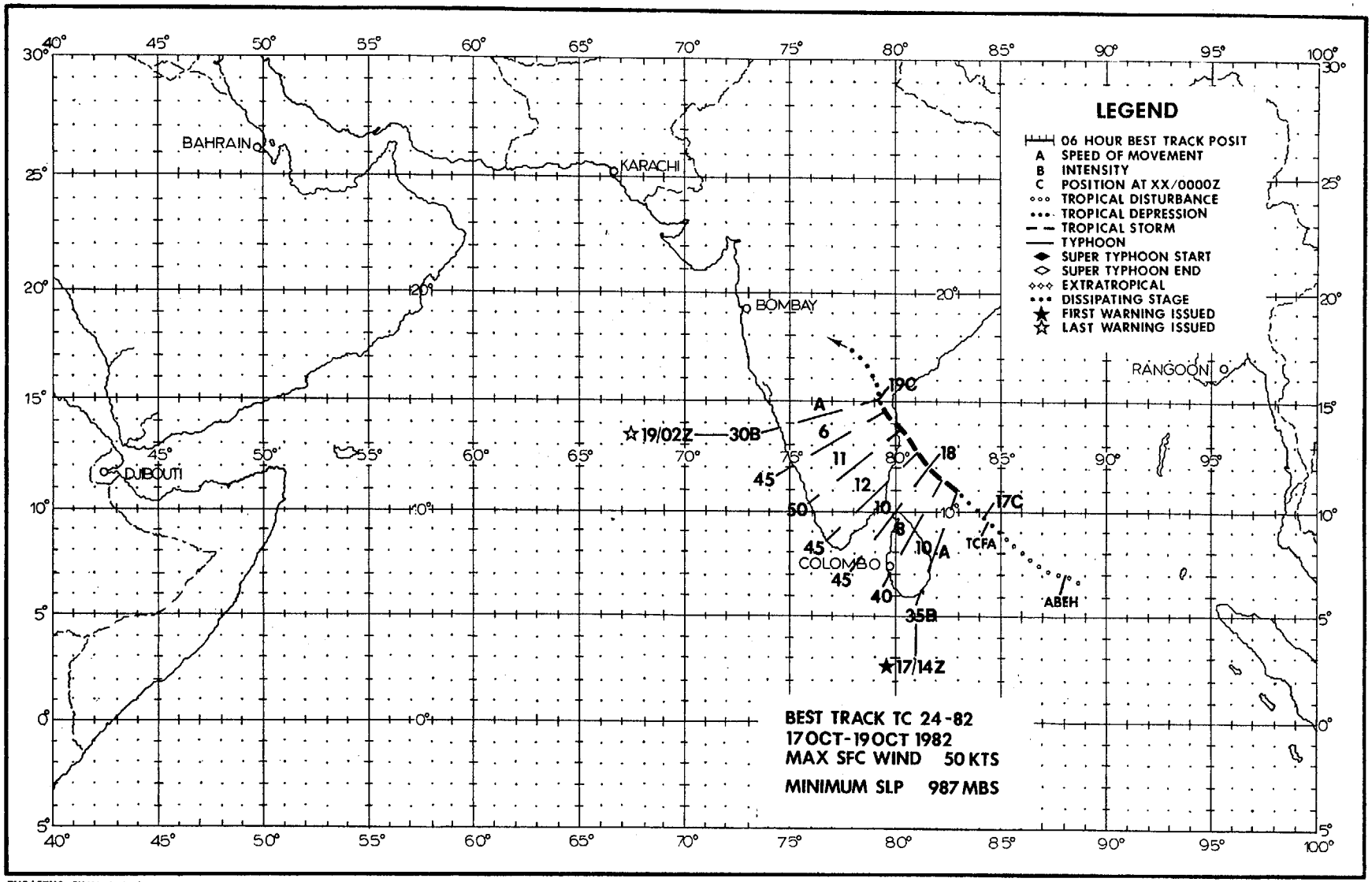

FWC/JTWC GUAM 3142/62 (NEW 2-76)

Tropical Cyclone 24-82 developed from an area of convective activity first observed on 15 October about 400 nm (740 km) east of Sri Lanka in the Bay of Bengal. No surface circulation was present but a weak upper-level anticyclone was evident on satellite imagery. During the next two days, the area was monitored for further development as it drifted slowly to the northwest. On the 16th, synoptic data and satellite imagery indicated that a loosely organized surface circulation had developed. In combination with the upper-level anticyclone, this circulation was considered to have good potential for intensification and a Tropical Cyclone Formation Alert was issued at 162300Z.

Subsequent satellite imagery indicated that the circulation had come together at the surface and mid-levels. JTWC issued the first warning on Tropical Cyclone 24-82 at 171400Z. Mid-level steering flow at the time was from the southeast due to the presence of a 500 mb anticyclone over Indochina. Numerical forecast products indicated that this mid-level anticyclone would retain its intensity and location throughout the ensuing 72 hours, thus, Tropical Cyclone 24-82 was forecast to continue moving northwestward. The system did move as expected, making landfall near Sriharikota Island at 181400Z with maximum sustained winds of 50 kt (26 m/sec).

Damage to private dwellings in Nellore District was extensive with an estimated 10,000 collapsed huts. Casualties were reported to be 5 dead and 10 injured. Tropical Cyclone 24-82 continued drifting northwestward after landfall and dissipated over central India.

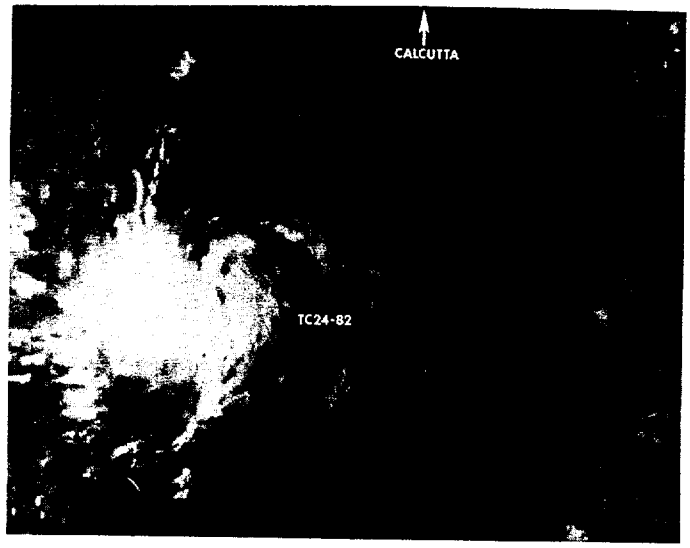

Figure 3-32-1. This satellite imagery indicated Tropical Cyclone 24-82 had organized sufficiently to warrant the issuance of tropical cyclone warnings. 170843Z October (NOAA 7 visual imagery from AFGWC Offutt AFB, Nebraska).

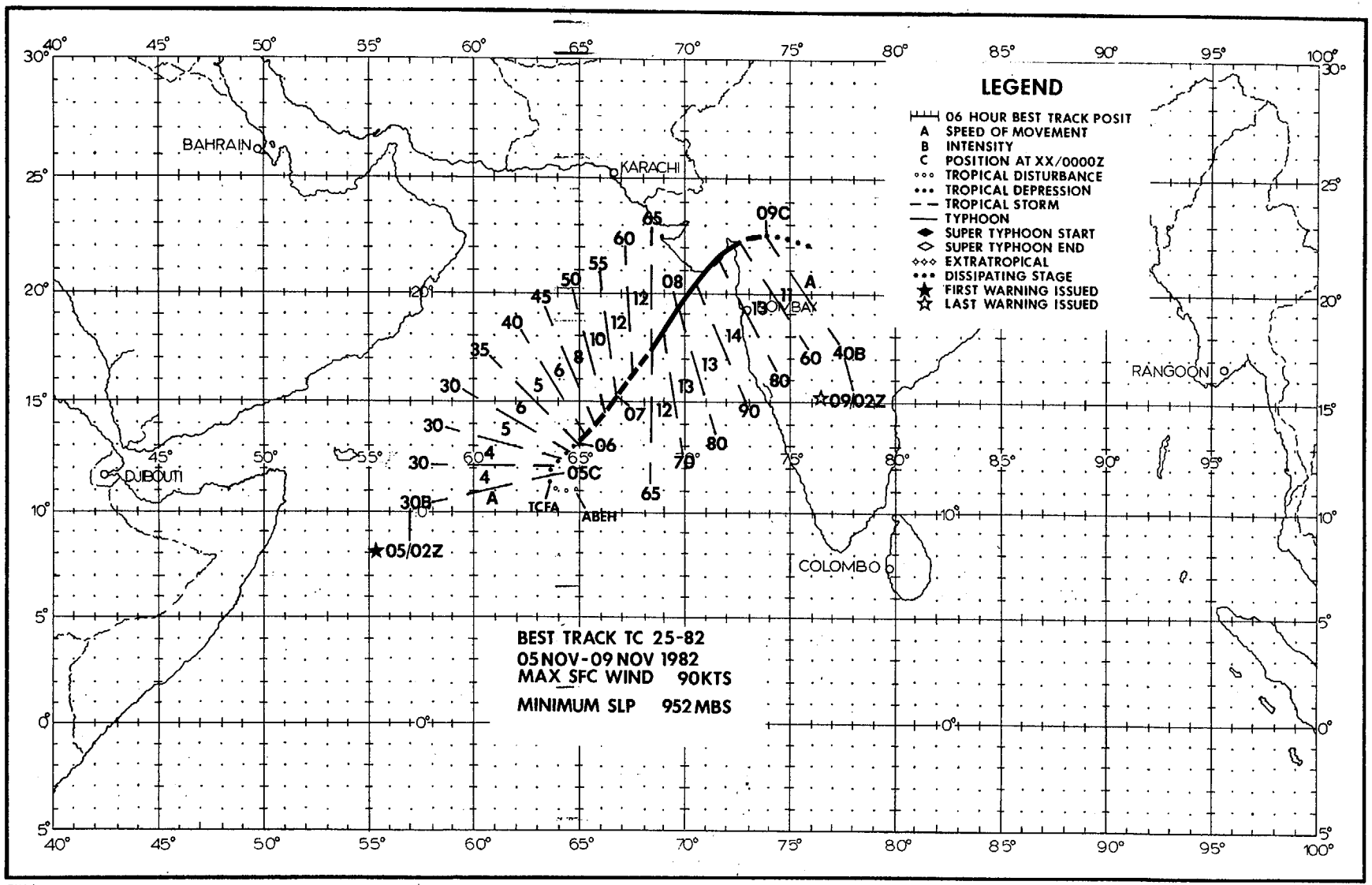

FWC/JTWC GUAM 3142/62 (NEW 2-76)

Tropical Cyclone 25-82 developed from an area of loosely organized convection in the central Arabian Sea. Although satellite images indicated that the convection and cloud system organization were increasing, shipboard synoptic reports were the first data to accurately describe the low-level circulation center. At 042000Z November, a Tropical Cyclone Formation Alert was issued when nearby shipboard observations indicated pressures near 1004 mb and winds of 20 kt (10 m/sec), confirming intensity estimates from earlier satellite data. Satellite and synoptic data during the subsequent 12-hour period indicated that development was continuing, prompting the first warning on Tropical Cyclone 25-82 at 050200Z.

Tropical Cyclone 25-82 slowly consolidated during the initial 24-hour period in warning status. Based on guidance from virtually every forecast aid, the first six warnings anticipated a movement toward the west-northwest. However, once the system organized and satellite fixes became more consistent, it became evident that Tropical Cyclone 25-82 was not moving westward as forecast. In the same time frame, a break developed in the mid-level subtropical ridge, which lay along 23N. As height falls occurred across the northern Arabian Sea coast, the tropical cyclone responded by accelerating toward the northeast and intensifying. Tropical Cyclone 25-82 continued to deepen until landfall at 081000Z near the Indian port city of Veraval (20.9N 70.4E). Veraval was particularly hard hit as the cyclone moved onshore with sustained winds of 90 kt (46 m/sec).

Once overland, and deprived of the low-level moist layer over water, Tropical Cyclone 25-82 rapidly dissipated, leaving in its wake at least 50,000 homes damaged or destroyed and a death toll in excess of 341.

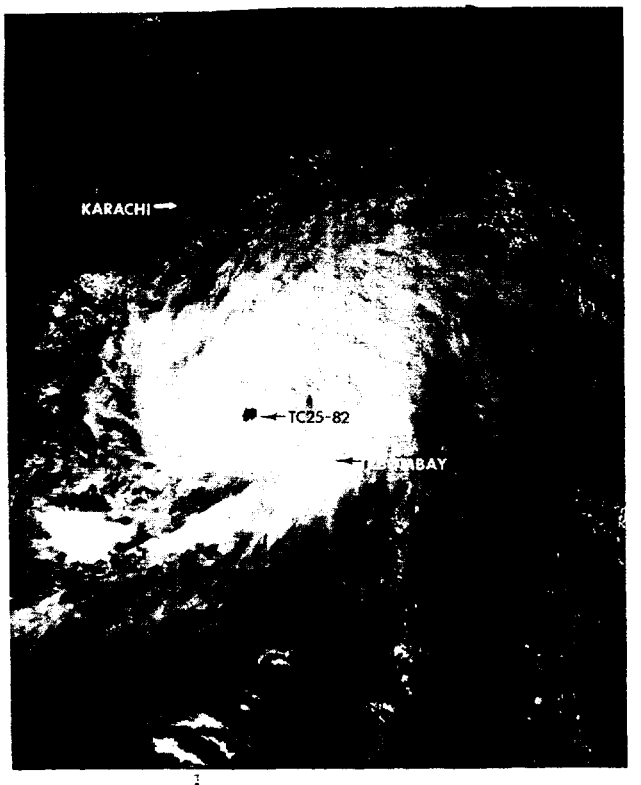

Figure 3-33-1. Tropical Cyclone 25-82 is at peak intensity with maximum winds of 90 kt (46 m/sec) and just making landfall on India's northwestern coast. 080921Z November (NOAA 7 visual imagery from AFGWC Offutt AFB, Nebraska)

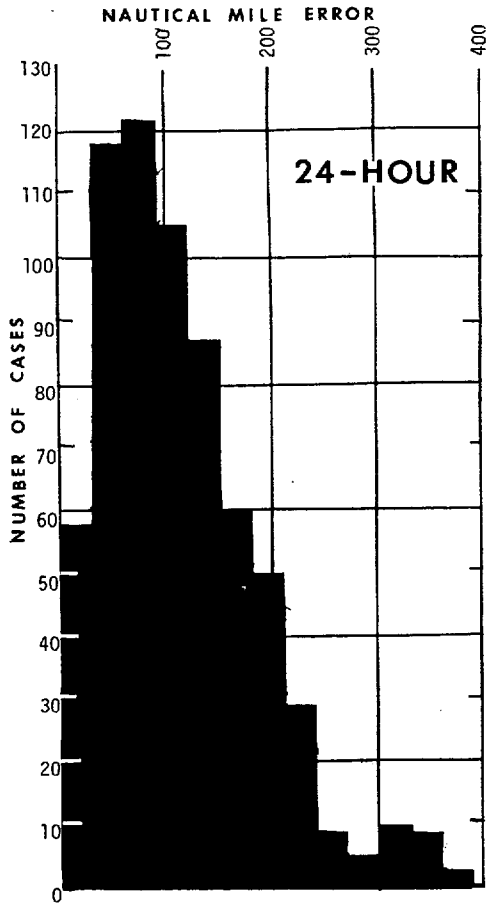

FIGURE 4-2. Frequency distribution of the 24-, 48-, and 72-hour forecast errors for all significant tropical cyclones in the western North Pacific during the 1982 season.

FORECAST ERRORS (nm)

	24-HR	48-HR	72-HR
MEAN:	113	237	341
MEDIAN:	98	209	296
STANDARD DEVIATION:	73	158	225
CASES:	665	535	428